BOILING HEAT TRANSFER TO TURBULENT LIQUID FILMS

BOILING HEAT TRANSFER TO TURBULENT LIQUID FILMS

By

EDGAR DERNEDDE, B.Sc.

A Thesis
Submitted to the Faculty of Graduate Studies
in Partial Fulfilment of the Requirements
for the Degree
Master of Engineering

McMaster University
May 1966

MASTER OF ENGINEERING (1966) McMASTER UNIVERSITY
(Chemical Engineering) Hamilton, Ontario.

TITLE: Boiling Heat Transfer to Turbulent Liquid Films

AUTHOR: Edgar Dernedde, B.Sc. (University College, London)

SUPERVISOR: Dr. T. W. Hoffman

NUMBER OF PAGES: xiv, 216

ABSTRACT:

Benzene and water films were passed over an inclined, hot copper plate. The boiling heat transfer to the turbulent liquid films has been measured with local heat-flux meters. These meters have been adopted from a design suggested by Gardon (G10), and could be used to measure boiling heat fluxes with an accuracy of about -20,000 BTU/hr.sq.ft. The results indicate that the heat transfer to the liquid films compares well with that of forced convection subcooled boiling.

During boiling the liquid film is destroyed by the growing vapour bubbles and by the separation of the liquid from the hot plate. The break-up of the liquid films has been investigated with high-speed photography but an analysis of the hydrodynamics of this break-up has not been made.

ODE TO A FLAT PLATE HEAT FLUX METER

OR EDGAR'S LAMENT

Power in - I^2R

Heat Flux Meter out by far;

Tear it down, build again,

Gotta find that factor ten!

Boil up liquids in a pool,

Calibrate that heat flux tool;

Balance good - we're on the track,

Oops! Read the charts from the back.

Read them right - things still great,

At last we've got the true heat rate.

A few more runs and no more worry,

What the hell - I'm in no hurry.

Calculate and fudge and fidget,

Soon we'll have that last damn digit;

Then I'm gone from this old place,

No more V-L interface

To haunt my dreams and plague my mind,

'Cause factor ten we did find!

Ken Pollock
Chemical Engineering Department
McMaster University
1965.

ACKNOWLEDGEMENTS

The author is grateful to Dr. T. W. Hoffman for suggesting the problem and indebted to him for his enthusiasm and guidance.

Sincere thanks are extended to the machine shop of the Engineering Faculty for their co-operation and patience and to the staff of the Chemical Engineering Department for their helpful suggestions.

Sincere thanks are also extended to Mrs. Agnes Arsenault who transformed this thesis to a legible form.

The partial support of this work by the Federal Department of Forestry is gratefully acknowledged.

TABLE OF CONTENTS

FIGURE INDEX

PLATE INDEX

TABLE INDEX

A. INTRODUCTION

The boiling of liquid films is of importance in cooling operations such as the quenching of hot metal sheets, the extinction of forest fires and has also become of recent interest in the cooling of nuclear fuel elements.

The amount of cooling that can take place is however limited. This limit, called burn-out, occurs when vapour instead of liquid contacts the heating surface. Under those conditions the liquid film has either completely evaporated or the temperature of the heating surface is too high for the liquid to contact it. When either of these happen the heat transfer rate from the heating surface is decreased markedly, because the vapour acts as a large heat transfer resistance. A nuclear fuel element supplies heat at a constant heat flux. If the heat transfer rate is suddenly reduced by one of the above mechanisms the fuel element usually overheats to a temperature corresponding to its melting point, i.e. the fuel element burns out.

It is of interest to determine under what conditions the liquid film ceases to cool the heating surface and what would be the maximum attainable heat flux for each mechanism. The purpose of the present investigation was to explore the hydrodynamic and heat transfer aspects of the mechanism, in which the temperature of the heating surface was so high that no further wetting of the liquid occurred, (Plate 1).

As will be seen in the literature survey much work has been done in related fields, but little has been done in this particular direction.

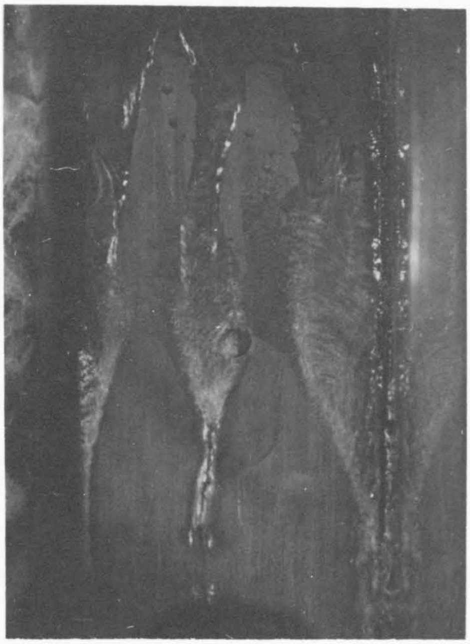

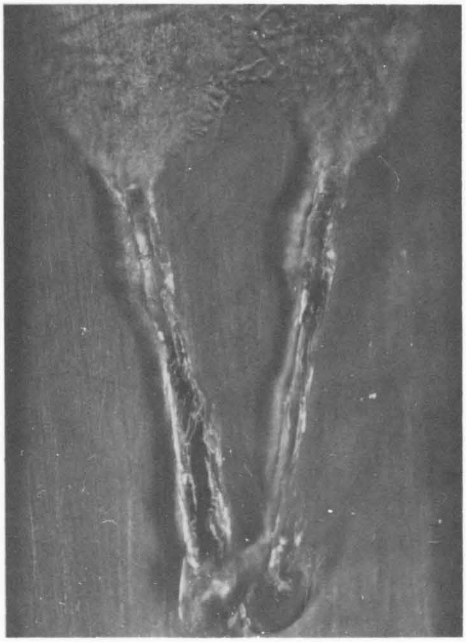

PLATE 1

B. LITERATURE REVIEW

1. Boiling Heat Transfer

1.1 Introduction

Over the last decade boiling heat transfer research has been intensified in order to apply this process to the cooling of nuclear reactors and rocket engines. The heat fluxes obtainable with nucleate boiling are very high and thus boiling seems a promising process for the above applications.

Boiling heat trasnfer is based on the change of phase from liquid to vapour at the heating surface. The temperature of the heating surface thus exceeds the saturation temperature of the liquid. The temperature gradient in boiling heat transfer is usually characterized by the temperature difference $\Delta T = T_W - T_{sat}$, where T_W is the temperature of the heating surface and T_{sat} the saturation temperature of the liquid. Depending upon the temperature difference ΔT three boiling regimes are known:

(i) nucleate boiling
(ii) transition boiling
(iii) film boiling.

These regimes can be identified by their heat transfer characteristics. Figure 1 shows a typical pool boiling curve of saturated water boiling on a horizontal surface at atmospheric pressure (G5) (H10). Region AB is the natural or forced convection regime. At B boiling commences by the generation of vapour bubbles at favoured spots on the heating

POOL BOILING CURVE OF WATER ON A HORIZONTAL SURFACE
(ATMOSPHERIC PRESSURE)

REF.: G5, H10

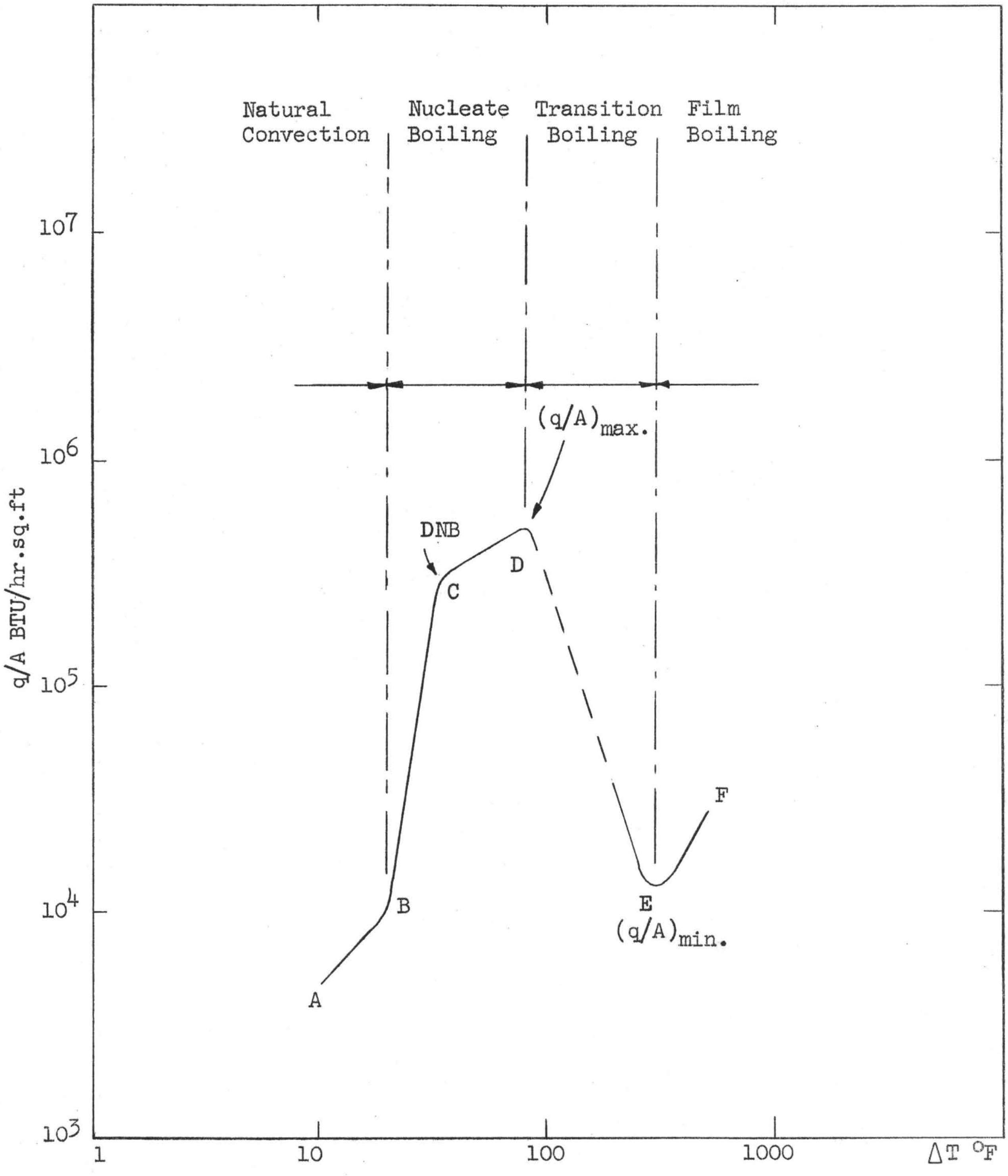

FIGURE 1

surface. An increase in wall temperature results in a steep increase of the heat flux due to the increasing number of bubble generating spots. This entire region, BC, is called the nucleate boiling regime. At C departure from nucleate boiling (DNB) occurs due to vapour patch formation on the heating surface. At D the maximum (critical or burn-out) heat flux occurs. Any further increase in wall temperature beyond D results in a decrease of the heat flux, because an unstable insulating vapour blanket forms over the heating surface. Region DE is called the transition boiling regime. At E, which is the position of the minimum heat flux, the vapour blanket stabilizes and the liquid no longer contacts the heating surface. Region EF is the film boiling regime, where the heat transfer takes place by conduction and radiation through the vapour film.

Nucleate and transition boiling are governed by local transient heat transfer phenomena, while film boiling is a steady-state process without periodic transients. The boiling theories available thus apply to one boiling regime only.

The boiling curve described above is characteristic of the boiling process, but its exact shape is determined by such a large variety of factors (liquid-solid combination, surface conditions, surface geometry, etc.) that it has been difficult for different observers to obtain reproducible results.

The influence of forced convection and subcooling on the boiling process is of practical importance. Subcooled boiling occurs when the liquid temperature is below its boiling point. Evaporation takes place at the heating surface with subsequent condensation of the vapour bubbles

EFFECT OF FORCED CONVECTION ON BOILING CURVE
(ATMOSPHERIC PRESSURE)

REF.: W3

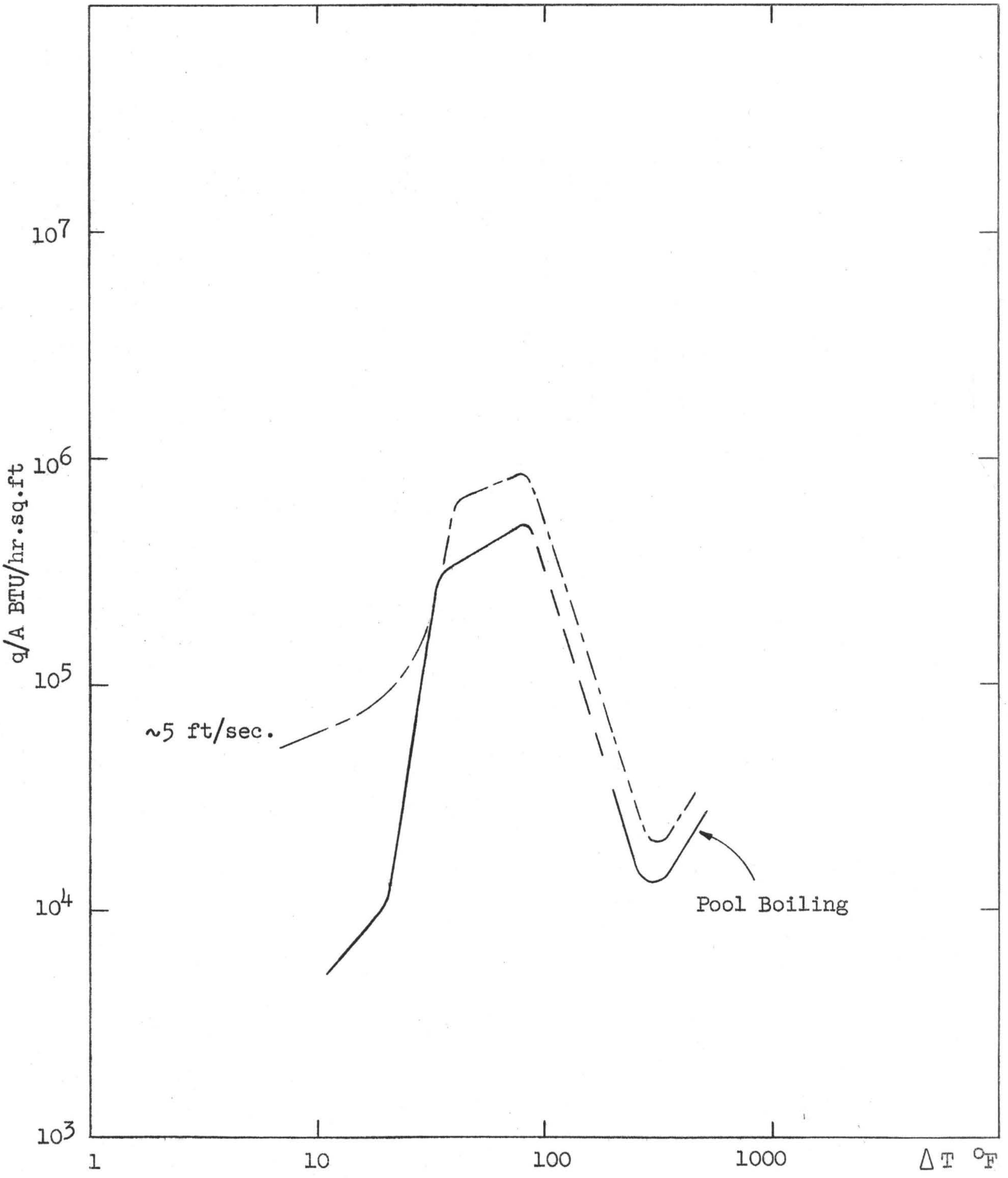

FIGURE 2

EFFECT OF SUBCOOLING AND FORCED CONVECTION ON BOILING CURVE
(ATMOSPHERIC PRESSURE)

REF.: B7, F4, E2, R2, M8, S2, G5, H10

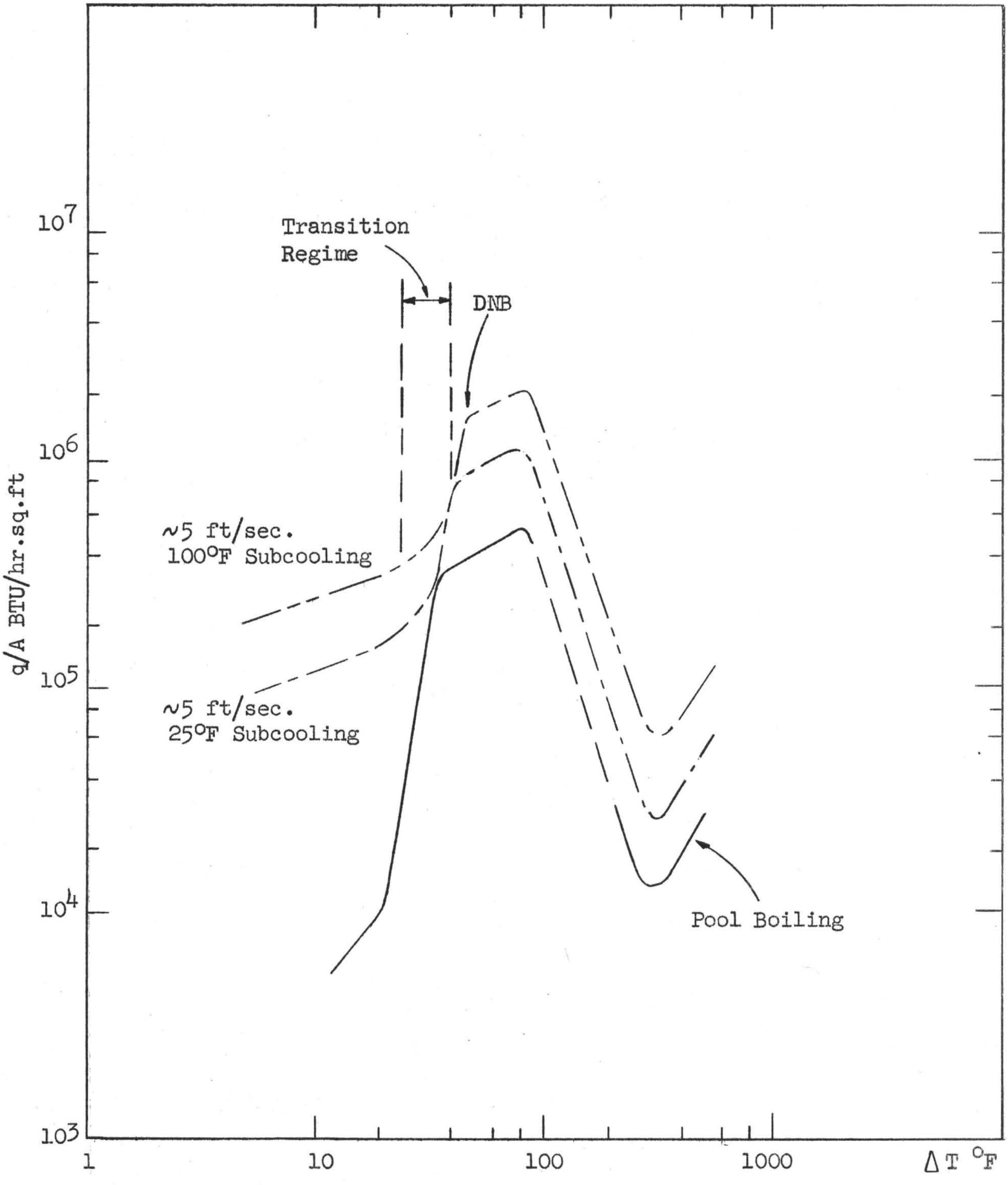

FIGURE 3

in the cold bulk liquid. There is no net evaporation. The heat transfer for subcooled boiling is exceptionally high. Figures 2 and 3 show the relative effect of forced convection and subcooling on the boiling curve. Few data besides those of Ellion (E2) are available which cover all the boiling regimes for a particular system and include these two effects. The values shown have been estimated and are presented only to indicate the trend. Further work in this area has been suggested by Bergles and Rohsenow (B7).

Extensive reviews of the literature on boiling have been given by Westwater (W3) (W4), Rohsenow (R2), Zuber (Z2) and Leppert and Pitts (L3). A brief survey of the boiling regimes is presented below.

1.2 Nucleate Boiling

A photographic study of nucleate boiling together with a determination of the boiling curve has shown that the nucleate boiling regime can be subdivided into four regions (G5):

(i) region of isolated bubbles
(ii) region of vapour columns (bubbles and mushrooms)
(iii) region of vapour mushrooms
(iv) region of vapour patches.

The mechanisms proposed for these regions will be discussed below.

In the first three regions the heat transfer is best represented by the equation (Z2) (K4)

$$q/A = a_1 \ (\Delta T)^{a_2} \left(\frac{n}{A}\right)^{a_3} \tag{B-1}$$

to include the independent effect of the nucleation site density (n/A). The nucleation site density is a function of the surface temperature T_w,

$$\frac{n}{A} = a_4 \exp\left(\frac{-K}{T_w^3}\right) \tag{B-2}$$

where K depends upon the surface characteristics and the physical properties of the liquid and the vapour, (G9). Equation (B-1) is more general for it makes allowance for the condition of the heating surface.

In the region of isolated bubbles the heat transfer is determined by bubble nucleation, bubble growth and bubble departure from the heating surface. The heat transfer can be controlled either by nucleation (at high pressures) or by bubble growth (at low pressures). At low heat fluxes vapour bubbles are formed at certain preferred sites on the heating surface. The areas between nucleating sites transfer heat by natural convection.

Surface nucleation

Since the vapour pressure over a concave liquid surface is less than that over a plane one, the liquid surrounding a vapour bubble must be superheated, in order that the bubble does not collapse. The excess pressure of the vapour bubble is given by the Laplace equation

$$\Delta p = p_V - p_L = \frac{2\sigma}{r} \tag{B-3}$$

where p_V and p_L are the pressure inside the vapour bubble and the liquid respectively, σ the surface tension and r the radius of the bubble. The presence of a superheated thermal boundary layer at the heating surface has been shown by Jakob (J2).

Theories of homogeneous nucleation predict liquid superheats of 100°F for the formation of vapour bubbles. However boiling usually begins at much lower superheats of about 10°F. It appears therefore that a starting cluster is already in existence, such that the large superheat required to form a vapour nucleus is no longer necessary.

It is known that a gas-filled cavity can act as a nucleating site. The gas can easily gain vapour and grow. The cavity may fill with vapour, when the initial gas is depleted and thus will continuously serve as a nucleating site. If boiling is discontinued such a nucleating site may be destroyed, because the cavity may fill with liquid. Bankoff (B6) has shown that the angle of the cavity and the solid-liquid contact angle determine the effectiveness of a cavity as a continuous nucleating site. An easily wetted cavity is a poor nucleating site.

Griffith and Wallis (G2) have shown that in a uniform temperature field the liquid superheat for bubble formation is directly related to the size of the cavity in the heating surface. Assuming a constant contact angle a growing bubble in the cavity passes through a stage of maximum curvature (minimum radius), which defines the superheat necessary for nucleation. The following equation, derived by substituting the Clausius-Clapeyron equation into equation (B-3) was verified.

$$T_H - T_{sat} = \frac{2\sigma T_{sat}}{r \lambda \rho_v} \qquad \text{(B-4)}$$

where ($T_H - T_{sat}$) is the superheat of the liquid, r the radius of the cavity, λ the latent heat of vaporisation and ρ_V the vapour density. However, the equation could not be used to predict the formation of vapour bubbles from the same nucleating site in a non-uniform temperature field. Higher superheats were required in that case.

Hsu and Graham (H8) have developed a procedure to determine when a nucleating cavity will nucleate in a non-uniform temperature field. The heating surface is considered to contain many cavities over a wide range of sizes. In the thermal boundary layer close to the surface the temperature profile, before boiling starts, is nearly linear and can be expressed by the heat transfer equation (natural or forced convection)

$$T_H = T_W - (q/A) \frac{1}{k_L} y \qquad \text{(B-5)}$$

It is postulated that a nucleus of hemispherical shape with radius r will grow, if the liquid temperature at a distance $y = r$ from the wall is greater than the critical liquid temperature T_H defined by equation (B-4). The corresponding wall superheat ($T_W - T_{sat}$) required to initiate boiling is best evaluated graphically, (Figure 4). The line tangent to the curve representing equation (B-4) establishes the minimum wall temperature required to initiate boiling. The size cavity that nucleates first is r_o. For a larger wall superheat cavities in the radius range from (r_1) to (r_2) are active. This method has been verified by Bergles and Rohsenow (B7) for subcooled boiling.

Hsu (H7) has extended the above model by considering transient conduction in the liquid near the heating surface. Transient conduction in the heating surface itself, as suggested by the work of Moore and Mesler (M5) has been neglected. The range of active nucleating cavities was determined by eliminating those which had an infinite waiting period; the waiting period being the time required for the liquid to attain a certain superheat. For the initiation of boiling of a saturated liquid the wall superheat was given by the relation

$$T_W - T_{sat} = \frac{8\sigma T_{sat} a_5}{\lambda \delta \rho_V} \qquad \text{(B-6)}$$

The importance of the thermal boundary layer thickness δ was stressed. Experimental data were available to support the model.

The frequency of nucleation (bubble frequency) is directly related to the waiting period and the bubble growth time.

INITIATION OF NUCLEATE BOILING

REF.: H8

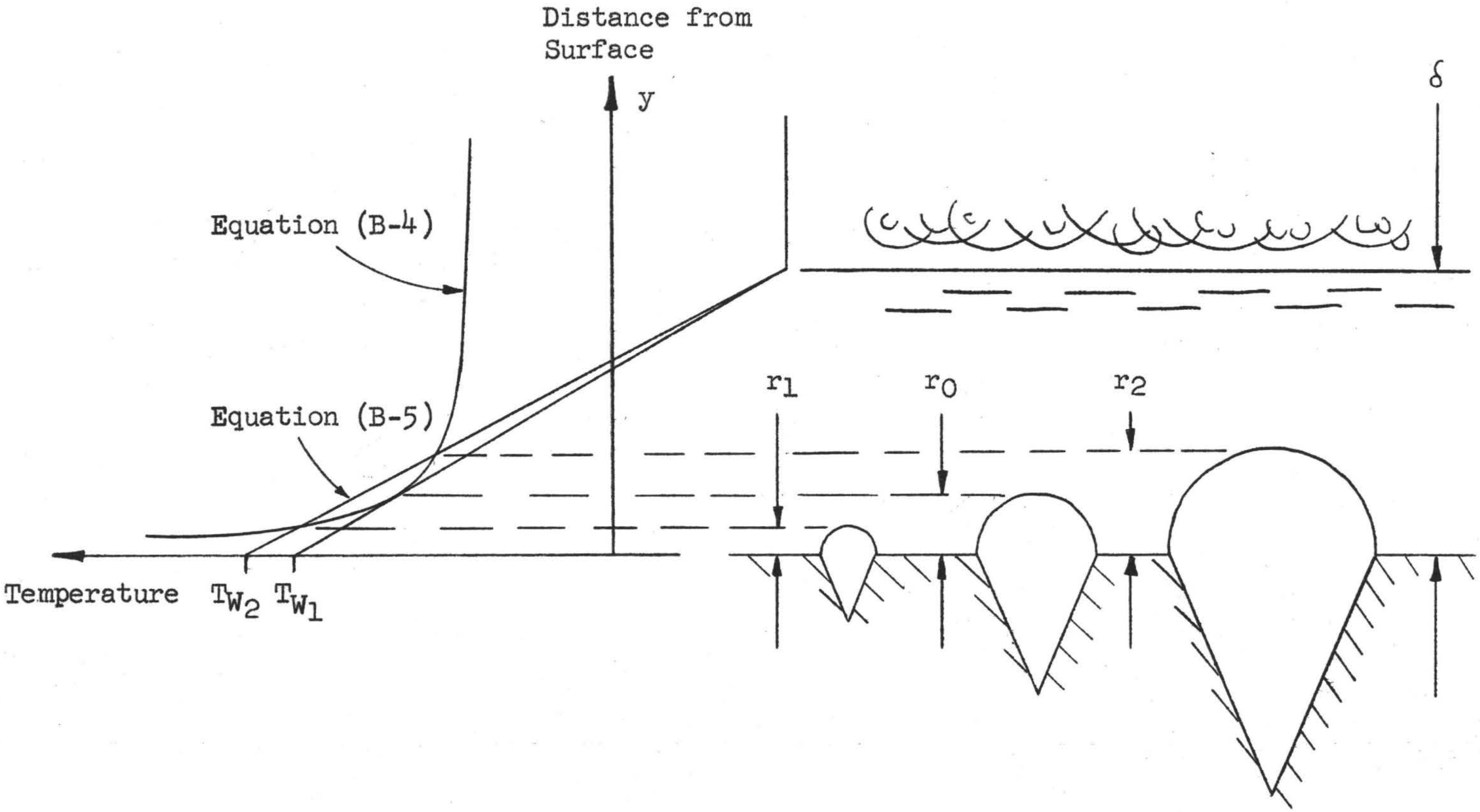

FIGURE 4

These considerations indicate that nucleation depends upon the physical properties of the liquid and solid, the cavity geometry and the thermal boundary layer thickness; the latter being dependent upon the hydrodynamic condition near the nucleating site.

Measurements have shown that the population of nucleating sites increases with surface temperature. At low heat fluxes the nucleating sites have been counted visually. For high heat fluxes Gaertner and Westwater (G3) devised an electroplating technique, which has shown that the nucleating sites are randomly spaced on the heating surface, (G9).

At a given surface temperature the population of active nucleating sites also depends upon the size distribution of the cavities in the heating surface. It has been suggested (W4) that boiling curves as shown in Figure 5 can be obtained for various surfaces. Curve A is the nucleate boiling curve for uniform large-sized cavities, while curve C is that for uniform small-sized cavities. The large slope of these two curves arises because all cavities will start nucleating at the same superheat. The superheat required for curve C will however be greater than for curve A, because of the smaller cavity size. Curve B relates to a surface with a range of cavity sizes and thus as the superheat is increased the corresponding cavities will start nucleating. Some of these considerations had already been established by Corty and Foust (C6), who performed experiments with boiling surfaces of different surface roughness.

Bubble growth

When the liquid has attained sufficient superheat, the vapour nucleus in the cavity grows into a bubble. The growth is the

EFFECT OF CAVITY SIZE DISTRIBUTION ON NUCLEATE BOILING CURVE

REF.: W4

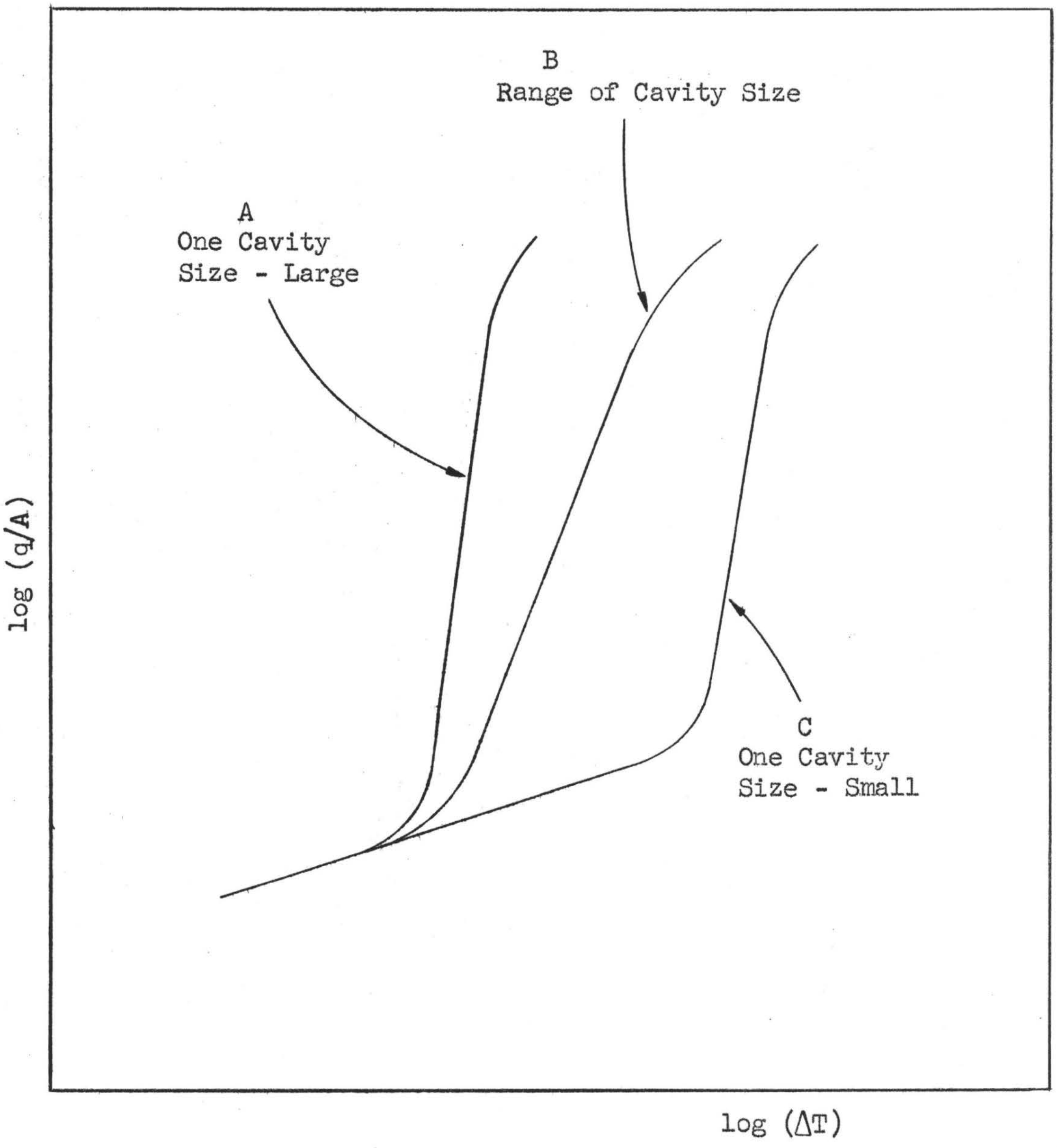

FIGURE 5

result of the evaporation from the liquid-vapour boundary. Thus heat flows from the surrounding superheated liquid to the bubble boundary, which is at a lower temperature. The growth of a vapour bubble is a dynamic process involving simultaneous heat and mass transfer.

Forster and Zuber (F2) combined the equation of motion of the bubble boundary with the transient heat conduction equation, to solve for the bubble growth in a uniform temperature field. The following equation was obtained

$$r = \frac{\pi C_L \rho_L \ (T_H - T_{sat})}{\lambda \quad \rho_V} \left(\frac{t}{\pi \alpha_L}\right)^{1/2} \qquad \text{(B-7)}$$

The controlling factor in the bubble growth was the heat transfer across an assumed thin liquid shell surrounding the bubble. The effects of surface tension and liquid inertia were found to be small.

The bubble growth is rapid during the initial stages and slow during the later ones. Such behaviour however cannot be fully portrayed by the constant time exponent of 1/2. A variable exponent permits much better agreement with experimental data. Zuber (Z3) and Griffith (G4) were able to predict the bubble growth rates much more accurately by including the effect of a non-uniform temperature field.

Bubble growth however is by no means a uniform process. In a microscopic study Strenge, Orrell and Westwater (S4) observed bubble growth rates at low heat fluxes and found considerable variations in growth rates and bubble emission frequency for a single nucleating site. The statistical nature of bubble generation and bubble growth has been attributed to turbulent liquid eddies (Z2).

The work by Moore and Mesler (M5) suggests that the growth of vapour bubble could largely be determined by the evaporation of a thin liquid film at the base of the bubble, (Figure 6). The thermal properties of the heating surface were shown to be significant in this transient conduction problem.

Bubble rise

When the radius of the bubble is about 0.05" the buoyant force becomes large enough to separate the bubble from the heating surface. The bubble departure is inhibited by surface tension forces at the triple interface and by inertia forces of the liquid. The bubble will be nearly spherical when limited by surface tension forces and ellipsoidal (with the major axis parallel to the heating surface) when limited by inertia forces of the liquid (R4). Since the bubble is situated in a non-uniform temperature field, the bubble experiences a surface tension gradient along the bubble boundary which holds the bubble to the heating surface.

It has been observed that at a single nucleating site the bubble departure diameter and the bubble frequency follow statistical distributions. For low heat fluxes the product of departure diameter and bubble frequency is constant and independent of the heat flux and nature of the liquid. For large heat fluxes the hydrodynamic condition of the liquid changes and this simple relation no longer holds, (Z4). The bubble size and frequency depend also upon the active nucleating site population immediately surrounding that bubble (G5).

Schlieren photographs by Hsu and Graham (H8) have shown the existence of the thermal boundary layer next to the heating surface. They observed that as a bubble departs, it carries away hot liquid

THIN FILM EVAPORATION

REF.: M5, K5

Low Heat Fluxes:

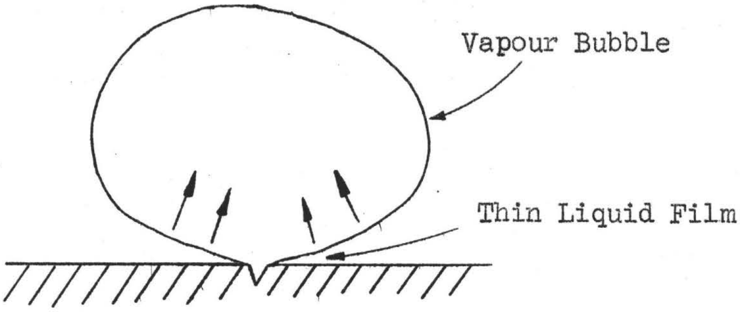

High Heat Fluxes:

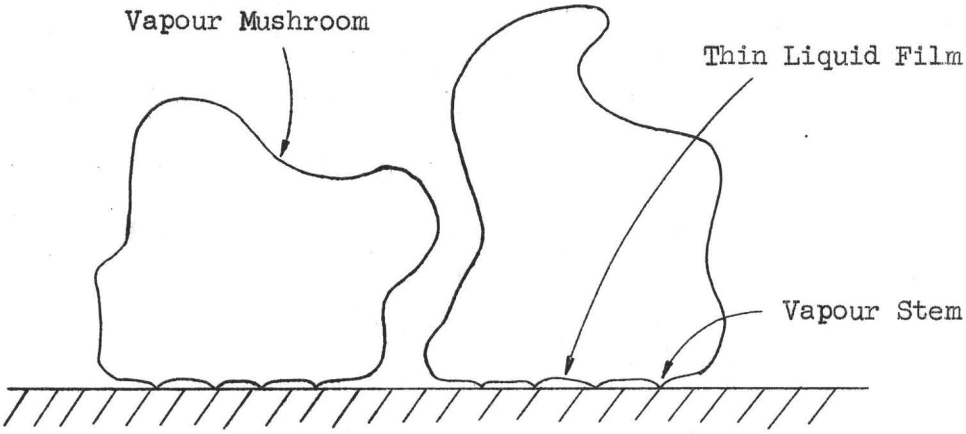

FIGURE 6

from the thermal boundary layer in a "region of influence" of size equal to twice the bubble diameter. During bubble rise the bubble is sourrounded by superheated liquid which causes further bubble growth.

Mechanisms of nucleate boiling

The multitude of the mechanisms proposed for nucleate boiling indicates the complexity of the process and the difficulty observers have in the interpretation of their data. Heat transfer can be considered to occur in two stages:

(i) heat transfer from the solid to the liquid in the thermal boundary layer (conduction and/or turbulent convection) and

(ii) heat transfer out of the thermal boundary layer.

The second stage can occur by the removal of either vapour (latent heat transport) or superheated liquid (enthalpy transport) from the thermal boundary layer.

It was originally perceived by many of the early workers that the motion of the vapour bubbles provided excellent agitation in the thermal boundary layer and thereby reduced the heat transfer resistance (F3). This mechanism has been supported by experiments in which vapour at saturation temperature was injected at the heating surface. The heat transfer was thereby increased in the lower heat flux region of nucleate boiling only.

Han (H9) has presented a mechanism for nucleate boiling in the region of isolated bubbles. By detailed examination of the processes of bubble nucleation, growth and departure, it has been possible to relate these to the boiling curve directly. The mechanism was based upon enthalpy and latent heat transport from the thermal boundary layer to the bulk of the liquid. Agreement with experimental data was satisfactory.

By comparing the heat transfer processes in dropwise condensation to those in nucleate boiling, Kast (K2) points to the similarities in nucleation and growth during the change in phase. Both processes are local transient ones, in which periodic removal of the new phase eliminates the heat transfer resistance it creates. The model considered latent heat transport from the thermal boundary layer, but neglected enthalpy transport as suggested by Hsu and Graham (H8).

Tien (T3) developed a hydrodynamic model for nucleate pool boiling in the region of isolated bubbles. The model asserted an inverted stagnation flow caused by the rising vapour bubbles. The vapour phase has been neglected, but its motion is considered to remove continually superheated liquid from the thermal boundary layer. Kutateladze (K3) has proposed a similar model by considering the stagnation flow of the liquid flowing towards the heating surface.

Zuber (Z4) emphasized the importance of the hydrodynamic factor in nucleate boiling and pointed out the similarities in the formation of gas bubbles from perforated plates. In the region of isolated bubbles the liquid flow could be idealized by source flow (displacement of superheated liquid from the thermal boundary layer by the growing bubble) and wake flow (entrainment of superheated liquid from the thermal boundary layer behind the rising bubble). The problem was then formulated as one of turbulent, natural convection from a horizontal heating surface. The limit of this mechanism occurred, when the hydrodynamic flow pattern changed and the bubbles interferred with each other vertically. A transition region occurs in which the heating surface is covered with vapour columns, vapour bubbles and vapour mushrooms. This transition probably accounts for the point of inflection observed in some boiling curves. Then follows the region of vapour mushrooms. The vapour mushrooms are fed with vapour from the heating surface through numerous thin vapour stems, (Figure 6). The vapour is most probably produced by continuous vaporization of a pulsating micro-layer of liquid at the base of the vapour stems, (Z4). At these high heat fluxes the dominant heat transfer mechanism appears to be latent heat transport, (R6).

Support for this micro-layer vaporization has been obtained experimentally by Moore and Mesler (M5), who have observed sudden temperature drops in the heating surface at a nucleating site. A local heat flux of almost 10^6 Btu/hr.sq.ft.has been observed for water boiling on a nichrome strip. The average heat flux under those conditions was however only 200,000 Btu/hr.sq.ft. A photographic examination by Rogers and Mesler (R3) showed that the large temperature drop occurred during bubble growth and that the surface temperature recovered during bubble departure. Further evidence has been supplied by Hospeti and Mesler (H11), who measured the scale deposited at the base of vapour bubbles in nucleate pool boiling of calcium sulphate solutions. The use of radioactive calcium sulphate permitted the evaluation of the micro-layer thickness. Their results were in agreement with measurements of Moore and Mesler (M5).

A detailed photographic study by Gaertner (G5) supports the above considerations of the nucleate boiling regions. He also observed the existence of another region, which occurs when the slope of the nucleate boiling curve decreases sharply, (Figure 1). It has been suggested that one call this point the departure from nucleate boiling DNB. In this region the vapour stems under the mushrooms collapse and local vapour patches are formed. A photographic study by Kirby and Westwater (K5) has shown the existence of dry areas (vapour patches) on the heating surface. Such vapour patches would result in local film boiling and thus show a much reduced heat transfer rate. The number of active nucleating sites could no longer be determined accurately, indicating that the nucleating sites were not active continuously (G3). The surface temperature has been observed to make large excursions in this region (L3). As the surface temperature is increased the number of vapour patches increases and the flow of liquid towards the heating surface becomes restricted.

Such a restriction of liquid flow by the vapour leads to a two-phase flow instability. The situation has been idealized by Zuber (Z5) and Moissis and Berenson (M6) by considering vertical flow of rising vapour jets and falling liquid jets. The maximum heat flux was assumed to be the result of the onset of the Kelvin-Helmholtz hydrodynamic instability of the interface between the counter-flowing columns of vapour and liquid. When instability occurs the liquid columns begin to interact with each other and trap large amounts of vapour at the heating surface. At the same time the liquid flow towards the heating surface is considerably reduced. Markels and Durfee (M7) and Donald and Haslam (D3) have shown with electrical resistance measurements that at the maximum heat flux about 50% of the heat transfer area is covered with vapour.

According to the above model the maximum heat flux is governed entirely by a hydrodynamic situation and should be independent of the heating surface condition and surface temperature. Berenson (B8) was able to verify this by changing the surface finish of the heating surface. Increased roughness of the heating surface resulted in decreased surface temperatures at the same maximum heat flux.

It has been shown by Costello et al (C7) that the maximum heat flux is affected by the hydrodynamic condition near the heating surface and by the surface condition of the heater. Their experiments indicated that enhanced liquid flow towards the heating surface from the sides increased the maximum heat flux. Such an increase was also observed when the heating surface was treated with materials (surface deposits) which increased the wetting. On the other hand Gaertner (G5) treated the heating surface with materials which decreased the wetting. His experiments demonstrated that thereby the maximum heat flux was decreased. It appears that the maximum heat flux is not governed solely by a hydrodynamic instability. Kirby and Westwater (K5) have suggested that the burn-out mechanism may be due to an increasing number of dry patches on the heating surface. The problem is a dynamic one because of the continual alternation between formation of dry patches and rewetting by the liquid. The stability of these vapour patches probably depends upon the hydrodynamic condition surrounding that patch, while the extent of the rewetting of the liquid on the dry area beneath the vapour patch depends upon the thermal conductivity of the solid and the liquid, the contact angle and the thermal capacity of the heater.

1.3 Transition Boiling

At surface temperatures exceeding those necessary for the maximum heat flux the vapour forms a very unstable vapour film over the heating surface. Liquid frequently penetrates the vapour film and contacts the surface at certain localities. Since part of the heating surface is covered with vapour, the local heat flux during contact must be much higher than the average heat flux over the entire heating surface. During such contacts the liquid becomes superheated and vaporizes explosively. The vapour film is then reformed locally. This process repeats itself at a rapid rate and can easily be identified by the noise of the explosions.

At increasing surface temperatures the increased conduction through the vapour film leads to an increase in the evaporation at the liquid-vapour interface. This evaporation exerts a stabilizing effect on the vapour film by preventing liquid-solid contact, (B9). The contact frequency and heat flux thus decrease with increasing surface temperature, until no further liquid-solid contact occurs at the position of the minimum heat flux. Although the vapour generation near the maximum heat flux is much larger than at the minimum heat flux, the vapour film is not stabilized thereby.

By electrical resistance measurements Markels and Durfee (M7) have shown that solid-liquid contact occurs over the whole transition boiling regime. They also suggest a relation between the wetted area per contact and the heat flux.

Berenson (B8) has obtained data for n-pentane in transition pool boiling. It was observed that solid-liquid contact occurred and that the surface roughness decreased the heat flux at a given surface temperature. The addition of surface active agents, which improved the wetting of the liquid during contact with the heating surface, resulted in an increase in heat flux.

On the basis of these findings Bankoff and Mehra (B10) developed a quenching theory, which postulates that the heat transfer occurs by periodic quenching of the heating surface. The heat transfer process during solid-liquid contact was considered to be transient conduction. Using Berenson's data it was shown that the heat flow per contact remained constant with surface temperature, but that the contact time decreased with increasing surface temperature. The contact frequency was determined from hydrodynamic considerations as proposed by Zuber and Tribus (Z6).

Because of the inverse heat flux-surface temperature relationship in the transition boiling regime, stable conditions in this regime can only be obtained by using a heating system that operates at a constant temperature difference (condensing steam). Electric heaters operate at constant heat flux and the boiling may easily change to nucleate or film boiling. The operating temperature in film boiling usually causes melting (burn-out) of the electric heater.

1.4 Film Boiling

In film boiling the heating surface is surrounded by a very stable vapour film. Such an arrangement is hydrodynamically unstable (Rayleigh-Taylor instability), but the inversion of the phases is prevented by the heat transfer process. The heat transfer across the vapour film occurs by conduction and radiation; the contribution by convection is usually small. The vapour is generated entirely at the vapour-liquid interface. Since there is no solid-liquid contact the nature of the heating surface has little effect on the heat transfer. The film boiling curves for most liquids, including cryogenics, are very similar.

The vapour-liquid interface oscillates and regularly discharges vapour bubbles into the liquid. The bubbles, which are umbrella shaped, are normally much larger than those in nucleate boiling. Photographic studies have shown that vapour bubbles are discharged simultaneously at certain distances between bubbles, (W3).

At temperature differences greater than 1000°F heat transfer by radiation becomes significant. Radiation may affect the temperature distribution in the vapour film by absorption and emission by the vapour. The simple supposition of conduction and radiation heat transfer is then no longer permissible. Sparrow (S5) has shown, however, that vapour participation in radiation heat transfer at low pressures is negligible.

Because film boiling is such a steady process, it was the first regime to be attacked theoretically. A similarity between film condensation and film boiling was apparent and Bromley (B11) presented a derivation for film boiling outside a horizontal tube. A force and heat balance for an element of vapour yielded an expression for the conduction heat transfer coefficient. It was shown experimentally that the supposition of conduction and radiation was correct.

The minimum heat flux condition is best approached from the stable film boiling regime. At decreasing surface temperatures the vapour-liquid interface becomes more wavy. The wave amplitude grows and eventually the wave-crests contact the heating surface. It was polstulated by Zuber (Z5) that the minimum heat flux was governed by the onset of the Rayleigh-Taylor instability. The wave which has the maximum growth rate determines the hydrodynamic transition and its wavelength is called the dominant wavelength.

Using Zuber's equations and the law of corresponding states Lienhard and Schrock (L4) were able to show a thermodynamic similarity between the maximum and minimum heat flux, both of which are essentially governed by hydrodynamic considerations. The instability theories (Kelvin-Helmholtz and Rayleigh-Taylor) apply to hydrodynamic transitions and thus give only two point values on the boiling curve.

Berenson (B12) applied the Taylor instability theory to the film boiling regime in order to obtain the bubble spacing and thus determine the heat transfer coefficient. Hosler and Westwater (H10) have conducted film boiling experiments on a horizontal plate and obtained good agreement with Berenson's equation. The average distance between rising vapour bubbles was found to be the dominant wavelength as was predicted by the model of Berenson.

The Leidenfrost phenomenon occurs when a drop of liquid rests on a heating surface without contacting it. The liquid drop is supported by a thin vapour film, which is maintained by evaporation from the lower surface of the drop. The temperature difference between the liquid drop and the heating surface corresponds to the film boiling regime. The heat transfer to small and large spheroids in film boiling was examined by Borishansky (B13).

1.5 Factors Affecting Boiling

The shape of the boiling curve depends upon a variety of factors, some of which will be discussed below. The following approximate figures are given in Table 1.

TABLE 1

	$(q/A)_{max}$ BTU/hr.sq.ft.	ΔT_{max} °F	$(q/A)_{min}$ BTU/hr.sq.ft.	ΔT_{min} °F
Water	450,000	80	15,000	250
Organics	150,000	80	10,000	180

Solid-liquid combination

Since nucleate and transition boiling are governed by local transient conduction the thermal conductivity of the solid and the liquid are of importance. Experiments have indicated that copper and water give the best heat transfer, provided other conditions are not changed.

In nucleate boiling, surface tension affects the nucleation process and the bubble growth during the initial stages. Jontz and Myers (J3) have shown experimentally that a decrease in surface tension increased the heat flux. Roll and Myers (R4) extended the model proposed by Hsu (H7) to show that a decrease in surface tension resulted in an increase in bubble emission frequency and that boiling was initiated at a lower superheat. Since surface tension has a stabilizing effect on the vapour-liquid interface, the hydrodynamic transitions occurring at the maximum and minimum heat flux are affected by a change in surface tension.

Exact knowledge of the dynamic behaviour of the triple interface does not appear to be available from the literature. It would be of great value to have more information on interfacial surface tensions, contact angles and wetting effects. Work has however been done which detected a thin liquid film adjacent to the heating surface, (M5), (H12), (K5), (G8). The experiments support the no-slip condition, which states that the growing bubble cannot displace the liquid directly in contact with the heating surface. A thin liquid film is thus formed beneath the bubble. The rapid vaporization of such a film can cause large local heat fluxes.

Another property which affects the bubble nucleation and bubble growth is the latent heat of vaporization. A choice of a liquid fixes four significant properties (viz, thermal conductivity, surface tension, contact angle and latent heat of vaporization) and it becomes experimentally difficult to estimate the importance of a single one.

Surface conditions

In nucleate boiling the surface condition can significantly alter the slope and intercept of the boiling curve. It was observed by Courty and Foust (C6) that a rough surface yielded larger boiling heat fluxes than a smooth surface at the same temperature difference. The effect was attributed to different cavity size distributions, which affected the surface nucleation. These aspects have already been discussed above.

By treating the heating surface with non-wettable materials the boiling phenomena can be altered significantly. Young and Hummel (Y2) have treated the heating surface with small teflon spots, which served as effective nucleating sites. The surface temperature for boiling in the region of isolated bubbles was reduced and the bubble size at departure was increased. Gaertner (G5) treated the heating surface with thin layers of teflon or silicon grease. During boiling large-sized bubbles were generated, which coalesced and formed a continuous vapour blanket on the heating surface. The transition to film boiling (maximum heat flux) occurred at a much lower heat flux. Similar hydrodynamic behaviour has been observed by boiling at low pressure or at zero gravity.

Impurities in the liquid are deposited on the heating surface. If the deposit is very thin, it may produce effective nucleation sites and improve the heat transfer. For thicker deposits however the temperature drop across the deposit decreases the effective wall temperature. Such a coating on a hot surface can be used to advantage by encouraging a rapid transition from film to nucleate boiling, (C11). A low thermal conductivity material which also has good wetting properties (sodium silicate) is applied in thin layers to the heating surface. Due to the low thermal conductivity, the thin layer rapidly attains a surface temperature corresponding to nucleate boiling. The quenching of metal objects thus occurs much more rapidly.

When a liquid, which contains dissolved gases, is heated gas bubbles are formed at the heating surface. These gas bubbles can then displace liquid from the cavities in the heating surface. As discussed earlier very effective nucleation sites are thus formed. The boiling of such a liquid is an unsteady-state process until all the gas is depleted.

Wayner and Kesten (W6) investigated saturated pool boiling of water using a porous heat source. The generated vapour was withdrawn through the pores instead of rising through the bulk liquid. Heat fluxes corresponding to those of the isolated bubble regime were obtained at much lower surface temperatures.

In the film boiling regime the surface characteristics are not significant except that the emissivity affects the rate of radiant heat transfer. The film boiling heat transfer can be significantly improved by using a porous heating surface through which the vapour is withdrawn, (W5).

Effect of forced convection on boiling

For saturated boiling forced convection has little effect on the nucleate boiling curve (Figure 2). Boiling seems to be the dominant mechanism. The superheat required for the initiation of boiling however is increased. This effect can be predicted by the model of Hsu (H7). The maximum heat flux is increased, which could be due to enhanced vapour removal from the heating surface.

Boiling inside a heated tube leads to two-phase flow as shown in Figure 12. The flow patterns depend upon a variety of factors such as heat flux, liquid temperature and flow rate. The different heat transfer mechanisms along the tube are discussed below. Most attention has been paid to the burn-out problem, which appears to depend upon the hydrodynamic stability of a thin liquid film adjacent to the tube wall (T2). The burn-out for boiling outside a tube with the liquid flow parallel to the tube is determined by similar hydrodynamic criteria.

For boiling of a liquid, which is flowing normal to a heated tube the flow conditions are quite different to those described above. Vliet and Leppert (V1) observed the presence of a vapour cavity and a thin liquid film at the back of the tube. The depletion of this liquid film caused by evaporation leads to local burn-out.

Effect of subcooling on boiling

Subcooling of the liquid causes the vapour bubbles, which are generated at the heating surface, to collapse in the bulk of the liquid. At large subcooling the vapour bubbles collapse on the heating surface itself. The hydrodynamic situation as compared to saturated nucleate boiling is different, because bubble rise and vapour columns are absent. The processes occurring directly on the heating surface, i.e. nucleation, bubble growth and latent heat transport are common to both subcooled and saturated nucleate boiling.

For steady-state subcooled boiling, a flow system is required and thus the factor of forced convection is always included in the boiling curve. The initiation of subcooled boiling occurs at a larger superheat, but once boiling is fully established subcooling has little effect on the boiling curve, (Figure 3). However, the maximum heat flux is considerably increased as shown in Figure 7. The maximum heat flux is probably determined by vapour bubble coalescence, because the bubble population on the heating surface is extremely high under those conditions.

Gunther (G6) studied subcooled boiling of water flowing parallel to a horizontal strip. Measurements of the burn-out heat flux, bubble population and bubble size were made at different pressures. The bubble size was found to be less, while the bubble population was greater than in nucleate boiling. The bubbles were almost hemispherical in shape and grew and collapsed in a rapid cycle. An analysis of bubble growth and collapse has been made successfully by Zuber (Z3) and Hsu and Graham (H8).

EFFECT OF FORCED CONVECTION AND SUBCOOLING ON THE MAXIMUM HEAT FLUX OF WATER

REF.: G6

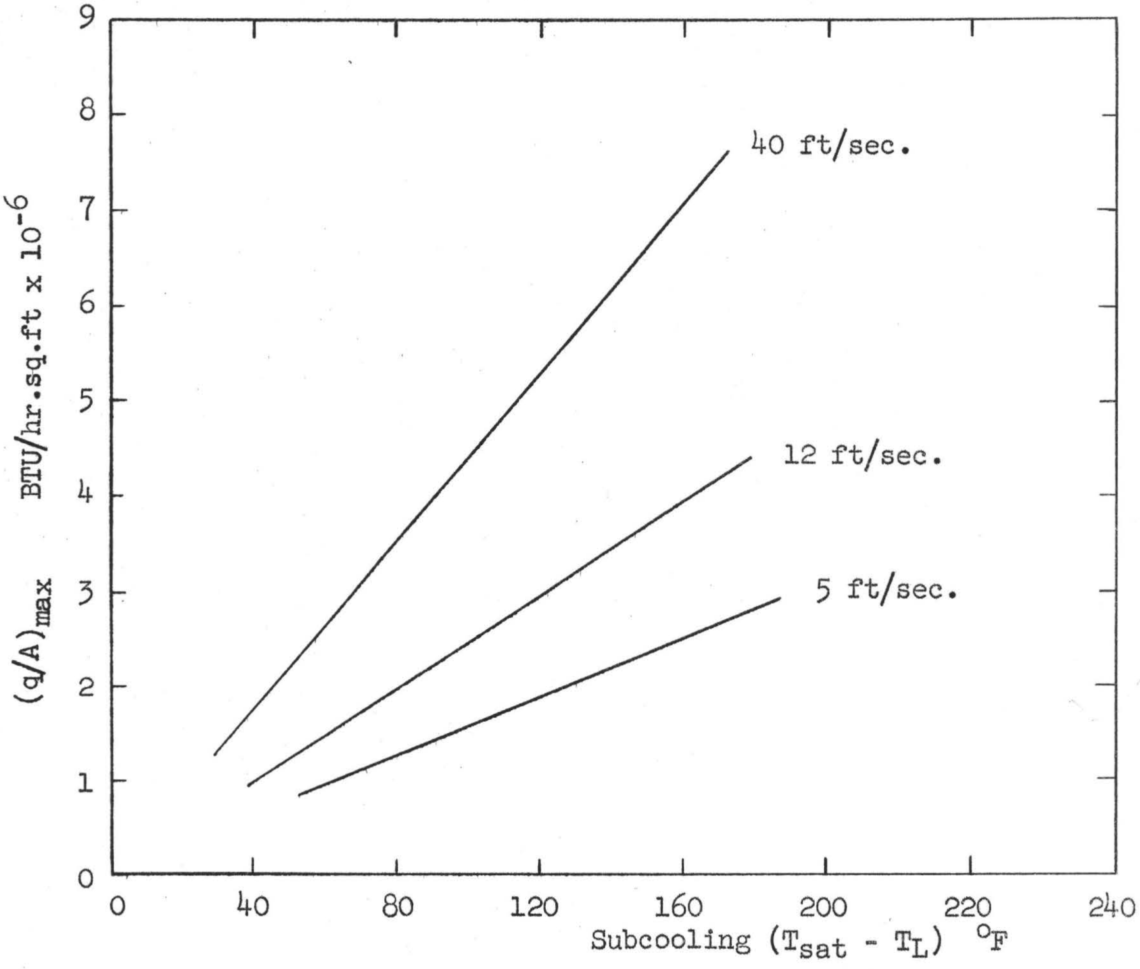

FIGURE 7

Shadowgraphs by Gunther (G6) indicated that the thermal boundary layer was continually disturbed by the vapour bubbles, thus providing strong micro-convection in that layer. At that time this mechanism was considered to account for the large heat fluxes of 10,000,000 BTU/hr.sq.ft. at burn-out. Rohsenow and Clark (R5) came to the same conclusion after showing that the latent heat carried by the vapour bubbles is relatively small.

Forster and Greif (F4) suggested that the growing bubbles displace the superheated liquid into the cold bulk of the liquid. After collapse the place of the vapour will be occupied by cooler liquid, which becomes superheated before nucleation occurs again. Thus a pumping action results in the thermal boundary layer, such that the heat flux is relatively unaffected by the level of subcooling or forced convection.

Bankoff (B14) observed very high condensation heat transfer rates to single bubbles growing in subcooled water. It was concluded that mass transfer (latent heat transport) across the bubble by evaporation at the bubble base and condensation at the bubble top was dominant at high heat fluxes. Bankoff's work is therefore complementary to the work by Moore and Mesler (M5). The heat transfer appears to be a two-stage process of thin film evaporation and subsequent condensation. An increase in subcooling or forced convection will essentially affect the rate of condensation resulting in a reduction of the maximum bubble size and bubble life as observed by Gunther (G6).

In the transition and film boiling regimes the heat transfer has been observed to increase significantly with subcooling (M8). A theoretical analysis of subcooled film boiling has been made by Cess and

Sparrow (C10), (S6).

Geometry and orientation

The geometry of the heater determines its thermal capacity and influences the hydrodynamic flow patterns in the liquid.

If the heating wire is less than the maximum bubble size, coalescence of vapour bubbles can easily occur. The wire then becomes locally insulated by the vapour and because of its low thermal capacity rapidly overheats at constant heat-flux operation. A low maximum heat flux can be obtained and the curvature of the boiling curve at the maximum heat flux can be significantly changed. Electric heaters with a large thermal capacity can be considered as operating at constant temperature, (H7), (G5).

The liquid flow patterns on a horizontal plane surface differ from those from a tube and could affect the boiling curve near the maximum heat flux (C9).

The orientation of a plane heating surface in the gravitational field has a significant effect on the nucleate boiling heat transfer. The heat transfer in the region of isolated bubbles is largest for a vertical heating surface and smallest for a surface facing downwards (G7), the difference being probably due to bubble motion in the thermal boundary layer.

In film boiling a horizontal plane surface yields about the same heat flux as a small vertical surface at the same surface temperature. In both conditions the flow in the vapour film is considered to be laminar. A tall vertical plane surface, however, allows a larger heat flux due to turbulent convection in the vapour film, (H13).

2. Liquid Film Flow

2.1 Introduction

Because of the improved heat and mass transfer, much attention has been given to thin film flow over the last 50 years.

The studies were usually restricted to two-dimensional flows by considering film flow inside and outside of vertical tubes and also on inclined planes. The effect of a stationary gas phase is negligible and thus is omitted from these studies. The surface of the liquid film is usually disturbed by waves and ripples, which make an exact study of the flow difficult.

The flow of liquid films is characterized by a relation between the film Reynolds number (Re) and a dimensionless film thickness (N_T), (Figure 8). Depending upon the Reynolds number three regimes of flow can be identified:

(i) smooth-laminar flow

(ii) wavy-laminar flow

(iii) turbulent flow

The transition to wavy-laminar flow occurs at Re = 10. For inclined planes, the angle of inclination has an effect on this transition. The transition to turbulent flow occurs at Re = 400. The flow is considered to be fully turbulent at Re > 800.

The disturbances in the liquid film are characterized by the Froude and Weber numbers, which determine the onset of waviness and the wave properties.

An extensive review of thin liquid flow has been presented by Fulford (F1).

LIQUID FILM THICKNESS AGAINST FILM REYNOLDS NUMBER

REF.: F1

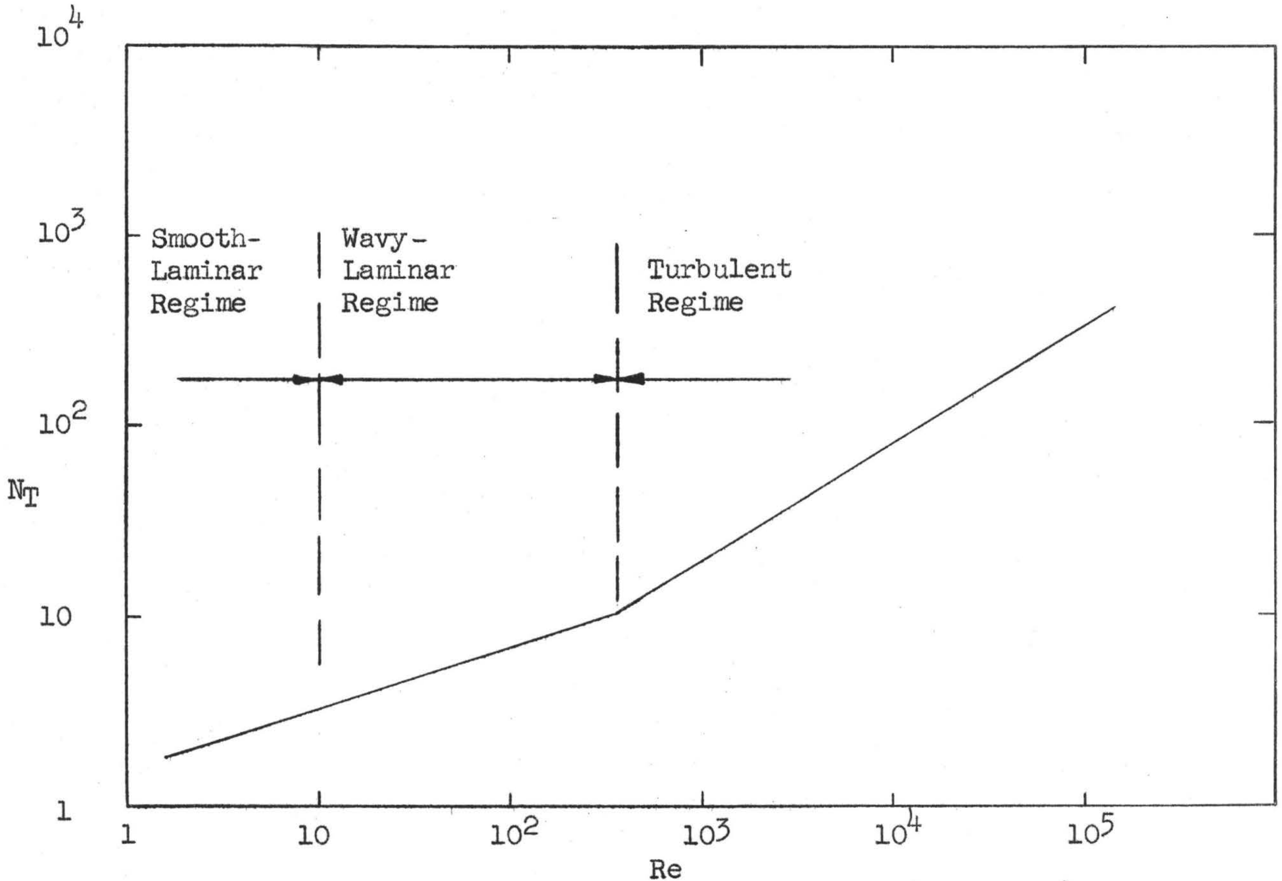

$$Re = \frac{\bar{u} b \rho_L}{\mu_L} = \frac{G}{\mu_L} \qquad N_T = b \left[\frac{g \sin\theta \ \rho_L^{\,2}}{\mu_L^{\,2}} \right]^{1/3}$$

FIGURE 8

2.2 Laminar Film Flow

In the laminar flow regimes the film flow is essentially streamline. In the smooth-laminar regime the surface of the film is smooth and without any disturbances. In the wavy-laminar regime the surface is disturbed by waves, which however do not disturb the streamline flow. Using Poiseuille flow Nusselt derived the equation for smooth-laminar flow. It has been shown experimentally, that this theory can be applied up to Re = 300. Wavy-laminar flow has been examined by Kapitza (L1) and it was shown that, for a first approximation, the waves do not affect the mean film thickness.

At low liquid flow rates regular waves occur, while higher flow-rates cause roll waves, which have a steep front and a sloping back. It is observed that if the Weber number (We) is greater than 1.0, capillary waves (short wavelength) are formed. If the Froude number (Fr) is greater than 1.5, gravity waves (long wavelength) are formed. The wave velocity is usually greater than the surface velocity of the film.

For very thin liquid films the capillary (surface tension) forces play an important part in the flow pattern, since they have about the same magnitude as the viscous forces. Uniform wetting of the solid surface becomes difficult and dry patches easily form.

2.3 Turbulent Film Flow

The turbulent flow is initiated at the break in the curve of Figure 8. Although the turbulent film is usually very rippled, the theoretical treatments assume a smooth turbulent film. Dukler and Bergelin (D1) have applied Nikuradse's universal velocity profile to thin film flow. The film is divided into a sublaminar layer, a buffer layer and a turbulent layer. The dimensionless velocity is a unique function of the dimensionless distance from the wall. The theory covered the laminar and turbulent flow regime and predicted the transition and film thickness fairly well.

Levich (L1) has pointed out that the velocity component of the eddy velocity in a direction perpendicular to the interface must vanish. Hence the turbulence is damped in the vicinity of the free surface by forces opposing that component. The turbulence damping is said to be caused by surface tension, which prevents the turbulence eddies from splashing through the liquid surface.

2.4 Factors Affecting Film Flow

The behaviour of the liquid film can be altered by effects such as parallel gas flows, surface active agents and surface waves. The effects of hydrodynamic and thermal instabilities on the liquid film flow will be discussed separately.

Entry zone

When a liquid film is formed on an inclined plane a smooth region exists before surface waves appear. The length of this region depends upon the liquid flow rate, the parallel gas flow rate and the flow-entry conditions. The length of the smooth region increases with the liquid flow rate. It has been observed that the length of the smooth region coincides with the position where the boundary layer thickness equals the film thickness. A cocurrent or countercurrent gas flow decreases the length of the smooth entry region considerably.

In the smooth entry zone the liquid film thickness is usually larger than in fully established flow.

Parallel gas flows

A gas flow, either cocurrent or countercurrent, parallel to the liquid film usually introduces an interfacial shear. In general it is found that for all flow regimes the film thickness decreases with increasing cocurrent flow and increases with increasing countercurrent flow. In a turbulent liquid film, the film thickness is not affected at low gas flow rates. Dukler (D2) has presented an analysis of the velocity distribution in cocurrent downward flow. The model considered turbulence near the wall and showed that the dimensionless velocity was dependent upon the dimensionless distance from the wall and upon a parameter involving the interfacial shear. Agreement with data was good.

Surface waves

When a horizontal liquid interface is subjected to random disturbances the interface becomes locally displaced and is no longer in equilibrium. The surface energy and potential energy are a minimum for a plane surface. Thus the restoring forces are surface tension and gravity for horizontal film flow, and only surface tension for vertical film flow. Because of inertia the liquid particles at the displaced interface overshoot the equilibrium position and surface waves are produced. If no damping is present these oscillations continue indefinitely. The viscosity of the liquid has a damping effect on the waves by dissipating energy into heat. Waves of small wavelength are damped more rapidly by viscosity than those of long wavelength. The presence of a wall also causes some damping; the thinner the liquid film the greater is the effect of the walls on the damping of the waves.

To maintain a wave in a viscous liquid, the energy that is dissipated by the wave-motion must be continually supplied to the liquid. This can occur by energy transference from a parallel gas stream or by loss of potential energy in gravity flow. If the energy transfer exceeds that of dissipation the waves grow, leading to spray formation at the wave-crests. The flow instabilities leading to wave-formation and wave destruction will be considered below.

Surface-active agents

Experiments have shown that surface waves are damped by surface-active agents. This has been predicted theoretically by Levich (L1), (W1). The change in surface tension itself does not cause damping. The surface-active material produces a film on the liquid surface which is subjected to stretching. A change in concentration of the surface-active material at the liquid surface results in a tangential surface-tension force, which stabilizes the interfacial motion. The liquid surface is said to exhibit surface elasticity. Only capillary waves, however, are affected by surface-active materials. This applies to soluble and insoluble surface-active agents. For soluble ones it is assumed that the diffusion is slow compared to the rate of surface deformation. If the concentration of the surface-active material is high, however, the change in concentration due to surface deformation becomes small and the damping effect is reduced again. This has been observed experimentally.

3. Hydrodynamic Instabilities of Liquid Films

A liquid film becomes hydrodynamically unstable when its flow pattern changes (O1). The onset of the transition to another type of flow is of importance in equipment design and theories have been developed to predict the transition. A linearized perturbation theory is usually used, which predicts the onset of the transition, but which yields no information about the new flow pattern. The theory considers small disturbances with exponential time growths in two-dimensional models.

A flow however may be metastable in that the instability has not been triggered, i.e. there are no small disturbances in the flow. No exact knowledge of the triggering mechanism appears to be available, except that it can be internal or external of the flow. This trigger effect could account for some of the discrepancy between the predicted and experimentally determined values for the onset of the transition. The behaviour of the smooth entry zone with respect to a parallel gas flow and the stability of the liquid flow on a vertical plate (T1) (B1) should be noted here.

Some of the instabilities in thin film flow will be mentioned below. The effect of heat transfer on the stability of liquid films is discussed in a later section.

3.1 Tollmien-Schlichting Instability

The flow of a homogeneous fluid at low flow-rates and for a particular geometry can be considered streamline. The liquid under those conditions can sustain the imposed shear stress. At a certain larger flow rate and when small disturbances are present in the liquid, the shear stress becomes larger than that which can be sustained by viscosity. The disturbances are then selectively damped or amplified in the boundary layer and produce a travelling wave. When these waves grow, the flow becomes unstable and transition to turbulent flow occurs. This transition has been described by the Tollmien-Schlichting instability (S1) (R1) and is characterized by the Reynolds Number.

The mean flow (laminar) with the superimposed disturbances is assumed to obey the Navier-Stokes equations, which simplify to the Orr-Sommerfeld equation (S1). The Orr-Sommerfeld equation thus describes the transition and an analysis has shown that the velocity profile in the boundary layer is of prime importance in determining stability.

Heat transfer to a fluid changes the velocity profile and Schlichting (S1) postulates that heating of a liquid would render the flow more stable.

3.2 Gravity Flow

An instability in thin film flow arises when it is subjected to gravity flow on an inclined plane. Benjamin (B1) has examined this case for laminar flow, where the instability leads to surface waves. The analysis is also based on the Orr-Sommerfeld equation. It is shown that the flow on a vertical plate is always unstable. Smooth films have been observed however and Benjamin explains this by the great length of the liquid film that is required for the amplification of the waves.

Tailby and Portalski (T1), who extended the theory of Kapitza (L1), predict stability below a certain liquid flow rate on a vertical plate. They have confirmed this with experimental data. Their theory is based upon an integral solution of the Navier-Stokes equation upon which small perturbations are superposed.

3.3 Parallel Gas Flow

An instability of a horizontal liquid film occurs, when a gas stream passes parallel over it. The shear at the interface leads to crinkling and wave formation. Various models dealing with uniform flows have been proposed, of which the Kelvin-Helmholtz model is one.

A perturbation approach is commonly used leading to the Orr-Sommerfeld equation. The models differ in their assumptions of the boundary conditions.

In the Kelvin-Helmholtz model (C1) the plane interface is found to be unstable for any velocity difference between the film and the gas. An energy transfer across the interface due to the shearing action accounts for the Kelvin-Helmholtz instability. The energy supplied must be sufficient to overcome the inertia and the surface tension in the plane interface, since the viscosity is being neglected. Thus a criterion is established for the onset of the Kelvin-Helmholtz instability which is characterized by the Richardson number (J). Surface tension has a stabilizing effect on this instability. If the film is very thin, the shear in the liquid is no longer negligible and work must be done against viscosity. The wall thus has a stabilizing effect.

Miles (M1) considers the Kelvin-Helmholtz instability as a static instability in which the shear produces disturbances that are in phase with the displacement of the film surface. Miles (M2) has proposed a model for liquid films in Couette flow, in which only those waves for which the wave speed is equal to the mean flow speed of the cocurrent gas, can absorb energy from the gas stream. Thus the disturbances in phase with the slope of the waves are considered as leading to instability. The component of the disturbance in phase with the slope of the wave is much more effective for a relatively inviscid fluid like water than for a very viscous fluid like oil, whereas static instability appears as the more efficient mechanism for the viscous fluid. Miles (M1) concludes that the Kelvin-Helmholtz instability is not responsible for the initial formation of water waves.

The models are simplified by not taking account of the full interaction between the gas and liquid flow, i.e. the effect of waves on gas velocity profile. Benjamin (B2) has described some of the more complicated models.

At the present time experiments have not shown clearly what model of instability can be observed, (K1), (H1), (O1), (C14).

At large gas flow rates the wavy flow becomes unstable; large disturbance waves are formed which travel rapidly along the surface of the liquid film. The waves have a milky appearance due to a very ruffled surface. The wave amplitude is usually sufficiently large to cause a break-up of the wave-crests into liquid drops. Thus entrainment into the gas stream results (N2). A thin substrate of film remains attached to the wall, while most of the liquid moves in the waves. It appears that the substrate is just able to sustain the shear due to the gas flow, (A1).

The onset of these conditions is of importance in determining equipment size. The perturbation theories have been extended by Ostrach and Koestel (O1) and also by Zuber (Z1), although it is realized that they only apply to small wave amplitudes. Little is known about the energy and momentum transfer between the gas and the liquid at large wave amplitudes. The form drag on the waves must also be considered. At present the onset of entrainment from the wave-crests is determined experimentally.

Entrainment is well known in annular two-phase flow, but insufficient data are available. A critical review of the knowledge in this field has been given by Acrivos (A1). Observation by Collier and

Hewitt (C2) showed that the liquid entrainment increases with liquid and gas flow rate as would be expected. At large total water flow rates, the liquid film thickness and film flow rate were observed to be independent of the total water flow rate and decreased with increasing gas flow rate. An increase in the total water flow rate resulted in an increase in entrainment while the liquid film flow rate remained constant. In two-phase flow two mechanisms of liquid transfer occur: the entrainment of drops from the liquid film and the droplet deposition from the gas core. The interchange of liquid is very rapid.

3.4 Gravity Flow with Parallel Gas Flow

This is an extension of the two cases discussed above. The instability is due to two factors; gas flow and gravity flow and easily leads to formation of roll waves with long wavelengths. Hanratty and Hershman (H2) have examined this instability for a turbulent gas. Integral mass and momentum balances for the combined gas and liquid flows were used together with superposed small disturbances. The results were in agreement with experiments and compared well with the Benjamin model, if the gas flow was zero.

3.5 Rayleigh-Taylor Instability

Another type of instability occurs when two fluids of different density (gas and liquid) are in contact and an acceleration is directed from the dense to the less dense fluid. The denser fluid thus tends to displace the less dense fluid. The instability of the plane interface between the two fluids is called Rayleigh-Taylor instability.

The mathematical analysis based on small disturbances is presented by Chandrasekhar (C1) for various properties of the fluids.

Surface tension and viscosity have small stabilizing effects by influencing only certain wavelengths. If the effects of surface tension and viscosity are neglected, the arrangement is always unstable. Again the stability theory only applies to small disturbances and cannot be applied to the large amplitudes observed by Emmons et al (E1). They have obtained some data for the disintegration of liquid spikes, which may have some relevance to the entrainment from wave crests.

4. Heat Transfer to Liquid Films

It has been known for a long time that the heat transfer rate to liquid films is greater than that for full pipe flow. Much work has been done on liquid film heat transfer in the thirties, but attention has essentially been focussed on overall heat transfer coefficients. The study of local heat transfer coefficients however leads to a much better understanding of the processes involved.

4.1 Stationary Liquid Films

Heidrich (H14) has investigated the evaporation without boiling from superheated water. The observed mass flux corresponded to a heat flux of 6,000 BTU/hr.sq.ft for an average superheat of 16°F.

Jakob and Linke (J1) and Yamagata et al (Y1) have observed that the heat transfer coefficient for nucleate boiling from a horizontal plate increased with decreasing liquid depth, (Figure 9). The liquid thickness approached the thickness of the thermal boundary layer described by Jakob (J2).

It would be of interest to study the effects of a parallel gas flow (steam or air) on these evaporation processes.

BOILING HEAT TRANSFER COEFFICIENT AGAINST LIQUID DEPTH OF WATER

REF.: J1

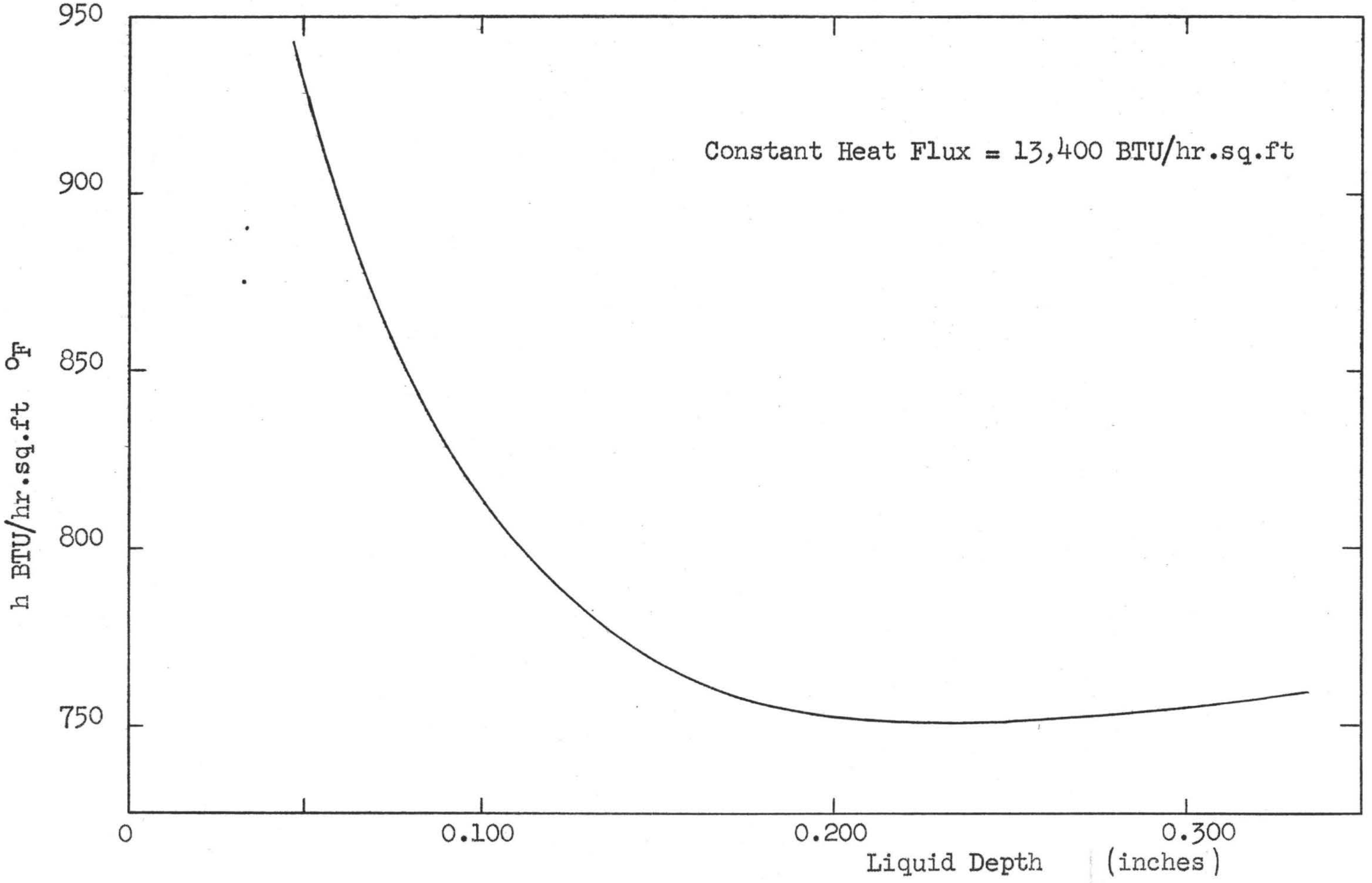

FIGURE 9

4.2 Gravity Flow

For wall temperatures well below the boiling point of the liquid it has been shown by McAdams (M3) that the film heat transfer coefficient can be described by

$$\frac{h_F}{h_P} = \frac{D^2}{4b(D-b)} \qquad (B-8)$$

where h_P is the heat transfer coefficient when the pipe is flowing full at the same mass flow rate. Both flows are turbulent. D is the inside diameter of the pipe and b the film thickness. Usually the heat transfer coefficient is found to be increased by a factor of about 2.2.

Nusselt was first to derive the equation for heat transfer to smooth-laminar liquid films. He found that the heat transfer decreased with Reynolds number due to the increasing film thickness. Dukler (D2) used the universal velocity profile to estimate the local heat transfer coefficient and was thereby able to cover the laminar and turbulent flow regimes quite successfully.

Portalski (P1) has shown that in wavy-laminar flow reverse flow occurs in the wave-valleys and that this leads to eddies. These provide good mixing in the liquid film and account for the high heat transfer. Chand and Rosson (C8) have measured the local heat flux to liquid films flowing down a vertical surface. Their results showed that the local heat flux oscillated with the same frequency as the waves on the film surface.

A detailed examination on heat transfer to thin water films flowing outside long vertical tubes has been made by Wilke (W2). The pipe was heated by an upward flow of hot water, such that heating occurred at constant temperature difference, but varying wall temperature. Measurements indicated that the thermal entry zone was about 1.5 ft long, after which the heat transfer coefficient remained constant. The length of the entry zone remained fairly constant for film Reynolds numbers up to 3000. A plot of the local average heat transfer coefficient (disregarding data from the entry zone) against the Reynolds number gave a curve with 3 breaks at Re = 200, Re = 400 and Re = 800, (Figure 10). The last two transition Reynolds numbers corresponded to the well-known change in hydrodynamic flow as outlined above. The first transition at Re = 200 could not be attributed to a change in the flow pattern. At Re $<$ 200 the measurements followed the Nusselt equation for heat transfer to smooth-laminar liquid films. The measurements of the velocity and temperature profile showed that at the first transition both profiles ceased to be linear for the whole film thickness and a thinner boundary layer was established in the liquid film. It is of interest to note here that the ratio of the wave-velocity to the mean stream velocity reaches a minimum value of about 1.5 at Re $\cong$ 100 for water (F1).

Garwin and Kelly (G1) have investigated the heat transfer to turbulent water films flowing over an inclined plate. The plate was heated by steam and gave a constant wall temperature. They obtained an equation for the heat transfer coefficient at a mean film temperature of 93°F.

$$h_F = 87\ (\sin\ \theta)^{0.2}\ (G)^{1/3} \qquad \text{(B-9)}$$

where θ is the angle of inclination of the plate and G the mass flow rate per unit breadth, (lb_m/hr.ft). The equation agrees satisfactorily

HEAT TRANSFER COEFFICIENT AGAINST REYNOLDS NUMBER FOR WATER FILMS

REF.: W2

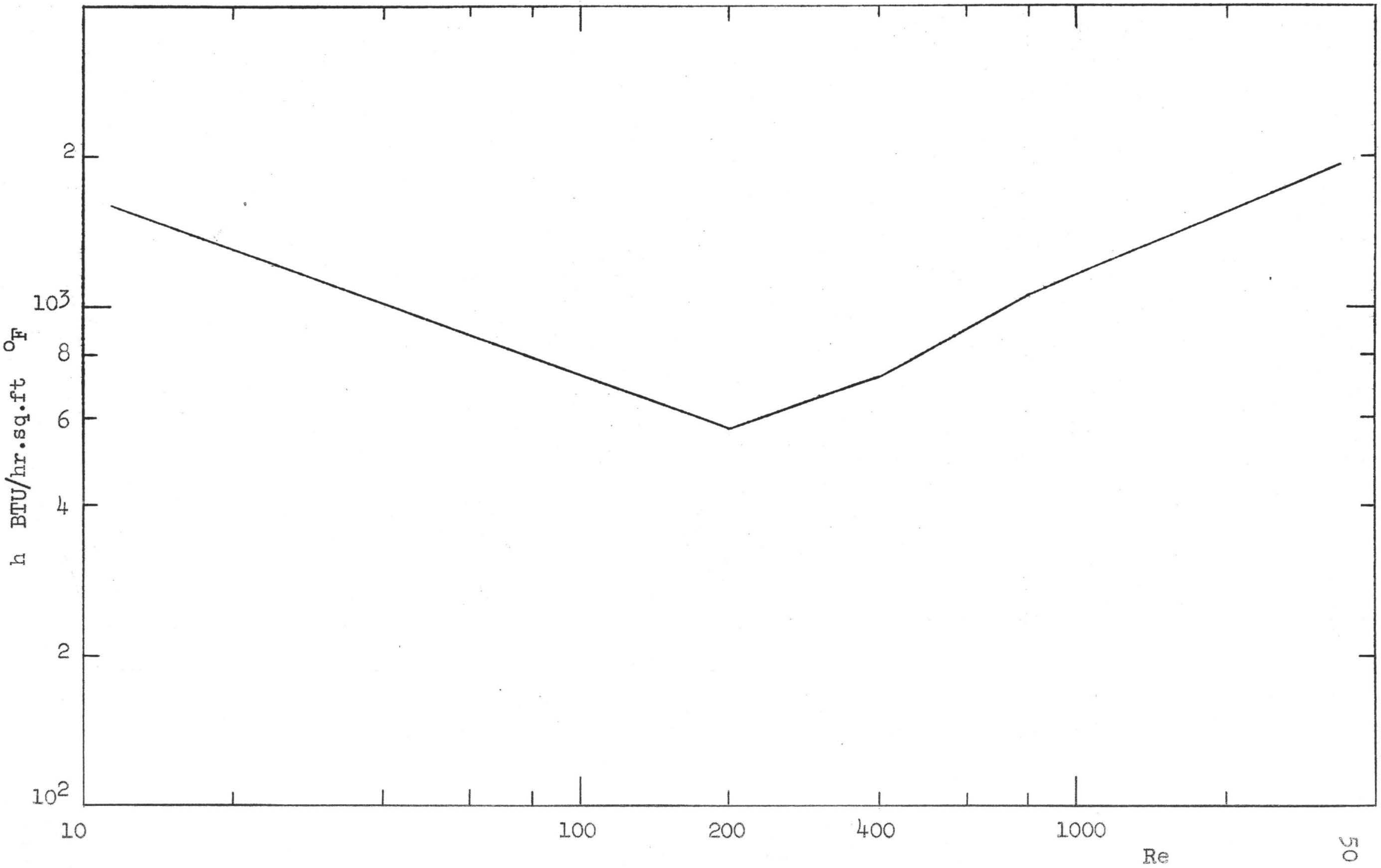

FIGURE 10

with the equation given by McAdams (M3) for film flow inside vertical pipes

$$\frac{h_F}{\left(\frac{k_f^3 \rho_f^2 g}{\mu_f^2}\right)^{1/3}} = 0.01 \left(\frac{c\mu}{k}\right)^{1/3} \left(\frac{4G}{\mu_f}\right)^{1/3} \qquad \text{(B-10)}$$

Bressler (B3) investigated the flow of water films flowing over a vertical plate which was heated by steam. The unheated plate was wetted well by the water, but small ripples were present. If the water was introduced at a higher temperature, the water surface was much smoother. When the plate was heated to near the boiling point, the liquid film contracted at the sides and the wetting was reduced. Intense evaporation occurred. Bubbles were formed at the limits of wetting. At higher wall temperatures still, the lower region of the film began to boil. The bursting of bubbles caused spray formation. Three regions were recognized: a heating section, a region where the first bubbles were formed and a region in a state of vigorous boiling. By blowing air over the film with a fan, the bubble size was reduced considerably and evaporation took place essentially from the film surface. At low water flow rates the heated plate was difficult to wet and the liquid passed along the plate in individual streams. Wetting was much improved by using surface active agents. Boiling occurred then at lower surface temperatures.

Heat transfer measurements were difficult in that the heat transfer area and film thickness changed continuously. The observed boiling heat transfer at low heat fluxes up to 60,000 BTU/hr.sq.ft agreed well with the boiling curve of Jakob and Linke (J1). The film thickness ranged from 0.008" to 0.032". No enhancement due to film flow was observed.

Similar experiments have been carried out by Norman and McIntyre (N1), who used a vertical tube heated externally by steam or rapidly-flowing hot water. Experiments under non-boiling conditions, but with surface temperatures close to the boiling point of water, showed that liquid films at $Re < 500$ were unstable. The Reynolds number at which instability occurred depended upon the liquid film temperature. The instability led to dry patch formation which caused a decrease in the apparent film heat transfer coefficient. The Nusselt equation for uniform film flow was no longer found to be applicable.

For the boiling experiments the water was introduced at its boiling point. At high surface temperatures the data fitted the nucleate boiling curve. However the flowrate (film thickness) appeared to have a significant effect at lower surface temperatures, (Figure 11). Although incomplete wetting took place at a low flow rate (0.0038") the average heat flux was of the same magnitude as at a greater film thickness (0.0056"), when complete wetting occurred. This probably indicates that the local heat flux for the thinner film is even higher than that indicated.

Complete wetting was said to ocucr at a film thickness of 0.0045"; high average heat fluxes of 40,000 BTU/hr.sq.ft were obtained at temperature differences of only 5-10°F. This was attributed to direct evaporation from the thin film surface with conduction and convection through the film, (Discussion N1). As the film thickness was increased the heat transfer rate decreased. This trend is in agreement with the Nusselt equation. However, the experimental heat transfer rates were from 3 to 5 times higher than the values calculated from

BOILING HEAT FLUX TO THIN WATER FILMS

REF.: N1

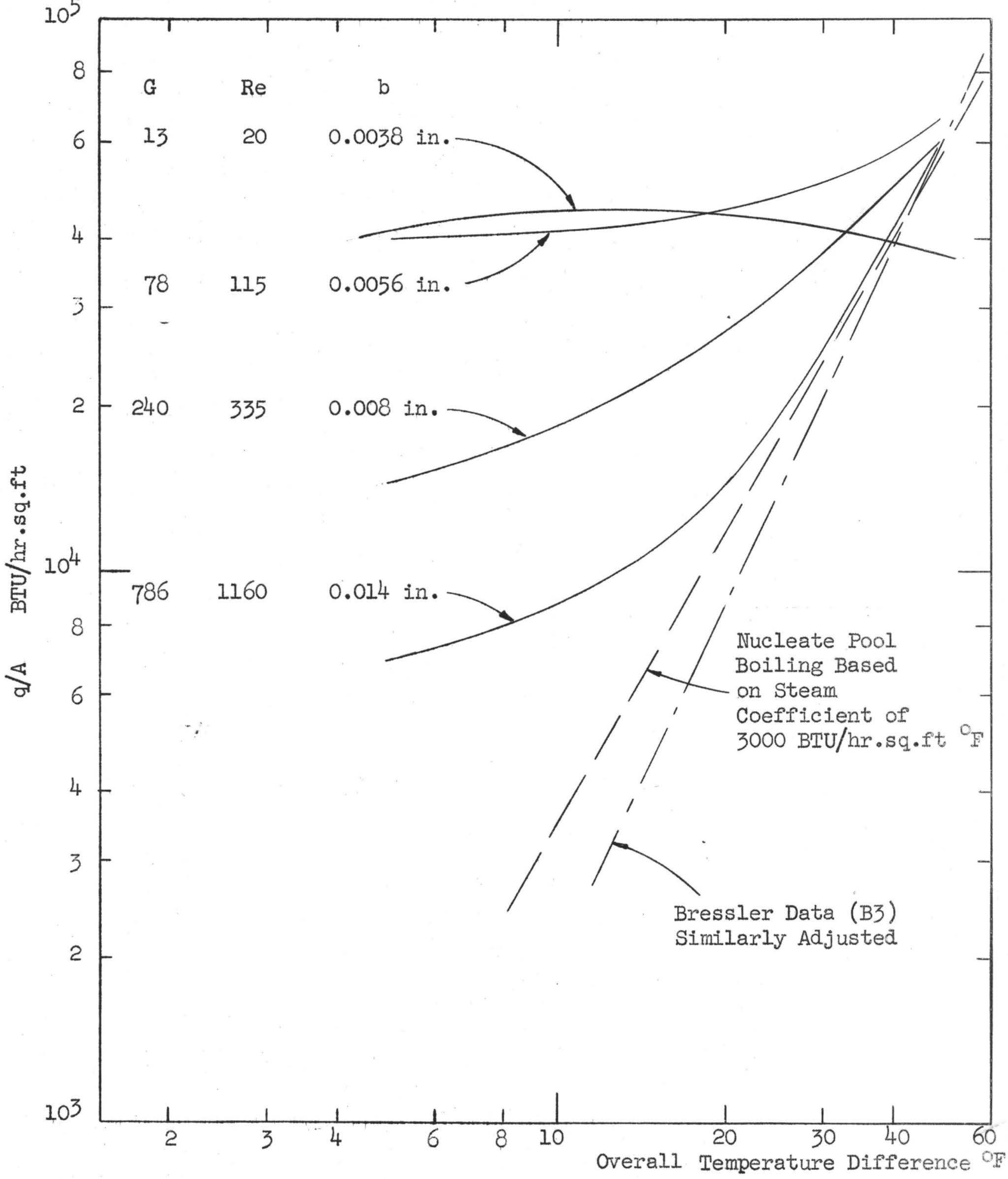

FIGURE 11

that equation.

The effect of surface evaporation on the heat transfer was apparently not observed by Bressler (B3), for film thicknesses greater than 0.008" were used.

4.3 Parallel Gas Flow

A shear on a liquid film produced by a parallel gas flow affects the velocity distribution in the film. The heat transfer is thereby increased as has been shown by Dukler (D2).

Studies have been made essentially in annular two-phase flows in vertical pipes, for this is the simplest geometry to analyse. Collier et al (C5) and Bennett et al (B5) suggest the following mechanisms for heat transfer, (Figure 12).

(i) subcooled nucleate boiling
(ii) saturated nucleate boiling
(iii) surface evaporation (two-phase forced convection of film)
(iv) two-phase forced convection (dry wall condition).

At a certain position along the tube saturated nucleate boiling in the liquid film is suppressed (H3). This is due to surface evaporation (equivalent to subcooling of the liquid film) and forced convection (because of the increasing shear on the liquid film by the vapour flow). Collier et al (C5) have used the model of Hsu (H7) to predict the wall temperature at the point of suppression of nucleate boiling. When the liquid film is in the state of nucleate boiling the heat transfer can be described by the pool boiling curve. However in the forced convective region of the film heat fluxes similar to those in boiling were obtained at lower wall temperatures. Heat may also be transferred from the liquid

FLOW PATTERNS IN TWO-PHASE FLOW HEAT TRANSFER

REF.: C5, B5

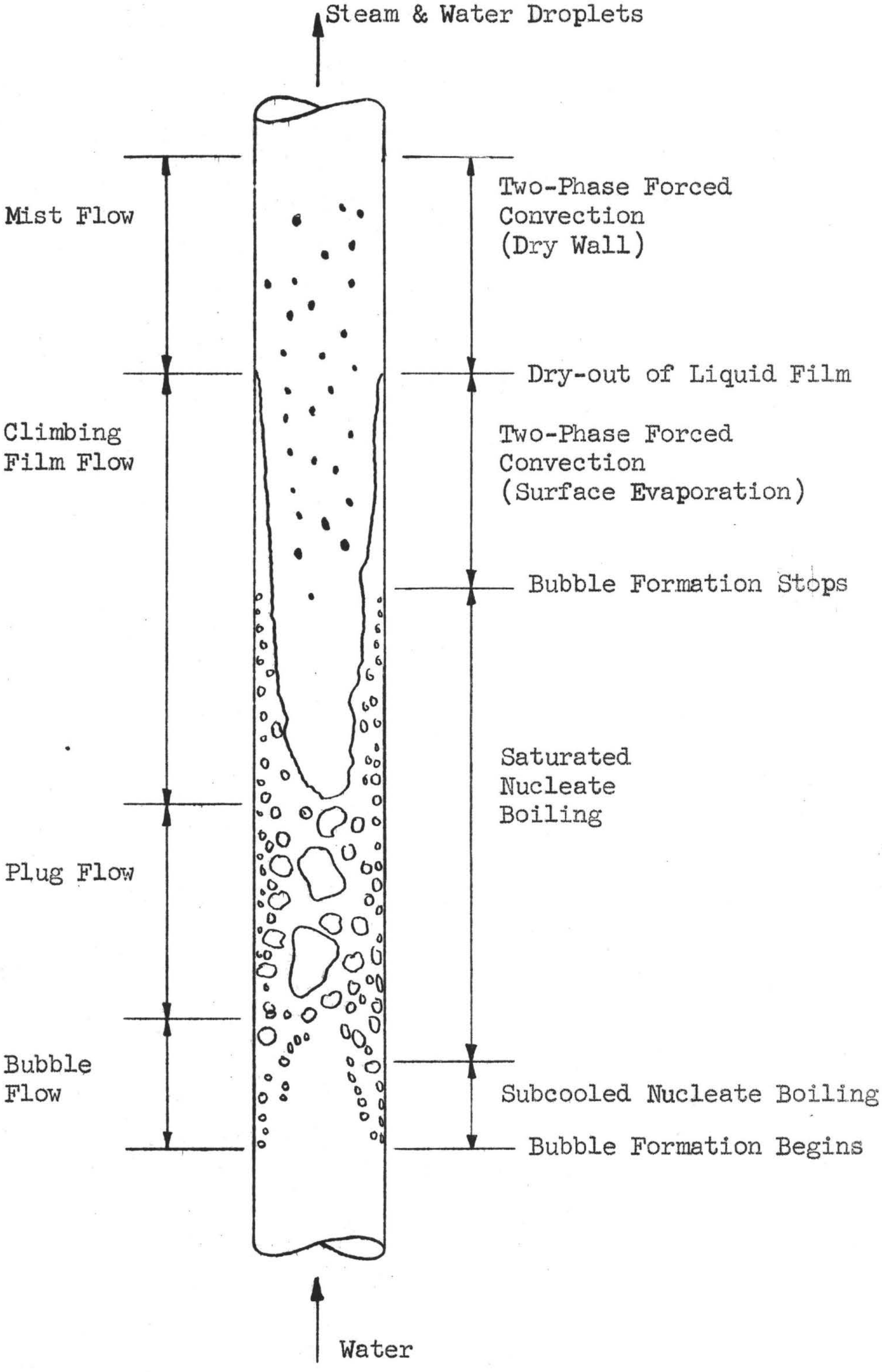

FIGURE 12

film to the vapour core by entrainment of superheated liquid. These hot droplets evaporate rapidly to decrease their superheat.

The occurrence of these four mechanisms depend upon the mass flow rate, heat flux and pipe length. They can be characterised by the steam quality of the flow. Each of these mechanisms can lead to burnout at different heat flux levels, (Figure 13). Burnout occurs when the liquid is no longer in contact with the heater surface. At low steam qualities the flow is essentially liquid and the burnout is due to the transition from nucleate to film boiling. In film boiling the heat transfer is considerably reduced and causes overheating of the wall. A region of burnout exists which appears to be independent of the heat flux. It is postulated that in that region the quality of the flow is such to make hydrodynamic instabilities dominant in determining burnout. Carr (C4) was able to correlate this hydrodynamic effect successfully using Zuber's mechanism (Z1) of droplet entrainment from a liquid film. At high steam qualities the flow consists of a vapour core carrying small droplets of liquid and a thin layer of liquid attached to the wall. The film thickness ranges from 0.001" to 0.010" and the film heat flux ranges from 10^5 to 10^6 BTU/hr.sq.ft. The film thickness in the direction of flow decreases due to evaporation and entrainment. The vapour flow and hence the interfacial shear on the liquid film increases in the direction of flow and causes surface waves. These waves can cause a break-up of the liquid film by encouraging dry spot formation, which then may lead to burnout. However, Berenson and Stone (B17) have made a photographic study of annular two-phase flow and concluded that the thin liquid film on the heating surface formed dry spots because of vaporization and not because

BURNOUT HEAT FLUX AGAINST STEAM QUALITY AT EXIT

REF.: C4

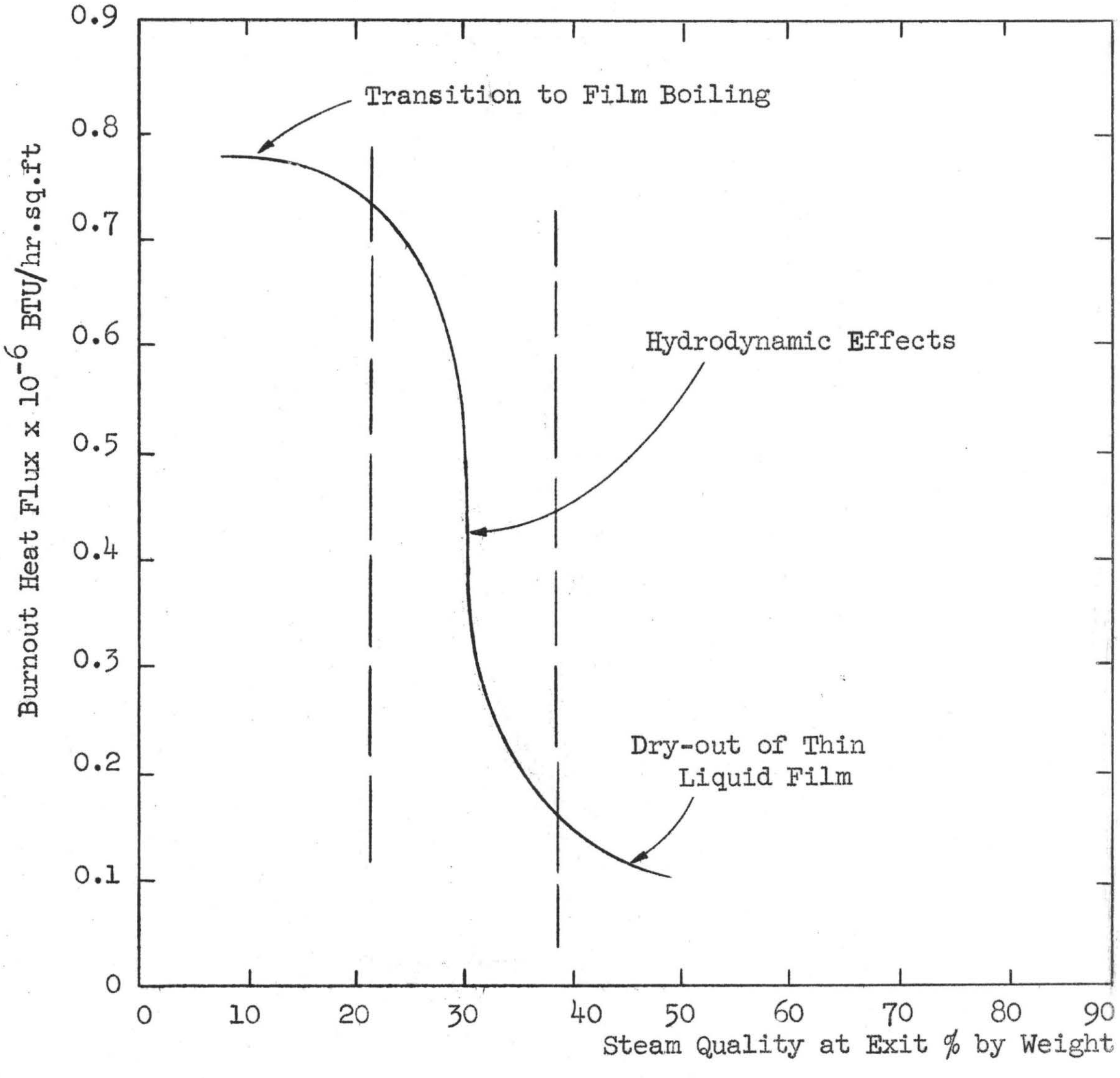

FIGURE 13

it was hydrodynamically unstable.

The theoretical models consider that the critical heat flux condition is obtained when the liquid consumption rate (vaporization and entrainment from liquid film) exceeds the liquid supply rate (from liquid upstream and by droplet deposition from vapour core). The particular flow visualizations for the models differ in stressing certain mechanisms, (C3), (B4), (T2).

5. Thermal Instabilities in Liquid Films

When a liquid film is heated effects occur which cause a change in flow pattern or lead to disruption of the continuous film. The hydrodynamic instabilities discussed above should be borne in mind here too.

5.1 Benard Instability

If a stationary liquid film is heated from below an adverse density gradient exists, such that the denser liquid rests upon a liquid layer of lower density. Such a system is top heavy and will rearrange itself in the gravitational field. The flow of the liquid is however inhibited by its viscosity. The system is potentially unstable, but the instability does not set in until the temperature gradient reaches a critical value. The onset of the instability is characterised by the Rayleigh number (Ra), (C1), (R1). Once the instability has set in, the liquid is divided into uniform cells, in which natural convection occurs. If the liquid film moves vortex rolls are produced, the nature of which depends upon the magnitude of the superposed velocity.

5.2 Liquid Film Break-Up

During the heating of flowing liquid films dry spots can be formed on the heating surface as a result of the heat transfer process. The liquid film under these conditions breaks up and no longer wets the surface uniformly. Some of the mechanisms of dry spot formation are discussed below, (Figure 14).

Thermocapillary effect

Thin film flow at low Reynolds numbers is usually wavy. Heat transfer to the liquid film enhances waviness due to the thermocapillary effect, (S3), (N1). A temperature gradient in the surface of the liquid causes a surface tension gradient. The temperature of the liquid surface in a wave valley is greater than that at the wave-crest. Thus a flow of liquid into the wave-crest occurs. The wave-valley is deepened, which increases the effect caused by further heat transfer to the thinner section. A dry spot may thus be formed from a deepened wave-valley.

Hsu et al (H4) have examined liquid film destruction by the thermocapillary effect. The theoretical treatment fixes an entry length for the thermal boundary layer to attain the film thickness of the wave-valley. Only after this entry length can temperature variations occur at the liquid-vapour interface. The magnitude of the temperature variation at the surface depends upon the heat flux and determines whether the flow of liquid away from the wave-valley is sufficiently large to cause the formation of dry spots. The experimental data were in fair agreement with the theory. As an example, unstable dry spots were observed at a film Reynolds number of 175 and a mean film thickness of 0.012"; the film temperature was 140°F and the heat flux 66,000 BTU/hr.sq.ft.

At large Reynolds numbers the surface waves cause sufficient mixing to eliminate the temperature gradient at the surface. For

MECHANISMS OF DRY SPOT FORMATION

REF.: S3

Thermocapillary Effect

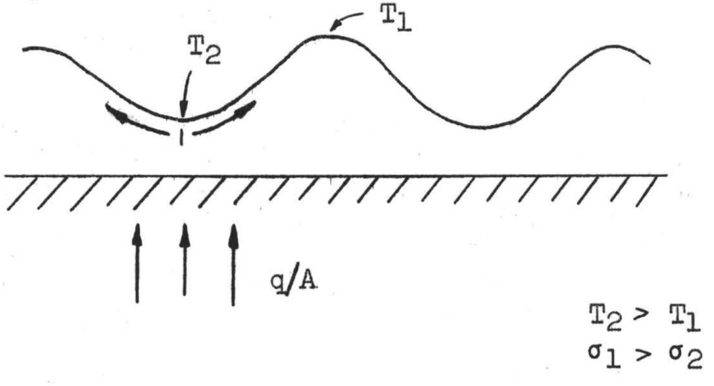

Vapour Thrust Effect

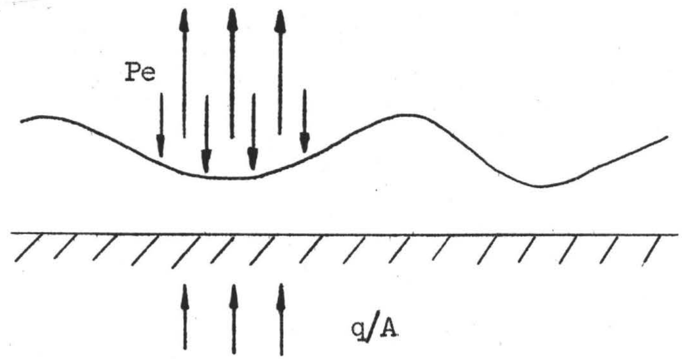

Bubble Growth Effect

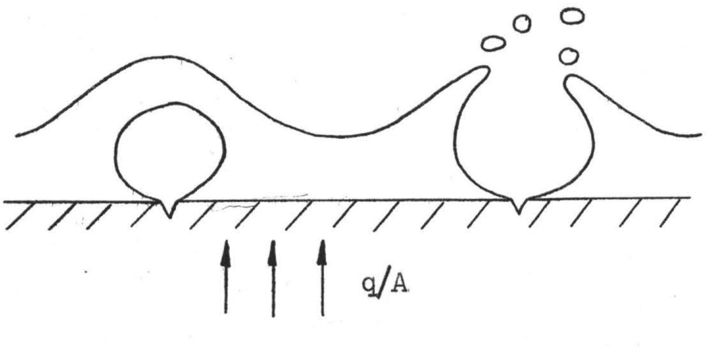

FIGURE 14

turbulent films this thermocapillary effect cannot occur.

Vapour thrust effect

At wall temperatures near the boiling point of the liquid, vaporization at the liquid surface becomes significant (S3). This vaporization causes a vapour thrust, because of the change of momentum at the evaporating interface. The vapour thrust acts towards the heating surface and thus tends to reduce the thickness of the liquid film. The pressure of the vapour thrust is given by

$$P_e = \rho_v \left(\frac{q/A}{\rho_v \lambda} \right)^2 \frac{\rho_L - \rho_v}{\rho_L} \qquad \text{(B-11)}$$

where (q/A) is the heat flux at the evaporating interface. At a heat flux of 1,000,000 BTU/hr.sq.ft the pressure of the vapour thrust is 0.012" H_2O for an evaporating waterfilm. For very thin films, which have a high rate of evaporation, this vapour thrust effect becomes dominant in determining the stability of the interface.

The presence of waves in the liquid film enhances dry spot formation in the wave-valleys, because the heat transfer and hence the vapour thrust is largest in such locations. The vapour thrust effect also occurs in turbulent liquid films.

Bubble growth effect

When the wall temperature exceeds the boiling point of the liquid, vapour bubbles are formed at the heating surface. At high liquid temperatures these bubbles grow and burst through the liquid film (S3). Liquid spray and dry spot formation result. The bubble size depends upon the film flow rate and subcooling; an increase in either of these factors decreases the bubble size and hence the bubble growth effect. An average maximum bubble size for subcooled nucleate boiling is 0.040", (G6).

Dry patch stability

Once a dry spot has been formed by one of the above mechanisms, it may expand into a dry patch or be wetted again with liquid. Surface tension forces, film flow conditions and the heat flux must be considered during this transient process. At very high heat fluxes the dry spot may easily overheat to wall temperatures corresponding to film boiling conditions.

Considering non-boiling conditions, the stability of a dry patch may be described by a simple force balance on the stagnation point D, (Figure 15).

$$\frac{\rho_L}{2}\int_0^b [u(y)]^2 \quad dy = \sigma_1 - \sigma_2 \cos\phi \qquad \text{(B-12)}$$

This equation indicates that the flow may sweep the patch downstream, while surface tension may move it upstream. Thus a criterion for the minimum wetting rate of the liquid on a solid surface is established. The liquid flow rate can be reduced however below the minimum wetting rate (M.W.R.), if there is no mechanism for dry spot formation.

Norman and McIntyre (N1) observed the minimum water flow rates required to wet the inside of a heated vertical tube. The M.W.R. was found to increase with wall temperature and decrease with the liquid entry temperature. This is in agreement with the above equation. The M.W.R. approached a maximum for all liquid entry temperatures at a wall temperature of about 220°F (when boiling was initiated) and then decreased again. At flow rates slightly larger than the M.W.R. the

DRY PATCH STABILITY

REF.: H5

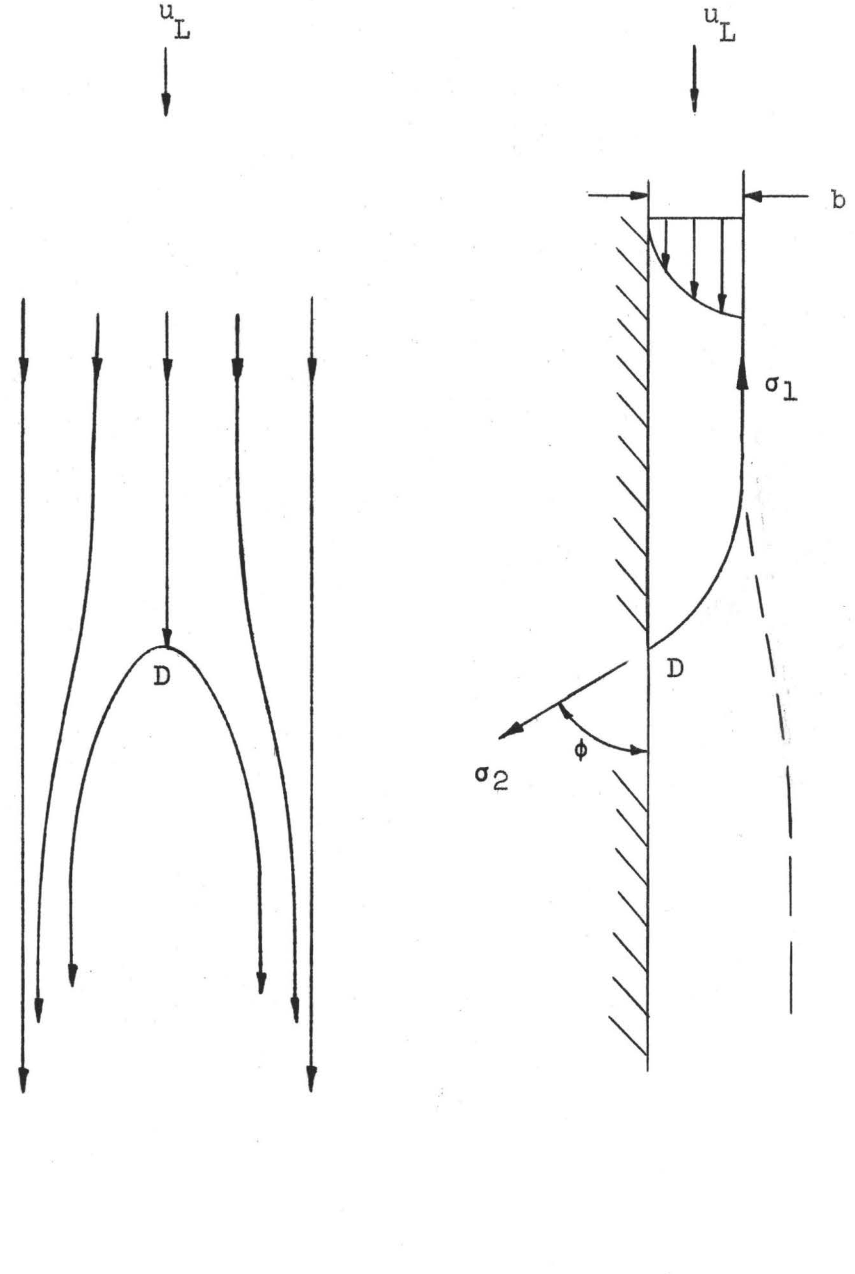

FIGURE 15

film surface was observed to be unstable, leading to local thickening and thinning of the film. The instability and dry patch formation was attributed to surface tension effects in the liquid surface.

A parallel gas flow changes the liquid film velocity and additional forces affect the criteria. Murgatroyd (M4) examined shear and form forces at the stagnation point and showed them to have a wetting effect as suggested by the data of Hewitt and Lacey (H6). The latter workers have confirmed the trend of the model, in that increasing gas flow rates decrease the M.W.R.

Staub and Zuber (S3) have also extended this model to account for surface tension variations and for the vapour thrust effect. The profile of the liquid at the stagnation point depends upon the contact angle as mentioned in the discussion of reference (N1). The profile may have a significant effect on the forces which determine the stability of the dry patch.

5.3 Liquid Film Destruction

When the heat flux to the liquid film is large, i.e. at large wall temperatures, vigorous boiling occurs in the liquid film. The boiling can lead to the destruction of the liquid film. Depending upon the film-flow rate two hydrodynamic patterns can develop. These may be compared to the burnout conditions in two-phase flow in a vertical pipe as mentioned above.

At low film-flow rates the bubble growth effect causes much spray formation and thereby reduces the film thickness. The liquid film then evaporates completely by surface evaporation and boiling.

At high film-flow rates the liquid does not evaporate completely, but will cover areas of the heating surface in which the wall temperature corresponds to the film boiling regime. In such areas the liquid will not contact the heating surface. The liquid film usually contracts into streams which flow over a vapour blanket on the heating surface, (Plate 1). Leidenfrost (L2) has described this hydrodynamic behaviour.

C. EQUIPMENT

1. Introduction

Some preliminary experiments were carried out by passing films of water and organic liquids over an electrically heated stainless steel plate. Besides giving some guidance for the construction of the final boiling equipment, some visual observations on the liquid film break-up were made. Plate 1 shows the complexity of the hydrodynamic pattern.

The hydrodynamic pattern was considerably simplified by introducing a thin section in the boiling plate as shown in Figure 16. A specific region of destruction of the liquid film could be observed where the liquid separated from the solid surface. Under steady conditions the flow pattern was stable with time, was two-dimensional and could be reproduced easily. Experimental investigation was greatly aided by this simplification.

2. Apparatus

The experiments consisted essentially of introducing water or benzene through a narrow slot to produce a thin liquid film over an inclined, hot metal surface. The break-up of the liquid film as it entered the film boiling regime was photographed with a high-speed Fastax camera. The heat transfer rate per unit area was measured under conditions of nucleate and film boiling by employing heat-flux meters which were an integral part of a copper plate. Two experimental boiling surfaces were employed, a chromed copper plate

DESTRUCTION OF LIQUID FILMS

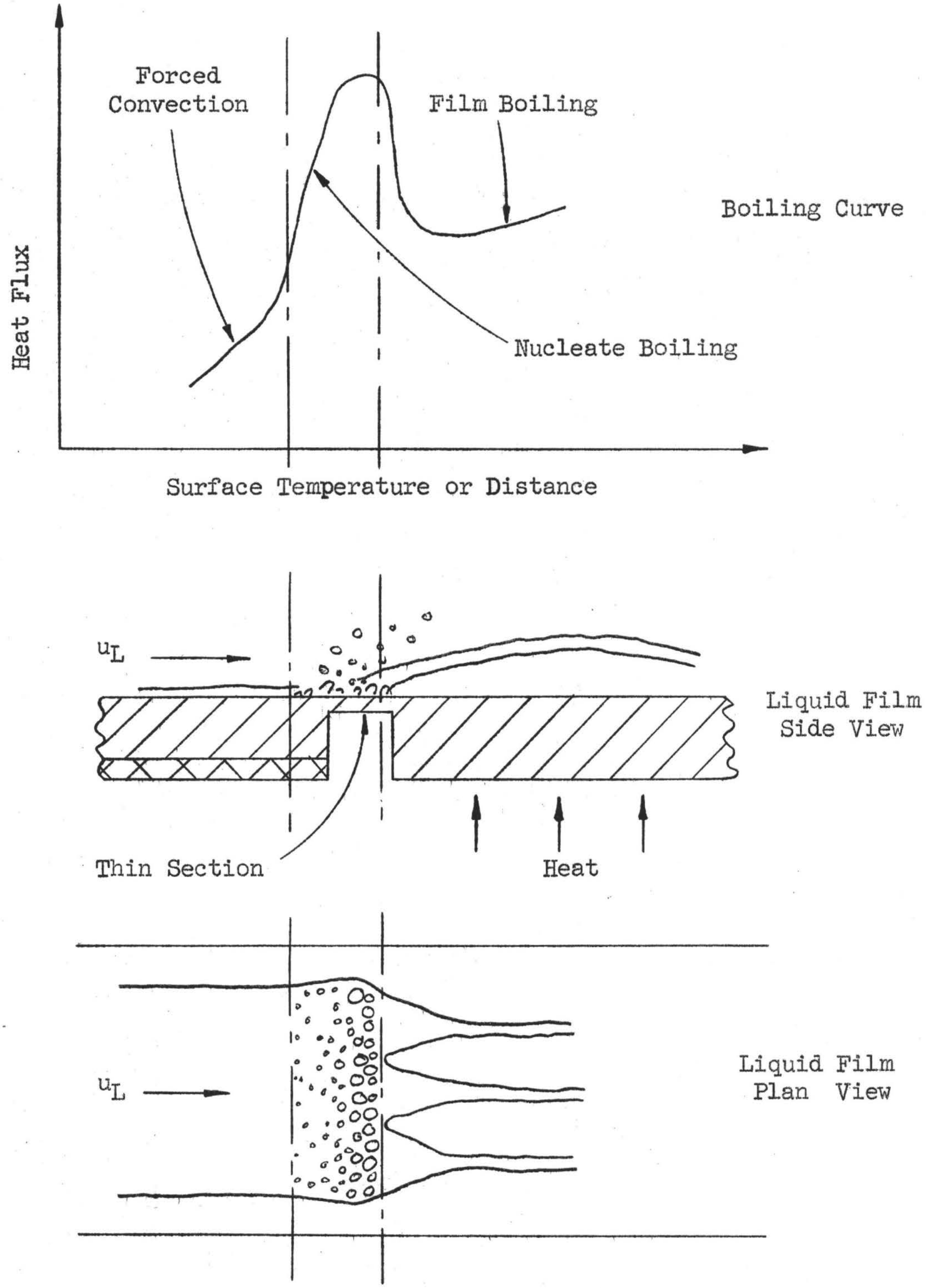

FIGURE 16

and an unplated copper plate. A detailed description of the apparatus is given below.

2.1 Liquid Circulating System

The liquid flowing over the boiling plate was continuously circulated as shown in Figure 17. The constant head tank supplied a constant flow rate to the boiling plate. The flow could be adjusted by a valve and was measured with a calibrated Fischer and Porter rotameter (FP 3/4 21G 10/80 tube, TGSVT-54 float).

The liquid after passage over the boiling plate flowed into a collecting tank from where it was pumped by a gear pump at about 5 gal./ min. into the constant head tank. An overflow line allowed some of the liquid to be returned to the collecting tank. The return line from the pump to the head tank was equipped with a water cooler and an electric heater, so that the temperature of the liquid could be controlled.

The vapour, which was generated on the boiling plate, was passed to a condenser, which was fixed to the tiltable plate supporting the boiler assembly. The condensate was collected in a glass vessel from which it was transferred at intervals to the collecting tank. Some vapour suction was applied to the condenser in order to reduce leaks into the atmosphere.

An electrically-heated preheater, which was installed after the rotameter, was used for experiments where operation was close to the boiling point of the liquid. The liquid entry temperature was measured with a copper-constantan thermocouple after the preheater. Other liquid temperatures were taken in the collecting tank and after the rotameter.

LIQUID CIRCULATING SYSTEM

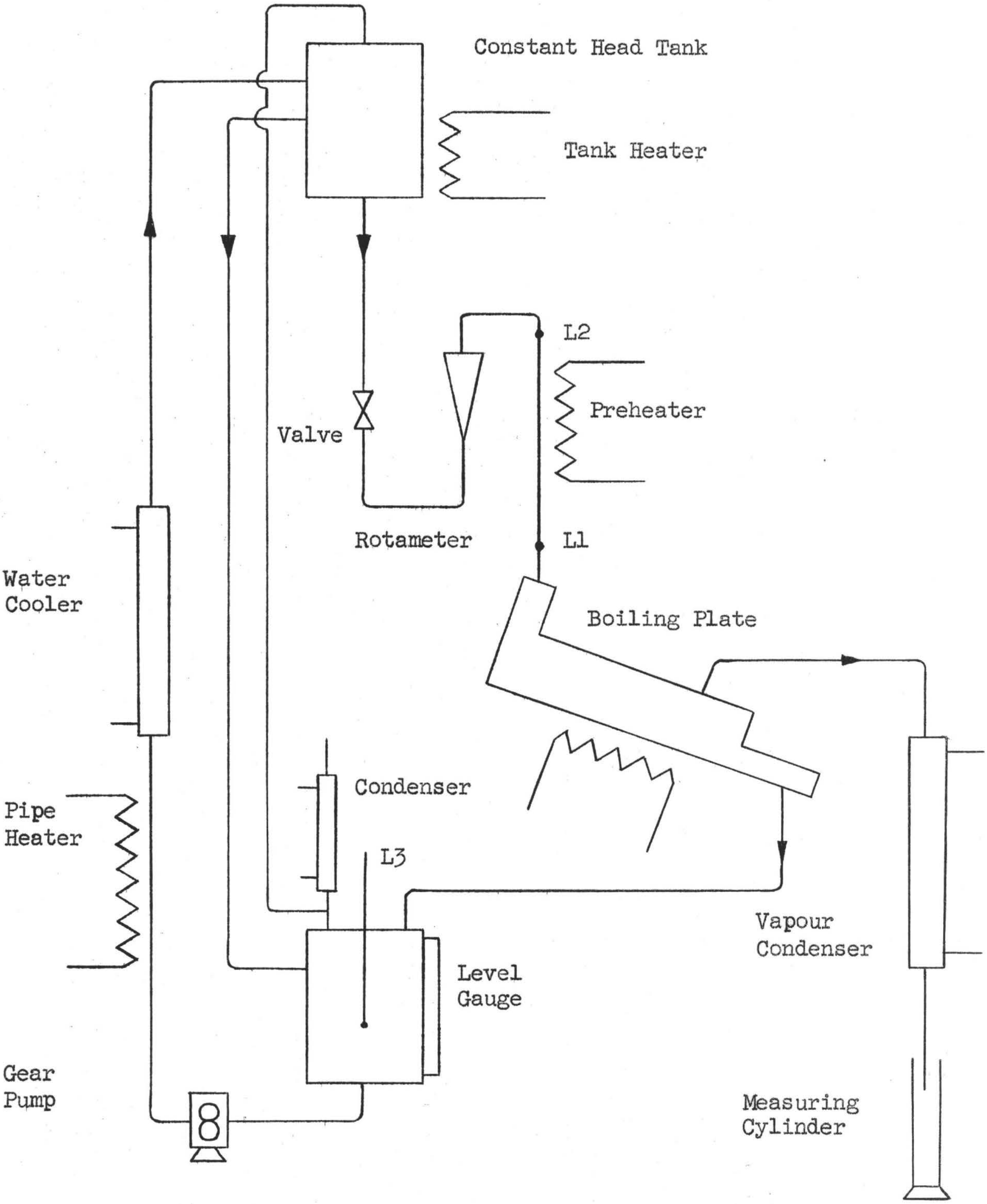

FIGURE 17

To avoid corrosion 1/2 in. stainless steel tubing and fittings were used for the liquid line and a 1 in. stainless steel pipe was used for the vapour line. All lines were insulated with 1 in. thick, low-temperature Fiberglas insulation.

2.2 Boiling Plate Enclosure

The illustrations of the boiler assembly (Figures 18, 19, 20 and Plate 2) show the boiling plate enclosure. The enclosure consisted of the liquid inlet and outlet sections which were machined from teflon to resist corrosion and prevent conduction of heat. Both sides were fitted with pyrex glass 2 1/2 in. x 16 in. x 1/4 in., such that the boiling plate was visible. The lid was made of 1/4 in. thick sheet of teflon, which carried a sheet of pyrex glass 3 1/2 in. x 8 in. x 3/16 in. for plan observations.

Asbestos tape, 1/16 in. thick, was used to seal the glass and the boiling plate. Teflon and glass were self-sealing.

The liquid entered through a slot, which distributed the liquid into a film. Since the wetting on the teflon was poor a clean gauze of stainless steel was placed over the teflon entry section and over part of the front lip of the boiling plate. Teflon guides were provided at the sides of the entry section to prevent the liquid film from flowing preferentially along the pyrex glass, (Plate 1). The liquid film was about 3 in. wide.

The vapour was removed under slight suction through a 1 in. stainless steel pipe and the liquid flowed out under gravity.

BOILER ASSEMBLY
(SIDE ELEVATION)

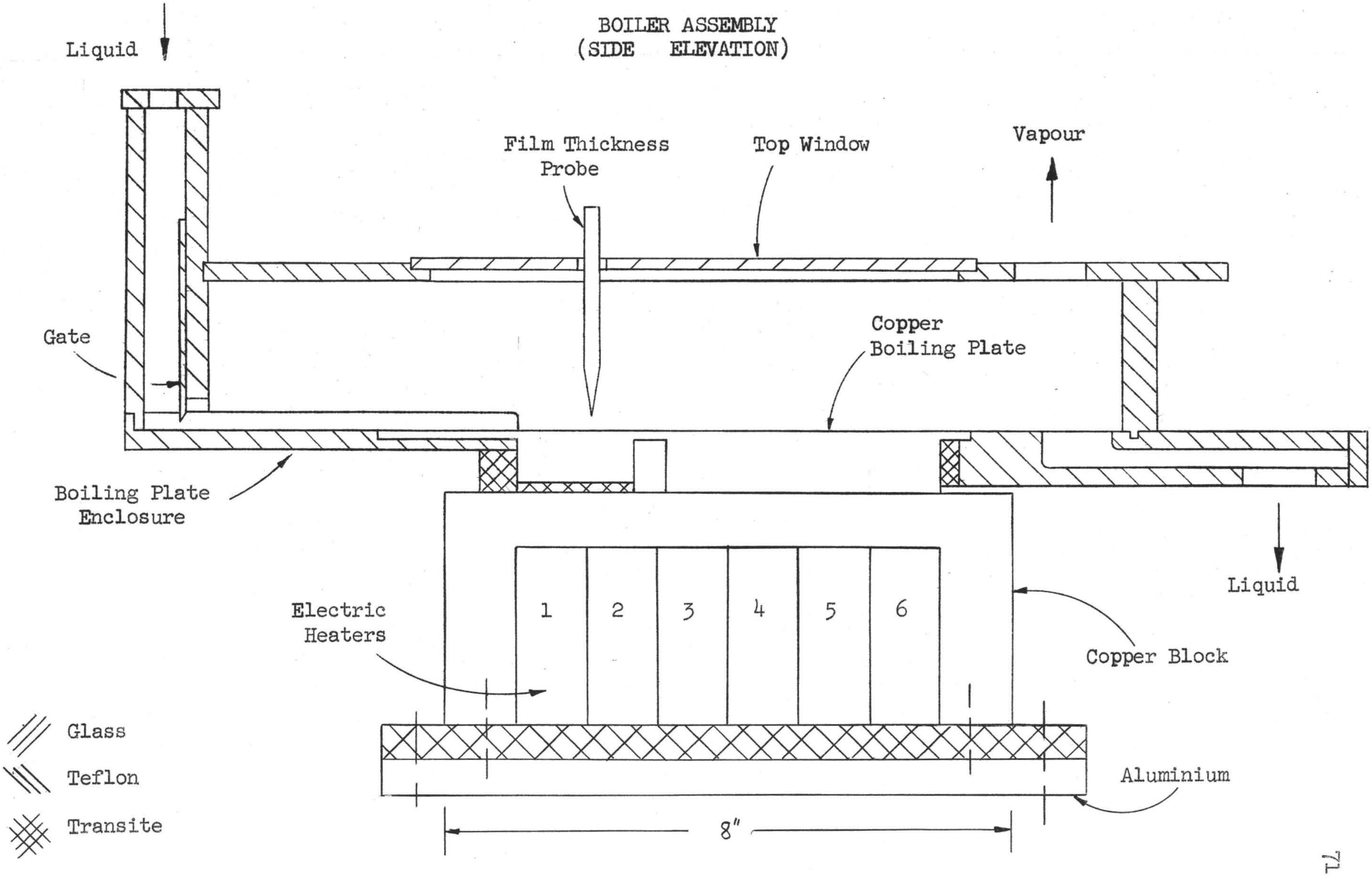

FIGURE 18

BOILER ASSEMBLY
(END ELEVATION)

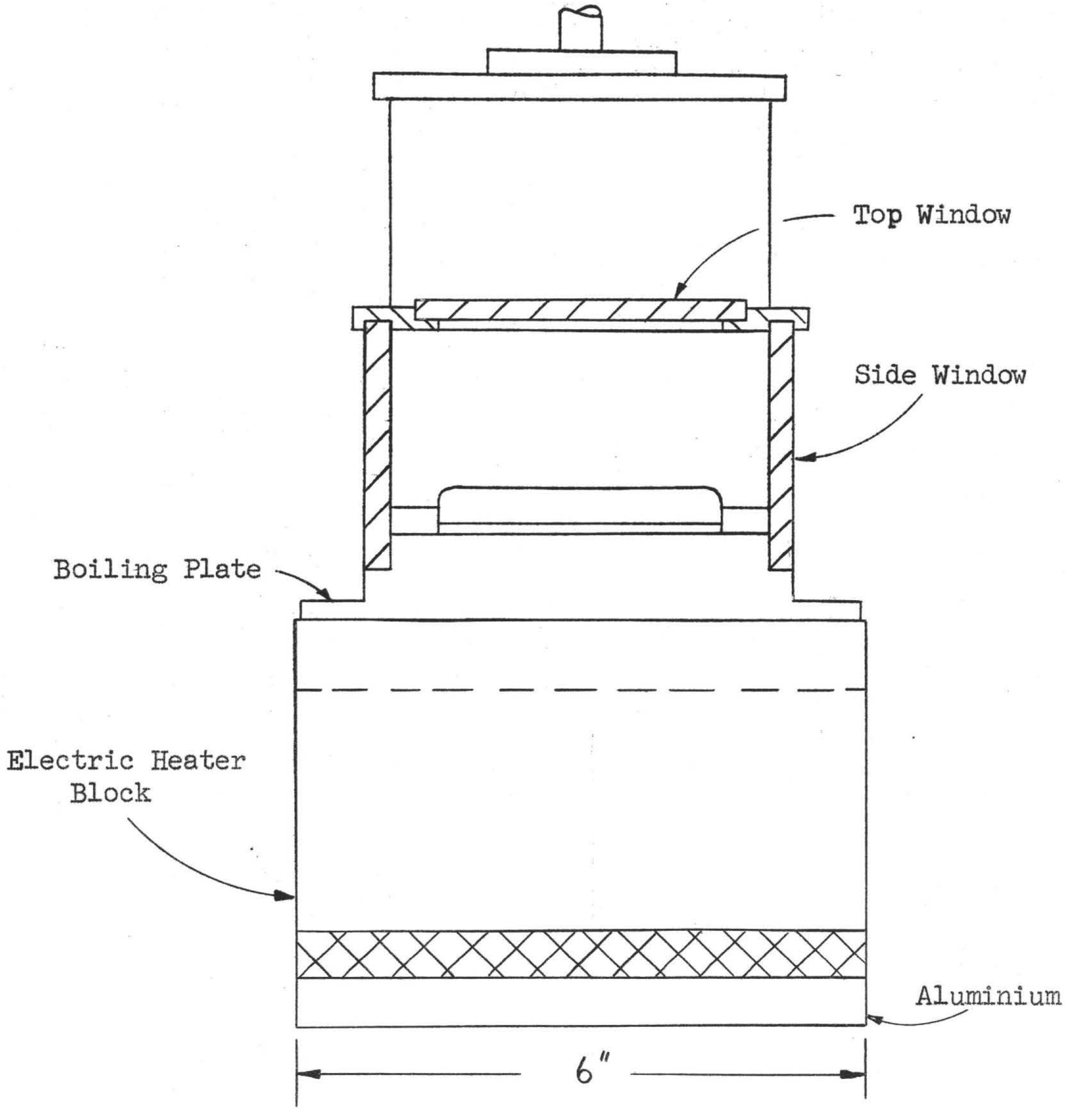

FIGURE 19

BOILER ASSEMBLY
(PLAN)

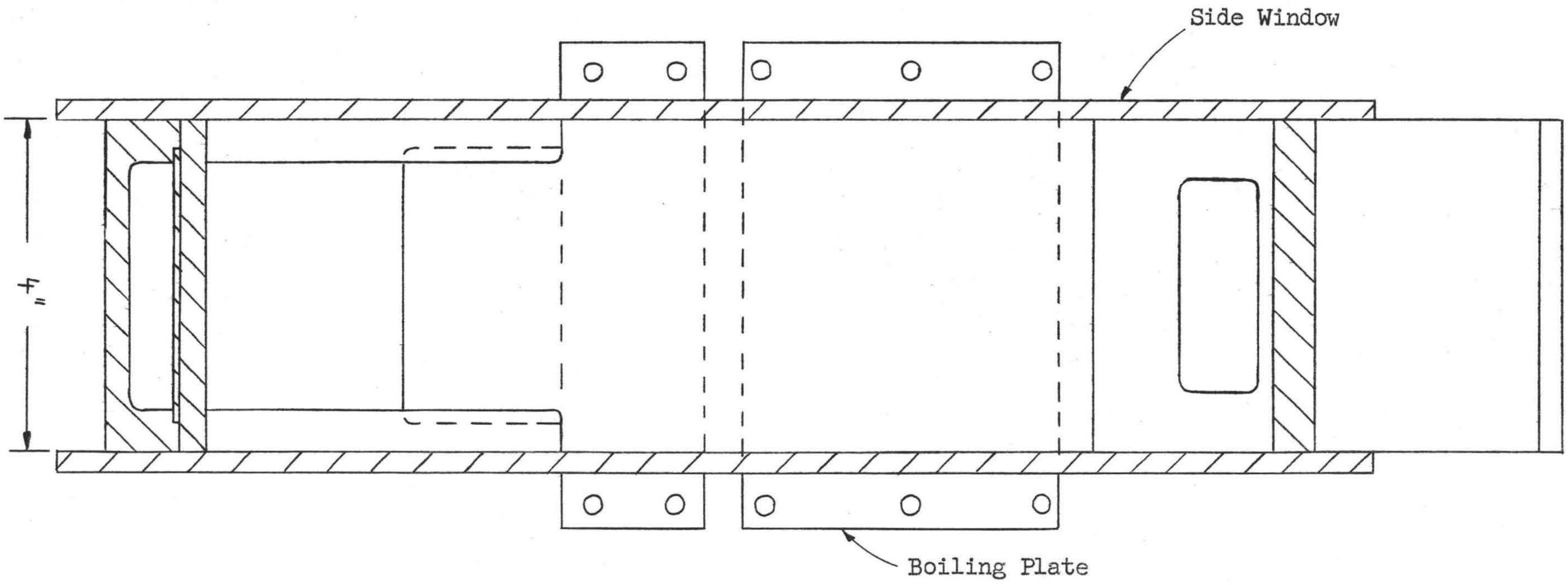

FIGURE 20

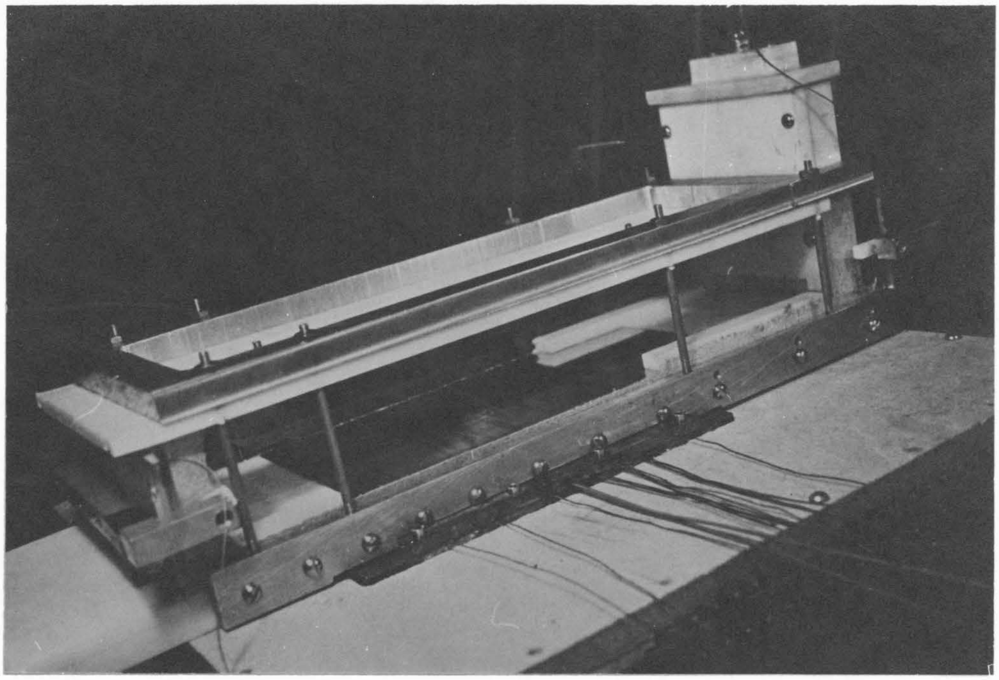

(a) ENCLOSURE

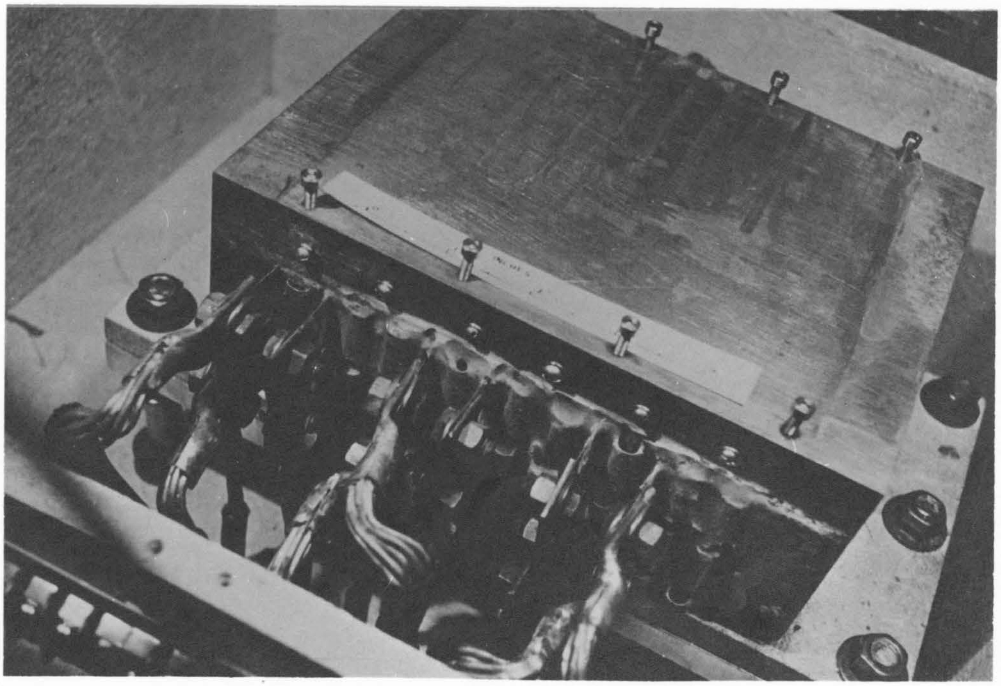

(b) HEATER ASSEMBLY

PLATE 2

The boiler assembly which consisted of the electric heater, boiling plate and boiling plate enclosure, was mounted on an aluminum plate, which could be tilted about a horizontal axis from 0° to 90°.

2.3 Electric Heater

The boiling plate was heated by means of an electric heater, which consisted of Kanthal "A"-1 heating strips embedded in a copper block. Copper was chosen for its good thermal conductivity. The block was divided into 6 separate heating sections to allow some control over the heat distribution to the boiling liquid film. Each heating section was designed for 2.5 KW at 24 V, to sustain the peak boiling flux of water over that section. By use of an additional heating strip in series a heating section could also be used for 1 KW operation, (Figure 21).

The electric heater was constructed by cutting twenty-four slots 2 1/2 in. deep and 1/8 in. wide into a copper block which was 8 in. long, 6 in. wide and 3 1/4 in. thick. Each heating section occupied four slots and these slots accommodated the Kanthal "A"-1 heating strips. The heating strips were arranged in the slots as shown in Figure 21. Two strip sizes were used 0.375 in. x 0.015 in. and 0.75 in. x 0.015 in. The strips were held centrally in the slots by Hiloset cement. The design calculations are shown in the appendix.

Six chromel-alumel thermocouples were screwed to the top of the fins in positions corresponding to the six heaters. An indication of the temperature distribution in the copper block was thus obtained.

To minimize heat loss by conduction the copper block was mounted on a 1/2 in. transite plate, which in turn was reinforced by a 1/2 in.

ELECTRIC HEATER

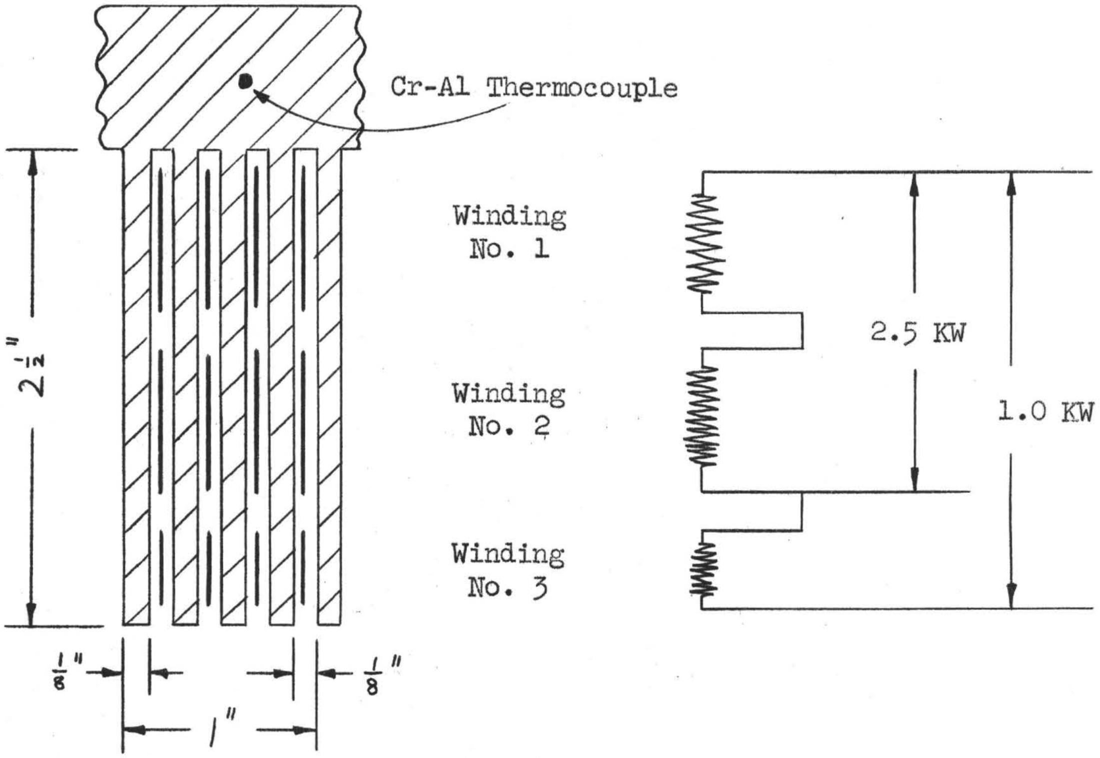

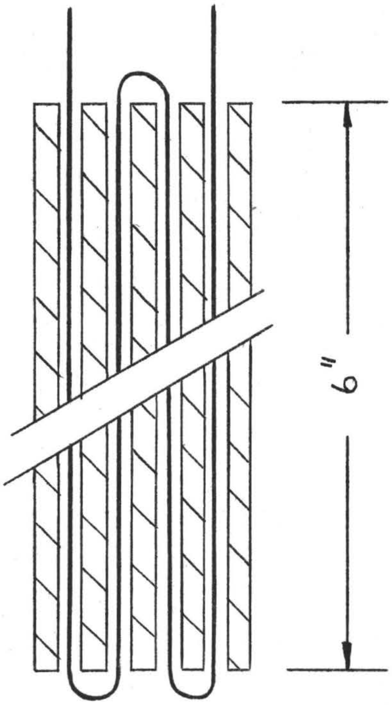

Further information is presented in Table 3 in the Appendix.

FIGURE 21

aluminum plate. The electric heater was surrounded by a transite box 16 in. x 14 in. x 7 in., such that the top surface of the copper block protruded by 1/8 in. Electrical connections to the heating strips were made through the bottom of the box using No. 2 and No. 6 flexible cable, (Plate 2).

To ensure better conduction from the electric heater to the boiling plate the two contact surfaces were machined flat and then tinned with ordinary soft solder. Additional soft solder paste was spread on the copper block surface. The electric heater and boiling plate were then screwed together. After the tin had melted during the first heating operation, the screws were tightened.

2.4 Power Supply

The electric power was controlled by two power units one rated at 7.5 KW, the other at 3 KW. Each power unit was connected to the 240 V, 3-phase power supply.

Since the Hiloset cement becomes conducting at high temperatures, low voltage power was used to avoid shorting difficulties. Power transformers with a 10:1 ratio were used to give a maximum secondary voltage of 24 V. The input voltage to the power transformers was controlled by variacs. For each power unit, three variacs were connected in delta as shown in Figure 22.

To give an indication of the power input the secondary of each power transformer was equipped with a voltmeter 0-30 V and an ammeter 0-5 A. The ammeters were connected via current transformers.

POWER SUPPLY CIRCUIT

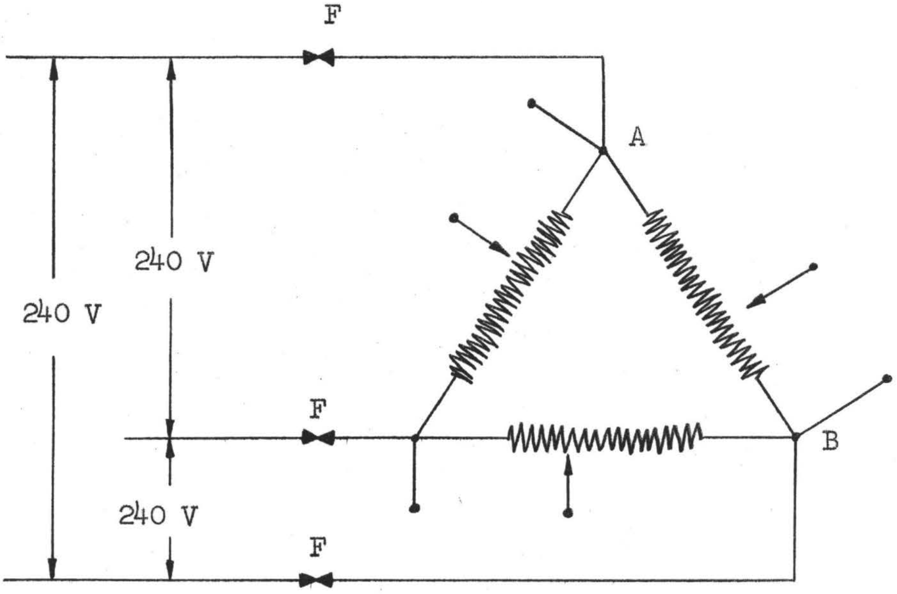

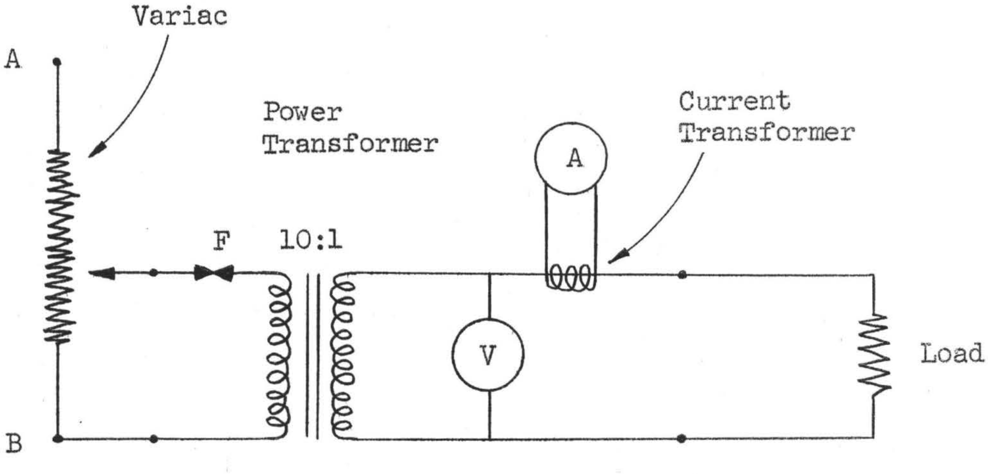

FIGURE 22

2.5 Boiling Plate (chrome-plated)

The material chosen for the boiling plate was copper, since good thermal conductivity was required for maximum boiling on thick plates. As will be seen later it was also necessary to use a good thermal conductor for the heat-flux meters.

The chromed boiling plate is shown in Figure 23. The liquid was introduced over a 2 in. long lip such that the flow could stabilize before reaching the region of destruction. To avoid preheating of the liquid before the thin section was reached, the front section of the boiling plate was insulated from the heater block with transite.

Fifteen surface thermocouples (copper-constantan) were installed into the boiling plate as shown. Nine of these were placed near the thin section, so that three temperatures could be measured in each regime of forced convection, nucleate boiling and film boiling.

Four heat-flux meters were installed into the boiling plate as indicated in Figure 23. These meters are described in detail below.

Grooves were machined on the underside of the boiling plate to act as passages for the thermocouple and heat-flux meter leads.

After installation of the surface thermocouples and heat-flux meters, the boiling surface of the boiling plate was polished with 4/0 emery paper and copper-plated 0.002 in. and chrome-plated 0.001 in.

Surface thermocouples

Philips Miniature thermocouple wire PR 6250 A/01 (copper-constantan) was used to prepare the surface thermocouples. The thermocouple wire was 0.028 in. in overall diameter with a constantan core 0.013 in. in diameter. Insulation between the core and the copper sheath was provided by a thin layer of magnesium oxide.

BOILING PLATE (CHROMED)

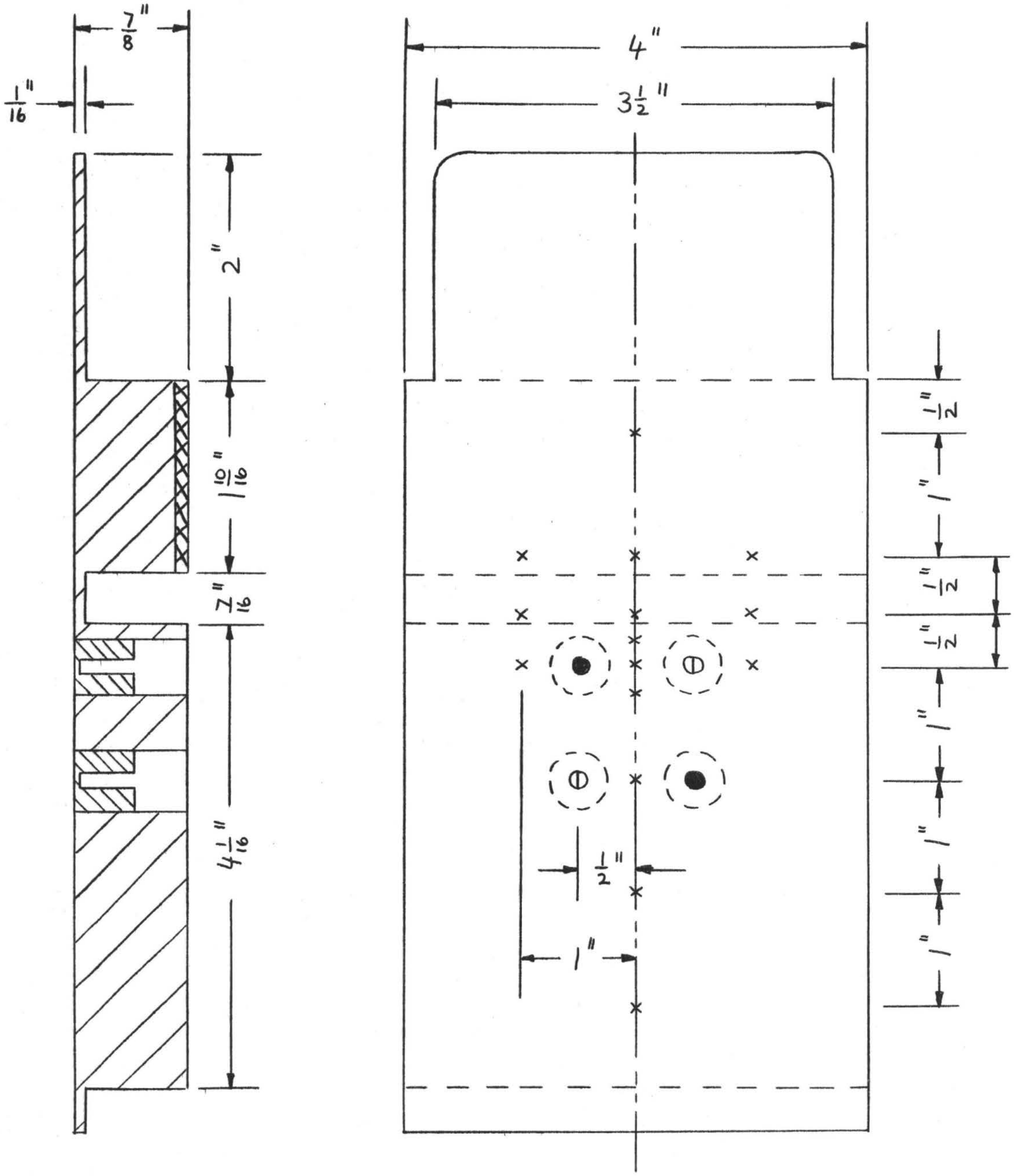

× Surface Thermocouple

● Heat Flux Meter Thin Copper Disc

⦶ Heat Flux Meter Constantan Disc

FIGURE 23

The tip of the thermocouple wire was filed flat and then polished with 4/0 emery paper. After standard cleaning and washing the tip was cold electroplated with a copper cyanide solution at 20 Amps/sq.ft for 24 hours. The tip was immersed about 1/8 in. into the solution. After plating the tip had a maximum diameter of about 1/8 in. Some gas bubbles were usually trapped underneath the thermocouple and reduced the copper deposition at the tip. The thermocouple tip was filed down to 3/32 in. diameter and the head was filed flat. Attempts to estimate the thickness of the thermocouple head with X-ray photography were unsuccessful. It probably varied from 0.005 in. to 0.025 in.

The thermocouple heads were heated slowly in a low Bunsen flame until oxidation began. A check for continuity was made before and after this heating test. Thermocouples not withstanding this treatment twice or which showed circular marks on the flat head were rejected.

The surface thermocouples were press-fitted into 5/64 in. diameter holes in the boiling plate, (Figure 24).

Heat flux meters

The heat flux meters were used to measure the local heat flux to the boiling liquid film. They were based on the design by Gardon (G10). The derivation of the basic equations and the calculation procedures are presented in the appendix.

The heat-flux meters were fabricated from copper cylinders as shown in Figure 25. Two types were made using a copper and a constantan disc to measure high and low heat fluxes respectively. The copper disc was an integral part of the cylinder, while the constantan disc was silversoldered into the cylinder.

SURFACE THERMOCOUPLES

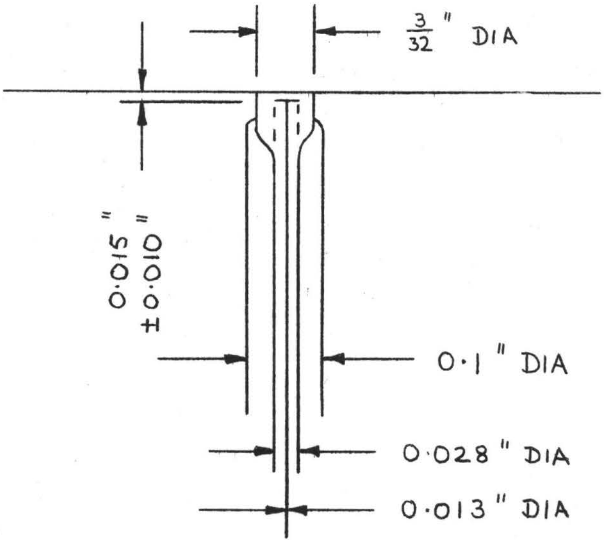

Press-Fitted

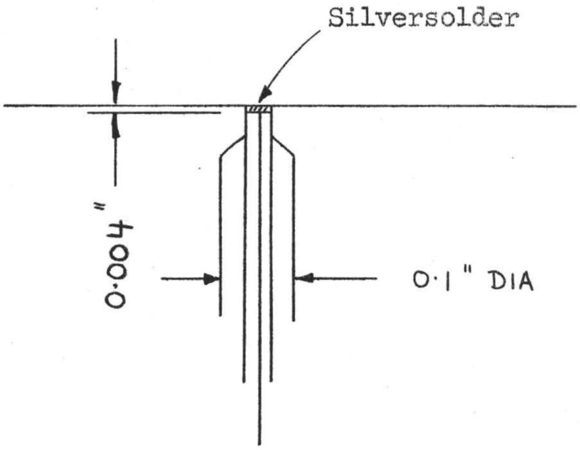

Silversoldered

FIGURE 24

HEAT FLUX METER PLUGS

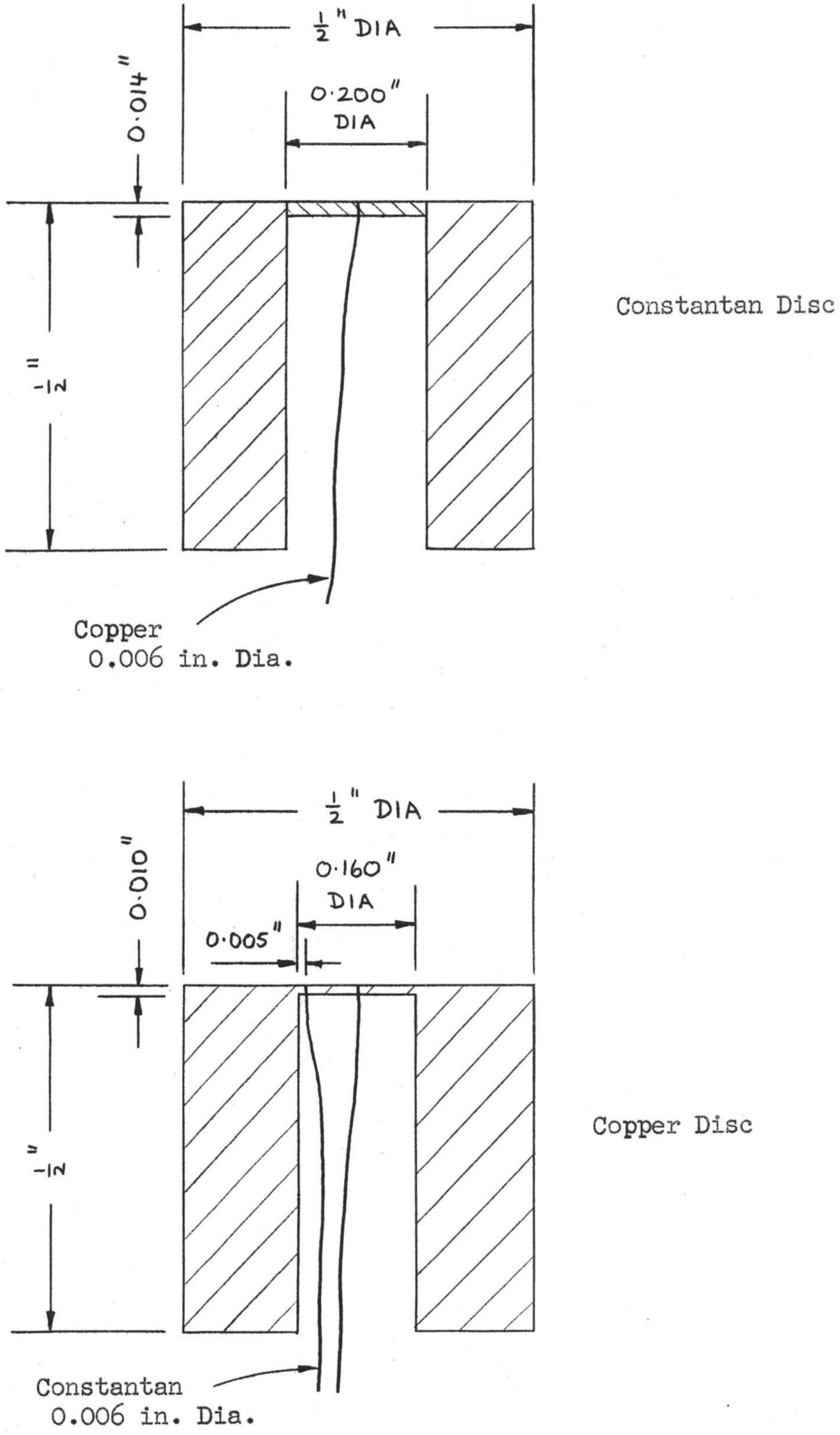

FIGURE 25

The thermocouple wires were silversoldered in holes which were drilled through the entire thickness of the disc. Small diameter thermocouple wires (0.006 in.) were used to reduce conduction errors. Their length was 1/2 in. after which connection to heavier 0.013 in. wire was made. The space behind the disc was filled with Sauereisen cement to hold the thin wires in position and to protect them from oxidation.

The heat-flux meters were press-fitted into 1/2 in. diameter holes in the boiling plate (Figure 23). For the copper disc, the meter was arranged such that the line between the two thermocouple junctions was perpendicular to the direction of flow.

2.2 Boiling Plate (unplated)

This design had similar features as the boiling plate described above except that the heat-flux meters were an integral part of the boiling plate, (Figure 26). The surface thermocouples were also modified and the chrome-plating was omitted.

Difficulty was experienced in drilling small thermocouple holes from the back of the heat-flux meters because of the thickness of the boiling plate. Thus a 1/4 in. deep area was machined out of the boiling surface and a corresponding copper plate (insert) was made up to fit into that space. The heat-flux meters were an integral part of the copper insert; eight surface thermocouples were also installed into the insert. Details of the surface thermocouples and the heat-flux meters are given below.

The insert was silversoldered into the boiling plate by the following method. The contact areas were fluxed and thin strips of silver solder 0.002 in. were placed into the machined area of the boiling plate.

BOILING PLATE (UNPLATED)

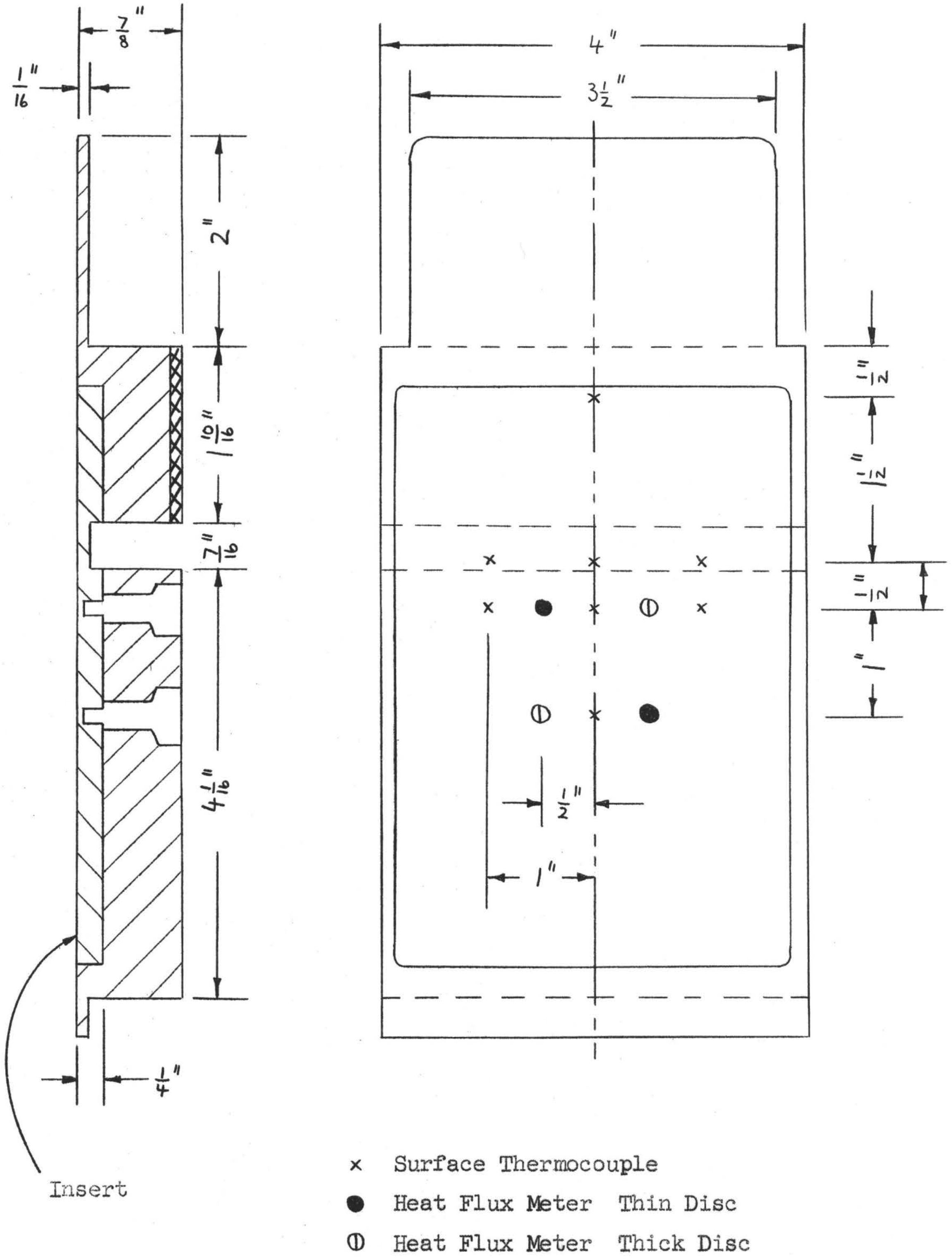

FIGURE 26

The insert, with all thermocouple wires for the heat-flux meters and surface temperature measurement already installed, was placed into the boiling plate. The assembled boiling plate was placed in a cold furnace, which was purged with argon in order to displace the air. Oxidation of the copper block before the silver-solder melted was thus avoided. The furnace was heated to 1400°F for 15 minutes and the boiling plate was allowed to cool. Argon was passed into the furnace during the entire heating and cooling operation. This method also served to silver-solder all the thermocouple junctions in the insert.

The boiling surface was ground flat to remove excess silver solder; 0.006 in. was taken off the entire surface during this operation.

Surface thermocouples

Philips Miniature thermocouple wire, as described above, was used. The end of the wire was filed flat and a junction was formed by dipping the tip into molten silver-solder. The wire was placed into a 0.030 in. hole in the boiling plate and the tip was depressed 0.010 in. beneath the boiling surface. The cavity was filled with silver-solder filings and flux. The surface thermocouples were then silversoldered in the argon-purged furnace. After grinding 0.006 in. off, the surface thermocouples were 0.004 in. beneath the boiling surface, (Figure 24).

Heat flux meters

The heat flux meters are shown in Figure 27. Two sizes were made using a thick and a thin copper disc to measure high and low heat fluxes respectively. An extra thickness of 0.006 in. was allowed for initially, to compensate for the grinding operation.

HEAT FLUX METERS

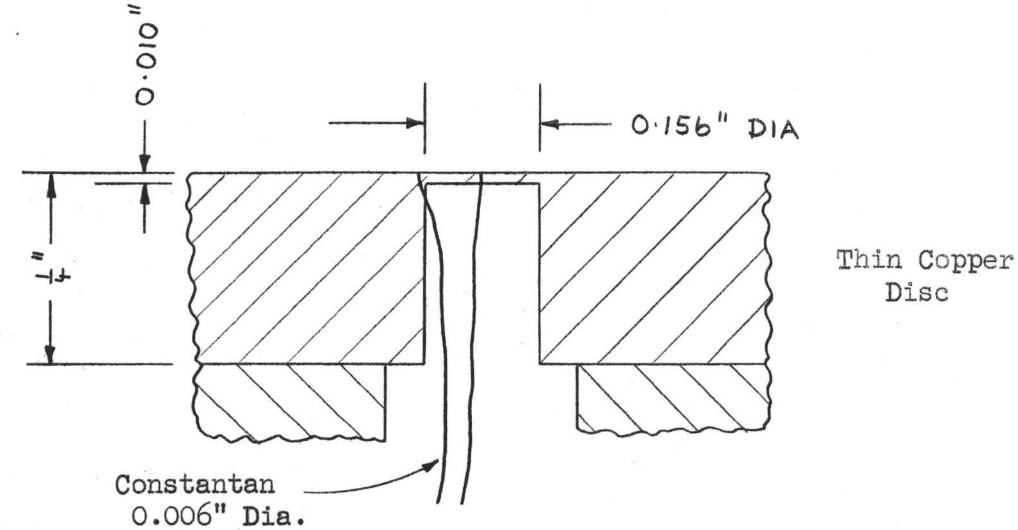

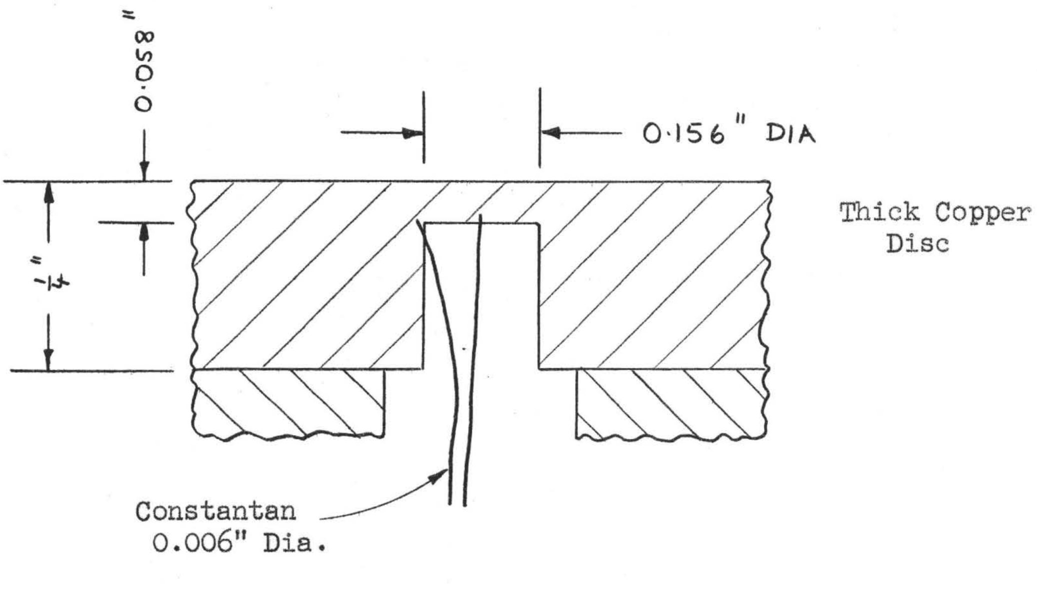

FIGURE 27

The thermocouple leads used were Philips Miniature thermocouple wire, which had been reduced in size from a diameter of 0.013 in. to 0.006 in. for 1/2 in. length by electro-deposition. The holes for the thermocouple wires (0.010 in. diameter) were filled with silversolder filings and flux. The copper was lightly punched to hold the thermocouple wire in its hole. The thermocouples were then ready to be silver-soldered in the furnace. For the thin disc the wires penetrated the entire disc, while for the thick disc the wires were inserted for about 0.015 in. The thermocouple wires were arranged such that the line between the two junctions was perpendicular to the flow of liquid.

The bottoms of the discs were insulated with cork and the remaining part of cavity was filled with Sauereisen cement to hold the thermocouple leads firmly.

3. Instrumentation

Measurements of surface temperature and heat flux were taken and also some photographic recordings were made.

3.1 Honeywell Visicorder

A Honeywell Visicorder 906 c was used to measure continuously one heat flux and one surface temperature. A surface thermocouple was chosen such that the line between the surface thermocouple and the heat-flux meter was perpendicular to the flow of the liquid film. The circuit is indicated in Figure 28.

Since the voltages encountered in the heat-flux meter circuit were low (0 - 1 mV), other thermocouple junctions were placed into a thermally insulated box. For the heat-flux measurement, a sensitive

VISICORDER CONNECTIONS

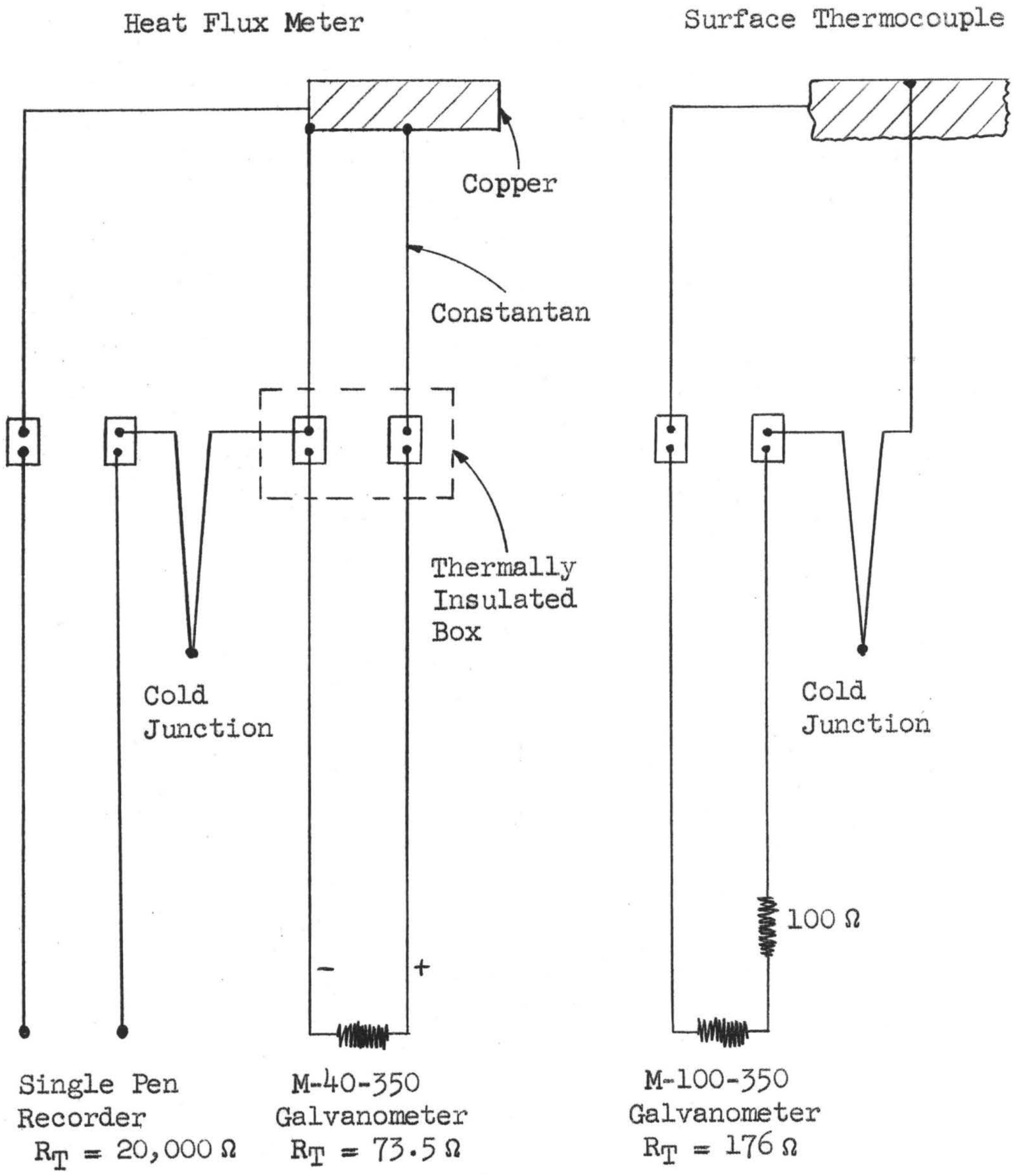

FIGURE 28

galvanometer M-40-350 without a damping resistor was used, to obtain full scale deflection in the range. The galvanometer was calibrated by measuring the voltage across the galvanometer with a single pen recorder, when operating with a constant heat flux under steady-state conditions. Further discussion is presented in the appendix.

The surface temperature was measured with a less sensitive galvanometer M-100-350 and a 100 Ω series resistance, to obtain greater sensitivity in the range used.

The chart speed used was 0.4 in./sec. and readability of the paper chart was ±0.2 mm (±3000 BTU/hr.sq.ft).

3.2 Honeywell Recorders

A single-pen Honeywell recorder was used to measure the temperature at the disc periphery of the heat-flux meter, (Figure 28). The Visicorder could not be used for this purpose because the low input impedance of a galvanometer affected the circuit of the heat-flux meter. The single-pen recorder had a high input impedance and thus did not affect the circuit of the heat-flux meter. The span used was 0-10 mV with a chart speed of 0.2 in./sec. Readability from the chart was ±0.02 mV (±0.5°F).

A 12-point Honeywell recorder was used to measure the surface temperatures of the boiling plate, the liquid temperatures and the copper-block temperature. The span used was 0-10 mV with a chart speed of 60 in./hr. Readability from the chart was ±0.05 mV, (±1°F).

3.3 High Speed Photography

A Fastax camera WF 4 ST with a synchronised stroboscope was used for exposing high speed Kodax Tri-X Reversal film (160 ASA). The camera was fitted with a 154 mm lens and extension tubes. The speed of the camera (6000 frames/sec maximum) was controlled by the Fastax Goose WF 358.

The stroboscope was a high pressure Xenon discharge tube which was triggered by a pick-up in the camera. The flash lamp had an intensity of 3 joules per flash; because of this large heat generation the number of flashes was limited to one thousand. A thousand consecutive flashes corresponded to about 25 ft. of film. The maximum frequency of the stroboscope was 6000 flashes/sec. and the flash duration was 3-4 μsec.

At camera speeds up to 2000 frames/sec. sufficient illumination could be provided by three 375 W spot lights. However this speed is not fast enough to resolve the activity in the region of destruction of the boiling film.

An optical system was devised for the Fastax camera in order to view the liquid film from two perpendicular directions simultaneously, (Figure 29). It consisted of a beam-splitter, two prisms and two convex lenses. The beam-splitter was masked such that one half transmitted light unreflected, while the other half reflected it through 90°. The achromatic lenses focussed the images on the centre of the beam-splitter. The camera was then focussed on the adjacent images of the object in the beam-splitter. The optical system was attached to the tiltable plate, which supported the boiler assembly.

Good illumination of the liquid film, such as to give high contrast, was difficult to achieve. Reasonable illumination however was obtained for both plan and side views by passing light onto the liquid film from a direction opposite to the film flow and at the smallest possible angle (30°) with the boiling surface.

OPTICAL ARRANGEMENT FOR HIGH SPEED PHOTOGRAPHY

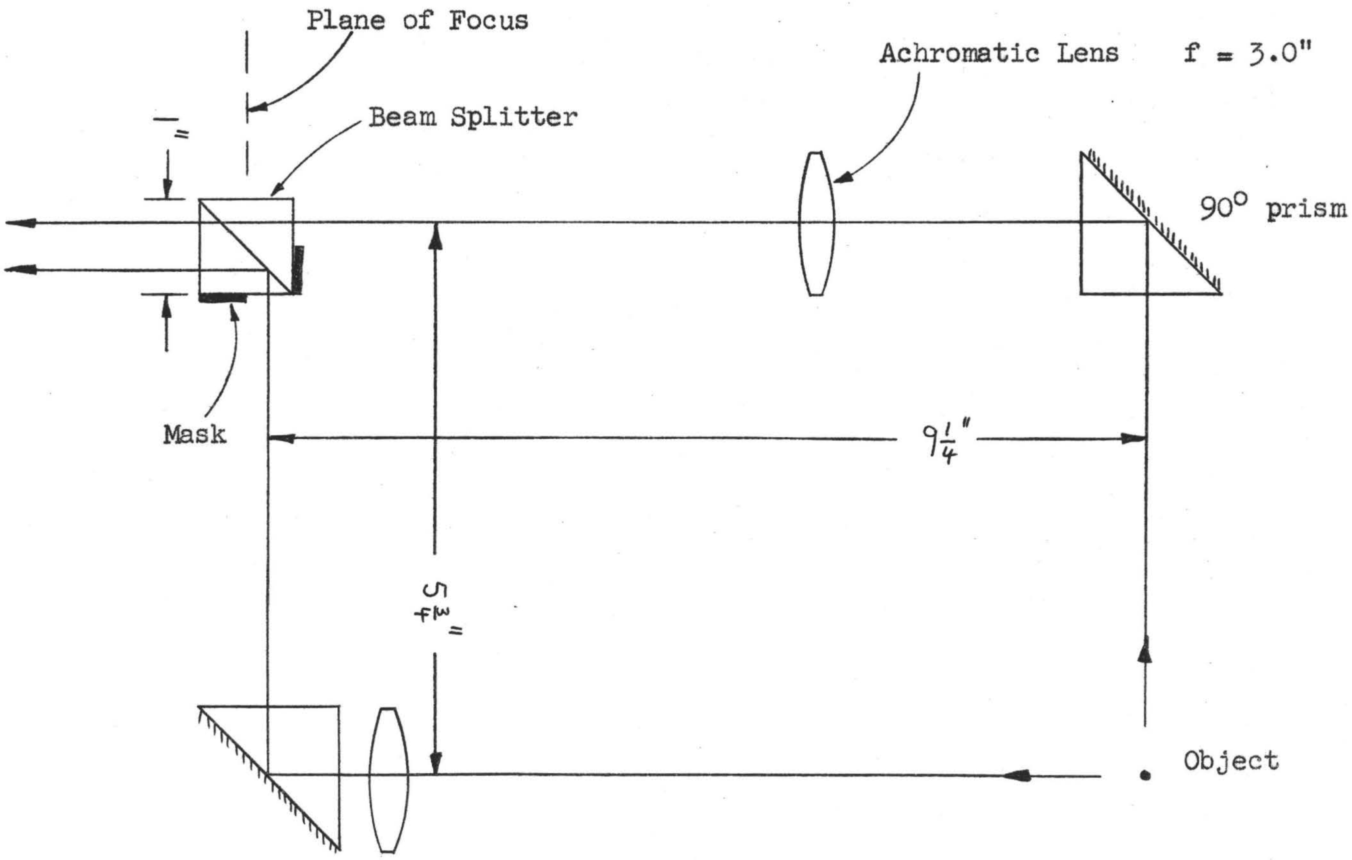

FIGURE 29

3.4 Instrument Synchronisation

The camera, visicorder and the two Honeywell recorders were synchronised by a timing circuit, (Figure 30). The Honeywell recorders were equipped with event timers, which were operated together with the Visicorder chart switch A.

The Fastax Goose Control was equipped with a camera and an event timer, which determined the camera running time and the stroboscope flashing time respectively. The event timer was set to start the flash stroboscope a certain time after the camera had started. The event and camera timers stopped simultaneously. The sequence was started by the camera timer switch B.

The event timer was also connected to a galvanometer in the Visicorder, in order to determine when the film was exposed in relation to the heat flux. The camera under these circumstances was focussed on the heat-flux meter. The electrical connection from the event timer was made using a 10:1 step-down transformer with a separate secondary winding. The output was rectified and connected to the galvanometer (M-1650) and a 7000 Ω series resistance.

3.5 Still Photography

For the plan views an Exacta Camera was used with a 102 mm lens and extension bellows. Kodax Tri-X film (160 ASA) was exposed for 1/150 sec.

For the side-views a Pentax camera was used with a 135 mm lens and extension bellows. Kodax Tri-X film (160 ASA) was exposed for 1/500 sec.

Illumination from the sides was provided by two 300 W photo-spots.

TIMING CIRCUIT

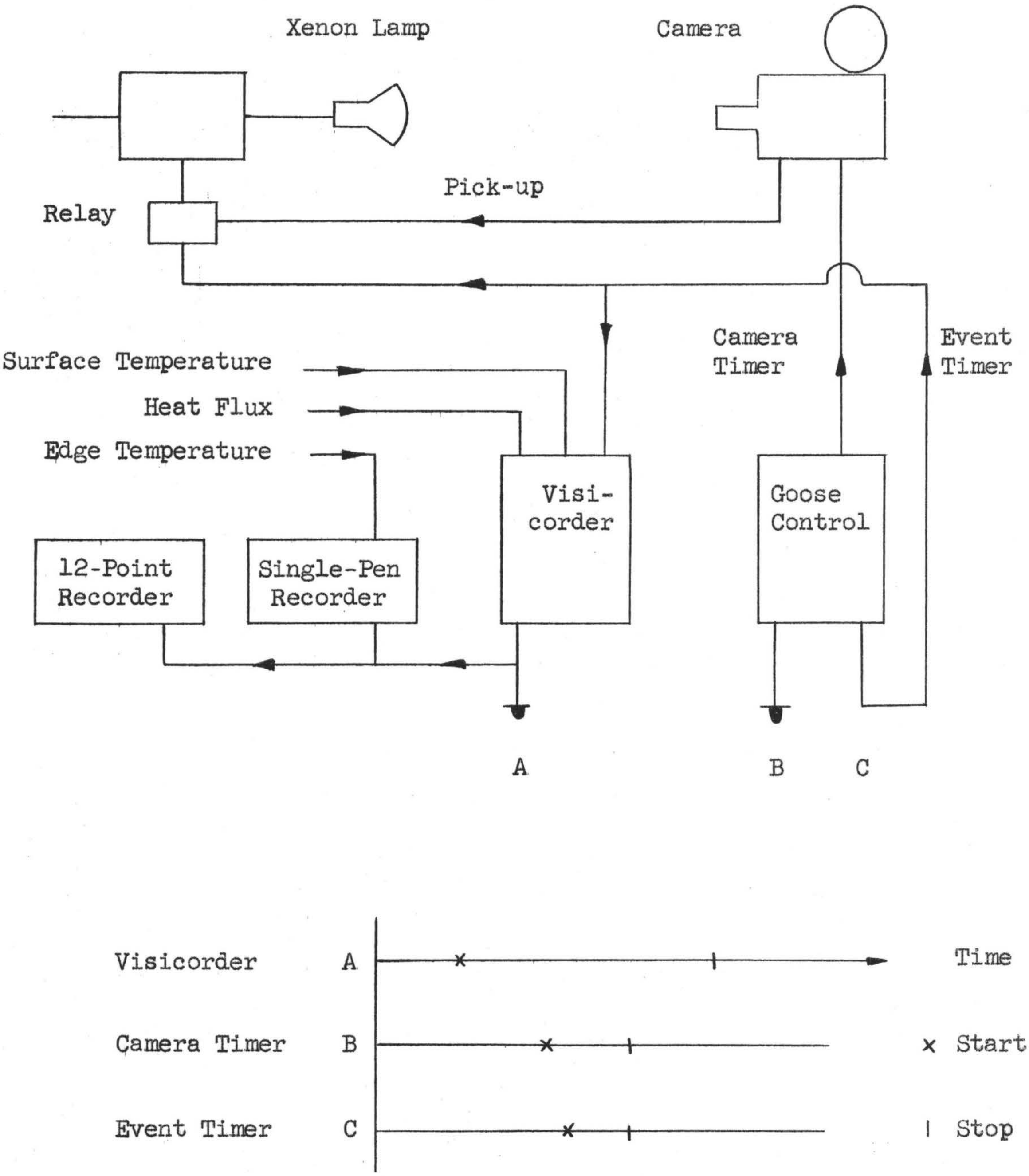

FIGURE 30

3.6 Film Thickness Gauge

The liquid film thickness was measured with a probe, which was attached to a micrometer. Micrometer readings were taken when the probe just contacted the free surface of the liquid film and when the probe touched the boiling plate. The first reading was indicated by the first formation of small ripples on the liquid film and the second was indicated by electrical contact between the probe and the boiling plate. The accuracy of the film thickness gauge was ±0.002 in.

D. EXPERIMENTS

The major concern of this study was the measurement of the boiling heat flux to liquid films with heat-flux meters. However, these heat flux meters needed calibration under boiling conditions and hence pool boiling experiments were performed. These pool boiling results could then be compared to the literature and the performance of the heat flux meters could be evaluated. Four types of experiments were thus carried out

(i) steady-state film flow (chromed boiling plate)
(ii) unsteady-state film flow (both boiling plates)
(iii) steady-state pool boiling (unplated boiling plate)
(iv) unsteady-state pool boiling (unplated boiling plate)

The two boiling plates were used for the experiments as indicated above.

1. Steady-State Film Flow

At the beginning of this project steady-state experiments were carried out with the chrome-plated boiling plate using distilled water and certified grade benzene. By steady-state it is meant that a region of destruction is obtained which stays stationary on the thin section, (Figure 16). Under these conditions the temperature profile along the centre line of the boiling plate remained constant with time. Adjustments to achieve steady-state conditions were made by changing the electrical heat input.

Still and high-speed photography were used to record a side view of the hydrodynamic phenomenon for varying flow rates, liquid temperatures and angles of incline. The thickness of the liquid film was also measured.

2. Unsteady-State Film Flow

Unsteady state experiments here refer to the condition when the region of destruction no longer is stationary on the thin section, but moves in the direction of flow. This behaviour is obtained by reducing the heat input to a value below that required for the steady-state condition. When the region of destruction passed over the heat-flux meters the entire boiling curve for film flow could be measured.

The apparatus was inclined at the desired angle. The liquid temperature was adjusted by means of the electric heater or cooler in the pump return line. The boiling plate was then heated to about 450°F for the benzene runs and to about 550°F for the water runs. The electrical power was then cut off. The liquid was passed over the boiling plate at the desired flow-rate. The two Honeywell recorders were started. When the region of destruction began to move from its position on the thin section the Visicorder was started and kept running until no more boiling could be observed on the heat-flux meters. Two flow rates (4.5 and 7.5 lb/min.) and three inlet temperatures were selected for each angle of inclination (90°, 60° and 30°) of the boiling plate.

During some experiments still photographs were taken showing a plan view of the boiling liquid film. A few high speed films were taken when the heat-flux meter indicated the maximum heat flux.

3. Steady-State Pool Boiling

The apparatus was adjusted to the horizontal position and modified to make a rectangular pool boiler 4 in. x 3 1/4 in. with a maximum liquid depth of 1 3/4 in. This was achieved by inserting two aluminium plates into the boiling plate enclosure and sealing them on the outside only with high-temperature silicon rubber cement, (Figure 31). The heat-flux meter was roughly central in the pool boiling area. The apparatus was sealed everywhere except for the vapour outlet line, where slight suction was applied. The liquid depth in the pool boiler was kept at about 1 1/2 in. by adding fresh liquid continuously through a stoppered hole in the top window. The liquid was added from a heated glass vessel. The temperature of the fresh liquid and the pool temperature were measured with copper-constantan thermocouples.

In order to increase the accuracy of the heat-flux measurement, the output from the heat-flux meter was connected through a Honeywell Deviation Amplifier to a galvanometer in the Visicorder, (Figure 32). The gain on the amplifier was set to take an input of ±0.25 mV. The set point unit was adjusted to give a constant voltage of -0.25 mV. The output from the amplifier was connected to a M-1000 galvanometer in the Visicorder. A series resistance of 220 Ω was used to give a full-scale deflection for the 4V output.

The power from the electrical heaters was severely limited due to large contact resistances which developed as a result of oxidation at the heater connections. Thus only benzene was used in these experiments.

The boiling plate was cleaned with 3/0 emery paper and the pool boiler was filled with hot benzene. The electrical heaters were then switched on. When the heat flux and the surface temperature as indicated by the Visicorder and single-pen recorder remained constant for

POOL BOILER

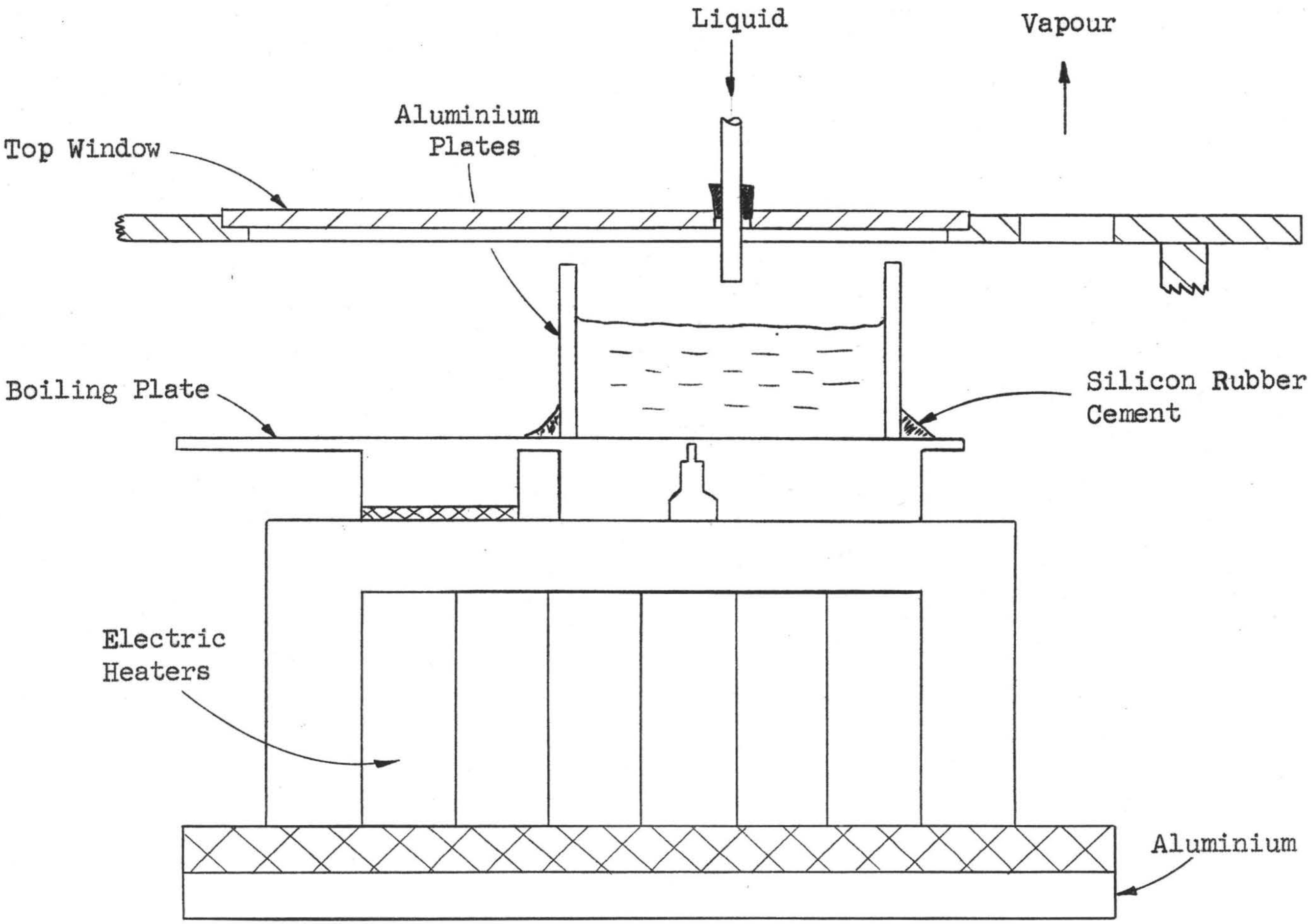

FIGURE 31

CONNECTION OF DEVIATION AMPLIFIER AND SET POINT UNIT

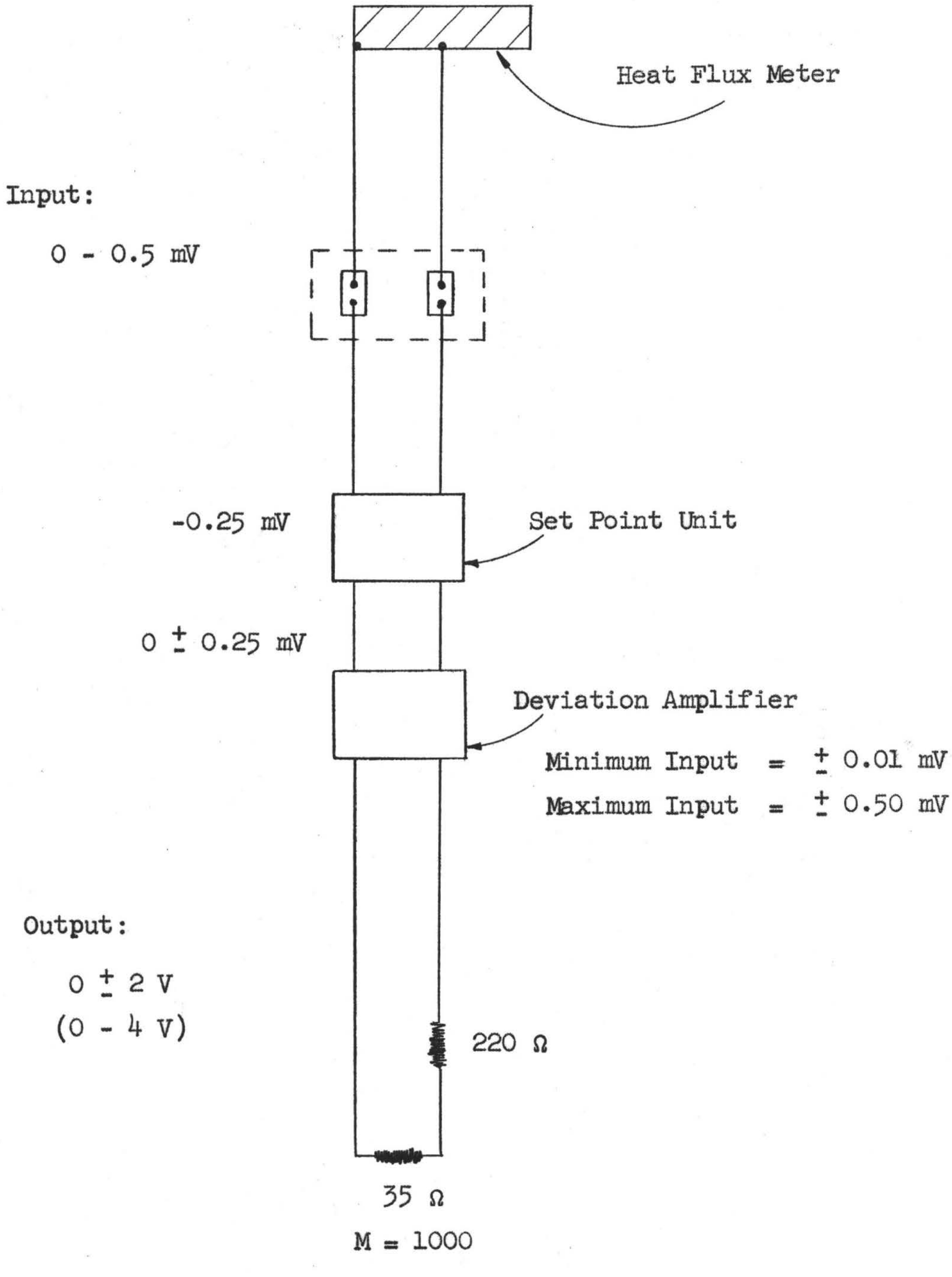

FIGURE 32

15 minutes, vapour collections were made and timed. The electrical power input was also noted.

The heat input was increased to obtain further steady-state measurements.

4. Unsteady-State Pool Boiling

The boiling plate was heated to 450°F. The heat input was then switched off. Certified grade benzene or distilled water was used in these experiments. The pool boiler was filled with the liquid through the stoppered hole. The liquid then cooled the boiling plate through all the boiling regimes starting with film boiling. Measurements of heat flux and surface temperature were taken continuously with the Visicorder and the single-pen recorder respectively. Liquid was added continuously to the pool boiler to keep the liquid level constant.

E. RESULTS

The results presented below have been obtained with two plates: a chromed boiling plate and an unplated boiling plate. Preliminary data were obtained with the chromed boiling plate. However these results were in poor agreement with the expected values. After some time these heat-flux meters failed due to oxidation around the edges of the plugs. The use of this plate was discontinued and a new unplated boiling plate with integral heat-flux meters provided good results.

1. Steady-State Film Flow

Essentially qualitative observations have been made of the hydrodynamic behaviour of the liquid film using the chromed boiling plate.

The liquid film was uniform before reaching the region of destruction. Surface ripples existed due to the edge effects from the teflon and the stainless steel gauze. At 90° incline of the boiling plate the liquid film was not very uniform in film thickness. The film thickness measurements for water and benzene films at a boiling plate inclination of 30° are shown in Figure 33. The measurements were taken in the entry zone of the liquid film where the equilibrium film thickness had not been established. It should also be noted that with the present method the maximum film thickness was measured. Both of these effects account for the deviation from the equation proposed by Brauer (B16). The liquid film width has been taken at 3 in.

On the thin section of the boiling plate nucleate boiling of the film occurred in a rather narrow band of 1/4 in. The bubble size increased

FILM THICKNESS MEASUREMENTS

REF.: B16

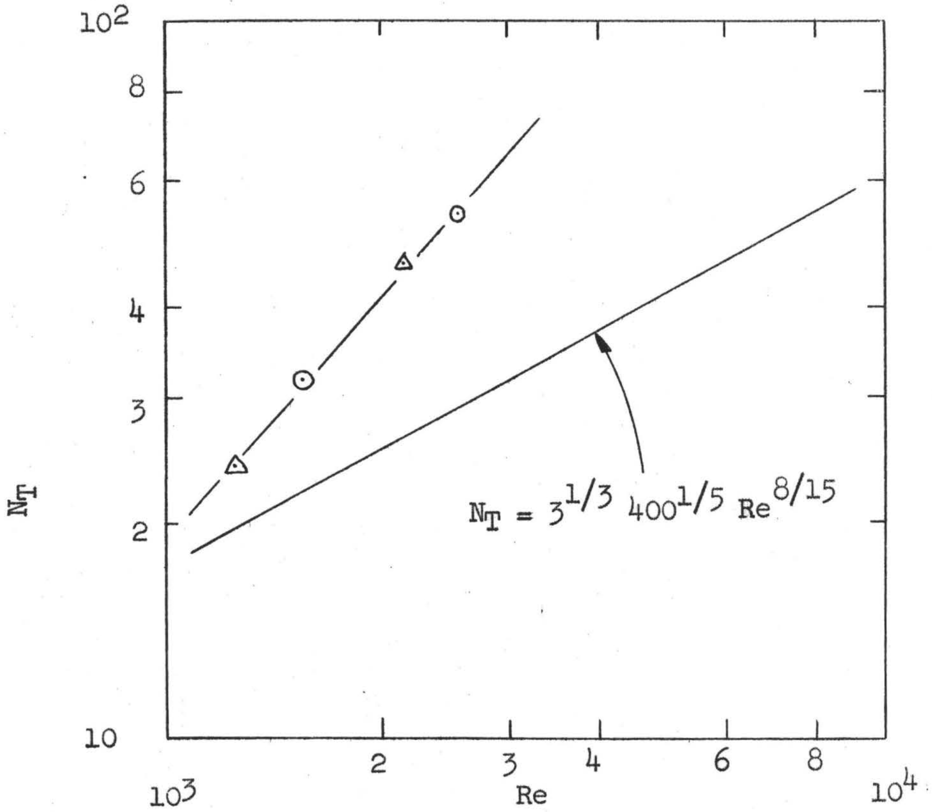

⊙ Water, 200°F, 30° incline

4.80 lb/min.	b = 0.035 in., Re = 1540
8.00 lb/min.	b = 0.059 in., Re = 2560

△ Benzene, 162°F, 30° incline

4.30 lb/min.	b = 0.031 in., Re = 1260
7.25 lb/min.	b = 0.060 in., Re = 2160

FIGURE 33

in the direction of flow. At the region of destruction vigorous activity took place, which was difficult to examine with the high-speed films taken at 3000 p.p.s. The liquid separated from the boiling plate with some spray formation near the end of the thin section, (Plate 3a).

The break-up behaviour of the liquid film depended upon the type of liquid, flowrate and subcooling. Benzene formed more liquid streams than water. The spray formation from a water film was much more than that from a benzene film.

At flow rates of 1.5 lb/min. or less the entry section was not wetted uniformly and dry patches tended to form in the liquid film. The break-up region did not discharge a continuous stream, but would accumulate liquid into drops, (Figure 34 and Plate 3c). These drops were regularly ejected from the break-up region. Flow rates of about 3 lb/min. caused the drops to coalesce into irregular streams. At flow rates of about 7.5 lb/min. the spray formation was reduced and the length of the nucleate boiling section was reduced slightly. Small triangular liquid sheets formed, which were particularly noticeable with water. The liquid sheets contracted into liquid streams. At flow rates of about 12.0 lb/min. the liquid sheets joined into a single sheet, which contracted into a single stream, (Figure 34).

Subcooling of the liquid has the effect of stabilizing the liquid film. The length of the nucleate boiling section and the bubble size was reduced. The boiling activity was much suppressed; thus the liquid film was less disturbed and separated smoothly from the boiling plate, (Plate 3b). There was a greater tendency for liquid sheets to form.

SIDE VIEW OF WATER FILMS

30° INCLINE

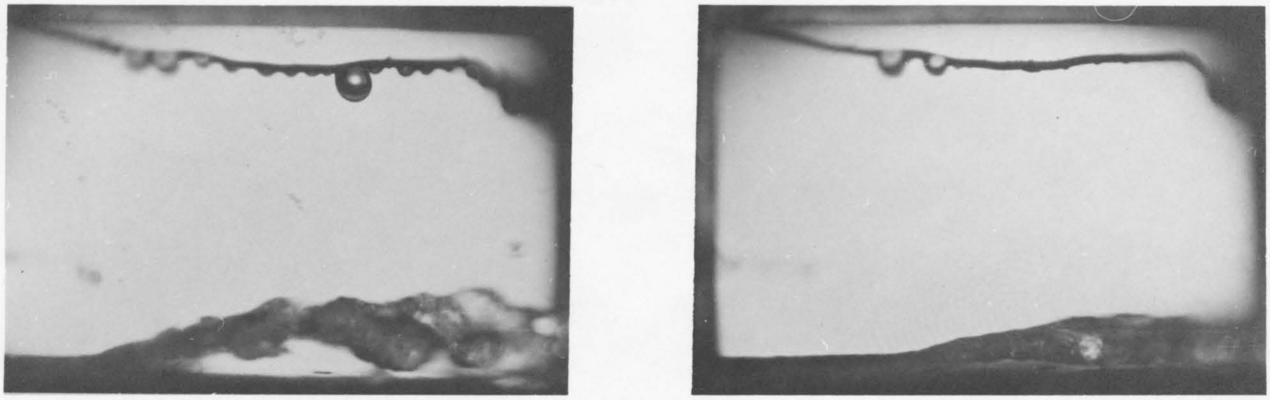

a) STEADY STATE
4.80 LB/MIN; 187°F

b) STEADY STATE
4.80 LB/MIN; 158°F

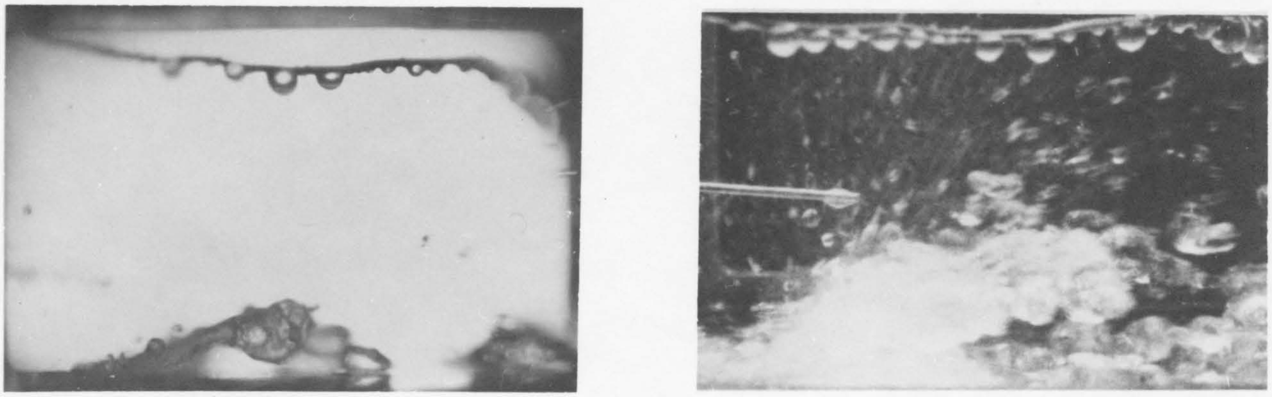

c) STEADY STATE
1.60 LB/MIN; 186°F

d) UNSTEADY STATE
2.50 LB/MIN; 202°F

PLATE 3

EFFECT OF FLOW RATE ON LIQUID FILM DESTRUCTION

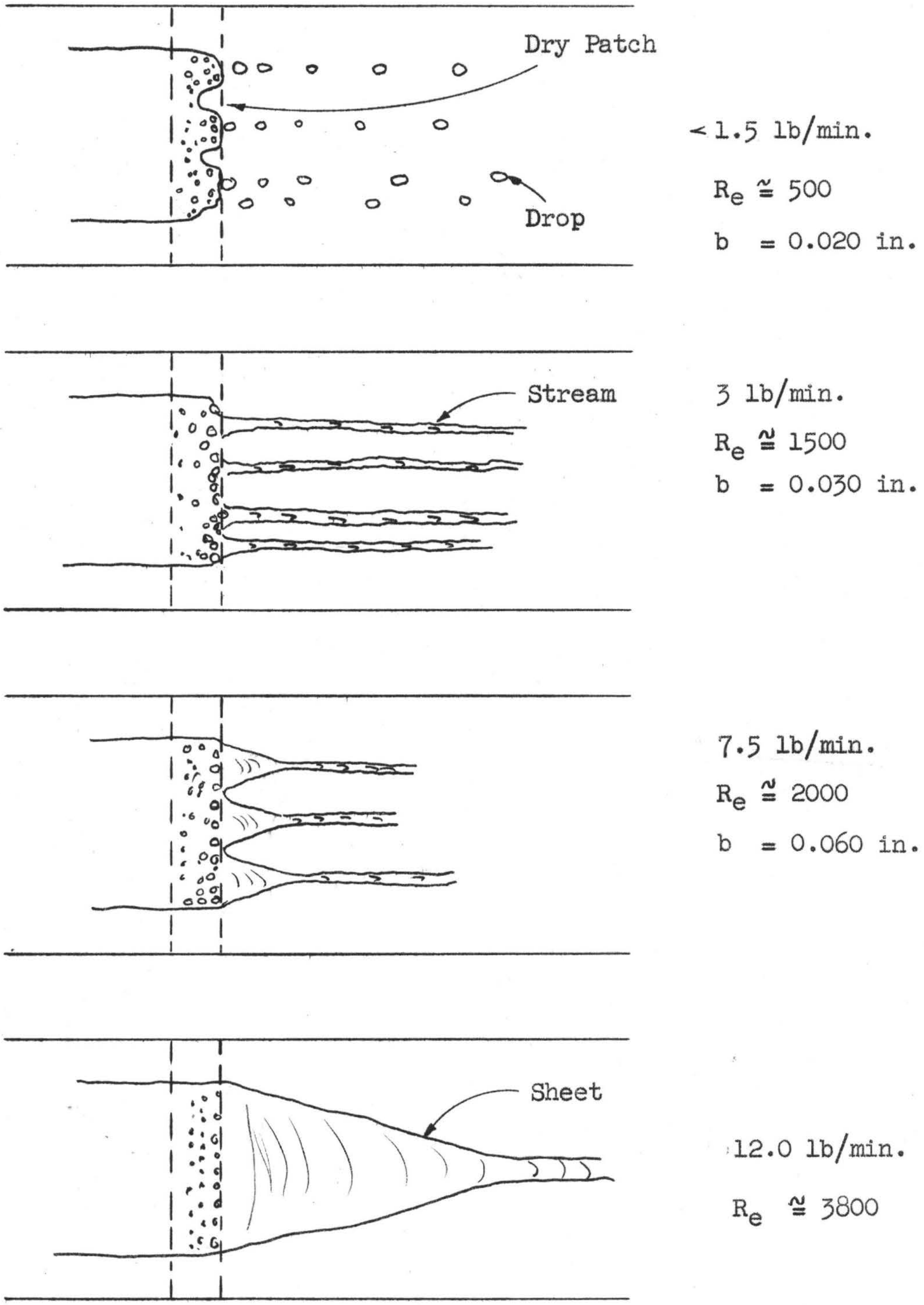

FIGURE 34

The angle of separation of the liquid from the boiling plate was observed to vary with the type of liquid and the subcooling. Water always separated at a greater angle than benzene. Increasing subcooling decreased the angle of separation, (Plates 3a and 3b). An effect due to flow rate was not observed. A large temperature gradient in the boiling plate increased the angle of separation.

A representative temperature profile along the centre line of the boiling plate is shown in Figure 35 for a water film. The temperatures depend upon the subcooling and angle of inclination of the boiling plate. Both of these determine the distance between the liquid streams and the boiling plate, i.e. the vapour film thickness in forced convection film boiling. At angles of inclination less than 60° the liquid fell back on the boiling plate. Greater cooling occurred at such locations.

It was noted that the thermocouples on the right of the boiling plate indicated lower surface temperatures than the left-hand thermocouples. The difference was of the order of 5°F and could perhaps be attributed to the grooves for the thermocouple leads since all the leads passed out at the right-hand side of the boiling plate, (Plate 2).

2. Unsteady-State Film Flow

In unsteady-state film flow the break-up region moved down the boiling plate and passed over the heat-flux meters. With this type of experiment the heat flux to the boiling film was measured in all the boiling regimes. Both boiling plates were used. Some photographic records were also made.

STEADY-STATE TEMPERATURE PROFILE ALONG CENTRE OF BOILING PLATE

WATER, 195°F, 3.3 lb/min., 30° INCLINE

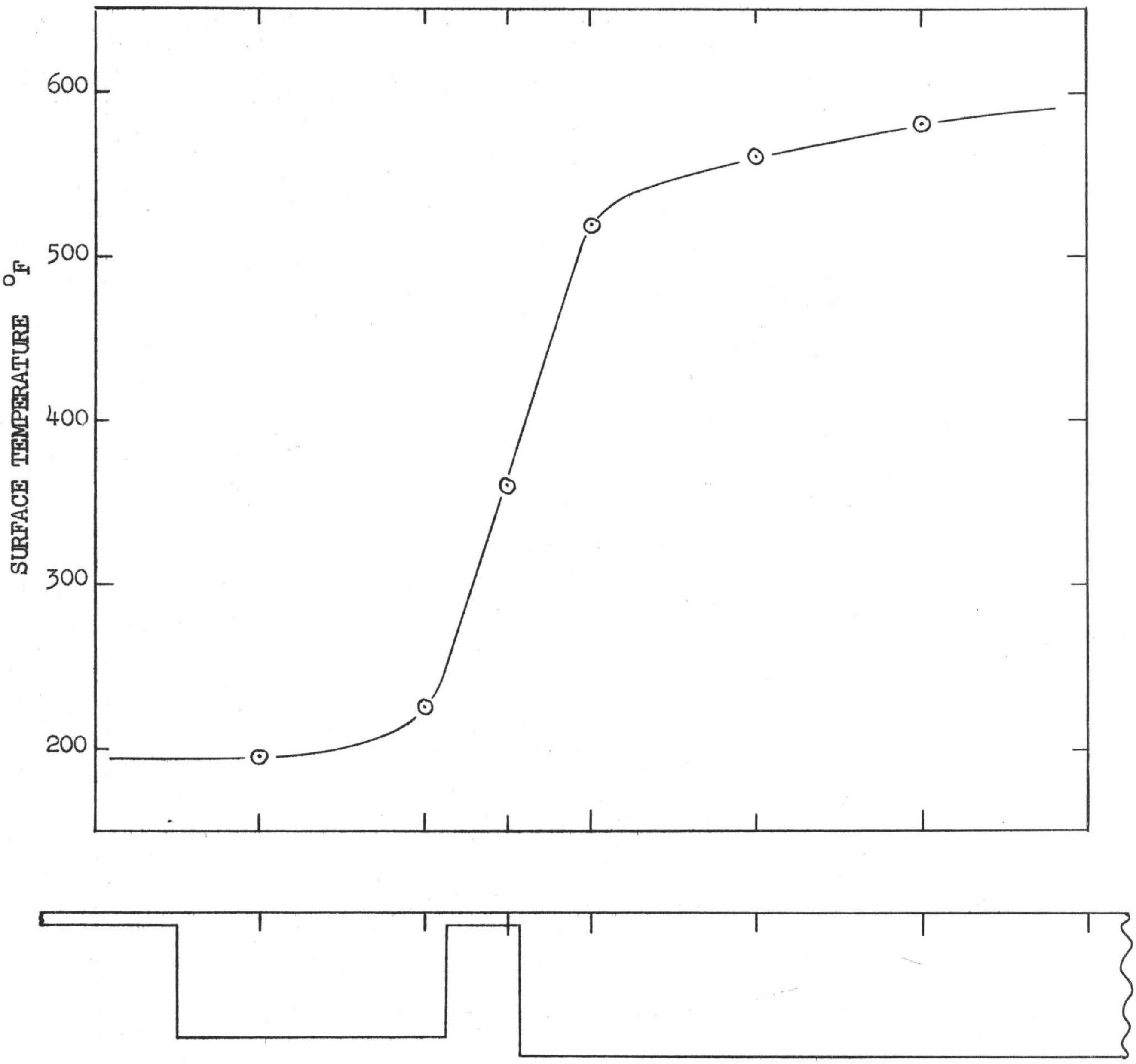

FIGURE 35

UNSTEADY-STATE TEMPERATURE PROFILE ALONG CENTRE OF BOILING PLATE

BENZENE, 168°F, 7.25 lb/min., 60° INCLINE

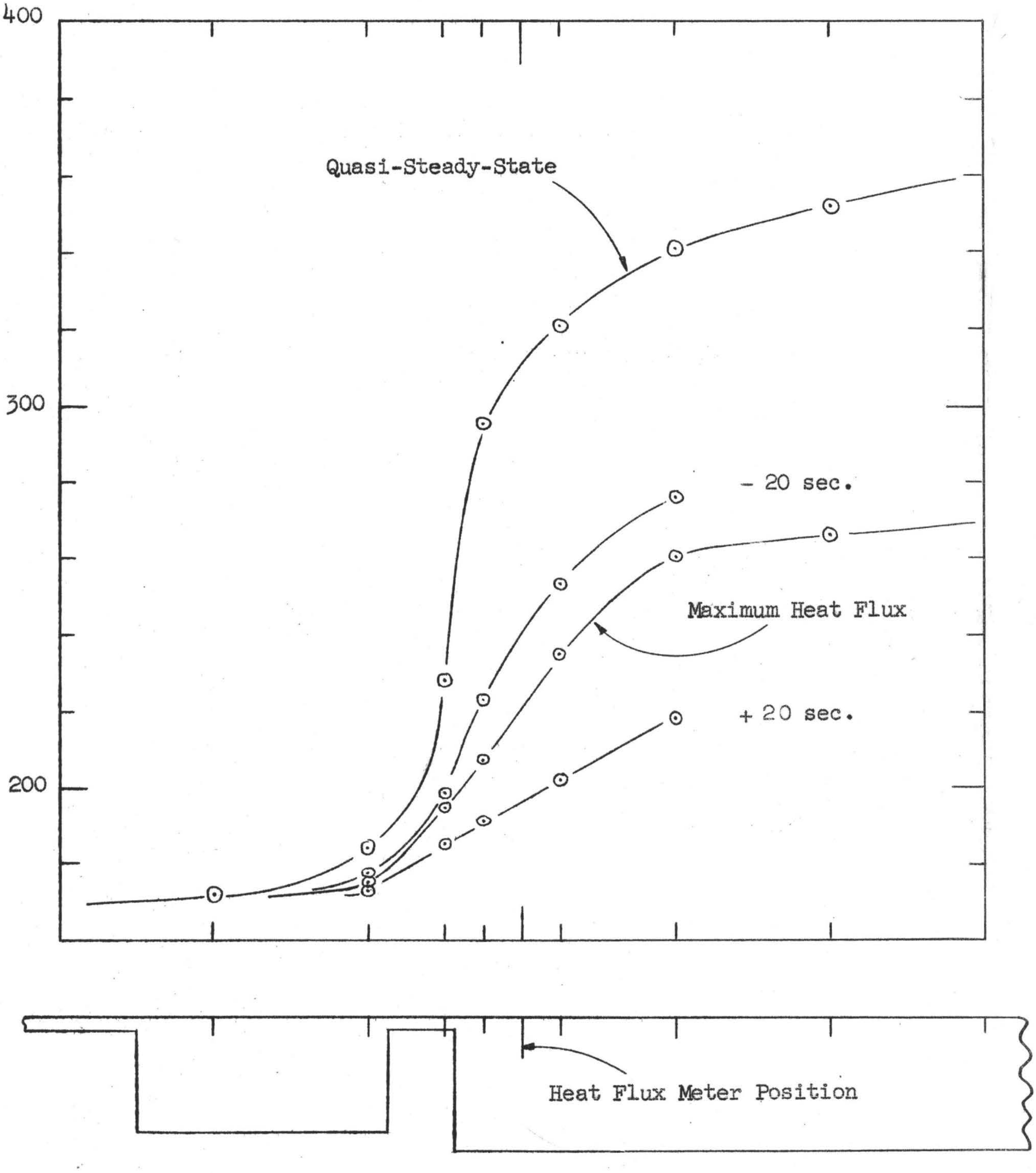

FIGURE 36

2.1 Hydrodynamic Behaviour

The break-up region would initially be fixed on the thin section of the boiling plate as in the steady-state experiments. When the surface thermocouple, which was 2 1/2 in. from the front lip, indicated a temperature of 275°F the break-up region of benzene would advance. For water the same occurred after the temperature had decreased to 450°F.

The temperature gradient along the centre line of the plate was initially high but decreased with time, (Figure 36). The angle of separation between the liquid and the solid decreased noticeably and when it almost reached zero the break-up region advanced. At large flow rates when liquid sheets were formed (Figure 34) part of the sheets looked milky, which was probably due to transition boiling. As the region of destruction advanced the nucleate boiling section of the film would expand along the plate, while the forced convection regime remained fixed on the thin section of the boiling plate. The noise level and the spray formation increased considerably, (Plate 3d). The increasing area of the nucleate boiling section caused increasing destruction of the liquid film.

The destruction of a boiling water film is shown in Plate 4. The water temperature was close to the boiling point. Many globules of water were formed during the destruction. This observation was confirmed by high-speed photography at 3000 p.p.s. The formation of these globules probably arose from perforations in the liquid film. The perforations could have been caused by bubbles bursting through the liquid film. Plate 5 shows a different kind of behaviour when the water was subcooled. The subcooling inhibited the boiling activity and smooth liquid sheets formed instead. Plate 6 shows

PLAN VIEW OF A WATER FILM

UNSTEADY STATE; 30° INCLINE

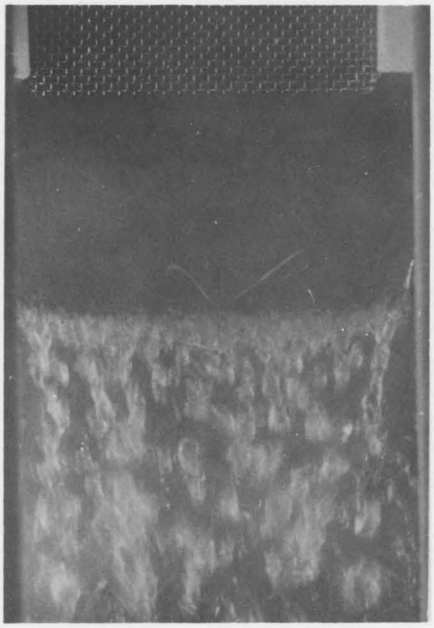

0 SEC; 4.80 LB/MIN; 201°F

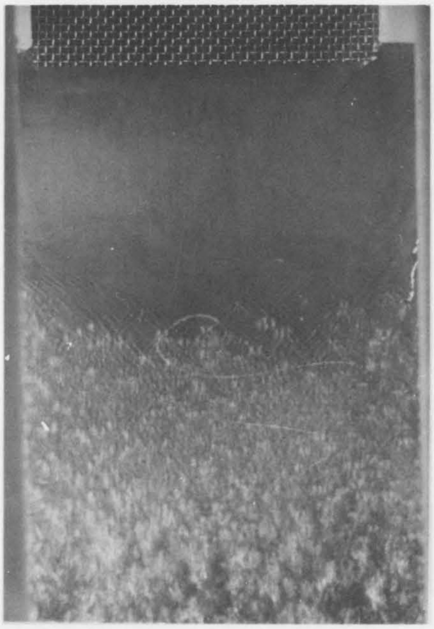

10 SEC; 4.80 LB/MIN; 201°F

PLATE 4

PLAN VIEW OF WATER FILMS
UNSTEADY STATE; 30° INCLINE

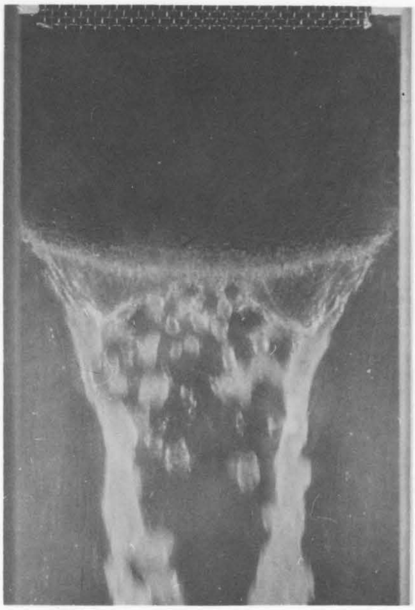

4.80 LB/MIN; 133°F

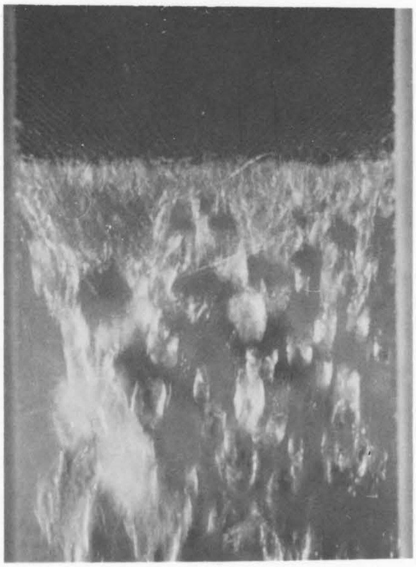

8.00 LB/MIN; 178°F

PLATE 5

HEAT FLUX METER POSITION

UNSTEADY STATE; 90° INCLINE

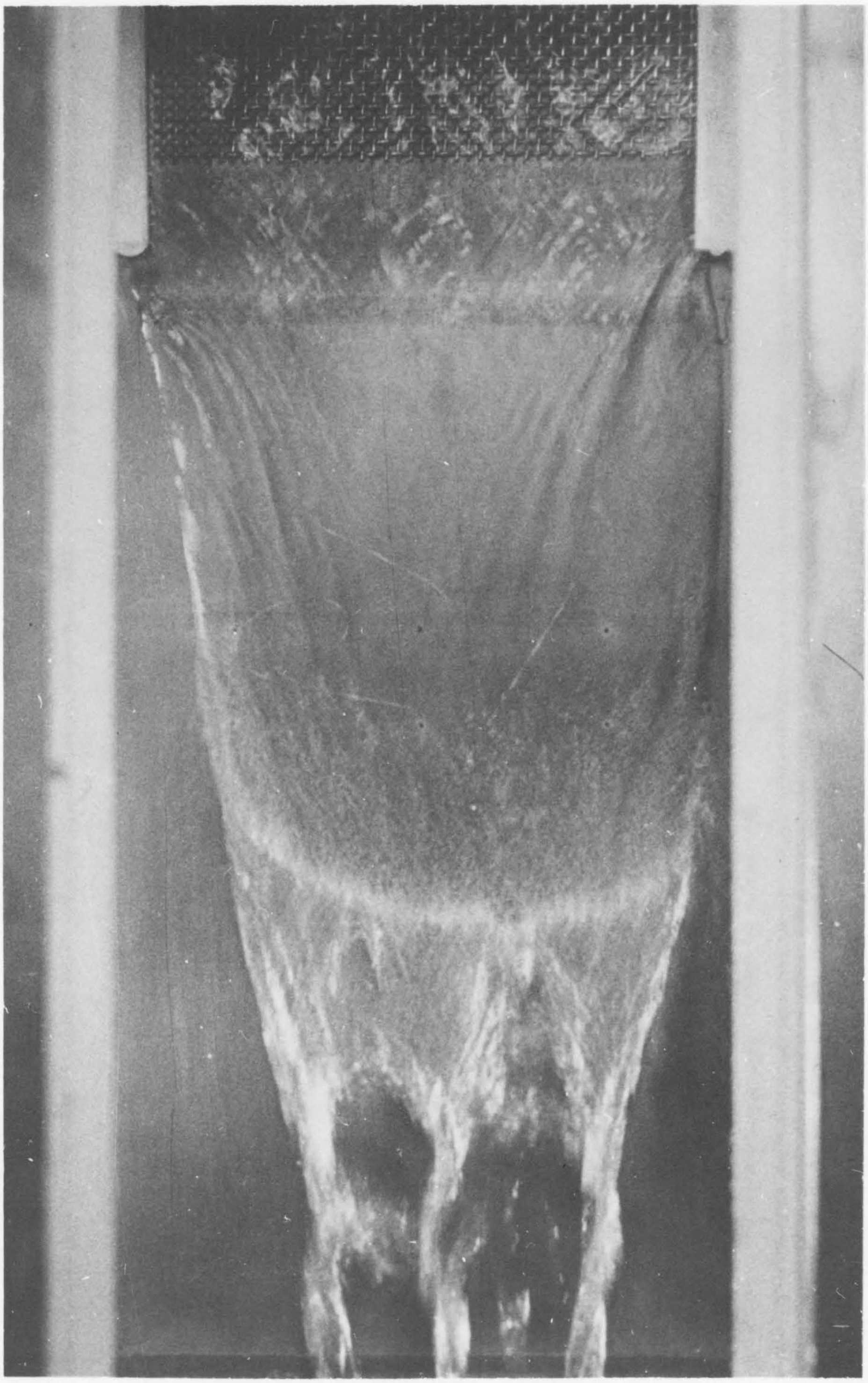

WATER; 8.00 LB/MIN; 152° F

PLATE 6

PLAN VIEW OF A BENZENE FILM

UNSTEADY STATE; 30° INCLINE

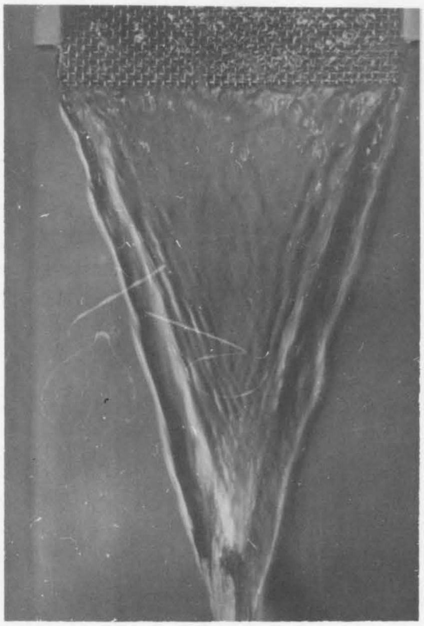

0 SEC; 4.30 LB/MIN; 75°F.

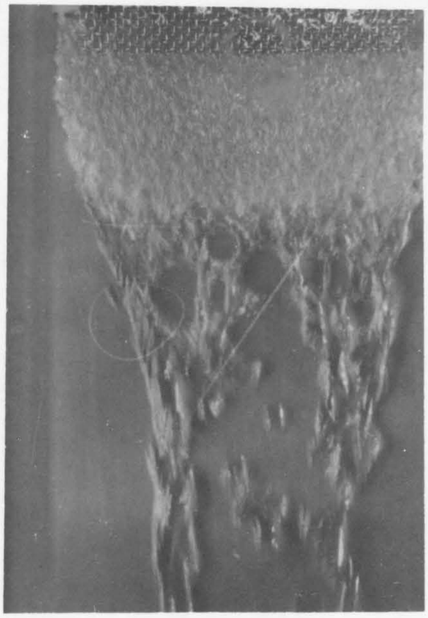

20 SEC; 4.30 LB/MIN; 75°F.

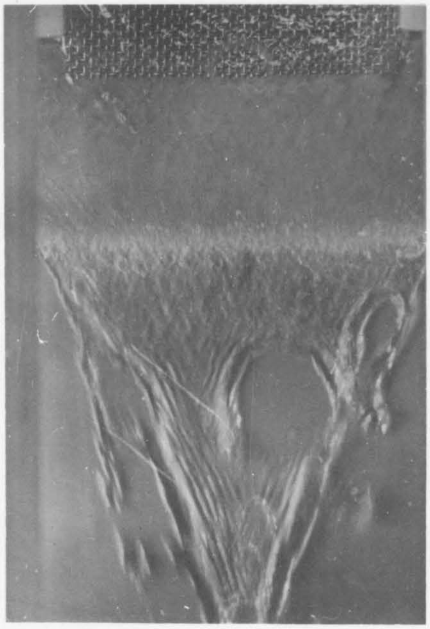

30 SEC; 4.30 LB/MIN; 75°F.

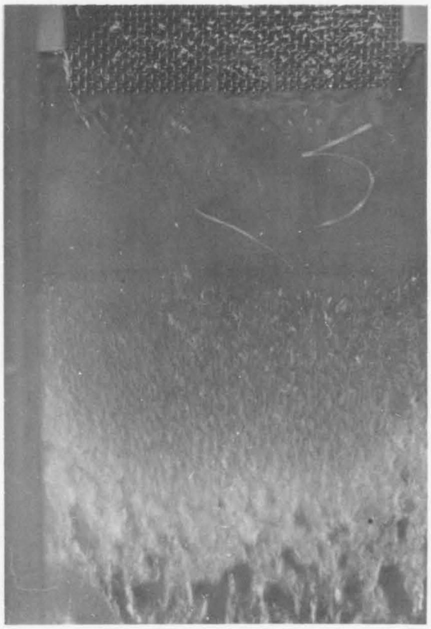

40 SEC; 4.30 LB/MIN; 75°F.

PLATE 7

PLAN VIEW OF BENZENE FILMS

UNSTEADY STATE; 30° INCLINE

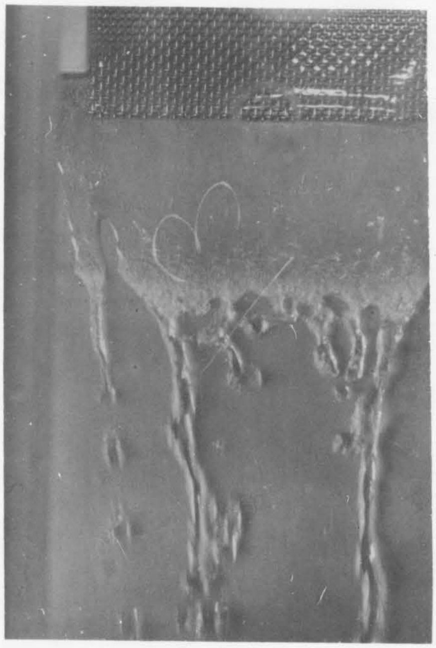

1.45 LB/MIN; 80°F.

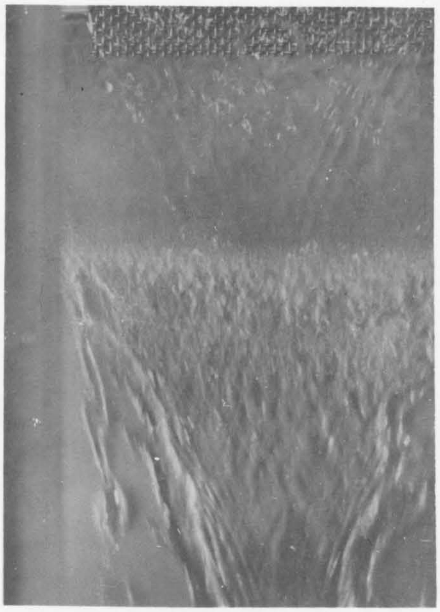

7.25 LB/MIN; 80°F.

PLATE 8

the same effect for a vertical plate; the more rapid advance of the break-up region over the heat-flux meter should be noted.

Plate 7 shows the destruction of a benzene film. Initially the break-up region was fixed on the end of the thin lip and the entire boiling plate was in film boiling. The break-up region rapidly advanced over the entry section and stopped again on the thin section of the boiling plate. After further cooling of the boiling plate the break-up region advanced again. The sequence shows the significance of the length of the nucleate boiling section on the film break-up. Plate 8 shows the break-up of a benzene film at different flow rates. At 1.45 lb/min. the tendency for dry patch formation can be seen. Subcooled benzene is shown in Plates 7 and 8 and hence liquid sheets are observed in those pictures in which the nucleate boiling section is short. It will be remembered that the nucleate boiling section in steady-state film flow was also short and hence the hydrodynamic patterns will be similar.

After the boiling plate had been cooled by the nucleate boiling of the liquid, the forced convection regime advanced. The transition point from nucleate boiling to forced convection was not so clearly defined as the transition point from film boiling to nucleate boiling (break-up region). As shown in Plate 4 the bubble size increased in the direction of the film flow. This was probably due to the increasing liquid film temperature along the boiling plate.

2.2 Boiling Heat Flux (Chromed Boiling Plate)

The first heat transfer data were taken with this boiling plate using benzene only. Some of the data obtained with the copper disc heat-flux meter which was 2 1/2 in. from the front lip are shown in Figure 37. The data indicate heat fluxes that were surprisingly large for

BOILING CURVE OF BENZENE FILM

4.30 lb/min., 30° INCLINE, 60° INCLINE

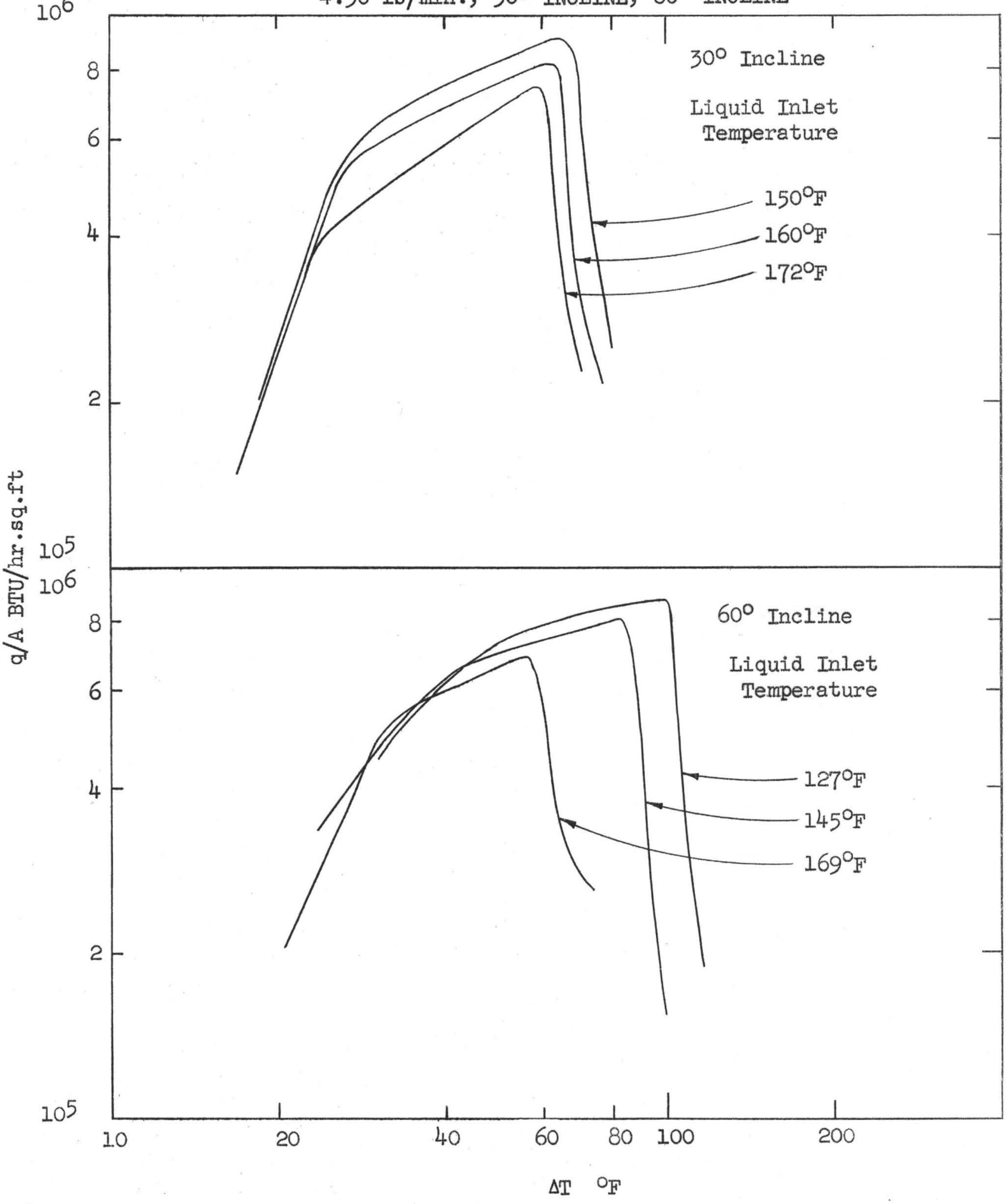

FIGURE 37

benzene (Figure 62). The heat fluxes appeared too large in the forced convection, nucleate boiling and film boiling regimes. In the film boiling regime of the liquid film the heat-flux meter showed a heat flux of 135,000 BTU/hr.sq.ft. The peak of the boiling curve (maximum heat flux) was extended over a large temperature range. Such behaviour was not expected. These errors could perhaps be attributed to the chrome-plating on the heat-flux meter and to the silver-solder joints of the thermocouple connections.

In order to check the thermocouples of the heat-flux meter each thermocouple was connected separately like a surface thermocouple. The data, shown in Figure 38, showed that the centre of the heat-flux meter cooled rapidly. Less boiling was taking place at the centre of the heat-flux meter, since the centre temperature was 44°F below the edge temperature. The edge temperature remained very steady, while the centre temperature fluctuated by about ±7°F. The centre temperature was steady, however, after indication of the maximum heat flux.

In these first experiments the wall temperature was measured with a surface thermocouple instead of using the edge thermocouple of the heat-flux meter. The maximum temperature decrease indicated by the surface thermocouple occurred always after the heat-flux meter had indicated the maximum heat flux. These two maxima should occur at the same time. The region of destruction, although initially in a straight line, took the form of a "parabola" with increasing speed of advance along the centre line of the boiling plate (Plate 6). For this reason it was not desirable to measure the heat flux and surface temperature in two different places. This error does not significantly effect the magnitude

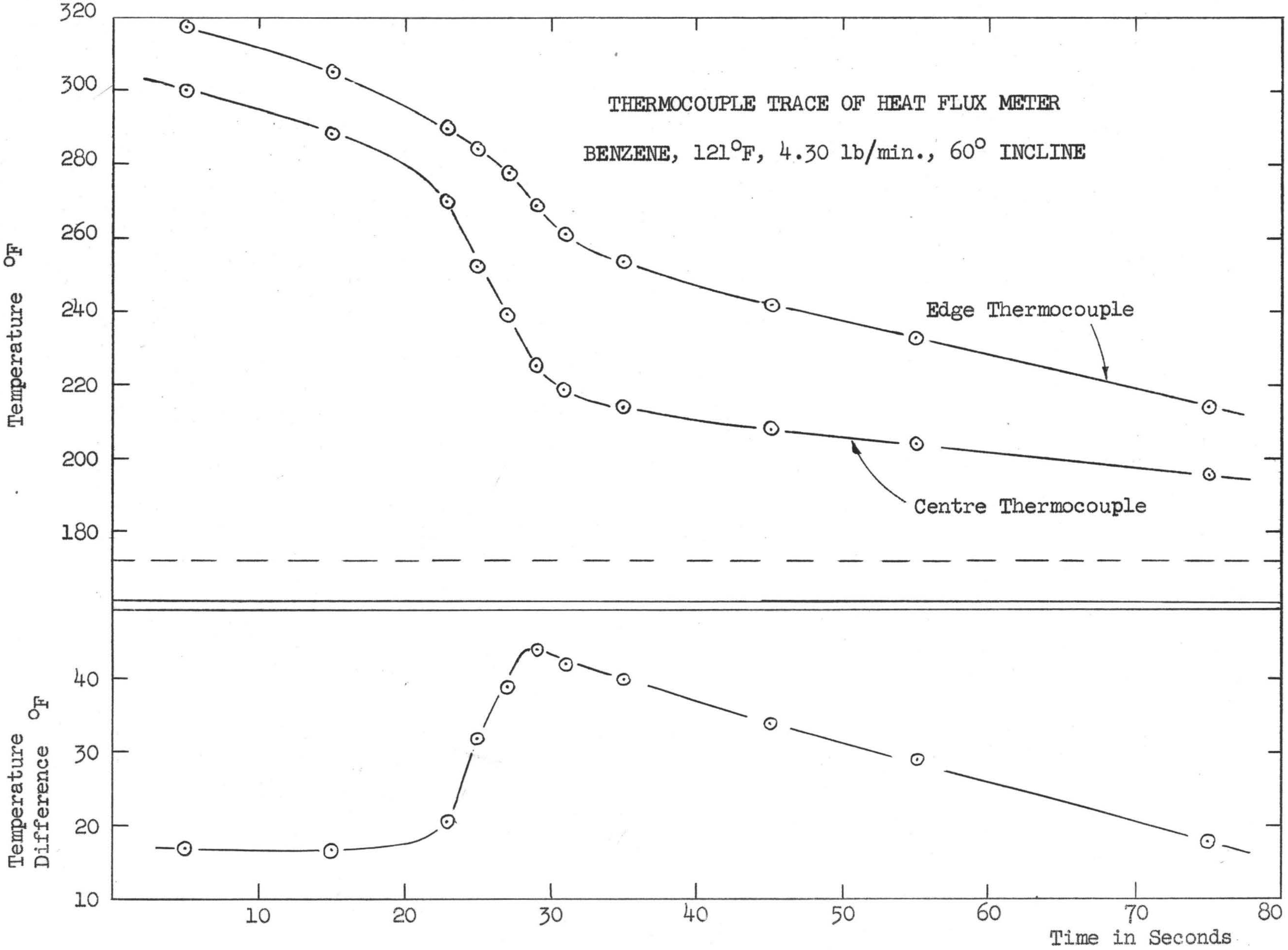
THERMOCOUPLE TRACE OF HEAT FLUX METER
BENZENE, 121°F, 4.30 lb/min., 60° INCLINE
Edge Thermocouple
Centre Thermocouple
Temperature °F
320
300
280
260
240
220
200
180
Temperature Difference °F
40
30
20
10
10
20
30
40
50
60
70
80
Time in Seconds

FIGURE 38

FORCED CONVECTION OF BENZENE FILM

30° INCLINE

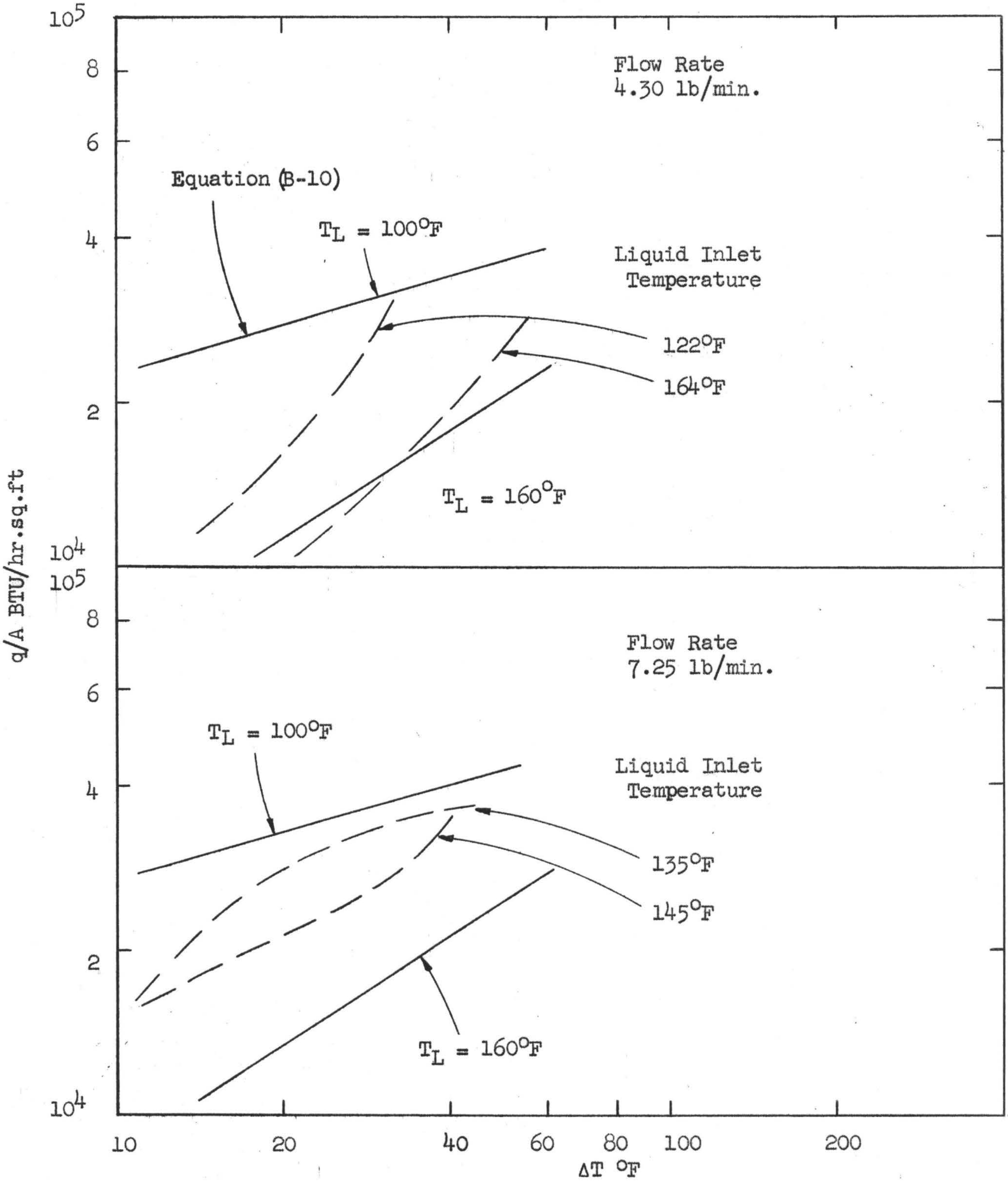

FIGURE 39

of the heat flux, but does yield an incorrect temperature difference.

The copper disc heat-flux meter 3 1/2 in. from the front lip was deformed during the press-fitting operation and could not be used.

The constantan disc heat-flux meters could be seen to cool rapidly whenever liquid boiled on them. Thus the boiling on these meters was not characteristic of boiling on the rest of the boiling plate. The constantan disc heat-flux meters indicated a maximum heat flux of about 35,000 BTU/hr.sq.ft for benzene. The constantan discs were designed to measure the heat flux in the film boiling regime. However these meters showed no response in that regime. It appears however that the constantan disc heat-flux meters can measure the heat fluxes in the forced convection regime. Figure 39 shows some of these results and equation (B-10).

The experiments were discontinued when the press-fitted heat-flux meter plugs oxidized around the edges. These plugs cooled rapidly then and did not act as the rest of the boiling plate. On the basis of these experiences another boiling plate with integral heat-flux meters was made. Instead of the constantan discs two thick copper discs were machined in the copper plate to measure the "large" heat fluxes observed.

2.3 Boiling Heat Flux (Unplated Boiling Plate)

With the second boiling plate, experiments were carried out with benzene and water. Measurements of heat flux were made with the thin copper disc heat-flux meter, which was 3 1/2 in. from the front lip, (Figure 26). Typical heat-flux meter traces of benzene and water are shown in Figures 40 and 41 respectively. From these traces the three boiling regimes could be identified. The film boiling regime was always smooth. The transition boiling regime was indicated by large

HEAT FLUX METER TRACE OF BENZENE FILM

156°F, 4.30 lb/min., 30° INCLINE, (BOILING CURVE IN FIGURE 46)

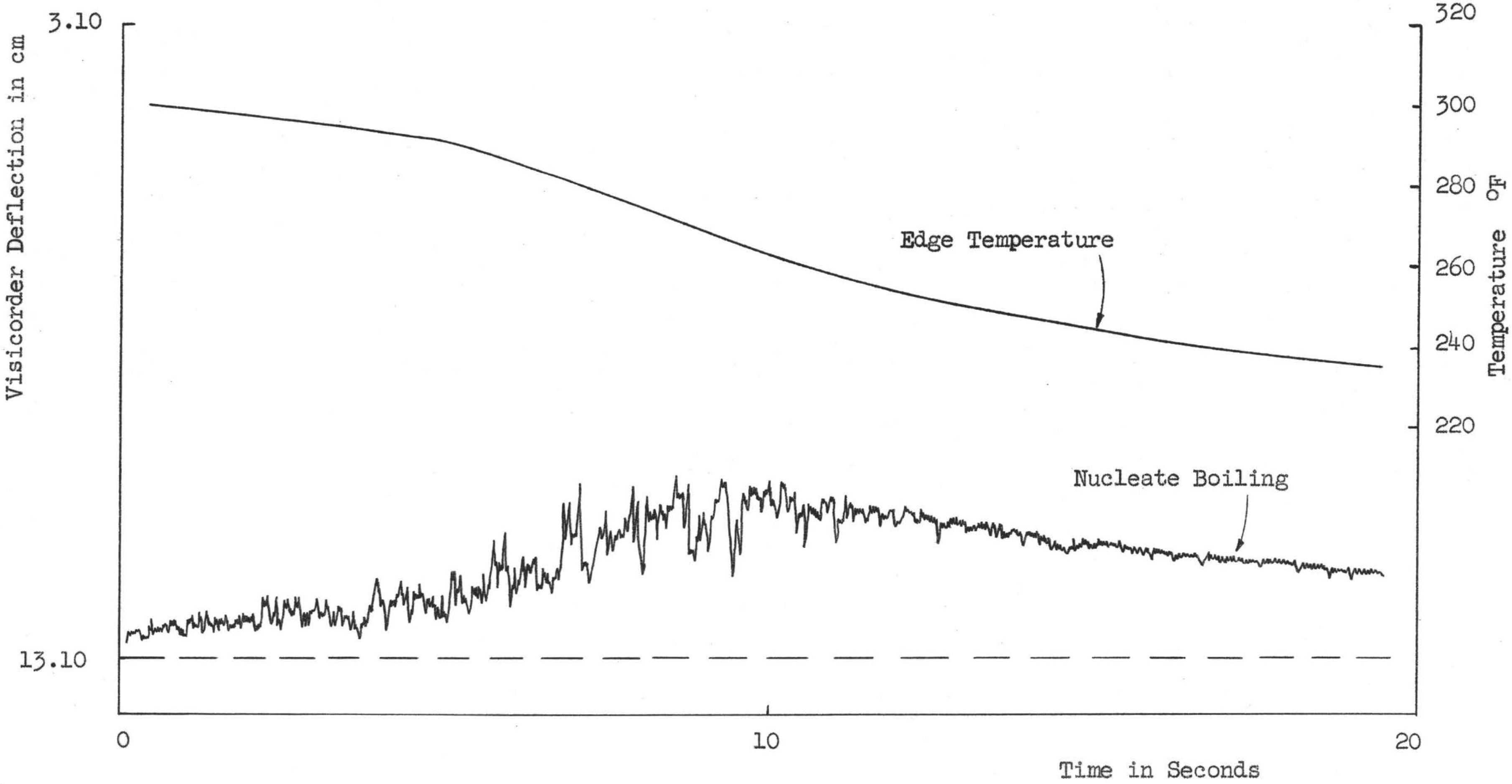

FIGURE 40

HEAT FLUX METER TRACE OF WATER FILM

201°F, 4.80 lb/min., 30° INCLINE, (BOILING CURVE IN FIGURE 50)

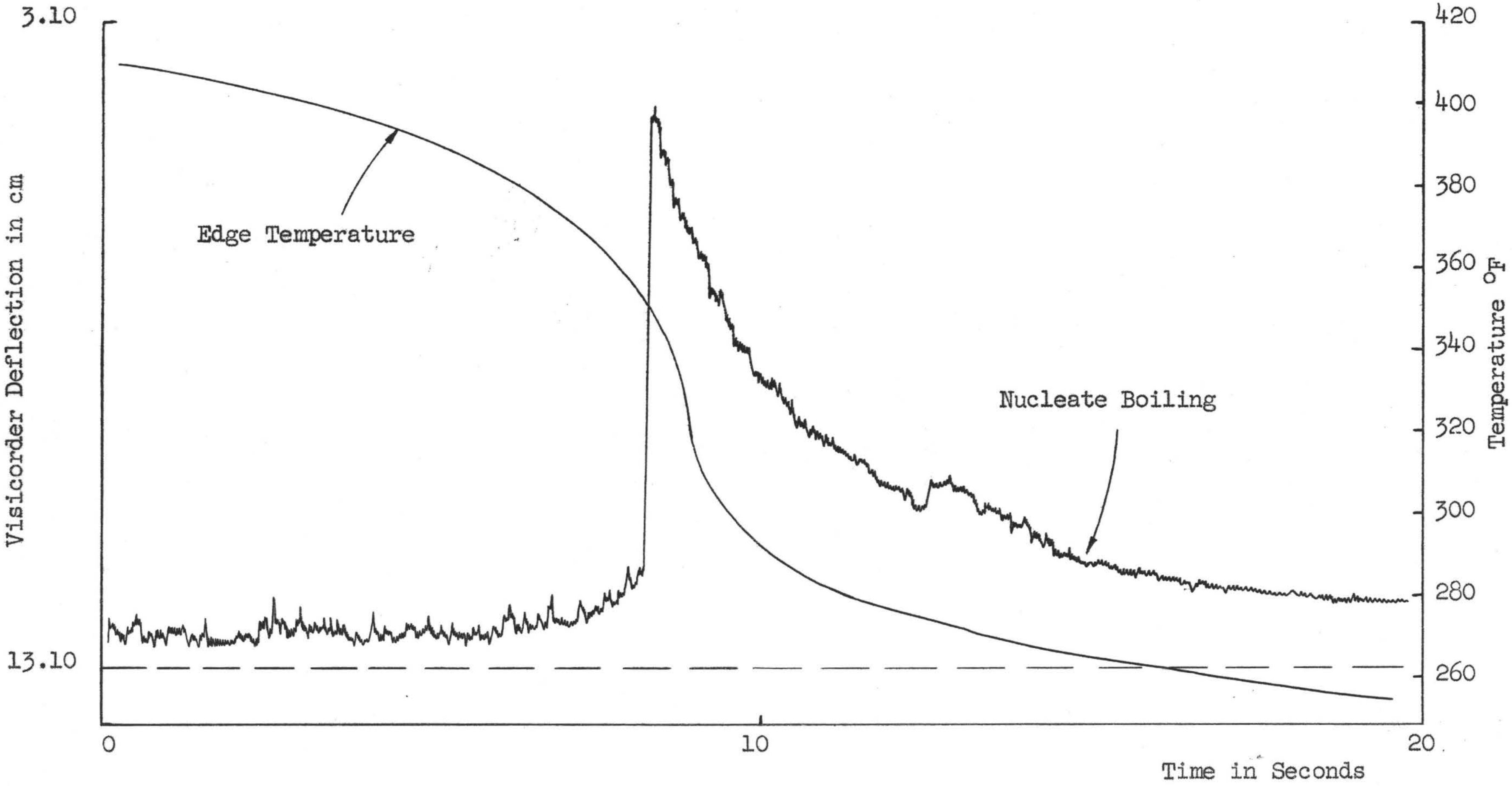

FIGURE 41

oscillations of the heat-flux meter. The nucleate boiling regime showed small oscillations not comparable to those in the transition boiling regime. The transition from nucleate boiling to forced convection could not be seen from the traces.

The boiling curves were constructed from the edge temperature of the heat-flux meter and the heat flux as determined by the temperature difference across the heat-flux meter. It was a simple matter to calculate the heat flux from the heat-flux meter traces except for the transition boiling regime. In this regime the large oscillations made a heat flux interpretation uncertain. The oscillations of the trace have been averaged by eye and a "mean" line has been drawn through them. The smallest and largest heat flux has been identified by the vertical bars shown in some figures.

The results for benzene are shown in Figures 42 to 47 and the results for water are shown in Figures 48 to 54. Due to the transient nature of the experiments an exact choice of the liquid temperature could not be made. Duplicate runs were made to check on the reproducibility of the results. The results of the duplicate runs in the three cases (Figures 45, 47 and 51) were identical with those of the previous runs.

The boiling-plate surface was cleaned with 3/0 emery paper at irregular intervals. Excessive cleaning with emery paper was avoided to prevent thinning of the heat-flux meter discs. During the benzene runs oxidation of the copper surface appeared to be inhibited. The surface always had a brown colour and felt smooth. When water was used, however, the copper surface appeared bluish, felt rough and oxidised rapidly. The surface conditions are described by the surface roughness, surface deposits and surface oxidation, but none of these were rigidly controlled during the present experiments.

BOILING CURVE OF BENZENE FILM

4.30 lb/min., 90° INCLINE

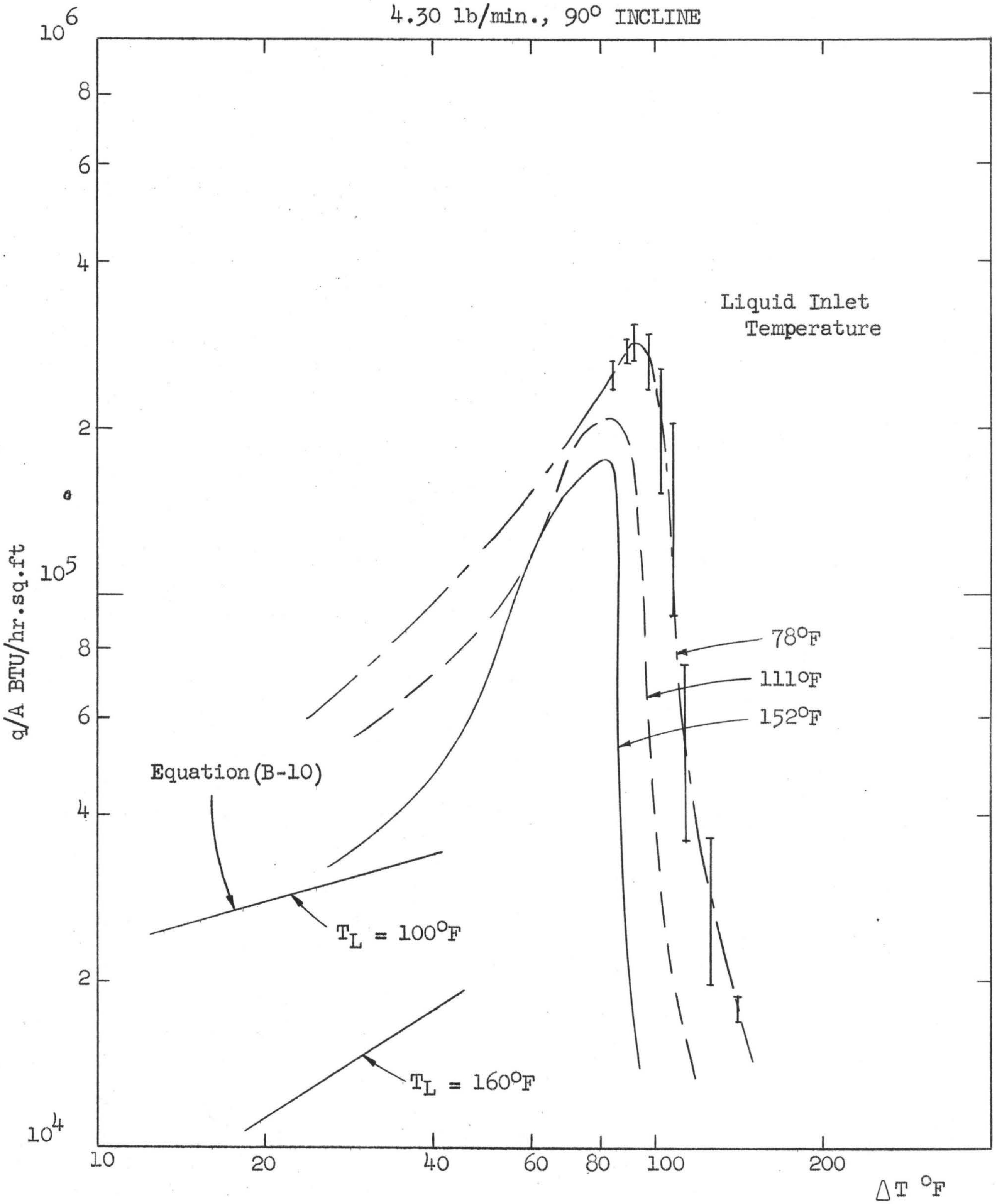

FIGURE 42

BOILING CURVE OF BENZENE FILM

7.25 lb/min., 90° INCLINE

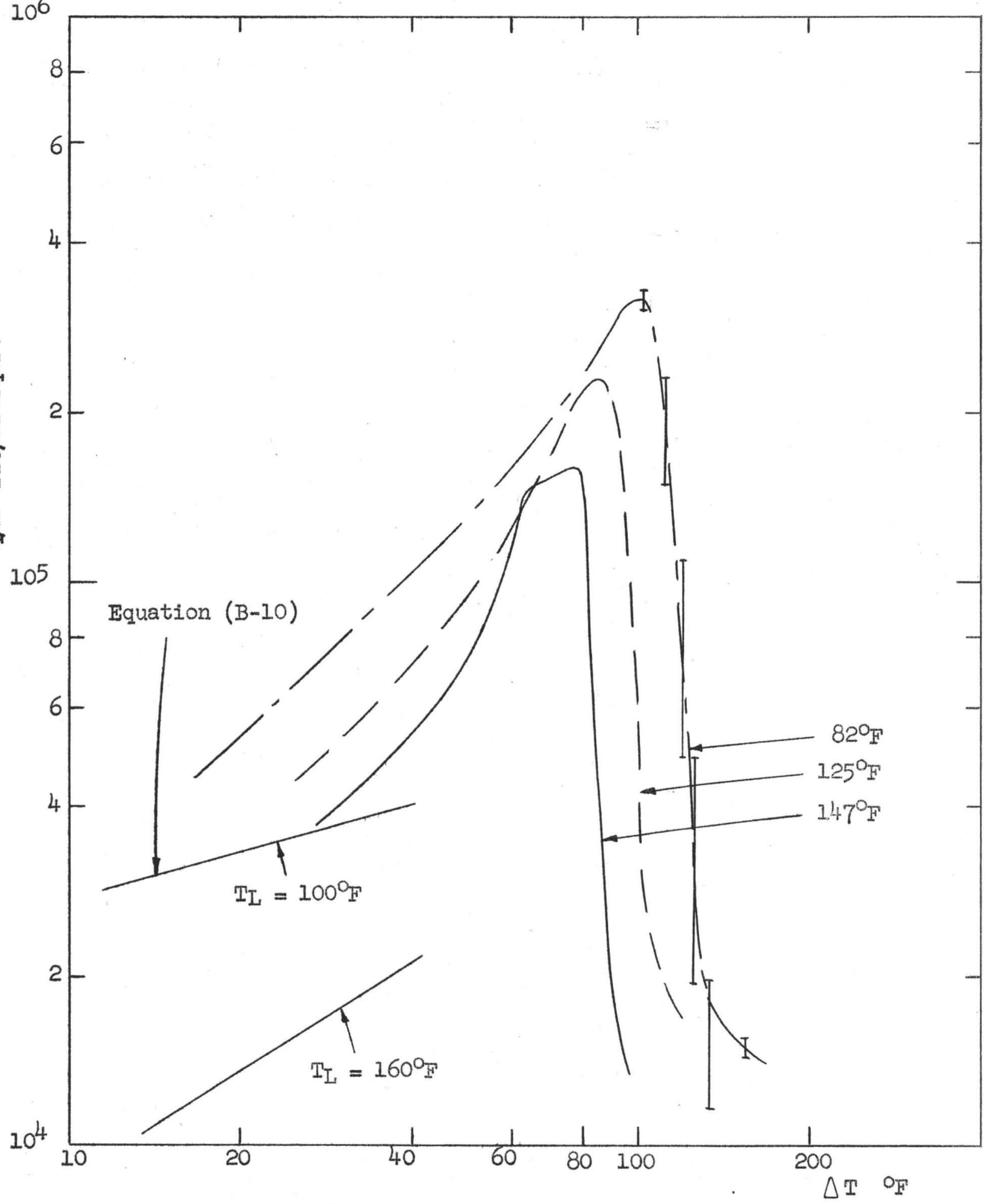

FIGURE 43

BOILING CURVE OF BENZENE FILM

4.30 lb/min., 60° INCLINE

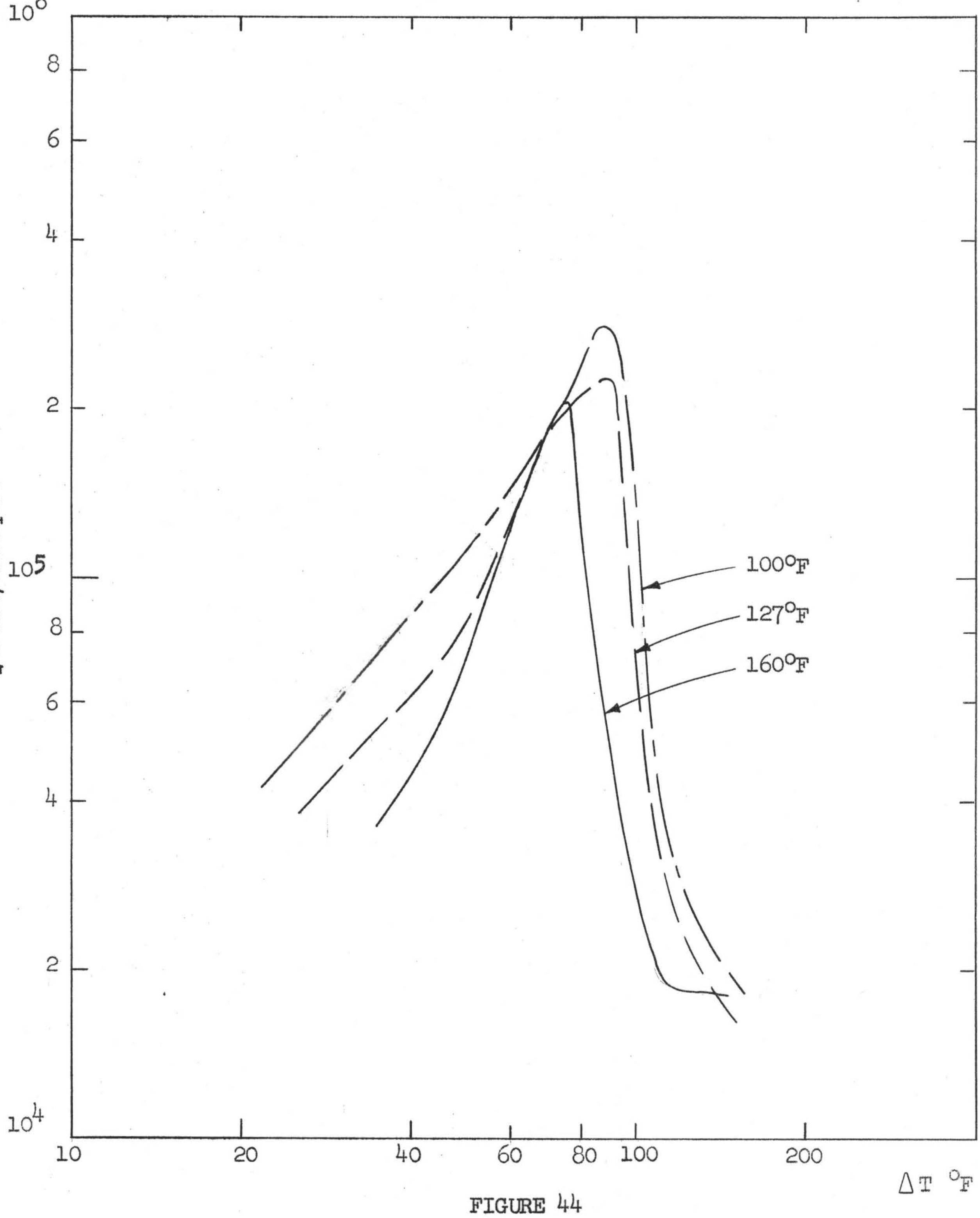

FIGURE 44

BOILING CURVE OF BENZENE FILM

7.25 lb/min., 60° INCLINE

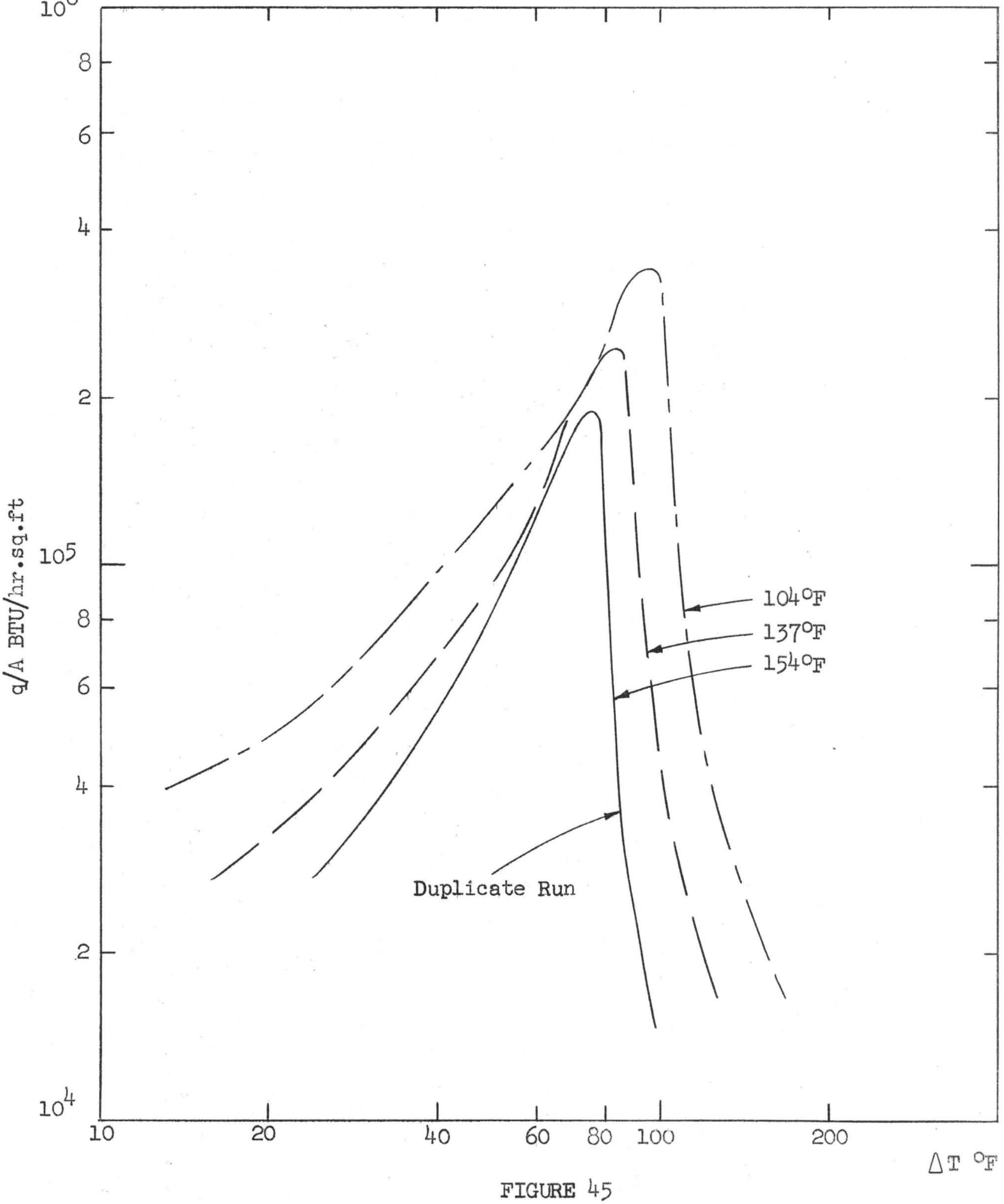

FIGURE 45

BOILING CURVE OF BENZENE FILM

4.30 lb/min., 30° INCLINE

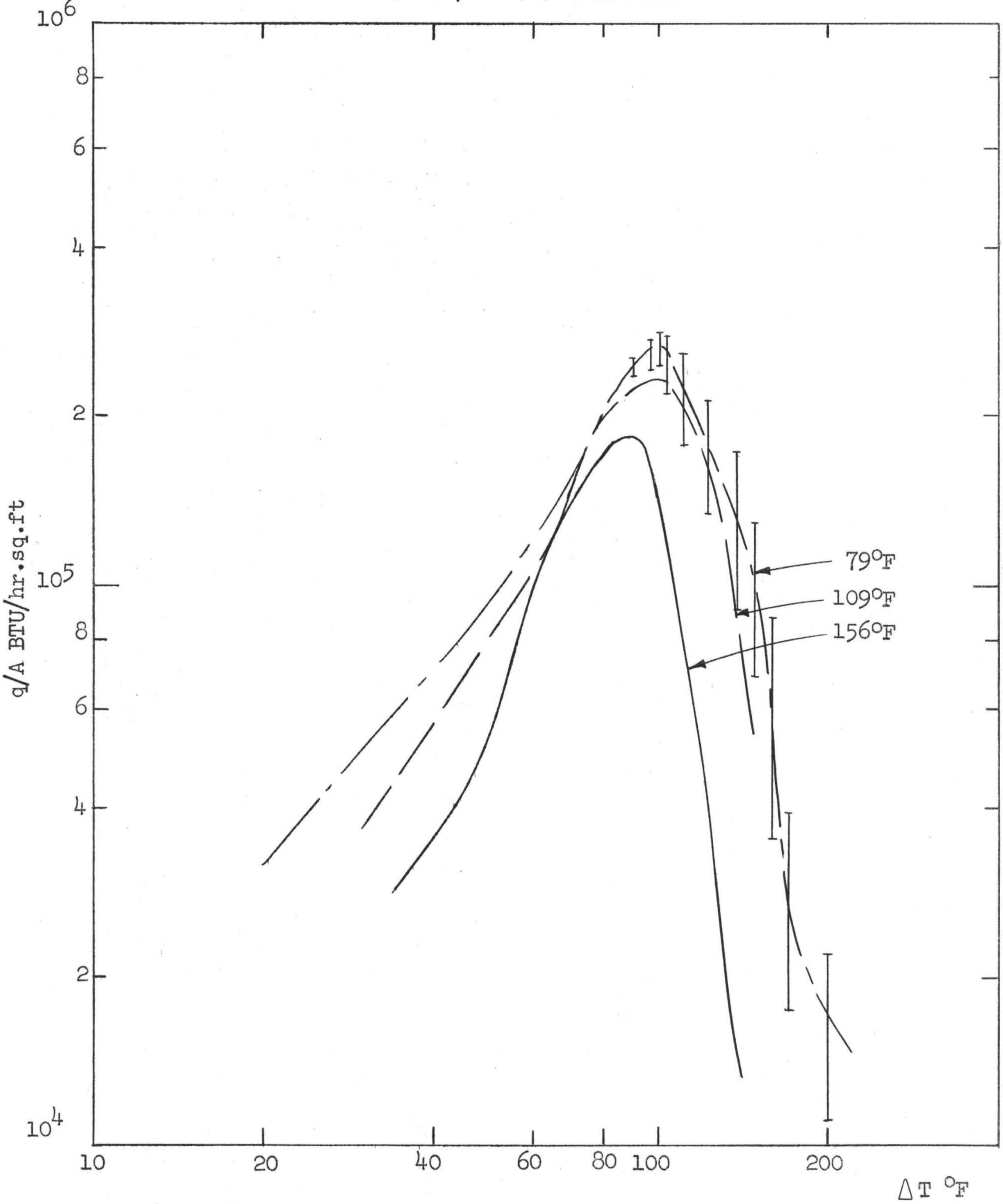

FIGURE 46

BOILING CURVE OF BENZENE FILM

7.25 lb/min., 30° INCLINE

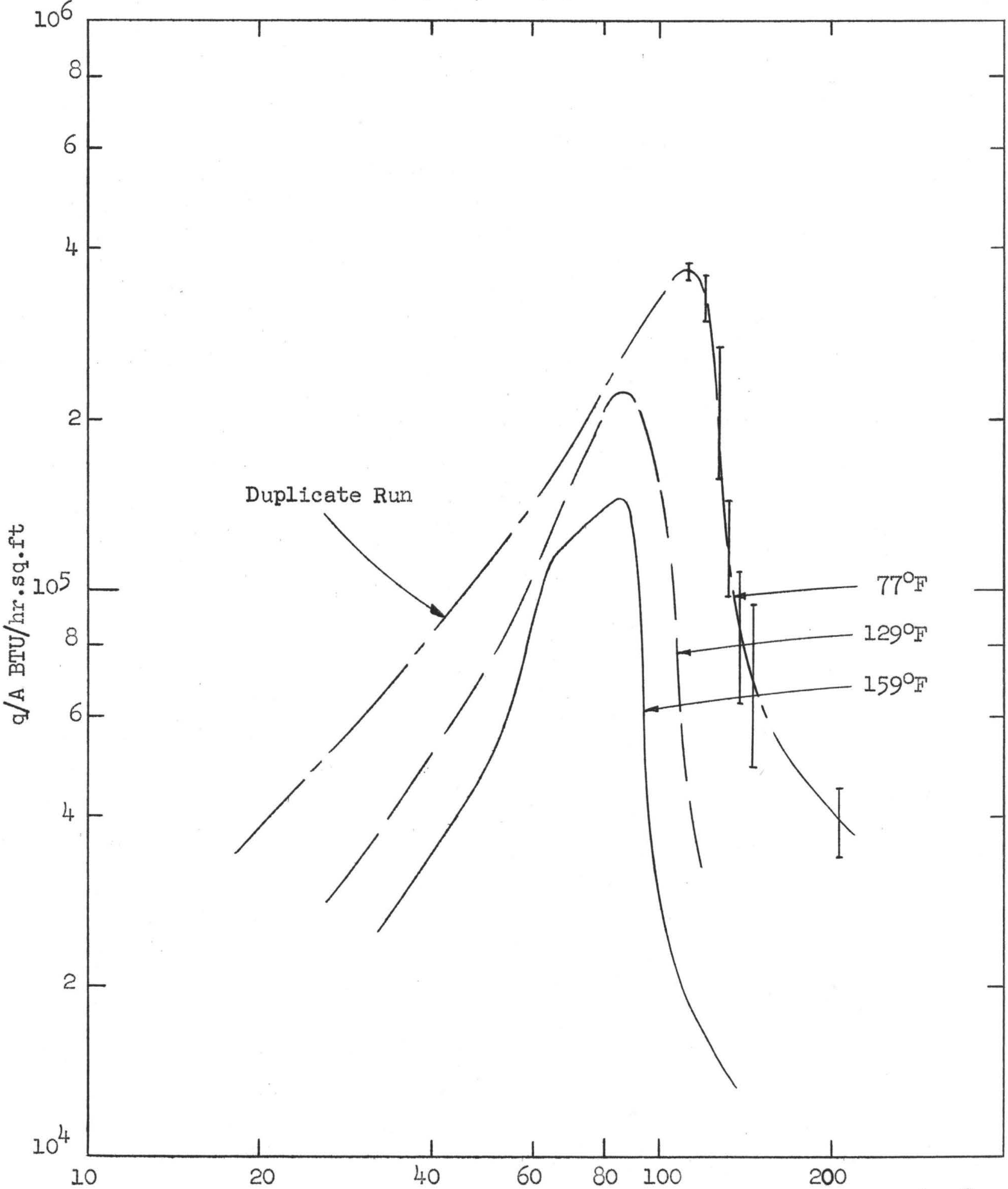

FIGURE 47

BOILING CURVE OF WATER FILM

4.80 lb/min., 90° INCLINE

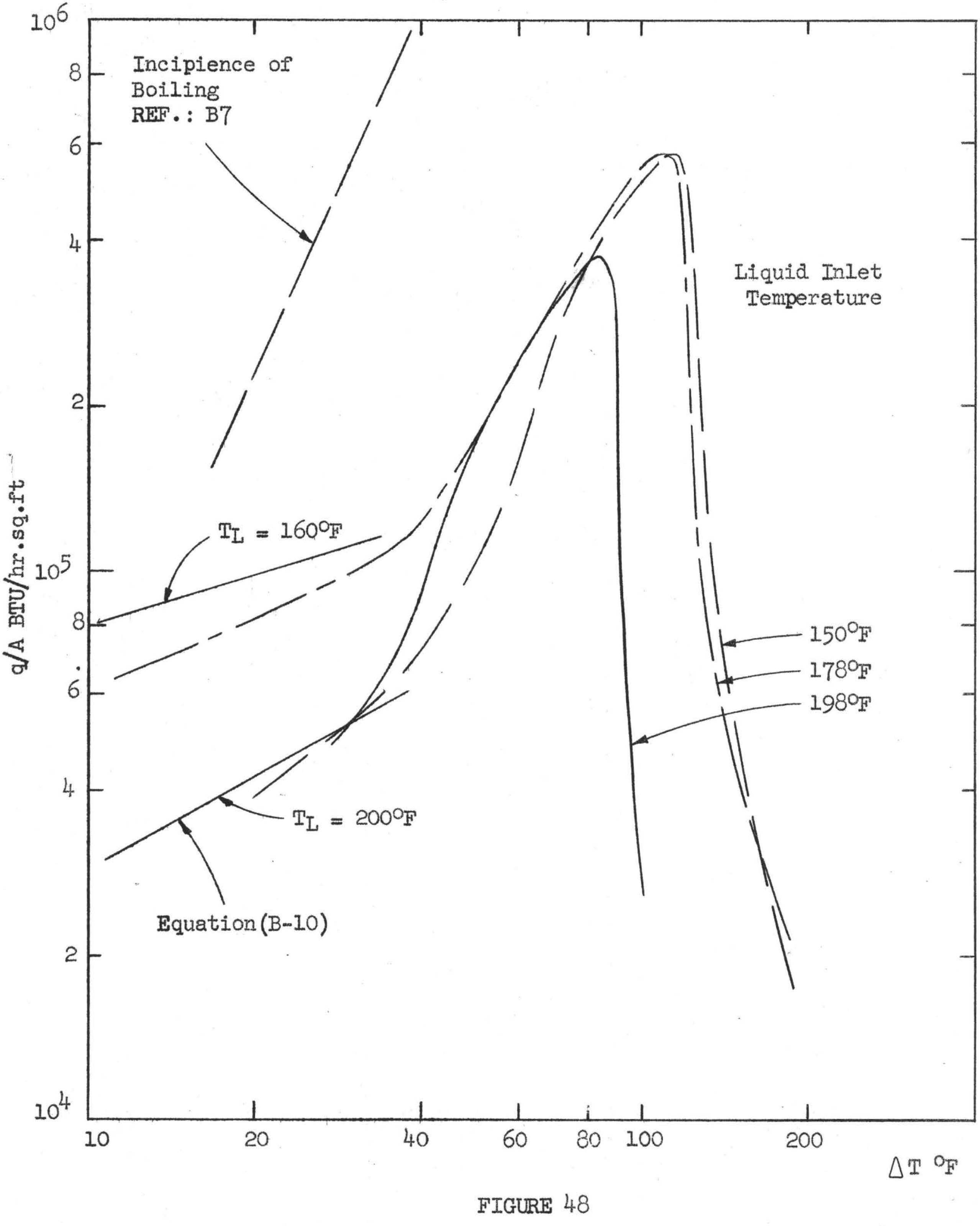

FIGURE 48

BOILING CURVE OF WATER FILM

8.00 lb/min., 90° INCLINE

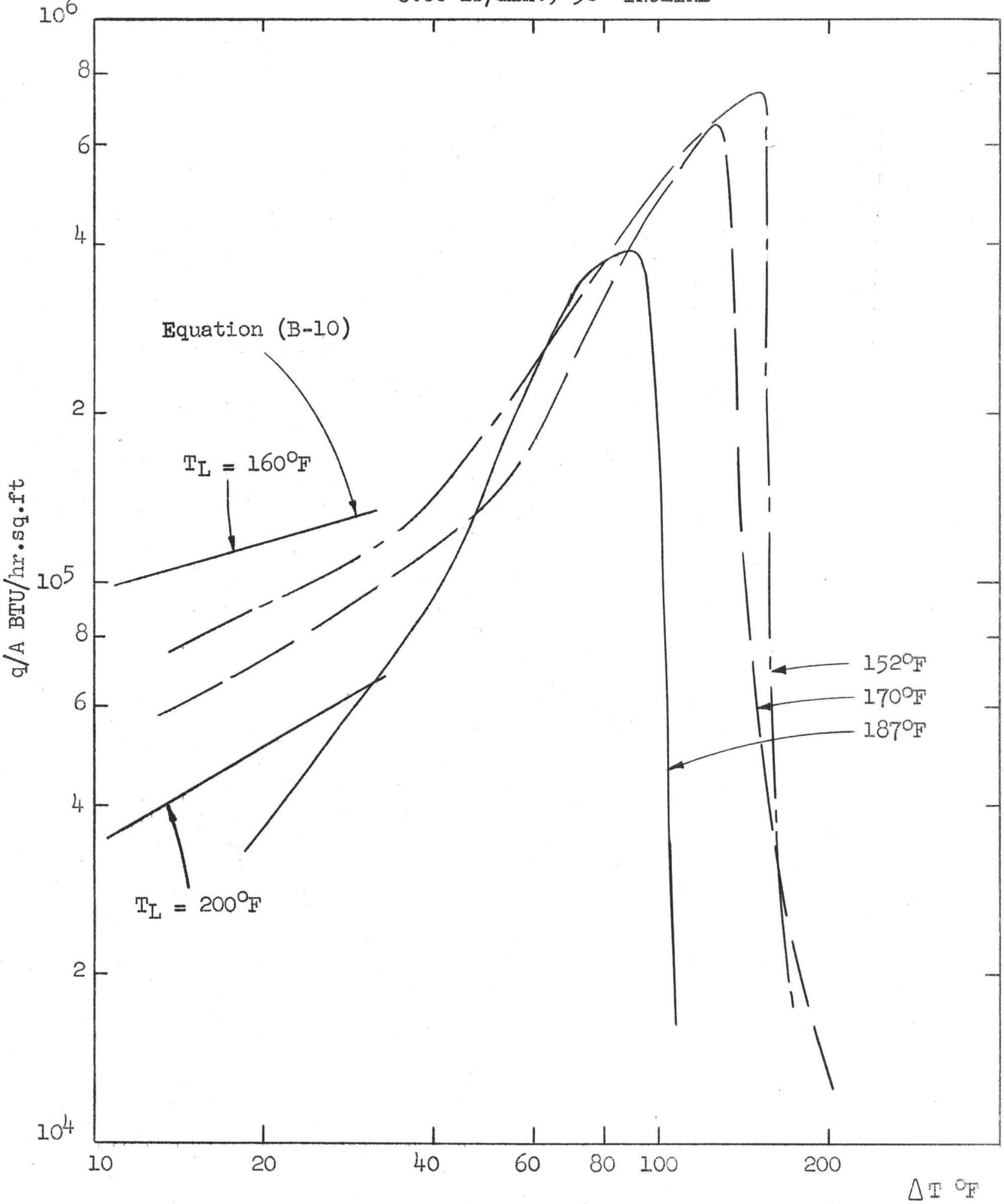

FIGURE 49

BOILING CURVE OF WATER FILM

4.80 lb/min., 30° INCLINE

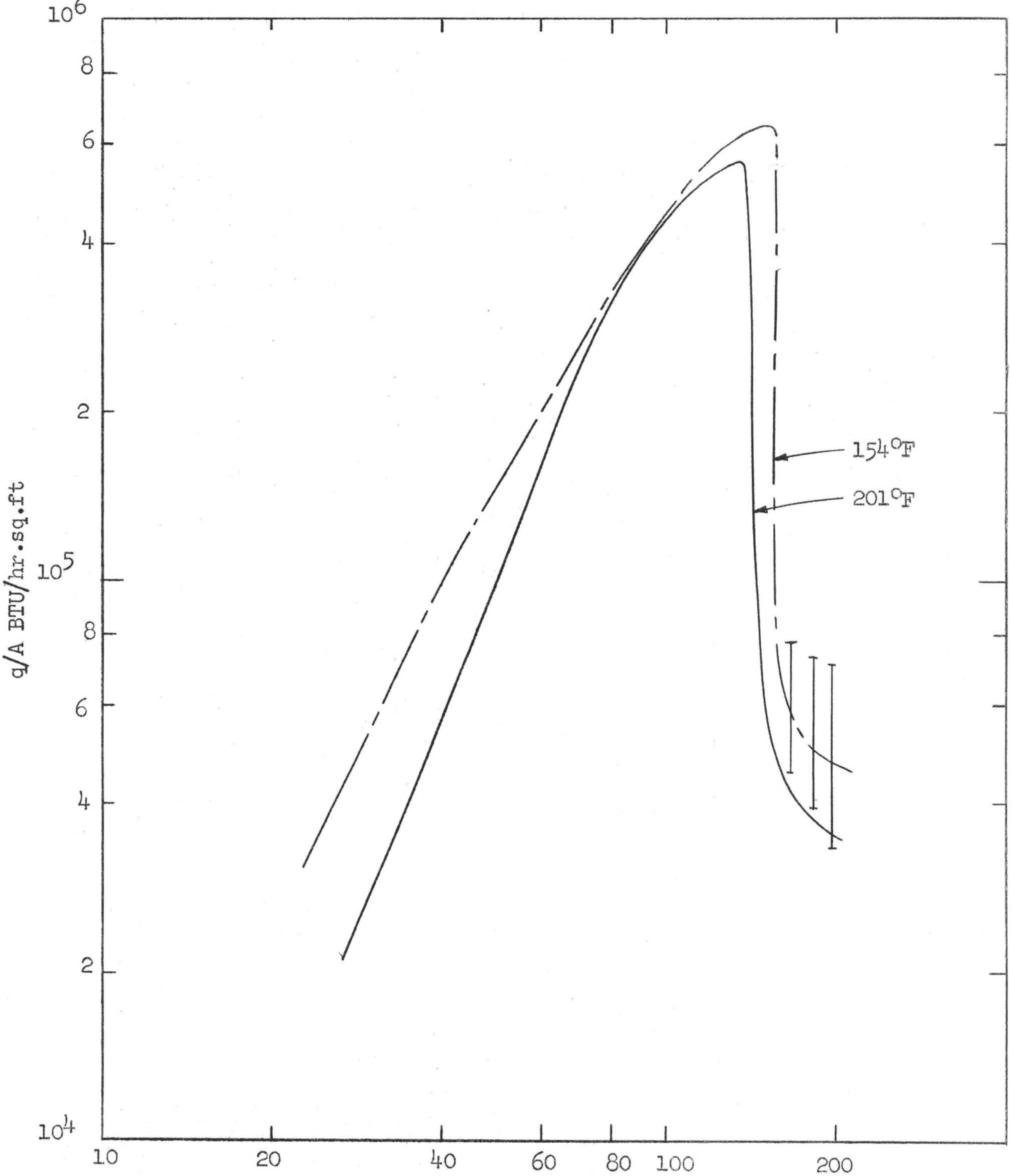

FIGURE 50

BOILING CURVE OF WATER FILM

8.00 lb/min., 30° INCLINE

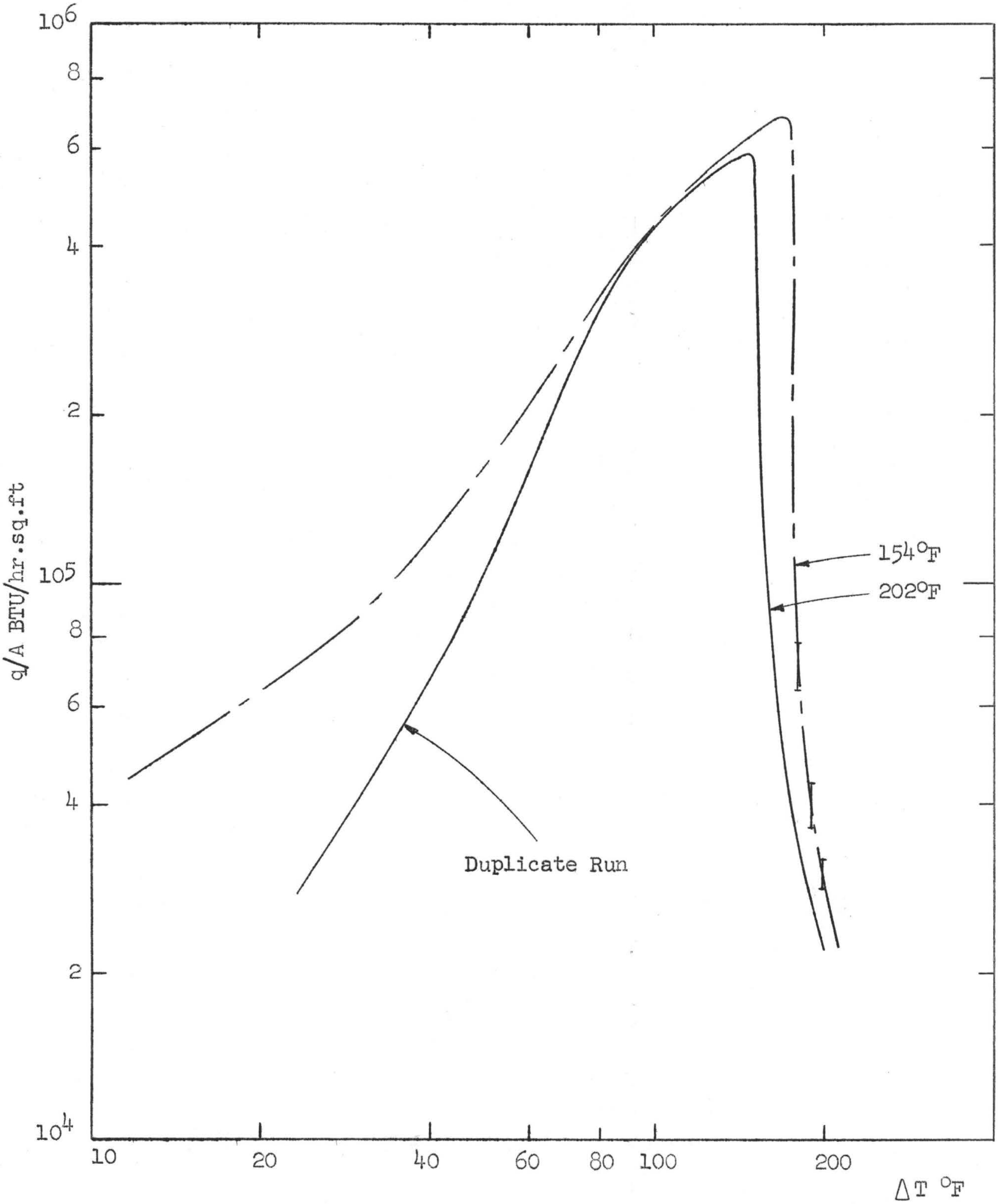

FIGURE 51

BOILING CURVE OF WATER FILM

4.80 lb/min., 30° INCLINE

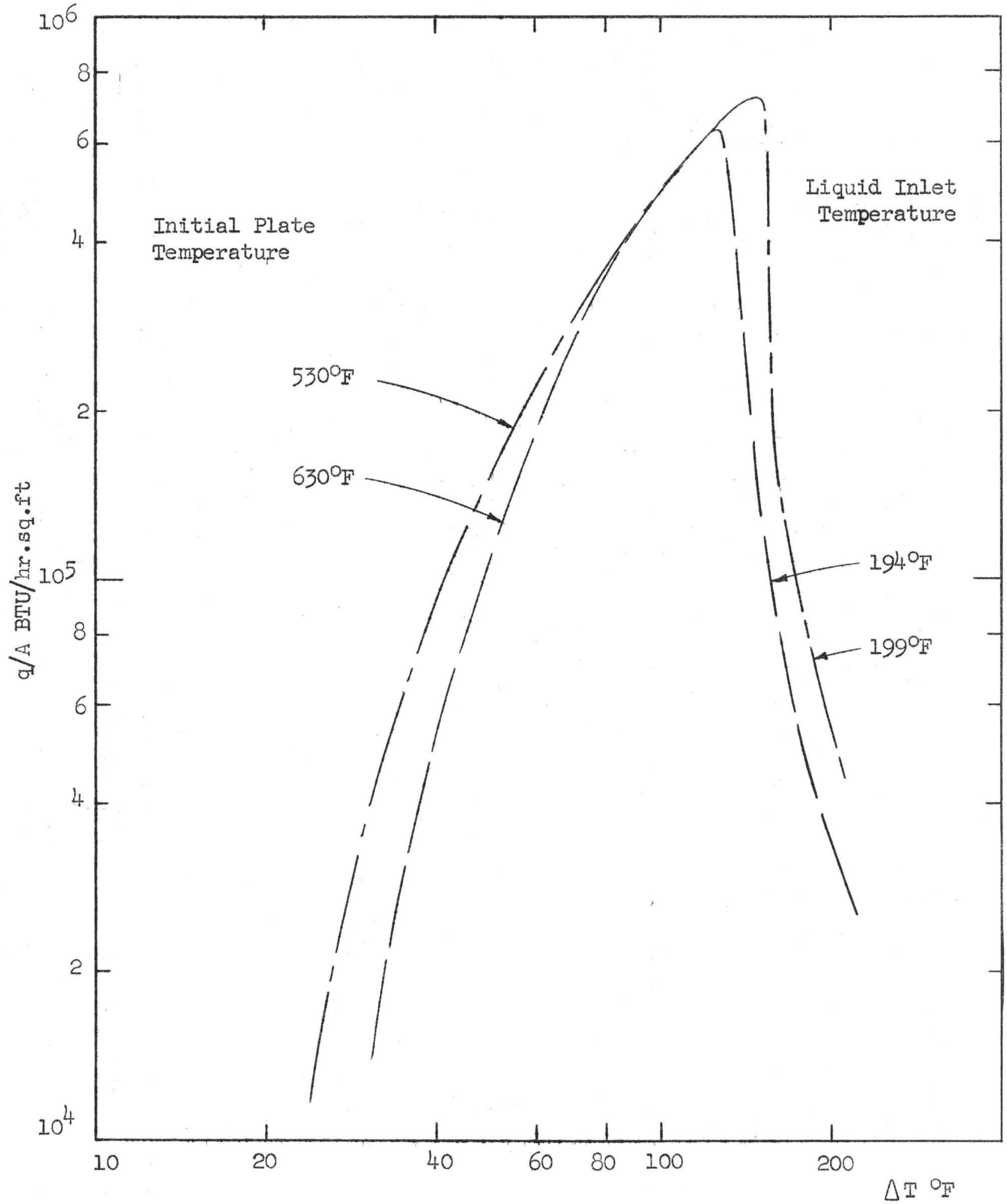

FIGURE 52

BOILING CURVE OF WATER FILM

4.80 lb/min., 30° INCLINE

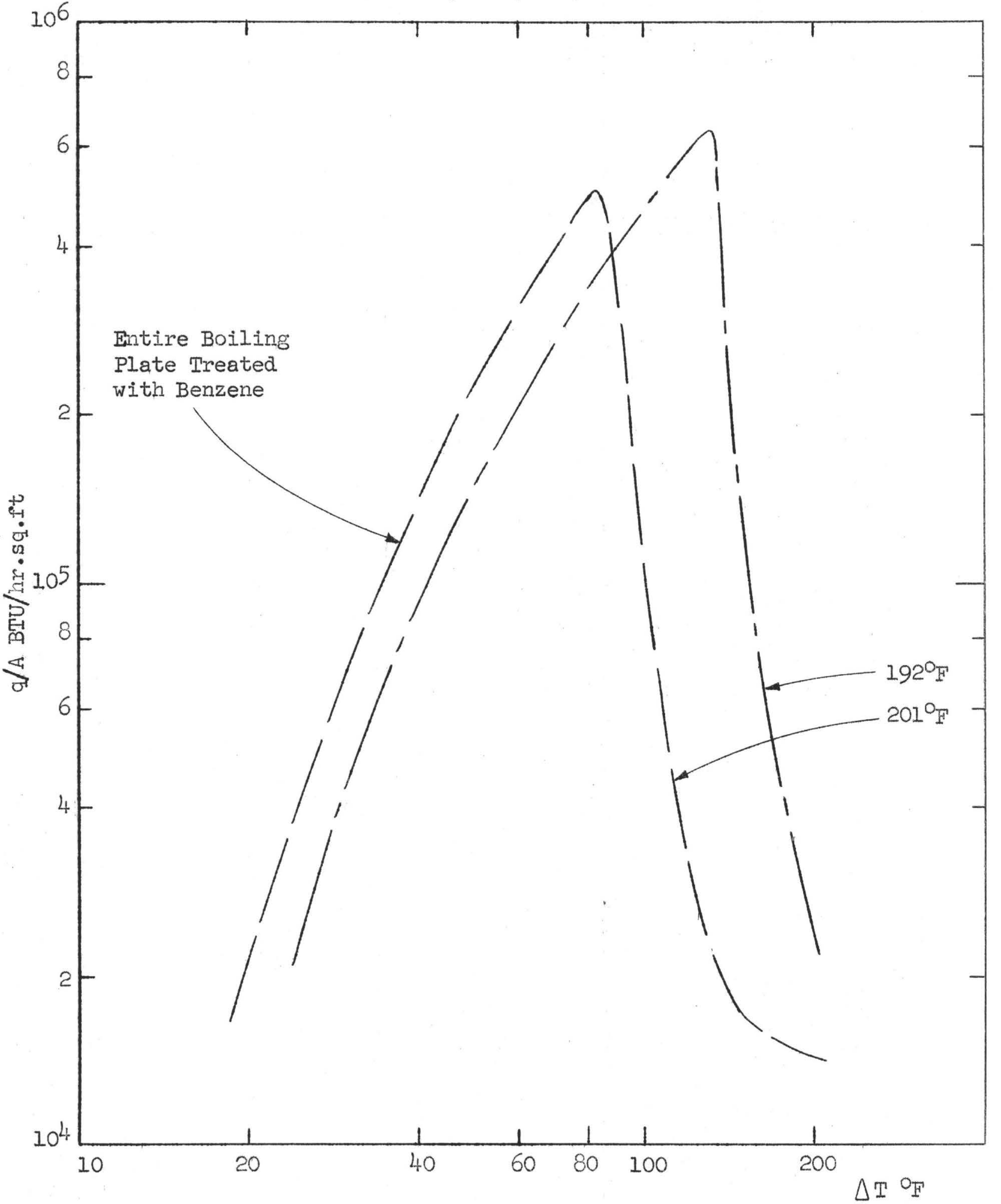

FIGURE 53

BOILING CURVE OF WATER FILM

4.80 lb/min., 30° INCLINE

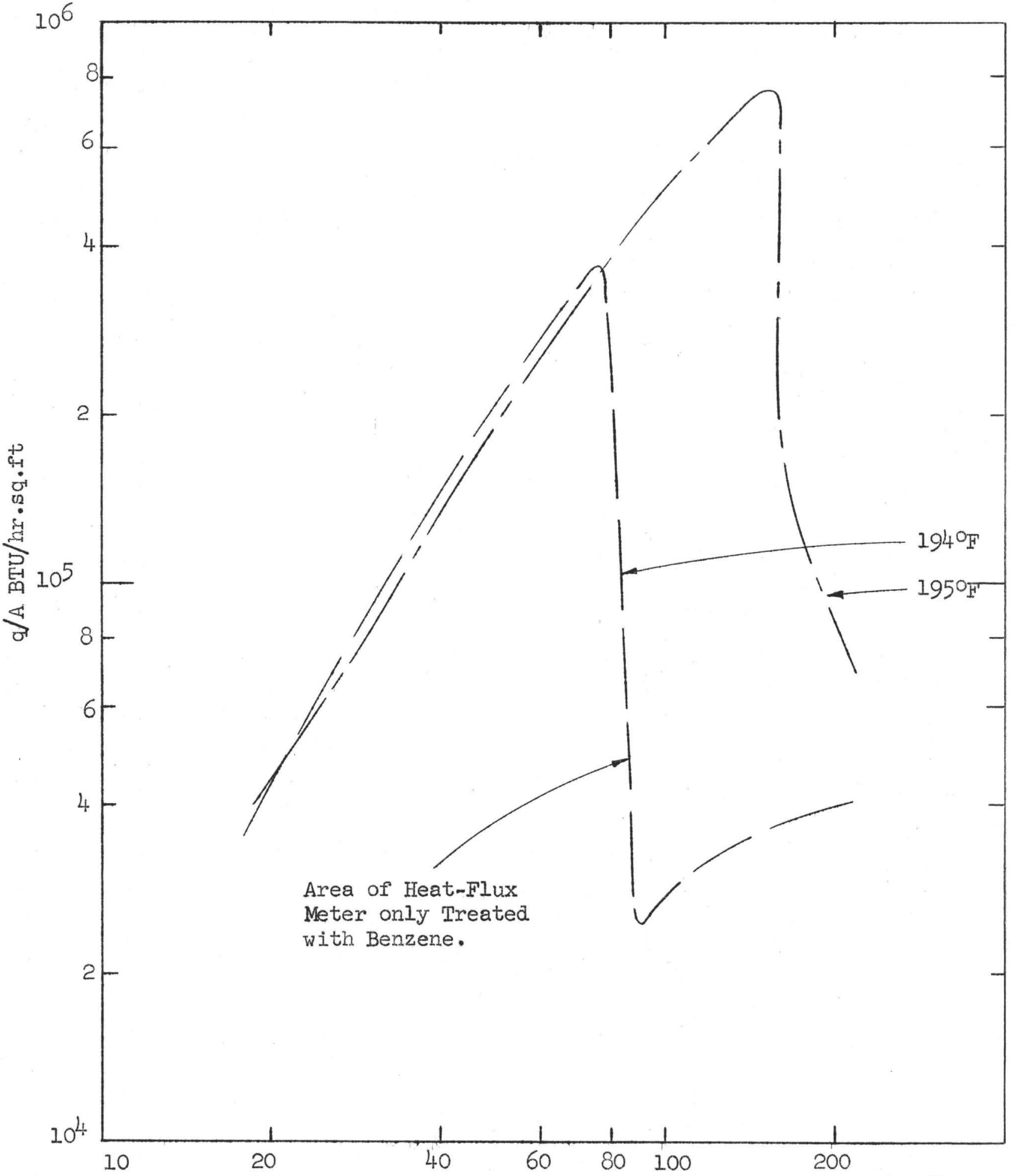

FIGURE 54

HEAT FLUX METER TRACE OF TRANSITION BOILING

WATER, 192°F, 201°F, 4.80 lb/min., 30° INCLINE, (BOILING CURVE IN FIGURE 53)

Boiling Plate Untreated

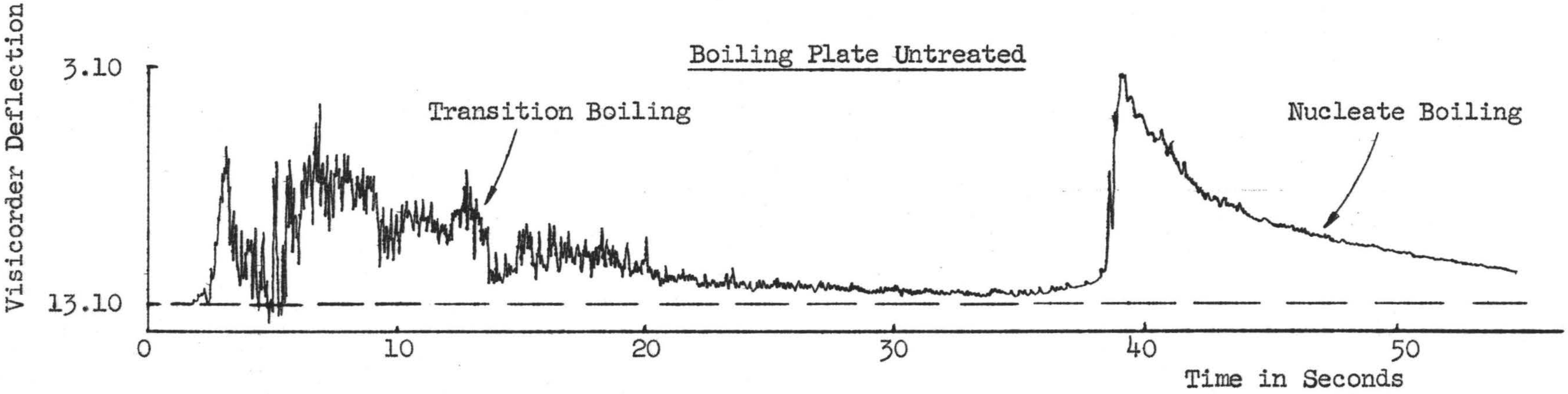

Entire Boiling Plate Treated with Benzene

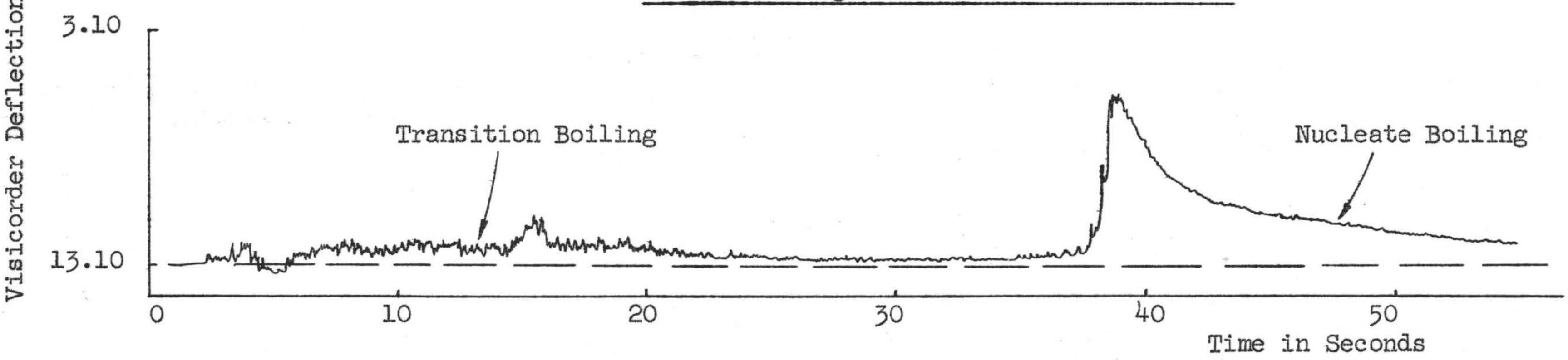

FIGURE 55

HEAT FLUX METER TRACE OF THICK COPPER DISC

WATER, FILM FLOW, 4.80 lb/min. 30° INCLINE
WATER, POOL BOILING (BOILING CURVE IN FIGURE 57)

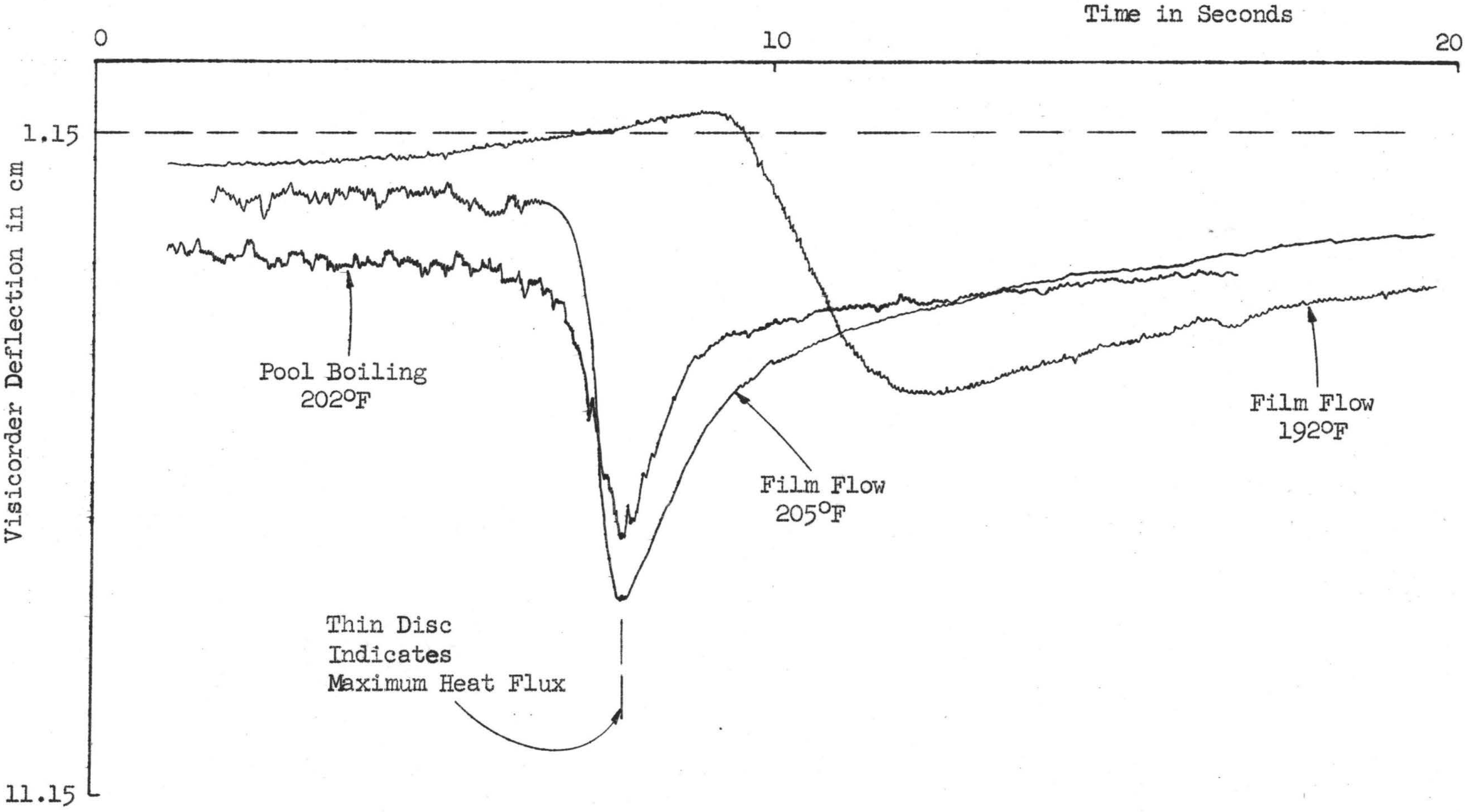

FIGURE 56

BOILING HEAT FLUX ON THICK COPPER DISC

WATER, FILM FLOW, 4.80 lb/min., 30° INCLINE

WATER, POOL BOILING

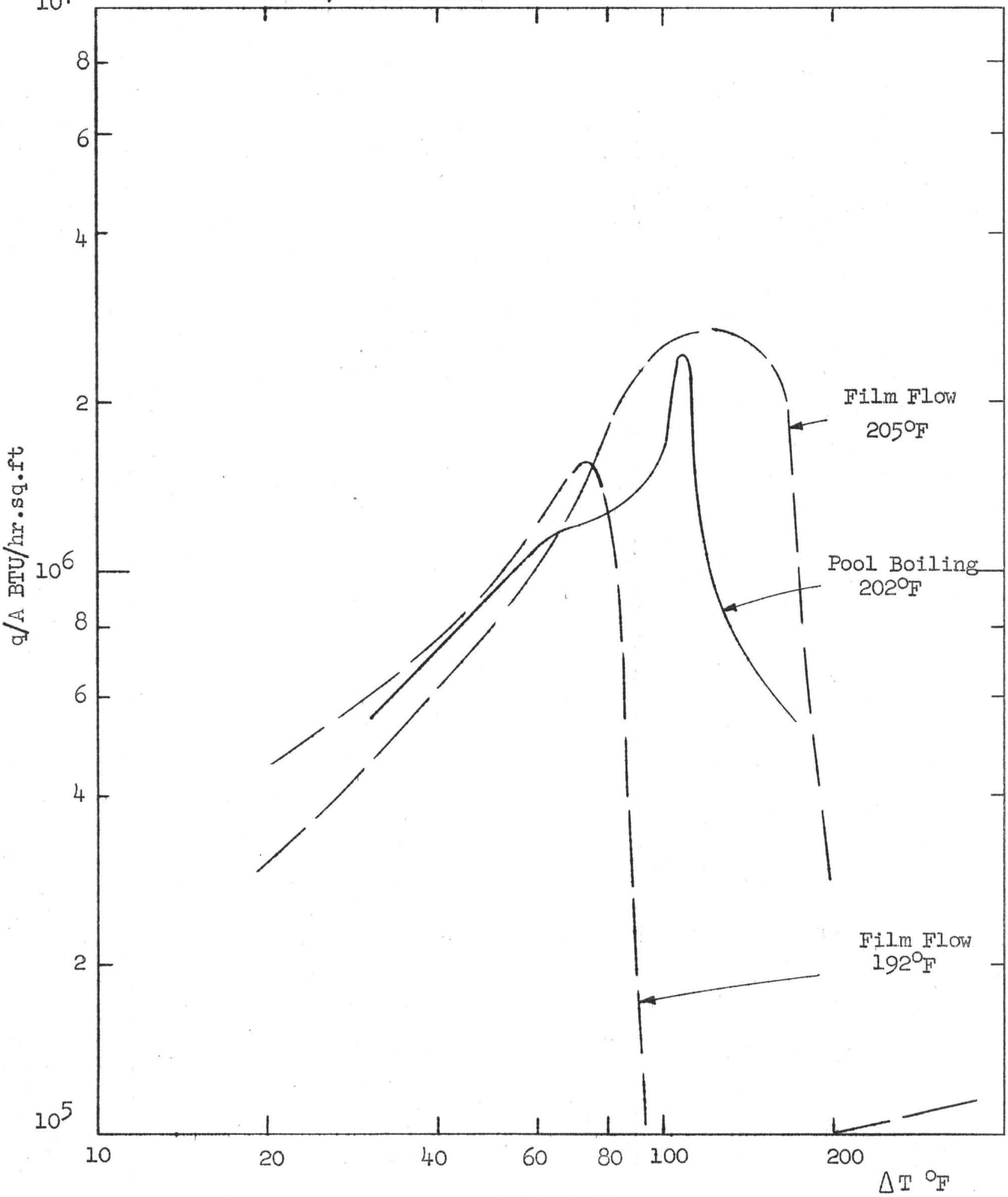

FIGURE 57

Two runs were made starting with different initial block temperatures. The results are shown in Figure 52 and there appears to be no significant effect.

After the experiments with water the boiling plate was cleaned and a further run with water was made. Then the surface of the boiling plate was brushed over with cotton wool soaked in benzene. This treatment was applied under film boiling conditions. The run with water was repeated at the same flow rate and water temperature. The boiling curves of the two runs are compared in Figure 53, and the two traces are compared in Figure 55. There appears to be a significant effect. The experiment was repeated except that this time only the immediate area of the heat-flux meter was treated with benzene. The results are shown in Figure 54. Observation of the film flow showed that the break-up region no longer advanced in a "parabolic" shape, but that it actually stopped in front of the heat-flux meter and continued to advance at the side of the heat-flux meter.

The thin copper disc heat-flux meter, which was 2 1/2 in. from the front lip, could not be used for comparison because of a damaged thermocouple connection.

Some characteristic traces of the thick copper disc heat-flux meter, which was 3 1/2 in. from the front lip are shown in Figure 56. The results of these two traces, which refer to water films, are shown in Figure 57. This meter always indicated very high heat fluxes.

3. Steady-State Pool Boiling

These experiments were performed to obtain an order of magnitude

NUCLEATE POOL BOILING OF BENZENE

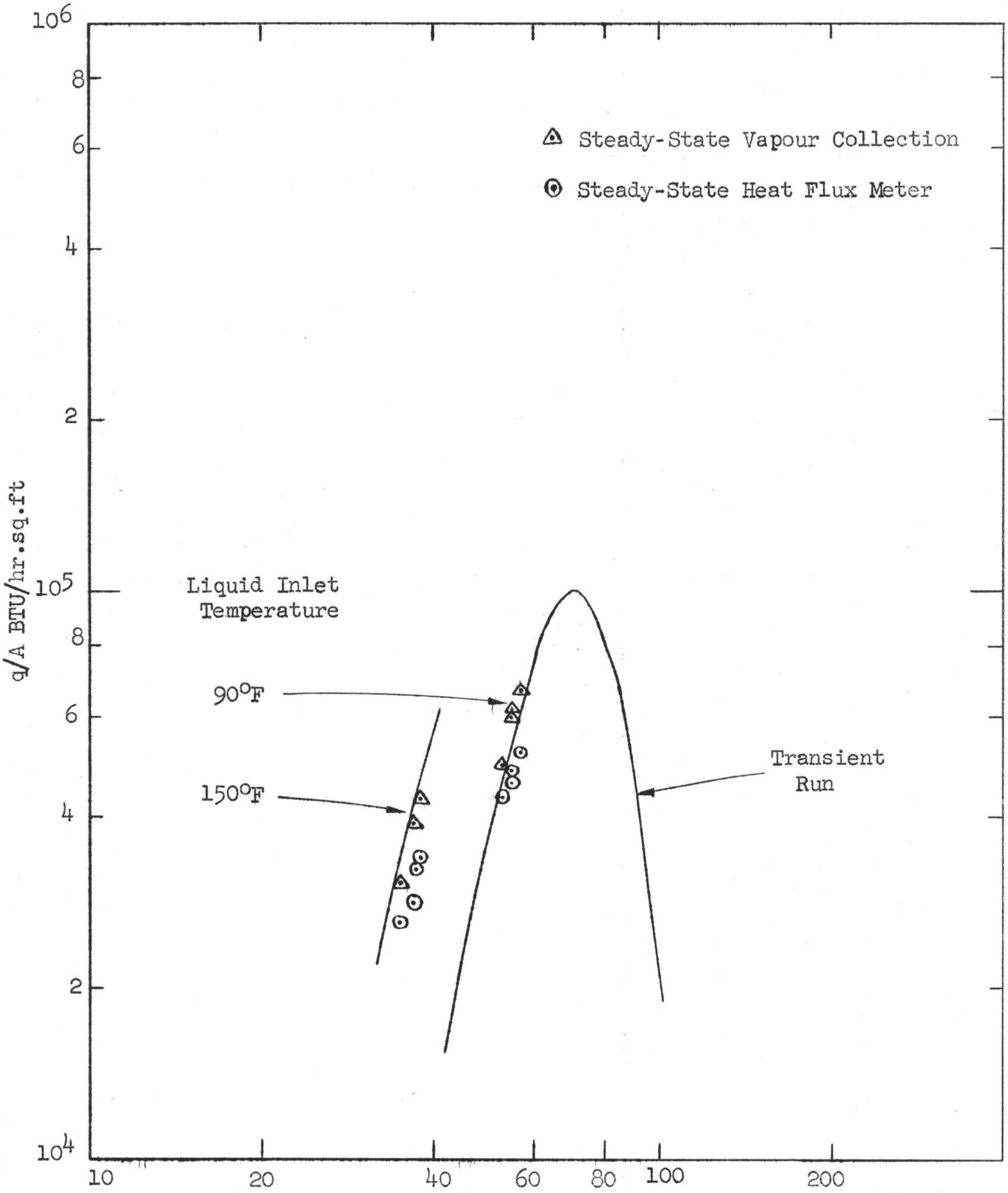

FIGURE 58

check on the heat-flux meters. The thin copper disc heat-flux meter which was 3 1/2 in. from the front lip of the unplated boiling plate, was used. A comparison between the heat fluxes obtained by the vapour collection method and the heat-flux meter method is shown in Figures 58 and 61. An unsteady-state pool boiling experiment performed shortly afterwards is also shown.

The heat fluxes as indicated by the vapour collection method were always found to be higher than those of the heat-flux meter method. More boiling activity was observed in the crevices at the periphery of the boiling area. This could account for some of the difference.

During these experiments considerable changes in the zero position of the heat-flux meter were observed. These changes were always on the negative side and indicated that the centre temperature of the heat-flux meter disc was higher than the edge temperature. In the appendix it is shown that such changes can be attributed to heat conduction into the heat-flux meter disc through the centre thermocouple. This heat conduction can also account for the low heat-flux readings of the heat-flux meter as mentioned above.

4. Unsteady-State Pool Boiling

These experiments were done to make a direct comparison between pool boiling heat fluxes and boiling heat fluxes of film flow. The thin copper disc heat-flux meter, which was 3 1/2 in. from the front lip of the boiling plate was used. Typical heat-flux meter traces for benzene and water are shown in Figures 59 and 60 respectively. The traces show the steady film boiling, transition and nucleate boiling regimes. The large oscillations of the heat-flux meter indicate transition boiling.

HEAT FLUX METER TRACE OF POOL BOILING OF BENZENE

LIQUID INLET = 90°F

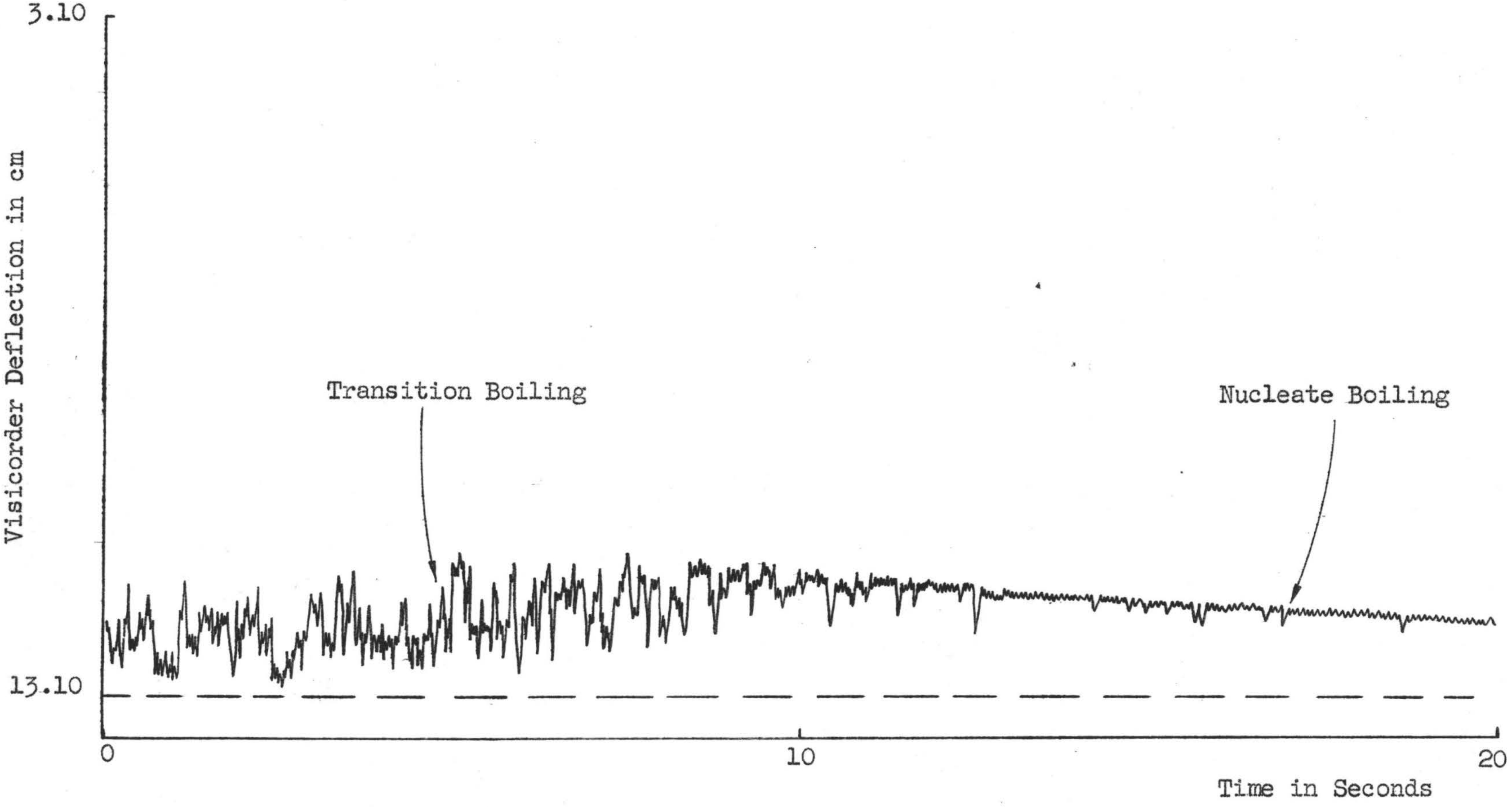

FIGURE 59

HEAT FLUX METER TRACE OF POOL BOILING OF WATER

LIQUID INLET = 202°F, (BOILING CURVE IN FIGURE 64)

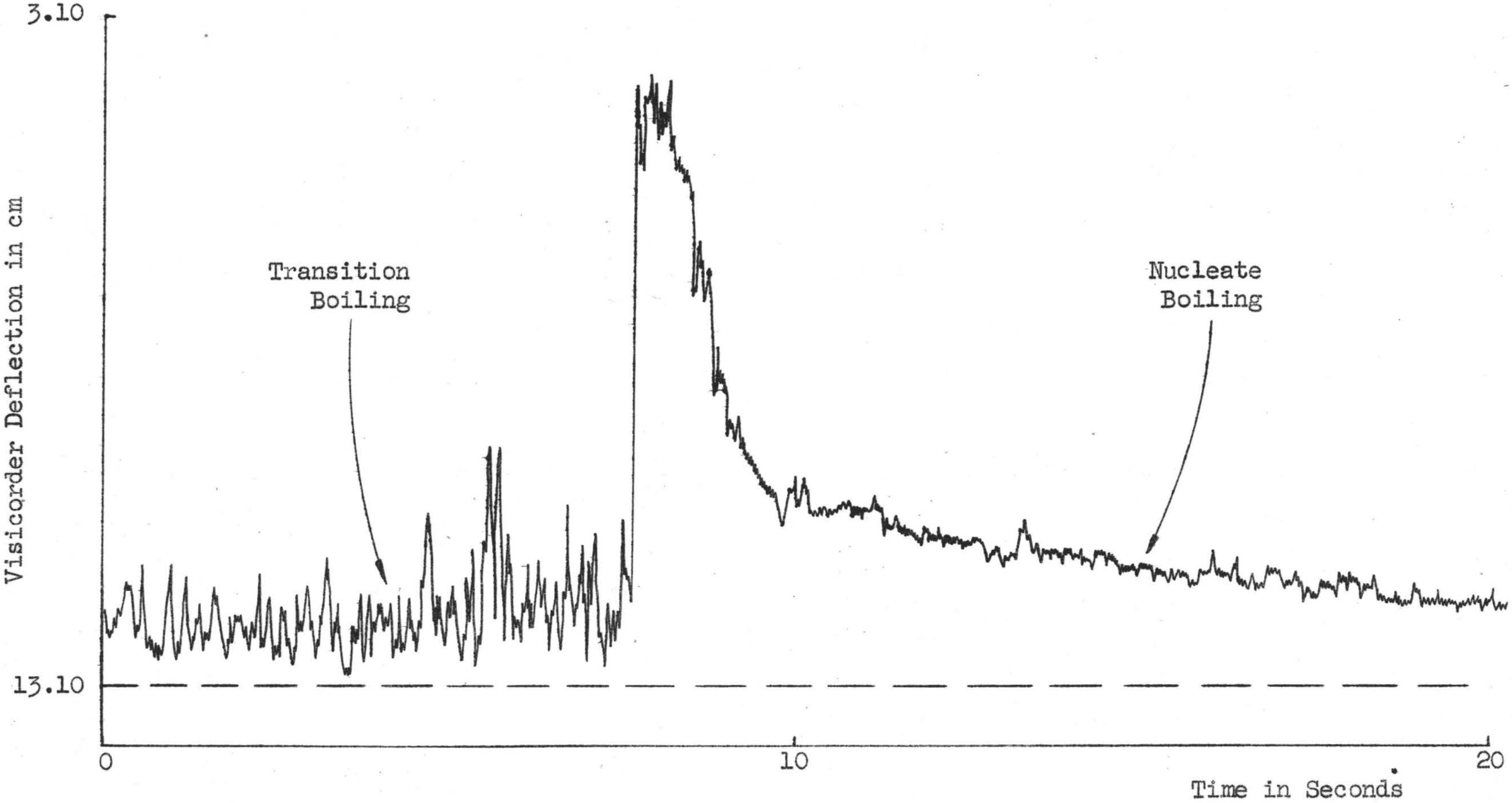

FIGURE 60

The traces during nucleate boiling were much more steady than those during transition boiling.

The results for benzene are shown in Figure 61 and the results for water are shown in Figures 63 to 66. The boiling curves for water in Figure 64 are unusual, because they show a point of inflexion in the nucleate boiling curve. Comparison of the heat-flux traces with the temperature traces showed a misalignment in that the sharp decrease of the temperature trace did not coincide with the maximum heat flux on the heat-flux trace. A timing error appeared evident as shown in Figure 65.

A trace during dry-out with water on the boiling plate is shown in Figure 68. Immediately after the dry-out, i.e. when all the liquid had boiled off, the heat-flux meter indicated a negative heat flux. This error diminished with time and was attributed to the thermocouple conduction.

The thick disc heat-flux meter, 3 1/2 in. from the front lip, showed characteristic responses as shown in Figure 56. A boiling curve for unsteady-state pool boiling of water is shown in Figure 57.

POOL BOILING CURVE OF BENZENE

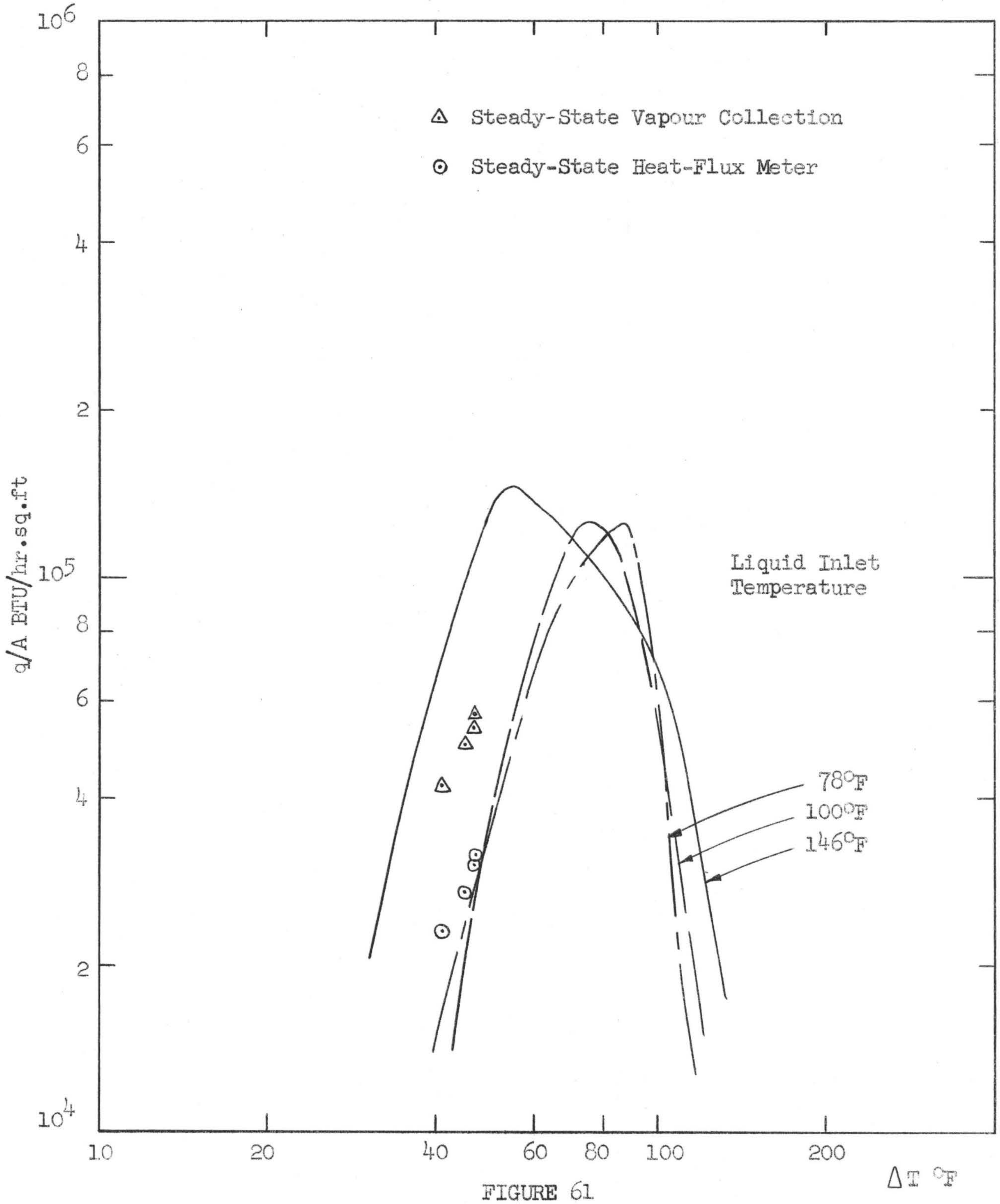

FIGURE 61

LITERATURE POOL BOILING CURVE OF BENZENE

REF.: C12, S7, B11, H15, H16

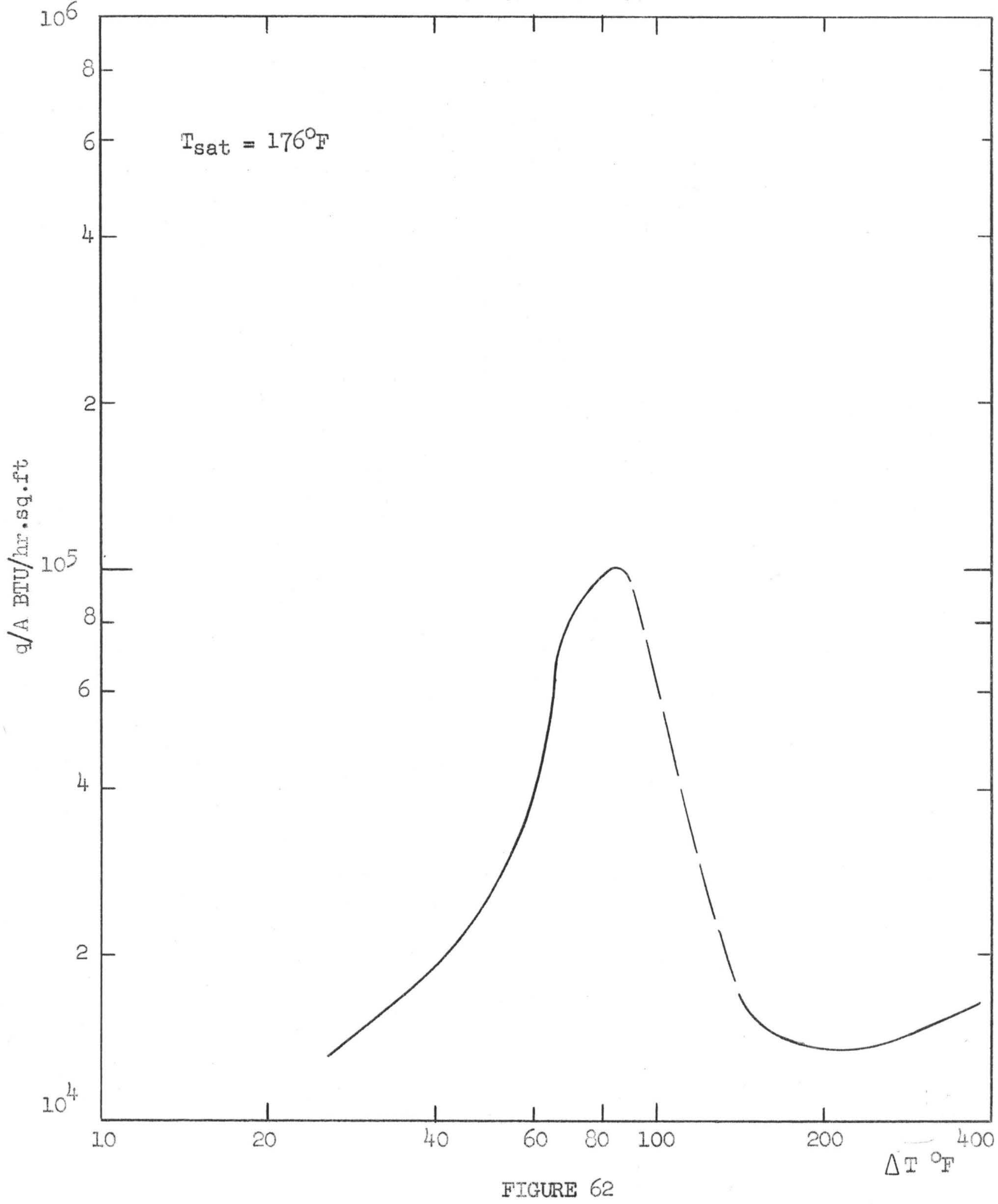

FIGURE 62

POOL BOILING CURVE OF WATER

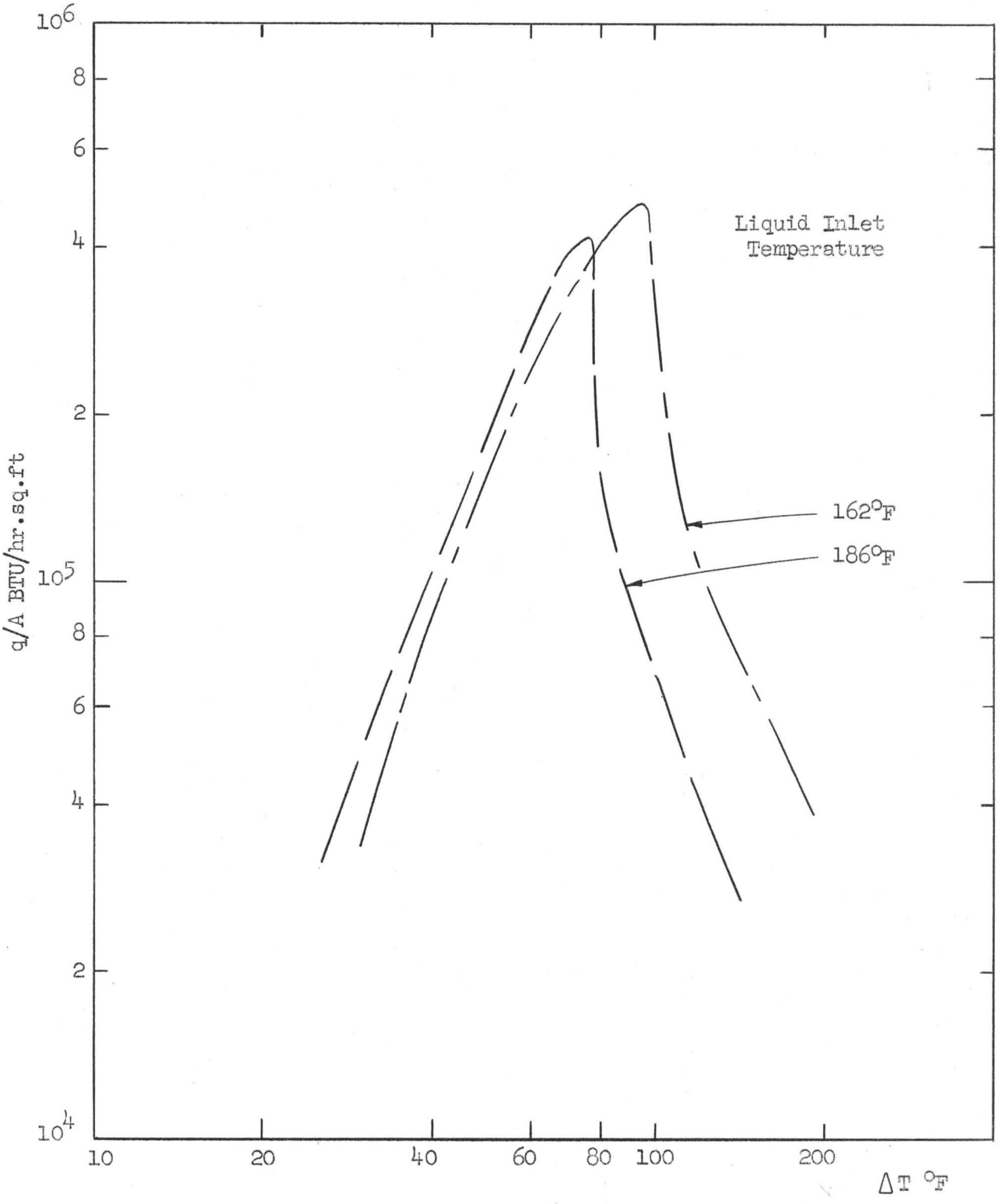

FIGURE 63

POOL BOILING CURVE OF WATER

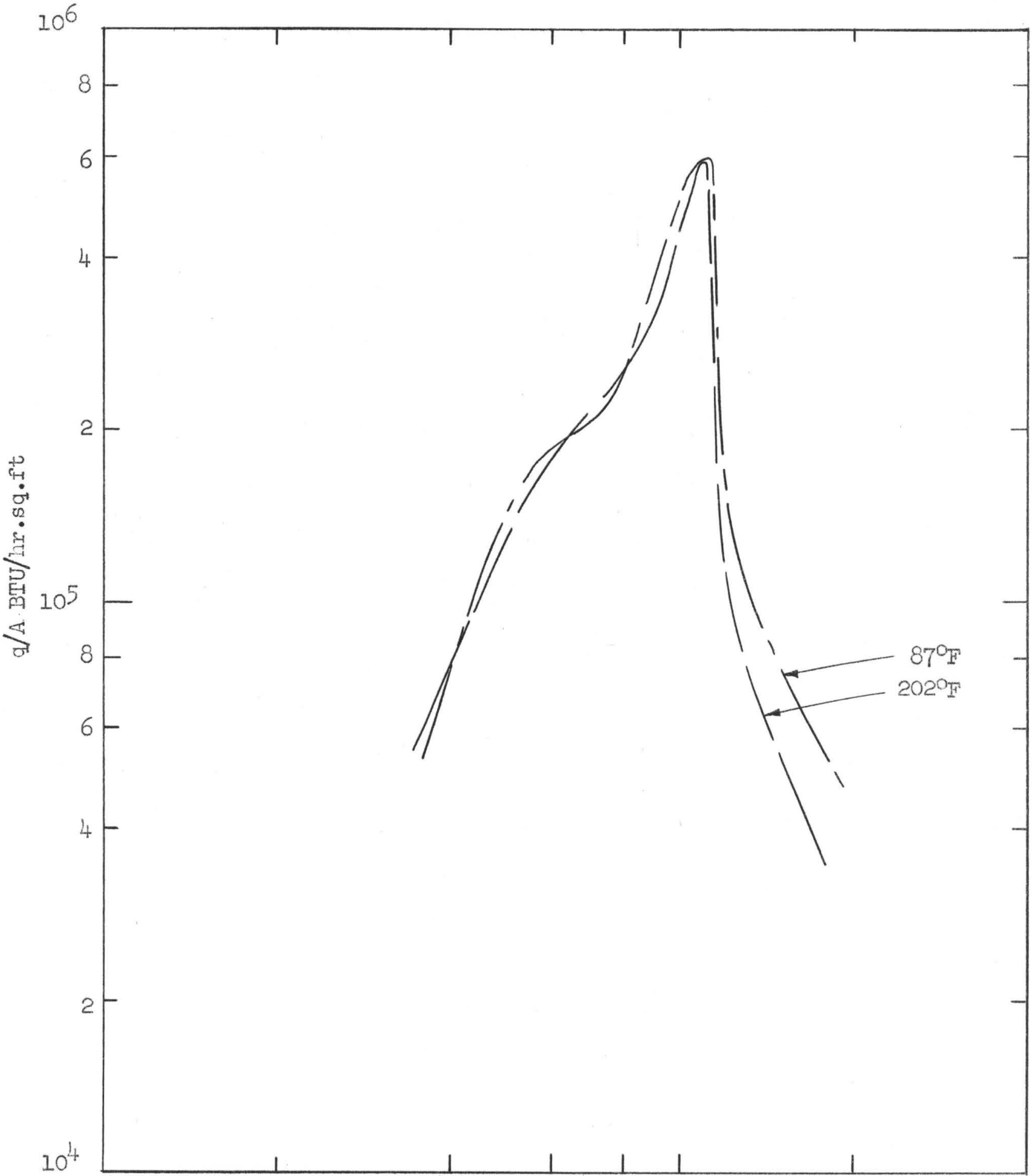

FIGURE 64

POOL BOILING CURVE OF WATER

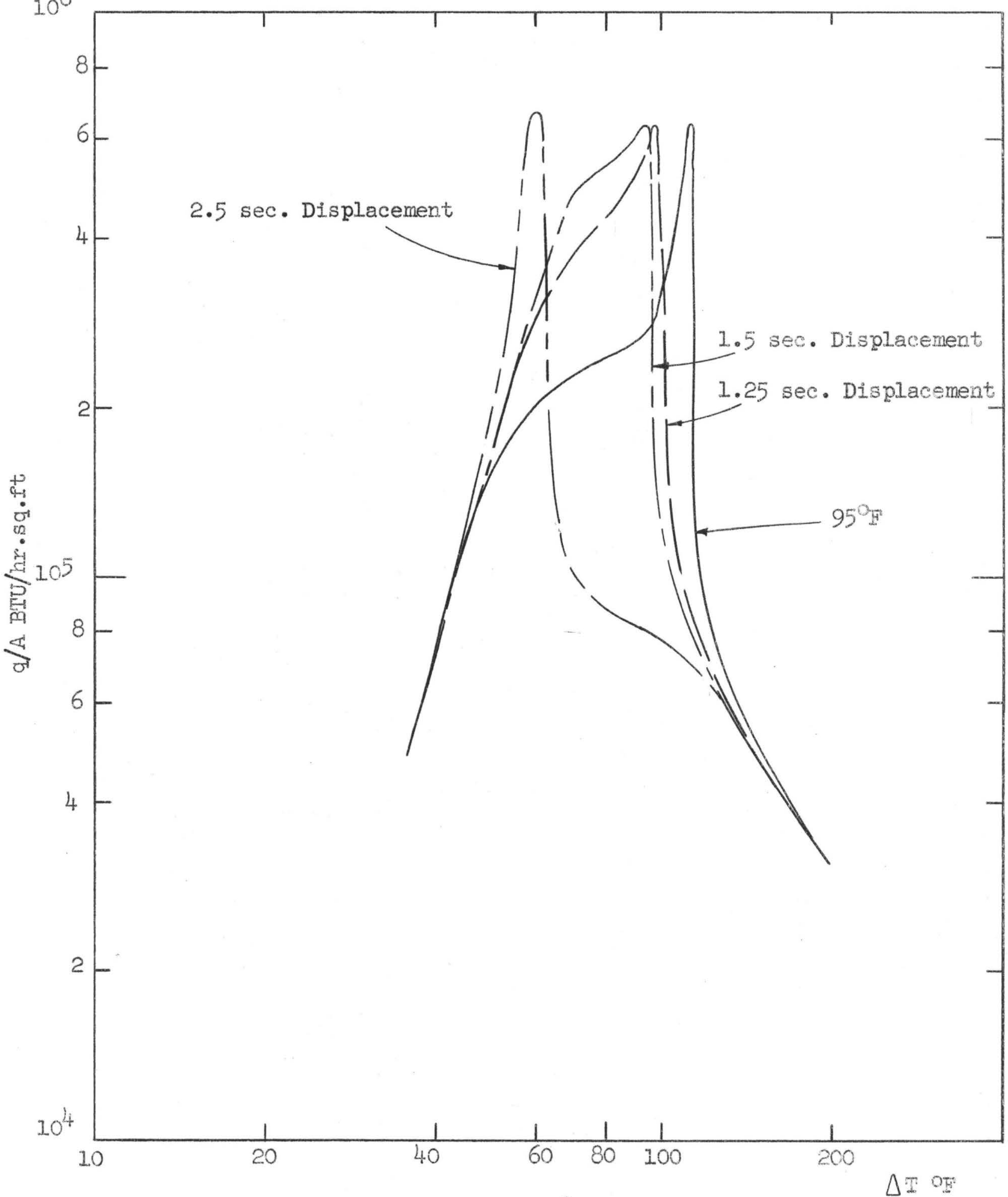

FIGURE 65

POOL BOILING CURVE OF WATER

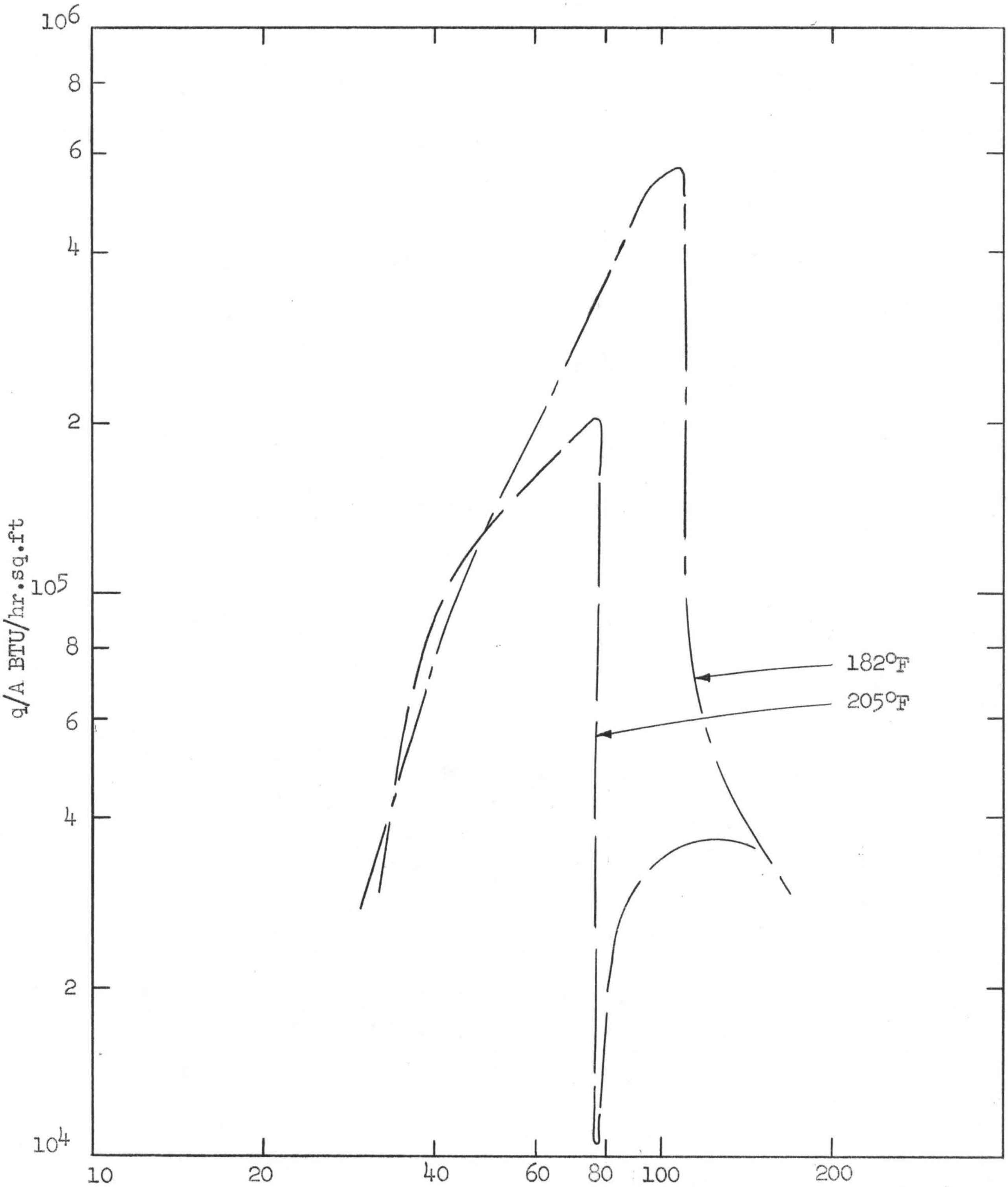

FIGURE 66

LITERATURE POOL BOILING CURVE OF WATER

REF.: G5, H10, C12, K4, J4, B18, M5

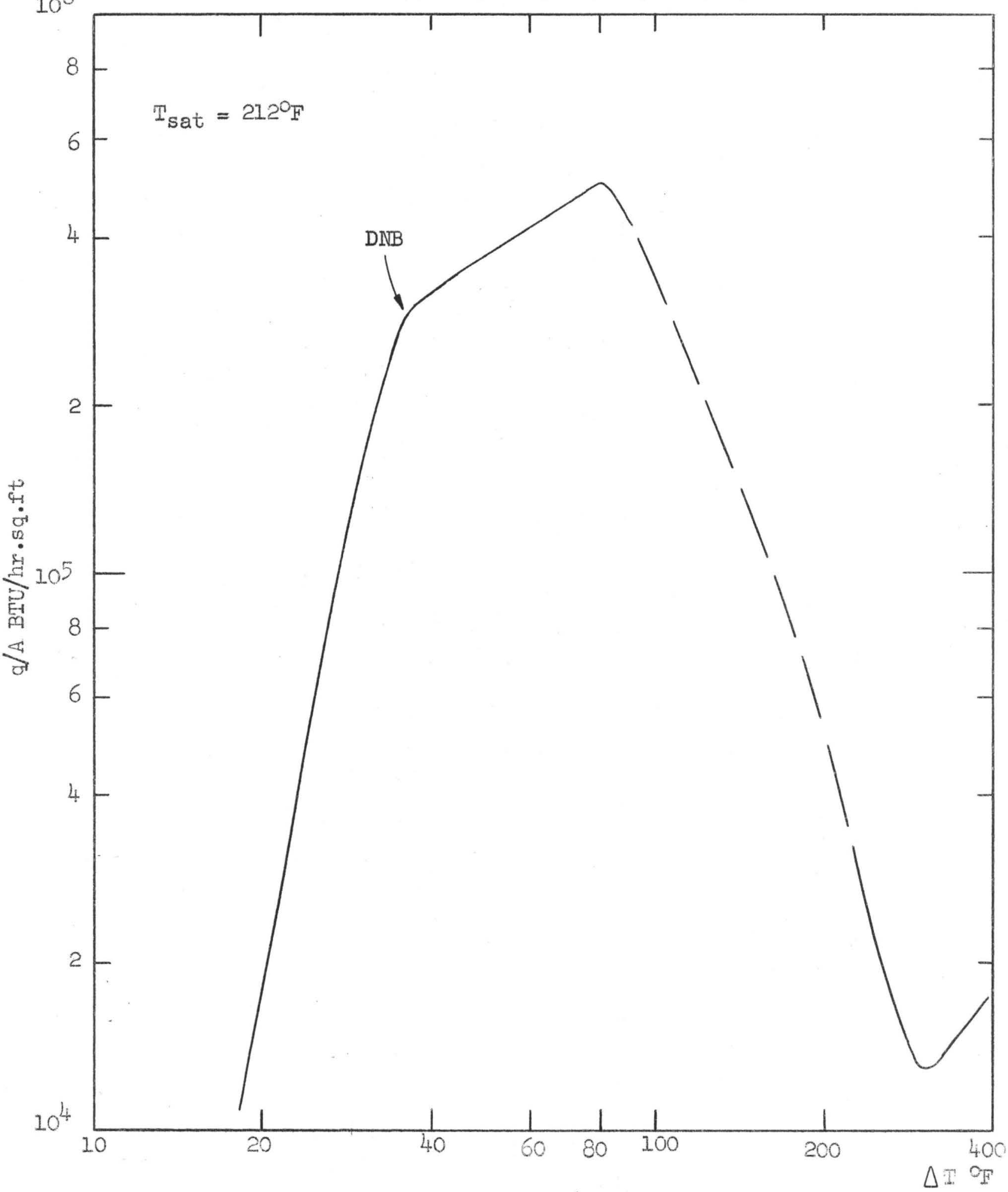

FIGURE 67

HEAT FLUX METER TRACE OF DRY-OUT IN POOL BOILING

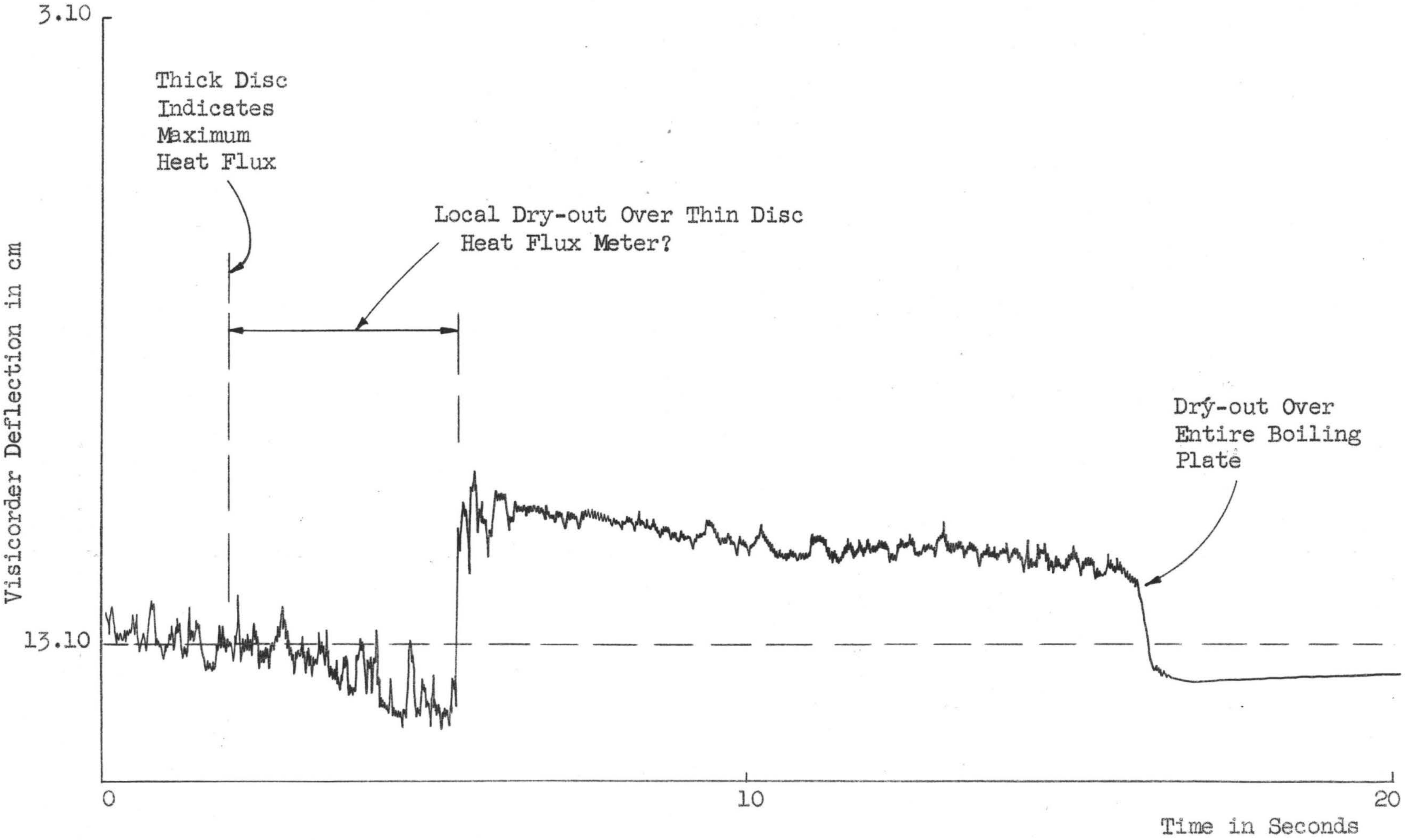

FIGURE 68

F. DISCUSSION

In this section the results of the film flow experiments will be discussed and related to the other experiments and established literature data. The use of the heat-flux meters under the conditions of boiling heat transfer is also discussed.

1. Hydrodynamic Behaviour

Plates 3 to 8 show that the hydrodynamic patterns of liquid film destruction under conditions of boiling heat transfer are quite complex. A detailed examination of the processes requires high-speed photography. However due to synchronisation difficulties only a few high-speed films were taken. From these films it was not possible to identify any growing bubbles on the boiling plate or see the hydrodynamic condition on the heat-flux meter.

Since the spray formation and boiling are suppressed at high subcooling of the liquid, a photographic study under those conditions might be simpler.

2. Heat Flux Measurements

The most significant results obtained are the heat-flux measurements of the boiling liquid films using the local heat-flux meters. These data are presented in Figures 42 to 47 for benzene and in Figures 48 to 54 for water.

2.1 Forced Convection

In these Figures the lines of low slope, where ΔT is less than about 30°F, are interpreted as pure forced convection heat transfer. In Figures 42, 43, 48 and 49 the equation (B-10) has been plotted for comparison at two liquid inlet temperatures. It appears from the data of benzene that the experiments were not carried out long enough to cover the forced convection regime. The experimental curves would join the equation (B-10) smoothly at low temperature differences of about 2°F. For water the agreement in intercept and slope between the experimental values and equation (B-10) is good. It should be noted that equation (B-10) has been based on experiments done with water.

Comparing the water data at 90° and at 30° incline, it will be noted that the forced convection curves appear to be absent in the runs made at 30°. From equation (B-9) it is, however, expected that the angle of inclination has only a small effect on the forced convection heat transfer. In these latter runs the water appeared to be boiling much more vigorously (larger bubble size).

In the present experiments no detailed examination was made when bubble nucleation on the heat-flux meter ceased. In future experiments the heat-flux measurements should be extended further into the forced convection regime.

2.2 Incipience of Boiling

An estimate of the temperature difference at the incipience of boiling can be made from the data of the water runs; (Figures 48 and 49). This temperature difference is about 30°F and is in general agreement with the evidence reported by Bergles and Rohsenow (B7) and Hsu (H7). The theoretical analysis by Hsu (H7) indicates that the temperature difference at the incipience of boiling increases with forced convection and subcooling. The effect of the subcooling seems to be confirmed by the data in Figure 48.

2.3 Transition Regime

This transition regime is meant to be the section on the boiling curve between forced convection and fully established nucleate boiling, (Figure 3). In this regime forced convection and subcooling increase the heat transfer. Qualitatively this is shown by the present data of benzene and water, i.e. at temperatures differences up to 60°F the colder liquid always allowed larger heat fluxes. Within the small experimental range the effect of forced convection was negligible in this regime. The range of this transition regime appears to be much greater for benzene (2-60°F) than for water (30-60°F).

Bergles and Rohsenow (B7) have proposed and verified an equation for this regime based on the superposition principle. By using the data of the water runs at 178°F and 170°F in Figures 48 and 49 respectively the superposition technique can be shown to apply in the transition regime provided the experimental forced convection and nucleate boiling curves are used. The equation for the heat flux at incipience of boiling, which was derived by Bergles and Rohsenow (B7), however does not apply to the present data, (Figure 48).

2.4 Nucleate Boiling

From the data it appears that at temperature differences above 60°F boiling becomes fully established. In this regime the boiling curves of benzene and water respectively follow a single line. The exponents a in the equation

$$q/A \propto (\Delta T)^a$$

are 2.6 for benzene and 1.7 for water. This observation is in agreement with statements of Forster and Greif (F4), who point out that the heat flux, once boiling is fully established, does not depend upon the degree of subcooling or forced convection.

The data indicate that the angle of inclination of the boiling plate has no effect on the nucleate boiling of the liquid films. Githinji and Sabersky (G7) have shown that the orientation of the heating surface effects the nucleate boiling heat flux in saturated pool boiling. This effect is absent in the present experiments due to the different hydrodynamic conditions, which now include forced convection and subcooling.

2.5 Maximum Heat Flux

At a certain temperature difference the boiling curve departs from the nucleate boiling line, (Figure 3). At a slightly greater temperature difference the maximum heat flux of the boiling curve occurs. The data of water and benzene show that the maximum heat flux increased with subcooling and forced convection. These results are in qualitative agreement with the results of Gunther (G6). However it should be noted that while the maximum heat flux of benzene was increased by a factor of 2, the maximum heat flux of water was not increased to such an extent. It was expected that the maximum heat flux of water would be increased by a greater extent than for organic liquids (Z5). This aspect will be discussed further in the section on heat-flux meters.

Westwater (W3) pointed out that the temperature difference at the maximum heat flux is only a small function of the subcooling or the forced convection. This, however, is not borne out in the present experiments, which show that this temperature difference increases with the subcooling of the liquid.

2.6 Transition Boiling

In the transition boiling regime the liquid contacts the heating surface intermittently at particular locations. Thus any point on the heating surface is subjected to cycles of low heat flux (no liquid contact) and high heat flux (liquid contact). This cycling is well indicated by the oscillations in the traces shown in Figures 40 and 41. The heat flux variations have been indicated in Figures 42, 43, 46, 47, 50 and 51.

These variations depend upon the angle of inclination of the boiling plate and on the angle of separation of the liquid film from the boiling plate. For benzene the angle of separation was always very low and hence the traces at 30° and 90° incline show the transition boiling regime. For water the angle of separation was large and hence at 90° incline of the boiling plate the transition boiling regime was not shown in the traces.

The present data show that increasing subcooling increases the heat flux (at the same surface temperature). Only one reference appears to be in the literature dealing with transition boiling to subcooled liquids. Stenzel and Schultze (S2) have shown that the heat transfer is increased in the transition boiling regime when the forced convection or subcooling is increased. The temperature difference at the minimum heat flux was found to be constant for any conditions of forced convection or subcooling.

2.7 Film Boiling

Due to the complex hydrodynamic flow patterns of the liquid film after it has separated from the boiling plate, it is difficult to discuss the heat transfer in the film boiling regime, (Plate 7). Also the error in the heat-flux measurement, due to the thermocouple conduction, would not permit accurate evaluation of the low heat fluxes in this regime.

The flow patterns depend upon the flow-rate, subcooling, liquid, length of nucleate boiling section on the boiling plate and the inclination of the boiling plate. These determine under what conditions the liquid passes over the local heat-flux meters.

In future experiments the film boiling regime might be covered better under conditions of large flow-rates, low angles of inclination of the boiling plate and a very short section of nucleate boiling in the liquid film. The flow patterns of the liquid film after the break-up region will then be much more uniform.

2.8 Surface Wetting

After the water runs the entire boiling plate was treated with cotton wool soaked in benzene and a further run with water was made.

The result of this experiment is shown in Figure 53. The maximum heat flux was found to be less and occurred at a much lower surface temperature. The temperature trace of the edge thermocouple was different to the water runs without benzene surface treatments. Repeated boiling with water removed this benzene, but the effect could be reproduced by a fresh application of benzene.

The results of water in Figures 48 and 49 at the highest liquid temperatures were the first that were obtained after the film flow runs with benzene. These boiling curves too indicate a rather low maximum heat flux at a low temperature difference. An examination of the edge thermocouple trace indicated a cooling pattern, which was similar to the temperature trace of the water experiments in which the surface was treated with benzene. The cooling rate of the boiling plate in these first water experiments was also much slower than in the later ones. Thus these first runs are probably not true water experiments.

When only the heat-flux meter itself was treated with benzene, the resulting flow patterns took quite a different shape. Instead of advancing in a "parabolic" curve, the break-up region stopped in front of the heat-flux meter, but continued to advance on both sides of the heat-flux meter. It appears that the benzene treatment altered the surface properties and reduced the wetting of the water on the copper heat-flux meter. No surface deposits or any other indication could be seen that the heat-flux meter was different from the rest of the boiling plate.

The resulting boiling curve (Figure 54) showed a low maximum heat flux at a low temperature difference. The decrease of the heat flux before the maximum heat flux should be noted; this was not observed in the other film flow traces. These results can be explained in terms of the film flow conditions: when the break-up region passed on both sides of the heat-flux meter (but not over it), the heat-flux meter was cooled by conduction through the copper. Thus the heat-flux meter was cooled below the temperature at which the maximum heat flux occurs. When the liquid did wet the heat-flux meter, it indicated a heat flux which corresponded to its surface temperature ($(\{80 + 212\}^{o}F$ in the present case). When maximum boiling occurred around the heat-flux meter (but not on it), the temperature gradient in the boiling plate was large. The conduction in the centre thermocouple was then also large and this could explain the decrease in heat flux before the "maximum" heat flux was indicated.

In Figure 55 two traces are compared; one refers to an ordinary run with water and the other to a run with a benzene-treated surface. The first peaks in the curves correspond to transition boiling on the heat-flux meter when the liquid fell back on the boiling plate (angle of inclination was 30°). The benzene-treated surface shows lower heat fluxes, which was probably due to the reduced wetting. This observation is in agreement with the findings of Berenson (B8) and Westwater (W3), who increased the heat flux in transition boiling by improving the wetting of the liquid on the solid.

It has been remarked in the section on forced convection that in the last water experiments the boiling on the plate was much more vigorous and that the forced convection curves were missing (compare Figures 48 and 52). It appears as if the data in Figure 52 give the pool boiling curve (Figure 63), indicating that the boiling in the liquid film was so vigorous that the effect of forced convection of the liquid film became negligible. This seems feasible if it is considered that the benzene on the copper surface (in the first water experiments) reduced the wetting of the water underneath the vapour bubbles and thus perhaps reduced the micro-layer vaporization (M5). It would be of interest to study this further.

2.9 Pool Boiling Heat Fluxes

The unsteady-state pool boiling experiments were done in order to judge the performance of the heat-flux meter by comparison with literature data. The literature data refer to horizontal plates with different surface materials. Figure 61 shows the unsteady-state pool boiling data for benzene. These boiling curves are in good agreement with the literature boiling curve shown in Figure 62. It is uncertain whether the effect of the inlet temperature is real.

Figures 63 to 66 show the unsteady-state pool boiling curves of water. These curves show consistent values and they are in fair agreement with the literature boiling curve shown in Figure 67. The position of the maximum heat flux and the transition boiling regime show good agreement with the literature curve. The maximum heat flux of water in the present experiments ranged from 430,000-630,000 BTU/hr.sq.ft. Gaertner (G5) boiled water on a horizontal copper surface and obtained a value of 500,000 BTU/hr.sq.ft for the maximum heat flux under steady-state conditions. The experimental nucleate boiling curve appears to join the literature curve at low heat fluxes. The characteristic knee (position of DNB) was not obtained in the present experiments. By careful experimentation Gaertner (G5) was the first to demonstrate the position of DNB in nucleate pool boiling. It is well known that nucleate boiling heat fluxes depend upon the surface conditions and in the present experiments these were not rigidly controlled. Thus a very precise comparison with the literature cannot be made. In these experiments there appeared to be little effect of the inlet temperature as shown in Figure 64.

It was thus confirmed that the heat-flux meters responded to the boiling conditions. Although the data range was small further evidence was taken from the steady-state experiments in which vapour collections were made (Figure 58). The heat-flux meters did measure the correct heat flux, if allowance was made for the thermocouple conduction along the centre wire. This is further discussed in the appendix.

2.10 Boiling Heat Flux to Liquid Films

When the film flow data and the pool boiling data of benzene (Figures 43 and 61) and of water (Figures 49 and 63) are compared, then the following trends (relative to pool boiling) will be observed: presence of forced convection, incipience of boiling at higher temperature differences, coincident nucleate boiling line once nucleate boiling is fully established, increased maximum heat flux and increased heat fluxes in the transition boiling regime. These trends are in agreement with forced convection subcooled boiling, which is shown in Figure 3.

The difference in the case of film flow is that the bulk of the liquid is absent and hence the liquid film rapidly heats up to its saturation temperature over a short length of the boiling plate. In the present experiments this heating length was only 1 1/2 in. and hence the boiling curve of a subcooled liquid film could be measured.

It may be expected that at very large film flow-rates ($Re > 4000$) the boiling of the liquid film resembles forced convection subcooled boiling under bulk flow conditions. The bulk flow could be considered as liquid film flow, in which the liquid film thickness was large. At large film flow rates the film thickness would be greater than 0.050 in., while the maximum vapour bubble diameter would be about 0.040 in. (G6).

The present data indicate that at lower film flow-rates ($1000 < Re < 4000$) the boiling of the liquid film still resembles forced convection subcooled boiling. It was also observed that at $Re < 500$ the heat transfer surface was not wetted uniformly and that dry patches tended to form at high surface temperatures, (Plate 8).

Bressler (B3) boiled water films at lower flow-rates ($350 < Re < 1200$) and low temperature differences ΔT. He observed that the boiling heat fluxes corresponded to the pool boiling curve of Jakob and Linke (J1). The boiling of these films was so intense that the effect of the small film flow was negligible. The subcooling of the water was about 15°F.

Norman and McIntyre (N1) have investigated the boiling heat flux to water films at lower film flow-rates still ($20 < Re < 1160$). No subcooling was employed and the temperature differences were low. These observers too concluded that at the higher film flow-rates the boiling of the liquid film could be described by the pool boiling curve. At very low flow-rates, however, they measured rather high heat fluxes at low temperature differences. This was attributed to direct surface evaporation (similar to microlayer evaporation underneath vapour bubbles).

The wetting of the heating surface under those conditions was possible, because lower surface temperatures were employed than in the present experiments.

Usually the average heat flux to a liquid film is measured over a certain boiling length. This leads to uncertainties because at low flow-rates ($Re < 1000$) much evaporation occurs, such that dry areas appear in the liquid film and the heating surface is not uniformly wetted. If the boiling length is long then the film may completely evaporate. At high heat fluxes (high temperature differences) this situation is even more severe, because more evaporation occurs and the wetting is further reduced. Thus at high heat fluxes a short boiling length should be chosen in order to ensure uniform hydrodynamic conditions over the area where the heat transfer is measured. The local heat-flux meter, which was used in the present experiments, fulfills this aim.

3. Heat-Flux Meters

In the case of pool boiling the use of the local heat-flux meter assumes (besides the assumptions presented in the appendix) that the local boiling occurring on the heat-flux meter is representative of the boiling over the rest of the boiling surface. The work of Gaertner (G5) suggests that after the DNB point on the boiling curve (i.e. when local vapour patches tend to form on the heating surface) the local conditions on the heating surface alternate between film boiling and thin liquid film evaporation. Because of its small size the heat-flux meter could measure either of the two conditions when the temperature difference on the boiling curve was between the DNB point and the maximum heat flux.

Similar considerations apply to the transition boiling regime in which the local heat flux changes as discussed above.

In a large number of pool boiling experiments with water it was observed that the heat flux decreased before the "maximum" heat flux was indicated, (Figure 68). The resulting boiling curve showed a low maximum heat flux at a low temperature difference, (Figure 66). These results could be interpreted by a local dry-out (vapour patch) on the heat-flux meter when the heat-flux meter should have indicated the true maximum heat flux. Under such conditions the heat-flux meter would indicate a zero heat flux before it indicated a "maximum" heat flux. In some traces the heat-flux meter indicated large variations from zero to the maximum heat flux near the expected maximum heat flux. The thick disc heat-flux meter could be used to identify at what time the thin disc should have indicated the maximum heat flux. In the traces which gave a low "maximum" heat flux the thick disc always indicated the maximum heat flux before the thin disc did, (Figure 68).

In the case of forced convection subcooled boiling the range between DNB and the maximum heat flux is reduced, such that DNB almost represents the maximum heat flux. Thus as soon as vapour patches begin to form on the surface, the heating surface overheats and burn-out (maximum heat flux) results. In the present unsteady-state experiments it is assumed that at the point of separation of the liquid film from the boiling plate the heat flux corresponds to the maximum heat flux under steady-state conditions.

During the heat transfer measurements the nucleate boiling section of the liquid films expanded along the boiling plate, (Plate 4).

Thus when the liquid film reached the heat-flux meter, it had already been heated by the nucleate boiling section. The amount of heating depends on the distance between the heat-flux meter and the thin section of the boiling plate. If this distance is very large, then the liquid film will attain its saturation temperature by the time it reaches the heat-flux meter. Thus in order to make a proper evaluation of the effect of subcooling on the maximum heat flux, the heat-flux meter should be placed close to the thin section.

The movement of the break-up region over the heat-flux meter causes an unsymmetric heat flux over the disc, (Plate 6). It is unknown how this disturbance affects the assumed operation of the heat-flux meter, i.e. a uniform heat flux over the entire disc. The two thermocouple junctions have been arranged so that the line joining them was parallel to the break-up region. For other positions of the edge thermocouple different "boiling curves" would be obtained. For example if the edge thermocouple was upstream of the centre one a negative heat flux would be recorded at the instant when the break-up region moved onto the meter.

The conduction along the centre thermocouple wire cannot be neglected as is shown in the appendix. This conduction error depends upon the temperature gradient in the thermocouple wire. No correction was made to the present results, because the exact value of the temperature gradient was not known. It was estimated that the maximum correction would amount to about +30,000 BTU/hr.sq.ft.

Using the data of Gaertner and Westwater (G3) the number of nucleating sites on the heat-flux meter can be roughly estimated in the case of water. The area of the heat flux meter was 1.33×10^{-4} sq.ft. Thus at a heat flux of 320,000 BTU/hr.sq.ft and 55,000 BTU/hr.sq.ft the number of nucleating sites would be 26 and 8 respectively. It should be noted, however, that their data were obtained under conditions of saturated pool boiling of water. From the data of Gunther (G6) it is known that the bubble population decreases with subcooling and forced convection and hence the values estimated above are on the high side.

The use of equation (K-1) requires precise machining of the heat-flux meter discs, accurate location of the thermocouples and good silver-soldering. The thermal conductivity of the material of the heat-flux meter must be precisely known at any temperature. The thermocouples must also be calibrated accurately.

3.1 Thin Disc Heat Flux Meter

The thin disc heat-flux meter gave results which were in general agreement with the literature data.

The maximum temperature difference observed across the thin disc was 20°F and 47°F for benzene and water respectively. Both of these temperature differences were too high because much less boiling would occur at the centre of the heat-flux meter. In the case of water probably no boiling occurred at the centre of the disc at all. This could explain why the maximum heat flux was not appreciably increased with subcooling and why the temperature difference (at the maximum heat flux) increased with subcooling in the case of water. The heat-flux meter was not acting as the rest of the boiling plate at these high boiling heat fluxes (Plate 6) and the heat-flux meter cooled rapidly.

The initiation of this cooling (probably by transition boiling) depended upon the liquid temperature, but the extent of the cooling remained about the same (i.e. until no further boiling could take place at the centre of the disc).

For the thin disc the centre thermocouple wire penetrated the entire disc. Thus at high heat fluxes, when a temperature gradient existed along the axis of the disc, the thermocouple would measure an "average" temperature of the disc axis. Provided the temperature gradient was small, then the thermocouple e.m.f. could be used in equation (K-1) without much error.

Moore and Mesler (M5) have shown that during bubble growth the heating surface is subjected to large local temperature variations. One of their results showed that an average local heat flux of 830,000 BTU/hr.sq.ft cooled the heating surface for 1.80 milliseconds. The heating surface then recovered during the following 12.5 milliseconds. After the 1.80 milliseconds the surface temperature of the nichrome strip had dropped by 24.2^{o}F. The depth of penetration of the temperature variation was 0.015 in. Assuming that the boiling on a copper surface is the same (i.e. same average local heat flux acting over the same length of time) as on the nichrome strip, then the surface temperature of the copper decreases by 6.2^{o}F and the depth of penetration of the temperature variation is 0.050 in. The copper surface would then recover to its initial temperature within 12 milliseconds. Since the heat-flux meter disc was only 0.010 in. thick, the centre thermocouple would probably not only respond to the average of all the nucleating sites on the heat-flux meter, but also to single nucleating sites near the centre of the disc. However such rapid temperature drops (1.80 milliseconds) were not measured because the maximum frequency response of the galvanometer M-40-350 was only 60 cycles/sec.

The response of the heat-flux measuring system can be judged from the trace in Figure 55. The trace shows the magnitude of transition boiling of water, when the liquid feel back on the heat-flux meter.

The further use of this heat-flux meter in the boiling field is recommended, since it provided reproducible results, which were in agreement with current knowledge. Its limitations have been discussed above.

3.2 Thick Disc Heat Flux Meter

Both thick copper disc heat-flux meters indicated large heat fluxes in all the boiling regimes and in the forced convection regime, (Figures 56 and 57). These results have been calculated using the temperature trace of the thin disc heat-flux meter. This does not affect the magnitude of the heat flux to a great extent, but does cause an error in the temperature difference.

In the case of benzene (film flow or pool boiling) the heat-flux meter hardly responded to the variable surface heat flux, but just indicated a steady large heat flux. In the film flow experiments with water two different characteristic traces could be obtained: one was an S-type trace and the other showed a sharp peak, (Figure 56). In the S-type trace the maximum heat flux always occurred after the thin disc had indicated the maximum heat flux. It should also be noted that the heat-flux meter always indicated a zero heat flux before indicating the maximum heat flux.

This type of trace was obtained in most experiments. However, in two film flow experiments the trace showed a definite peak (maximum heat flux) and this peak coincided exactly in time with the maximum heat flux of the thin copper disc.

The maximum heat flux for benzene and water at liquid temperatures close to the boiling point were about 700,000 BTU/hr.sq.ft and 2,000,000 BTU/hr.sq.ft respectively. For both liquids the film boiling heat flux was indicated to be about 170,000 BTU/hr.sq.ft. For the thick disc heat-flux meter the centre line temperature profile shows a large temperature gradient (Figure 74) and hence the centre thermocouple (being attached essentially to the bottom of the disc only) indicated the least temperature difference. Thus when the three-dimensional equation is applied the values for the heat fluxes would be higher still.

In the unsteady-state pool boiling experiments with water the response of the thick disc heat-flux meter was good and characteristic, (Figure 56). The peak of the trace coincided in time with the maximum heat flux of the thin disc heat-flux meter. As in the film flow experiments the heat fluxes were always indicated as too large in all the boiling regimes, (Figure 57).

When the film flow and the pool boiling traces are compared, it will be noted that the film flow traces are anomalous, because of their rounded peaks. Sharp peaks, as obtained in only two experiments, were expected. The reason for such behaviour and for the indication of these large heat fluxes is unknown. The answer may lie in the locations of the thermocouples.

3.3 Transient Heat Flux Measurement

Stenzel and Schultze (S2) have used a transient method for the measurement of boiling heat fluxes to various oils. Their apparatus consisted of a silver cylinder, which carried a thermocouple at its axis. The cooling rate of this thermocouple gave a measure of the surface heat flux. With this apparatus the heat flux was measured in all the boiling regimes. Effects such as forced convection, subcooling, surface roughness and surface tension were also studied. Their results were in qualitative agreement with the boiling curves shown in Figure 3. A notable exception was that no increase in the maximum heat flux was observed with increasing subcooling. This was attributed to the high viscosity of the oils at low temperatures. They note that such transient heat-flux measurements have a limited accuracy and that rapid cooling rates must be avoided.

The present experimental investigation has been carried out under transient conditions with a moving heat sink and a variable surface heat flux (advancing nucleate boiling region of the liquid film). However, since measurements were essentially taken at the solid-liquid interface, the true boiling heat flux - temperature difference relationship should be obtained with the present method. The cavity in the boiling plate (due to the heat-flux meter) probably has a negligible effect.

Good agreement between the film flow and unsteady-state pool boiling data was obtained. In the pool boiling experiments the boiling curve was obtained under transient conditions with a stationary heat sink and a variable surface heat flux and these data were in reasonable agreement with the literature boiling curve. Thus it appears that the present method can be used to measure boiling heat fluxes to liquid films.

G. CONCLUSIONS

From the present work the following conclusions can be drawn:

(i) The local heat-flux meter can be used to measure heat fluxes in pool boiling and in the boiling of liquid films. The present accuracy however is limited due to the uncertainty of the magnitude of the thermocouple conduction error.

(ii) The thin disc heat-flux meter, which was used in the present experiments, provided good results at low heat fluxes such as encountered in the boiling of benzene. This meter should not be used at large heat fluxes, which occur in the subcooled boiling of water films.

(iii) The film flow of benzene and water under boiling conditions resulted in boiling curves, which showed improved heat fluxes over the corresponding pool boiling curve. The boiling curves of the turbulent liquid films ($1000 < Re < 2500$) changed with flow-rate and subcooling in a manner, which was in agreement with forced convection subcooled boiling as shown in Figure 3.

The effect of the angle of inclination was unimportant in the forced convection and nucleate boiling regimes.

At the high surface temperatures (high heat fluxes) used in the present experiments $Re > 500$ in order for the liquid film to wet the boiling plate uniformly.

(iv) The pool boiling data of benzene was in good agreement with the literature pool boiling curve. In the case of water this agreement was fair.

(v) By treating the copper surface with benzene the heat flux to the water film is reduced in the transition boiling regime and at the maximum heat flux. This was attributed to the reduced wetting of the water on the copper surface.

(vi) The films taken at 3000 p.p.s. showed that the hydrodynamic factors governing the liquid-film destruction during the transition from nucleate to film boiling are complex.

(vii) The local heat-flux meter is a very useful tool for obtaining boiling data quickly, since a rapid transient method can be employed.

H. RECOMMENDATIONS

The present study was done to provide some general information on the hydrodynamic behaviour and heat transfer to turbulent liquid films under boiling conditions. During the study a heat-flux meter was developed; the use of such a meter for the measurement of boiling heat fluxes is possible and further work should be done on the meter.

1. Experimental Technique

(i) The heat-flux meters should be calibrated using steady-state pool boiling in all the boiling regimes.

(ii) The conduction along the centre thermocouple should be reduced or at least measured such that a correction can be applied to the data. The thermocouple conduction error can be reduced by using a thinner thermocouple wire and by decreasing the temperature gradient in the wire. The temperature gradient was high in the present apparatus because of the large heat transfer resistance between the copper block and the copper plate. This joint, at which the thermocouple was embedded, was at a high temperature.

(iii) At present only one heat-flux meter was used for the entire study. It would be desirable to check two similar heat-flux meters against each other. Also the effect of the geometry of the heat-flux meter should be studied further. Different meter sizes should give the same heat flux under the same conditions. This should lead to the development of a heat-flux meter which measured the large heat fluxes of subcooled water films more accurately.

(iv) The liquid entry and outlet sections of the boiler assembly could be improved. It was difficult to obtain a uniform film thickness at large angles of incline. Also the liquid should be removed more directly, since at large angles of incline liquid accumulated at the outlet and this increased leakages. The leakages that occurred were due to the deformed teflon.

2. Boiling of Liquid Films

(i) The present experiments should be repeated under controlled surface conditions and the present data range should be expanded into the forced convection and film boiling regime.

(ii) The boiling heat transfer to thin liquid films ($b = 0.003 - 0.030$ in,) might be investigated using the heat-flux meters.

(iii) The effect of wetting on the boiling heat flux, particularly the maximum heat flux, should be examined. In these experiments surface treatments (such as with benzene) or addition of surface-active materials or non-newtonian materials might be considered.

(iv) The thermal conductivity of the boiling plate affects the movement of the break-up region of the liquid film. The break-up behaviour of the liquid film using different boiling plate materials might be investigated.

I. NOMENCLATURE

a_1 - a_5	constants	
b	liquid film thickness	ft
c	specific heat	BTU/lb$^{\circ}$F
D	diameter	ft
g	acceleration of gravity	ft/hr^2
G	mass flow rate per unit wetted perimeter	lb/hr.ft
h	heat transfer coefficient	BTU/hr.sq.ft$^{\circ}$F
k	thermal conductivity	BTU/hr.sq.ft$^{\circ}$F/ft
n/A	number of nucleating sites per unit area	per sq.ft
p	pressure	lb/hr^{2}ft $\left(= 0.239 \times 10^{-8} \frac{\text{lb-force}}{\text{ft}^2}\right)$
Δp	pressure difference	lb/hr^{2}ft
P_e	pressure of vapour thrust	lb/hr^{2}ft
q/A	heat flux	BTU/hr.sq.ft
r	radius of bubble or cavity	ft
t	time	hr
T_L	bulk liquid temperature	$^{\circ}$F
T_H	temperature of superheated liquid	$^{\circ}$F
T_{sat}	boiling point of liquid	$^{\circ}$F
T_W	surface temperature	$^{\circ}$F
ΔT	temperature difference (surface superheat)	$^{\circ}$F
u	streamline velocity in liquid film	ft/hr
$\bar{u}$	average velocity of liquid film	ft/hr
y	distance from heating surface	ft

α	thermal diffusivity	ft^2/hr
β	coefficient of cubical expansion	per ^oF
δ	thermal boundary layer thickness	ft
Θ	angle from the horizontal	
λ	latent heat of vaporization	BTU/lb
μ	viscosity	lb/ft.hr
ρ	density	lb/cu.ft
σ	surface tension	lb/hr^2
ϕ	contact angle	

Subscripts

L	liquid
V	vapour
F	film
f	properties evaluated at the mean film temperature

Dimensionless Numbers

Re	film Reynolds number	$\frac{G}{\mu}$
N_T	film thickness number	$b\left[\frac{g \sin\theta\rho^2}{\mu^2}\right]^{1/3}$
We	Weber number	$\frac{\bar{u}}{(\sigma/\rho b)^{1/2}}$
Fr	Froude number	$\frac{\bar{u}}{(gb)^{1/2}}$
J	Richardson number	$-\frac{\left(g\frac{d\rho}{dz}\right)}{\rho\left(\frac{du}{dz}\right)^2}$

Ra	Rayleigh number	$\frac{\rho^2 b^3 c g \beta (T_W - T_L)}{\mu k}$

J. BIBLIOGRAPHY

A1 Acrivos, A. "Modern Chemical Engineering", Vol. 1, (1963), Reinhold.

B1 Benjamin, T.B. "Wave Formation in Laminar Flow down an Inclined Plane" J. Fluid Mechanics, 2, 554, (1957).

B2 Benjamin, T.B. "Shearing Flows over a Wavy Boundary". J. Fluid Mechanics, 6, 161, (1959).

B3 Bressler, R. "Versuche über die Verdampfung von dünnen Flüssigkeitsfilmen" Zeitschrift VDI, 100, 630, (1958).

B4 Becker, K.M., Persson, P., "An Analysis of Burnout Conditions for Flow of Boiling Water in Vertical Round Ducts". J. Heat Transfer, 86c, 515, (1964).

B5 Bennett, J.A.R., et al, "Heat Transfer to Two-Phase Gas-liquid Systems." Part I. Trans. Inst. Chem. Eng., 39, 113, (1961).

B6 Bankoff, S.G. "Entrapment of Gas in the Spreading of Liquid over a Rough Surface". A.I.Ch.E. J., 4, 24, (1958).

B7 Bergles, A.E., Rohsenow, W.H., "The Determination of Forced Convection Surface Boiling Heat Transfer." J. Heat Transfer, 86c, 365, (1964).

B8 Berenson, P.J. "Experiments on Pool Boiling Heat Transfer." Int. J. Heat & Mass Transfer, 5, 985, (1962).

B9 Boswirth, L. "Der Übergang von Blasen-zu Filmverdampfung." Atomkernenergie, 6, 93, (1961).

B10 Bankoff, S.G., Mehra, V.S., "A Quenching Theory for Transition Boiling." IEC Fundamentals, 1, 38, (1962).

B11 Bromley, L.A. "Heat Transfer in Stable Film Boiling." Chem. Eng. Progress, 46, 221, (1950).

B12 Berenson, P.J. "Film Boiling Heat Transfer From a Horizontal Surface." J. Heat Transfer, 83, 351, (1963).

B13 Borishansky, V.M. "Problems of Heat Transfer During Change of State." AEC tran - 3405, Chapter 4.

B14 Bankoff, S.G. "A Note on Latent Heat Transport in Nucleate Boiling." A.I.Ch.E. J., 8, 63, (1962).

B15 Burnett, D.R. "Transient Temperature Measurement Errors in Heated Slabs for Thermocouples Located at the Insulated Surface." J. Heat Transfer, 83, 505, (1961).

B16 Brauer, H. "Strömung und Wärme-übergang bei Rieselfilmen." VDI - Forschungsheft 457, (1956).

B17 Berenson, P.J., Stone, R.A., "A Photographic Study of the Mechanism of Forced Convection Vaporisation." Chem. Eng. Progr. Symp. Series, No. 57, 61, 213, (1965).

B18 Bonilla, C.F., Perry, C.W., "Heat Transmission to Boiling Binary Liquid Mixtures." Trans. A.I.Ch.E., 37, 685, (1941).

C1 Chandrasekhar, S. "Hydrodynamic and Hydromagnetic Stability." (1961). Oxford.

C2 Collier, J.G., Hewitt, G.F., "Data on the Vertical Flow of Air-Water Mixtures in the Annular and Dispersed Flow Regions." Part II. Trans. Inst. Chem. Eng., 39, 127, (1961).

C3 Collier, J.G. "Burnout in Liquid-Cooled Reactors." Nuclear Power, 6, 61, (June 1961).

C4 Carr, J.B. "Burnout in Net Quality by Liquid Film Destruction." AEC Report CONF-595-1 (1964).

C5 Collier, J.G., et al, "Heat Transfer to Two-Phase Gas-Liquid Systems." Part II. Trans. Inst. Chem. Eng., 42, 127, (1964).

C6 Corty, C., Foust, A.S., "Surface Variables in Nucleate Boiling."
Chem. Eng. Progr. Symp. Series, No. 17, 51, 1, (1955).

C7 Costello, C.P.et al, "A Study of Induced Convective Effects on Saturated Pool Boiling Burnout."
Chem. Eng. Progr. Symp. Series, No. 59, 61, 271, (1965).

C8 Chand, R., Rosson, H.F., "Local Heat Flux to a Water Film Flowing Down a Vertical Surface."
IEC Fundamentals, 4, 356, (1965).

C9 Costello, C.P., Adams, J.M., "The Interrelation of Geometry, Orientation and Acceleration on the Peak Heat Flux."
A.I.Ch.E. J., 9, 663, (1963).

C10 Cess, R.D., Sparrow, E.M., "Subcooled Forced Convection Film Boiling on a Flat Plate."
J. Heat Transfer, 83, 377, (1961).

C11 Cowley, C.N. et al, "A Method for Improving Heat Transfer to a Boiling Fluid."
IEC Process & Development, 1, 81, (1962).

C12 Cichelli, M.T., Bonilla, C.F., "Heat Transfer to Liquids Boiling Under Pressure."
Trans. A.I.Ch.E., 41, 755, (1945).

C13 Churchill, R.V. "Fourier Series and Boundary Value Problems."
(1941), McGraw-Hill.

C14 Cohen, L.S., Hanratty, T.J., "Generation of Waves in the Concurrent Flow of Air and a Liquid."
A.I.Ch.E. J., 11, 138, (1965).

D1 Dukler, A.E., Bergelin, O.P., "Characteristics of Falling Liquid Films."
Chem. Eng. Progr., 48, 557, (1952).

D2 Dukler, A.E. "Dynamics of Vertical Falling Film Systems."
Chem. Eng. Progr., 55, 62, (1959).

D3 Donald, M.B., Haslam, F., "The Mechanism of the Transition from Nucleate to Film Boiling."
Chem. Eng. Science, 8, 287, (1958).

E1 Emmons, H.W. et al, "Taylor Instability of Finite Surface Waves."
J. Fluid Mechanics, 7, 177 (1960).

E2 Ellion, M.E. "A Study of the Mechanism of Boiling Heat Transfer."
Ph.D. Thesis, Calif. Inst. Tech. (1954).

F1 Fulford, G.D. "The Flow of Liquids in Thin Films."
Advances in Chem. Eng., 5, 151 (1964).
Academic Press.

F2 Forster, H.K., Zuber, N., "Growth of a Vapour Bubble in a Superheated Liquid."
J. Applied Physics, 25, 474, (1954).

F3 Forster, H.K., Zuber, N., "Dynamics of Vapour Bubbles and Boiling Heat Transfer."
A.I.Ch.E. J., 1, 531, (1955).

F4 Forster, K., Greif, R., "Heat Transfer to a Boiling Liquid-Mechanisms and Correlations."
J. Heat Transfer, 81, 43, (1959).

G1 Garwin, L., Kelly, E.W., "Heat Transfer to Inclined Falling Films."
Ind. Eng. Chem., 47, 392, (1955).

G2 Griffith, P., Wallis, J.D., "The Role of Surface Conditions in Nucleate Boiling."
Chem. Eng. Progress Symp. Series, No. 30, 56, 49, (1960).

G3 Gaertner, R.F., Westwater, J.W., "Populations of Active Sites in Nucleate Boiling Heat Transfer."
Chem. Eng. Progress Symp. Series, No. 30, 56, 39, (1960).

G4 Griffith, P. "Bubble Growth Rates in Boiling."
Trans. A.S.M.E., 80, 721, (1958).

G5 Gaertner, R.F. "Photographic Study of Nucleate Pool Boiling on a Horizontal Surface."
J. Heat Transfer, 87, 17, (1965).

G6 Gunther, F.C. "Photographic Study of Surface Boiling Heat Transfer to Water with Forced Convection."
Trans. A.S.M.E., 73, 115 (1951).

G7 Githinji, P.M., Sabersky, R.H., "Some Effects of the Orientation of the Heating Surface in Nucleate Boiling." J. Heat Transfer, 85, 379, (1963).

G8 Golightly, D.R., McCartney, E.R., "A Study of the Effect of Air Bubbles on the Nucleation and Growth of Calcium Sulphate Scale on a Heat Transfer Surface." The Chemical Engineer, No. 169, CE 170, (1963).

G9 Gaertner, R.F. "Distribution of Active Sites in the Nucleate Boiling of Liquids." Chem. Eng. Progress Symp. Series, No. 41, 59, 52, (1963).

G10 Gardon, R. "A Transducer for the Measurement of Heat Flow Rate." J. Heat Transfer, 82, 396, (1960).

H1 Hanratty, T.J., Engen, J.M., "Interaction between a Turbulent Air Stream and a Moving Water Surface." A.I.Ch.E.J., 3, 299, (1957).

H2 Hanratty, T.J., Hershman, A., "Initiation of Roll Waves." A.I.Ch.E.J., 7, 488, (1961).

H3 Hewitt, G.F., et al, "Burnout and Nucleation in Climbing Film Flow." Int. J. Heat & Mass Transfer, 8, 793, (1965).

H4 Hsu, Y.Y., et al, "Destruction of a Thin Liquid Film Flowing over a Heating Surface." Chem. Eng. Progress Symp. Series, No. 57 , 61, 139, (1965).

H5 Hartley, D.E., Murgatroyd, W., "Criteria for the Break-up of Thin Liquid Layers Flowing Isothermally over Solid Surfaces." Int. J. Heat & Mass Transfer, 7, 1003, (1964).

H6 Hewitt, G.F., Lacey, P.M.C., "The Breakdown of the Liquid Film in Annular Two-Phase Flow." Int. J. Heat & Mass Transfer, 8, 781, (1965).

H7 Hsu, Y.Y. "On the Size Range of Active Nucleation Cavities on a Heating Surface". J. Heat Transfer, 84, 207, (1962).

H8 Hsu, Y.Y., Graham, R.W., "An Analytical and Experimental Study of the Thermal Boundary Layer and Ebullition Cycle in Nucleate Boiling." NASA, TND 594, (1961).

H9 Han, C.Y., Griffith, P., "The Mechanism of Heat Transfer in Nucleate Pool Boiling."
Int. J. Heat & Mass Transfer, 8, 887, (1965).

H10 Hosler, E.R., Westwater, J.W., "Film Boiling on a Horizontal Plate."
A.R.S. Journal, 32, 553, (1962).

H11 Hospeti, N.B., Mesler, R.B., "Deposits Formed beneath Bubbles during Nucleate Boiling of Radioactive Calcium Sulphate Solutions."
A.I.Ch.E. J., 11, 662, (1965).

H12 Hendricks, R.C., Sharp, R.R., "Initiation of Cooling Due to Bubble Growth on a Heating Surface."
NASA, TND 2290, (1964).

H13 Hsu, Y.Y., Westwater, J.W., "Approximate Theory for Film Boiling on Vertical Surfaces."
Chem. Eng. Progress Symp. Series, No. 30, 56, 15, (1960).

H14 Heidrich, A., Dissertation (1931), Reference from M. Jakob, "Heat Transfer," Vol. I, (1949).

H15 Hsu, Y.Y., Westwater, J.W., "Film Boiling from Vertical Tubes."
A.I.Ch.E. J., 4, 58, (1958).

H16 Huber, D.A., Hoehne, J.C., "Pool Boiling of Benzene, Diphenyl and Benzene-Diphenyl Mixtures under Pressure."
J. Heat Transfer, 85, 215, (1963).

H17 Hoffman, T.W. Private Communication, McMaster University, Hamilton, Ontario, (1965).

J1 Jakob, M., Linke, W., "Der Wärme-übergang beim Verdampfen von Flüssigkeiten an Senktechten und Waagerechten Flächen."
Phys. Zeitschrift, 36, 267, (1935).

J2 Jakob, M. "Heat Transfer in Evaporation."
Mech. Engineering, 58, 643, (1936).

J3 Jontz, P.D., Myers, J.E., "The Effect of Dynamic Surface Tension on Nucleate Boiling Coefficients."
A.I.Ch.E. J., 6, 34, (1960).

J4 Jakob, M., Linke, W., "Der Wärme-übergang von einer Waagerechten Platte an Siedenes Wasser."
Forschung auf dem Gebiete des Ingenieurwesens, 4, 75, (1933).

K1 Knuth, E.L. "The Mechanics of Film Cooling."
Jet Propulsion, 24, 359, (1954).

K2 Kast, W. "Bedeutung der Keimbildung und der Instationären Wärme-übertragung für den Wärme-übergang bei Blasenverdampfung und Tropfenkondensation."
Chemie-Ingenieur-Technik, 36, 933, (1964).

K3 Kutateladze, S.S., et al, "The Theory of Heat Transfer During Nucleate Boiling."
International Chem. Eng., 5, 474, (1965).

K4 Kurihara, H.M., Myers, J.E., "The Effects of Superheat and Surface Roughness on Boiling Coefficients."
A.I.Ch.E. J., 6, 83, (1960).

K5 Kirby, D.B., Westwater, J.W., "Bubble and Vapour Behaviour on a Heated Horizontal Plate During Pool Boiling to Burnout."
Chem. Eng. Progress Symp. Series, No. 57, 61, 238, (1965).

L1 Levich, V.G. "Physiochemical Hydrodynamics."
Prentice Hall, (1963).

L2 Leidenfrost, W. "Strömungs- und Wärme-übergangsverhältnisse bei frei Fallenden Rieselfilmen im Zustand der Verdampfung."
Naturwissenschaften, 43, 465, (1956).

L3 Leppert, G., Pitts, C.C., "Advances in Heat Transfer."
Vol. I, p. 185, (1964), Academic Press.

L4 Lienhard, J.H., Schrock, V.E., "The Effect of Pressure, Geometry and the Equation of State upon the Peak and Minimum Heat Flux."
J. Heat Transfer, 85, 261, (1963).

M1 Miles, J.W. "On the Generation of Surface Waves by Shear Flows - Kelvin-Helmholtz Instability."
J. Fluid Mechanics, 6, 583, (1959).

M2 Miles, J.W. "The Hydrodynamic Stability of a Thin Film of Liquid in Uniform Shearing Motion." J. Fluid Mechanics, 8, 593, (1960).

M3 McAdams, W.H. "Heat Transmission" p. 244, (1954), McGraw-Hill.

M4 Murgatroyd, W. "The Role of Shear and Form Forces in the Stability of a Dry Patch in Two-Phase Film Flow." Int. J. Heat & Mass Transfer, 8, 297, (1965).

M5 Moore, F.D., Mesler, R.B., "The Measurement of Rapid Surface Temperature Fluctuations During Nucleate Boiling of Water." A.I.Ch.E. J., 7, 620, (1961).

M6 Moissis, R., Berenson, P.J., "On the Hydrodynamic Transitions in Nucleate Boiling." J. Heat Transfer, 85, 221, (1963).

M7 Markels, M., Durfee, R.L., "Studies of Boiling Heat Transfer with Electrical Fields." A.I.Ch.E. J., 11, 716, 720, (1965).

M8 Motte, E.I., Bromley, L.A., "Film Boiling of Flowing Subcooled Liquids." Ind. Eng. Chem., 49, 1921, (1957).

N1 Norman, W.S., McIntyre, V., "Heat Transfer to a Liquid Film on a Vertical Surface." Trans. Inst. Chem. Eng., 38, 301, 317, (1960).

N2 Nedderman, R.M., Shearer, C.J., "The Motion and Frequency of Large Disturbance Waves in Annular Two-Phase Flow of Air-Water Mixtures." Chem. Eng. Science, 18, 661, (1963).

O1 Ostrach, S., Koestel, A., "Film Instabilities in Two-Phase Flows." A.I.Ch.E. J., 11, 294, (1965).

P1 Portalski, S. "Eddy Formation in Film Flow Down a Vertical Plate." IEC Fundamentals, 3, 49, (1964).

R1 Rosenhead, L. "Laminar Boundary Layers." (1963), Oxford.

R2 Rohsenow, W.H. "Developments in Heat Transfer", p. 169, (1964). M.I.T. Press.

R3 Rogers, T.F., Mesler, R.B., "An Experimental Study of Surface Cooling by Bubbles During Nucleate Boiling of Water."
A.I.Ch.E. J., 10, 656, (1964).

R4 Roll, J.B., Myers, J.E., "The Effects of Surface Tension on Factors in Boiling Heat Transfer."
A.I.Ch.E. J., 10, 530, (1964).

R5 Rohsenow, W.H., Clark, J.A., "A Study of the Mechanism of Boiling Heat Transfer."
Trans. A.S.M.E., 73, 609, (1951).

R6 Rallis, C.J., Jawurek, H.H., "Latent Heat Transport in Saturated Nucleate Boiling."
Int. J. Heat & Mass Transfer, 7, 1051, (1964).

S1 Schlichting, H. "Boundary Layer Theory." (1960), McGraw-Hill.

S2 Stenzel, W., Schultze, R., "Verdampfungs-kühlung I & II"
Chemie-Ingenieur-Technik, 30, 643, 720, (1958).

S3 Staub, F.W., Zuber, N., "A Program of Two-Phase Flow Investigation."
AEC Report, GEAP 4367, (1963).

S4 Strenge, P.H., et al, "Microscopic Study of Bubble Growth during Nucleate Boiling."
A.I.Ch.E. J., 7, 578, (1961).

S5 Sparrow, E.M. "The Effect of Radiation on Film Boiling Heat Transfer."
Int. J. Heat & Mass Transfer, 7, 229, (1964).

S6 Sparrow, E.M., Cess, R.D., "The Effect of Subcooled Liquid on Laminar Film Boiling."
J. Heat Transfer, 84, 149, (1962).

S7 Sauer, E.T., et al, "Heat Transfer to Boiling Liquids."
Mech. Engineering, 60, 669, (1938).

T1 Tailby, S.R., Portalski, S., "The Hydrodynamics of Liquid Films Flowing over a Vertical Surface."
Trans. Inst. Chem. Eng., 38, 324, (1960).

T2 Tippets, F.E. "Analysis of the Critical Heat Flux Condition in High Pressure Boiling Water Flows." J. Heat Transfer, 86, 23, (1964).

T3 Tien, C.L. "A Hydrodynamic Model for Nucleate Pool Boiling." Int. J. Heat & Mass Transfer, 5, 553, (1962).

V1 Vliet, G.C., Leppert, G., "Critical Heat Flux for Nearly Saturated Water Flowing Normal to a Cylinder." J. Heat Transfer, 86, 59, (1964).

W1 Whitaker, S. "The Effect of Surface Active Agents on the Stability of Falling Liquid Films." IEC Fundamentals, 3, 132, (1964).

W2 Wilke, W. "Wärme-übergang an Rieselfilme" V.D.I. - Forschungsheft 490 Forschung auf dem Gebiele des Ingenieurwesens, 28, (1962).

W3 Westwater, J.W. "Advances in Chem. Eng." Vol. I, (1956); Vol. II, (1958), Academic Press.

W4 Westwater, J.W. "Fundamental Research in Heat Transfer." p. 61, (1963), Pergamon Press.

W5 Wayner, P.C., Bankoff, S.G., "Film Boiling of Nitrogen with Suction on an Electrically Heated Porous Plate." A.I.Ch.E. J., 11, 59, (1965).

W6 Wayner, P.C., Kesten, A.S., "Suction Nucleate Boiling of Water." A.I.Ch.E. J., 11, 858, (1965).

Y1 Yamagata, K., et al, "Nucleate Boiling of Water on a Horizontal Heating Surface." Mem. Fac. Eng. Kyushu University 15, No. 1, 97, (1955).

Y2 Young, R.K., Hummel, R.L., "Improved Nucleate Boiling Heat Transfer." Chem. Eng. Progr., 60, 53, (1964).

Z1 Zuber, N. "On the Atomisation and Entrainment of Liquid Films in Shear Flow." General Electric, Report No. 62 GL 153, (1962).

Z2	Zuber, N.	"Recent Trends in Boiling Heat Transfer Research." Part I. Applied Mechanics Reviews, 17, 663, (1964).
Z3	Zuber, N.	"The Dynamics of Vapour Bubbles in Non-Uniform Temperature Fields." Int. J. Heat & Mass Transfer, 2, 83, (1961).
Z4	Zuber, N.	"Nucleate Boiling - The Region of Isolated Bubbles and the Similarity with Natural Convection." Int. J. Heat & Mass Transfer, 6, 53, (1963).
Z5	Zuber, N.	"Hydrodynamic Aspects of Boiling Heat Transfer." AEC Report, AECU 4439 (1959).
Z6	Zuber, N., Tribus, M.	"Further Remarks on the Stability of Boiling Heat Transfer." AEC Report, AECU 3631, (1958).

K. APPENDIX

1. Heat Flux Meter

The heat flux meter consists of a thin metal disc, which is in the heating surface and is insulated from below (Figure 69). When heat flows from the disc surface, the centre temperature of the disc is lower than the edge temperature. The magnitude of this two-dimensional temperature difference indicates the heat flux from the disc surface. The heat flux meter has been based on the design by Gardon (G10).

1.1 Assumptions

The following assumptions have been made for an analysis of the heat-flux meter when used under boiling conditions:

(i) Since boiling is a local transient process sufficient bubble nucleating sites must be on the disc such that a statistical average heat flux is measured at all times.

(ii) The heat flux from the disc should be the same at every point on the disc.

(iii) The thin disc should not interfere with the boiling phenomenon. Boiling heat flux is quite sensitive to the temperature difference (wall temperature) and thus the centre temperature should not be more than 5°F below the edge temperature:

$$T_W - T_{sat} \gg T_W - T_C$$

The material of the heat flux meter must have a high thermal conductivity (i.e. copper or silver), in order to keep ($T_W - T_C$) small under the conditions of the high heat fluxes encountered in boiling.

HEAT FLUX METER ANALYSIS

Two-Dimensional

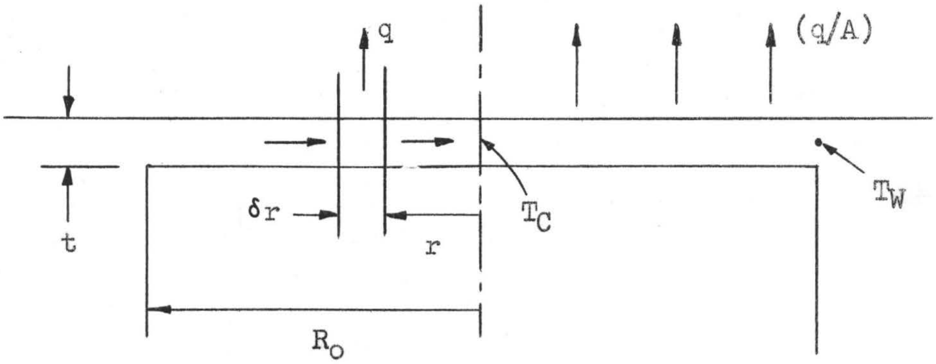

$$(q/A) = \frac{4\,k\,t}{R_o^2}\,(T_W - T_C) \qquad \text{(K-1)}$$

Three-Dimensional

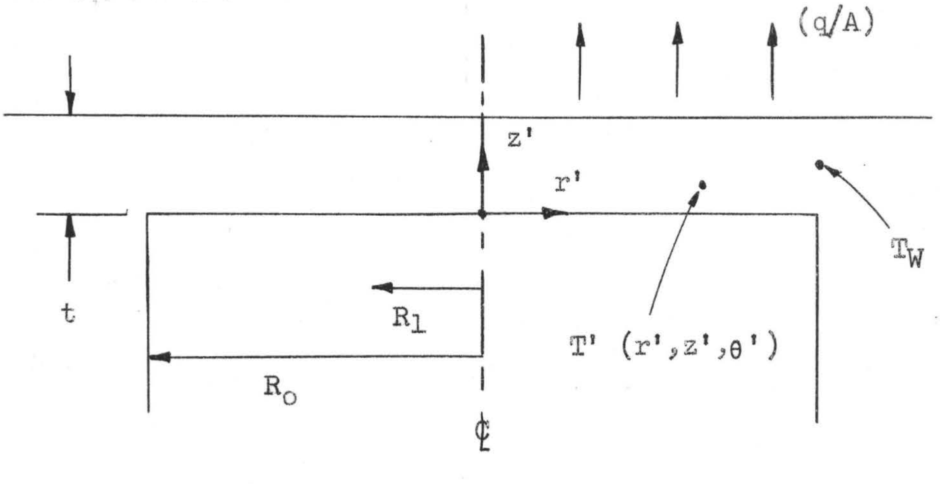

$$(q/A) = \frac{kt}{2R_o^2} \cdot \frac{1}{\sum\limits_{n=1} \frac{1}{\lambda_n^3\, J_1(\lambda_n)}} \cdot (T_W - T'_{\text{℄ ave}}) \qquad \text{(K-7)}$$

FIGURE 69

(iv) No conduction of heat along the thermocouple wires which measure the edge temperature T_W and the centre temperature T_C.

(v) A true two-dimensional conduction problem such that at the centre of the disc the top surface has the same temperature as the bottom.

(vi) The thin disc has a very fast response time, such that when the disc is subjected to a varying heat flux, the instantaneous heat flux is indicated by the steady-state temperature difference at all times. A material of high thermal conductivity is required for the heat-flux meter disc, if the time constant should be small.

1.2 Two-Dimensional Analysis

The following equation for steady-state conditions of the thin disc can be written (Figure 69):

$$q_r = -kA \frac{dT}{dx}$$

$$q = (-q_{r+\delta r}) - (-q_r)$$

$$(q/A)\, 2\pi r \delta r = 2\pi(r + \delta r)\, t \left[k \frac{dT}{dr} + \frac{d}{dr}\left(k \frac{dT}{dr}\right) \delta r \right] - 2\pi r t k \frac{dT}{dr}$$

$$\frac{(q/A)}{t} = \frac{k}{r}\frac{dT}{dr} + \frac{d}{dr}\left(k \frac{dT}{dr}\right)$$

$$= \frac{1}{r}\frac{d}{dr}\left(rk \frac{dT}{dr}\right)$$

The equation is solved with the following boundary conditions:

(i) $r = 0$ $\qquad T = T_C$ $\qquad \frac{dT}{dr} = 0$

(ii) $r = R_o$ $\qquad T = T_W$

and $k = k_o\,(1 + \alpha \Delta T)$ where $\Delta T = T - T_o$

$$\therefore\ (q/A) = \frac{4\ k_o\ t}{R_o^2}\ (T_W - T_C)\ \left[1 + \frac{\alpha}{2}\ (\Delta T_W + \Delta T_C)\right] \qquad \text{(K-1)}$$

The thermocouple voltage is given by the equation

$$E = \beta\,\Delta T + \gamma\,\Delta T^2$$

$$\Delta E = E_W - E_C = \beta\,(\Delta T_W - \Delta T_C) + \gamma\,(\Delta T_W^{\,2} - \Delta T_C^{\,2})$$

$$= (T_W - T_C)\left[\beta + \gamma\,(\Delta T_W + \Delta T_C)\right]$$

Substituting

$$(q/A) = \frac{4\ k_o\ t}{R_o^2}\ \frac{\left[1 + \frac{\alpha}{2}\,(\Delta T_W + \Delta T_C)\right]}{\left[\beta + \gamma\,(\Delta T_W + \Delta T_C)\right]}\ \Delta E$$

since $T_C \to T_W$ $\qquad \Delta T_W + \Delta T_C \approx 2\Delta T_W$

and then writing

$$\frac{1}{C} = \frac{(1 + \alpha\,\Delta T_W)}{(\beta + 2\gamma\,\Delta T_W)}$$

$$\therefore\ q/A = \frac{4\ k_o\ t}{R_o^2} \cdot \frac{\Delta E}{C} \qquad \text{(K-2)}$$

For the thin copper disc $t = 0.010$ in. $R_o = 0.078$ in.

$$(q/A) = 17{,}700\ \frac{\Delta E}{C} \qquad \text{(K-3)}$$

For the thick copper disc $t = 0.0575$ in. $R_o = 0.078$ in.

$$(q/A) = 102{,}000\ \frac{\Delta E}{C} \qquad \text{(K-4)}$$

These equations have been used for the evaluation of the boiling heat flux. The function C has been plotted in Figure 70 using values α, β and γ which have been obtained from the International Critical Tables.

Copper-Constantan thermocouple:

$$E = 0.0381\ \Delta T + 0.444 \times 10^{-4}\ \Delta T^2 \quad \text{mV}$$

VARIATION OF E.M.F. AND THERMAL CONDUCTIVITY WITH TEMPERATURE

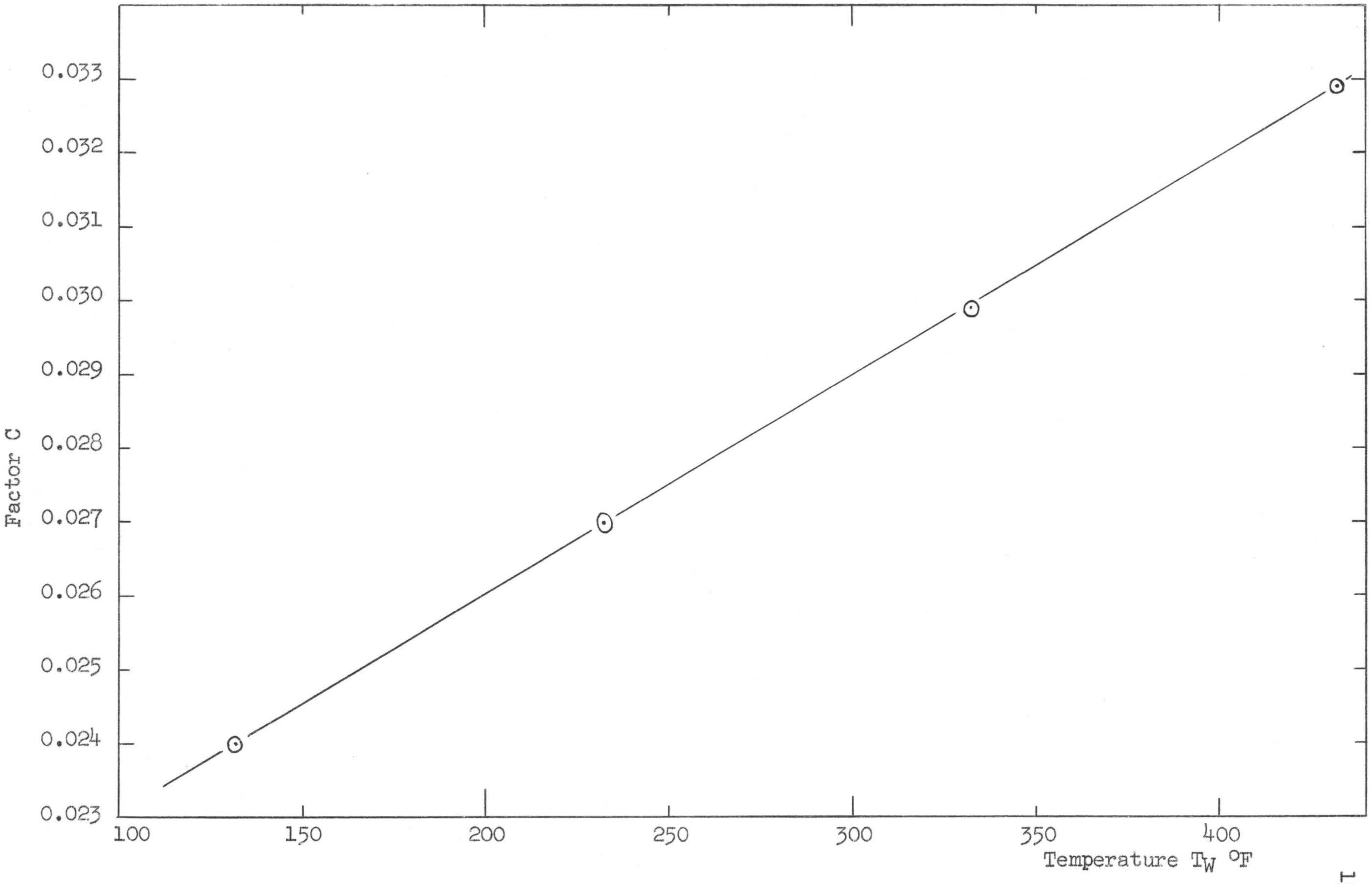

FIGURE 70

Thermal Conductivity of Copper ($76^o - 362^oC$):

$$k = 0.925\ (1 - 0.00009\ \Delta T) \qquad \text{cals/cm}^2\text{sec.}^oC/\text{cm}$$

where ΔT is in ^oC and $T_o = 0^oC$.

Converting to ^oF

$$E = 0.0212\ \Delta T + 0.137 \times 10^{-4}\ \Delta T^2 \qquad \text{mV}$$

$$k = 224\ (1 - 0.00005\ \Delta T) \qquad \text{BTU/hr.sq.ft.}^oF/\text{ft}$$

where ΔT is in ^oF and $T_o = 32^oF$.

1.3 Heat Flux Meter Calibration

The thermocouples of the thin copper disc heat-flux meter were checked individually with a potentiometer. Comparisons were made when the boiler assembly was at two uniform temperatures; one in air and the other when hot benzene was flowing over it.

TABLE 2

	Air	Benzene
Edge thermocouple	4.080 mV	2.800 mV
Centre thermocouple	4.080 mV	2.800 mV

The closed circuit of the heat-flux meter already carried a small current, when there was no temperature differential at the meter. The magnitude of the e.m.f. was +0.010 mV and probably arose from other junctions in the circuit. By use of the Deviation Amplifier it was shown that the e.m.f. source was on the galvanometer side of the circuit, (Figure 71). The initial current changed during the warm-up period of the Visicorder, because of the change of resistance of the

HEAT FLUX METER CIRCUIT

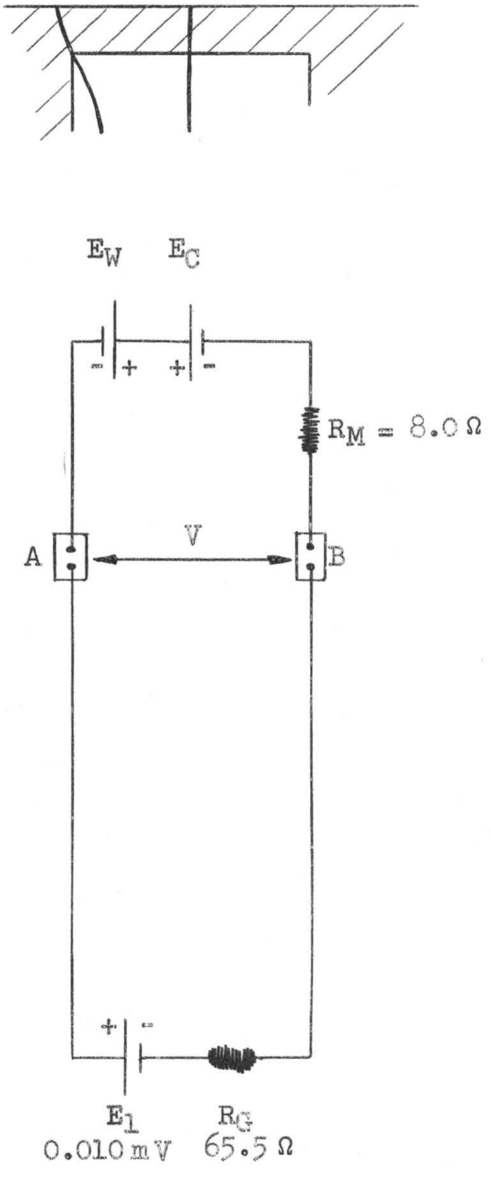

$E_M = E_W - E_C$

$E_M + E_1 = i\,(R_G + R_M)$

$V = E_M - iR_M$

$i = k(d)$

$k = 0.243\ \frac{\mu A}{in}$

FIGURE 71

HEAT FLUX METER CALIBRATION CURVE

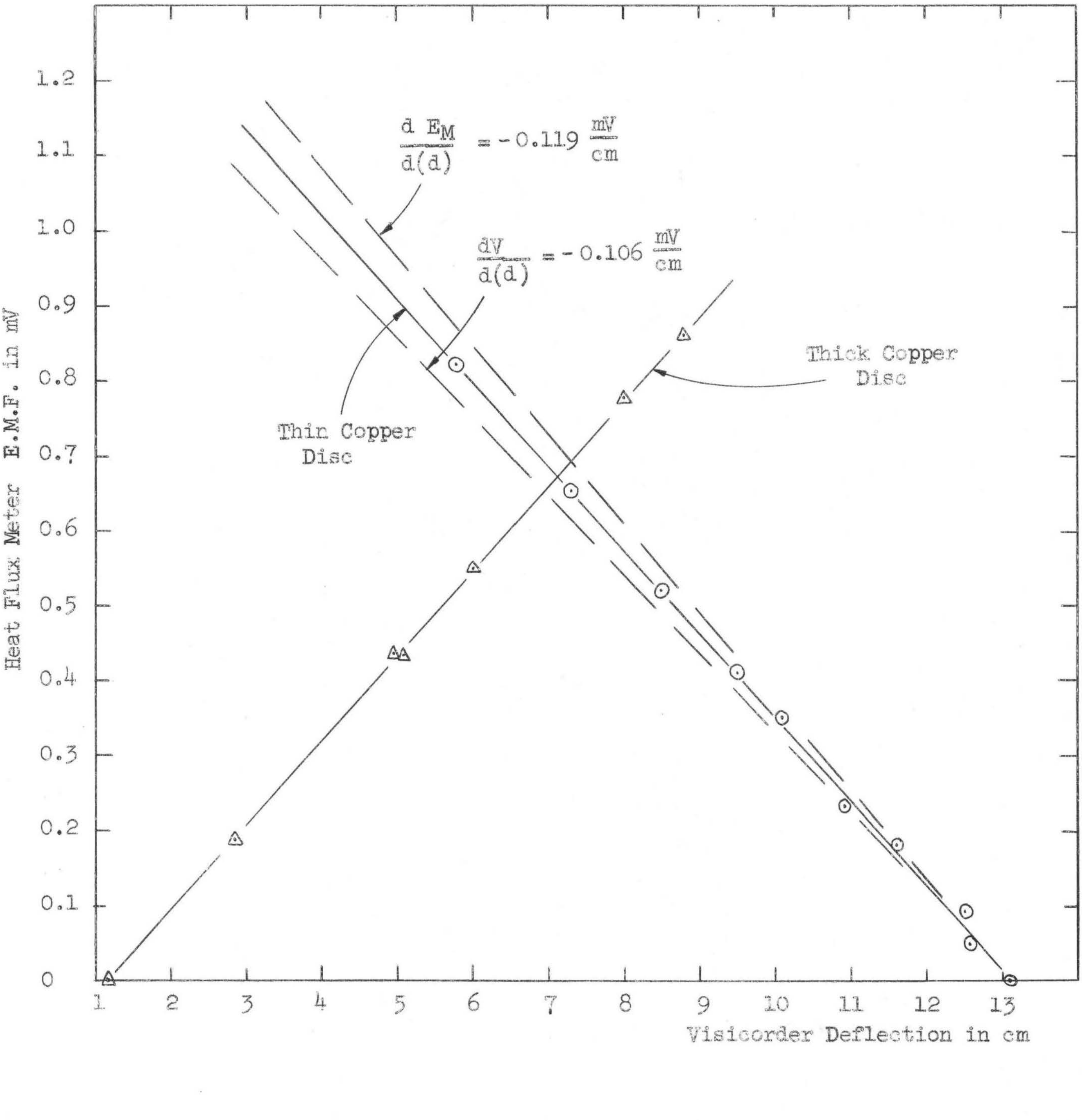

FIGURE 72

galvanometer coil. The resistance remained constant after 15 minutes warm-up of the Visicorder.

For calibration of the heat-flux meter a Honeywell single-pen recorder was adjusted to the range of 0 - 2 mV and connected across the terminals AB (Figure 71). Thus a measurement of the voltage, V. was obtained. Water was passed on the heat-flux meters such that the deflections on the single-pen recorder and Visicorder were steady. Steady deflections were compared and plotted as shown in Figure 72.

A comparison of the two theoretical curves of E_M and V against the Visicorder deflection is also shown. The galvanometer sensitivity was 0.243 μA/inch. The experimental curve of V had a greater slope than expected. The reasons for this are unknown. The experimental curve was taken as the calibration curve of the heat-flux meter.

The circuit of the thick disc heat-flux meter was electrically equivalent to the thin disc heat-flux meter. The calibration of this meter is also shown in Figure 72.

1.4 Three-Dimensional Analysis

The simplicity of the two-dimensional analysis presented above permits a direct relation between the heat flux and the differential e.m.f. The dependence of the thermal conductivity, although small in the case of copper, has also been incorporated in that expression. The following analysis (H17) was performed in order to determine the magnitude of the three-dimensional effects, the time constant of the heat-flux meter and the thermocouple conduction error.

The energy equation for heat conduction in a solid cylindrical system exhibiting radial symmetry and constant properties can be written as

$$\frac{\partial^2 T'}{\partial r^2} + \frac{1}{r}\frac{\partial T'}{\partial r} + \left(\frac{R_o}{t}\right)^2 \frac{\partial^2 T'}{\partial z^2} = \frac{\partial T'}{\partial \theta} \qquad \text{(K-5)}$$

where each variable has been normalised with

$$r = \frac{r'}{R_o} \qquad z = \frac{z'}{t} \qquad \theta = \frac{\alpha\theta'}{R_o^2}$$

The primed variables are defined in Figure 69.

Steady-state analysis

Under steady state conditions equation (K-5) can be written

$$\frac{\partial^2 T}{\partial r^2} + \frac{1}{r}\frac{\partial T}{\partial r} + \left(\frac{R_o}{t}\right)^2 \frac{\partial^2 T}{\partial z^2} = 0 \qquad \text{(K-6)}$$

where $T = T' - T_W$ and T_W is the temperature along the edge of the disc, i.e. at $r' = R_o$ for all z. In order that the analysis may be more general the heat-flux density was considered to be operable over the region $0 \leqslant r' \leqslant R_1$ and over the remaining annular ring, i.e. $R_1 \leqslant r' \leqslant R_o$ the heat flux was considered to be zero.

The boundary conditions may be written

(i) $r = 0$ $\frac{dT}{dr} = 0$, - radially symmetrical temperature distribution

(ii) $r = 1$ $T = 0$, - temperature at edge of disc for all z is T_W

(iii) $z = 0$ $\frac{dT}{dz} = 0$, - no heat loss from underside of disc

(iv) $z = 1$ $\frac{dT}{dz} = \frac{-(q/A)t}{k}$, - uniform heat flux away from upper region of disc. $r_1 = \frac{R_1}{R_o}$

$0 \leqslant r \leqslant r_1$

By the separation of variables with the equation

$$T\,(r\,,z) = R\,(r)\,.\,\mathcal{Z}(z)$$

two ordinary differential equations arise

$$\frac{d^2R}{dr^2} + \frac{1}{r}\,\frac{dR}{dr} + \lambda^2 R = 0$$

$$\frac{d^2\mathcal{Z}}{dz^2} - \left(\frac{\lambda^2 R_o{}^2}{t^2}\right)\mathcal{Z} = 0$$

where λ is the Eigenvalue. These equations are easily solved to yield

$$R = C_1\, J_o\,(\lambda r) + C_2\, Y_o(\lambda r)$$

$$\mathcal{Z} = C_3 \sinh\left(\frac{\lambda t}{R_o}\right) z + C_4 \cosh\left(\frac{\lambda t}{R_o}\right) z$$

The constants are evaluated by utilizing the boundary conditions and a Fourier-Bessel series representation (C 13) of the function

$$-\left[\frac{(q/A)t}{k}\right]$$

The final solution is

$$T_{ss} = \sum_{n=1}^{\infty} \frac{-2(q/A)R_o}{\lambda_n^2\; k\; r_1} \cdot \frac{J_1\,(\lambda_n r_1)\, J_o(\lambda_n r)}{\left[J_o{}^2(\lambda_n r_1) + J_1{}^2(\lambda_n r_1)\right]} \cdot \frac{\cosh\left(\dfrac{\lambda_n t z}{R_o}\right)}{\sinh\left(\dfrac{\lambda_n t}{R_o}\right)} \qquad \text{(K-7)}$$

where λ_n are the roots of $J_o\,(\lambda_n) = 0$

With $r_1 = 1$ the steady-state temperature profile within the heat-flux meter can be compared with that predicted from the two-dimensional equation (K-1). The value of the thermal conductivity of copper has been taken at 220 BTU/hr.sq.ft.^{o}F/ft. Figures 73 and 74 indicate this comparison for the meters used in this study. It can be seen that the two-dimensional equation predicts satisfactory results for the thin disc. For the thick disk there is a significant temperature difference between the top and bottom of the disc.

TEMPERATURE PROFILE OF THIN COPPER DISC

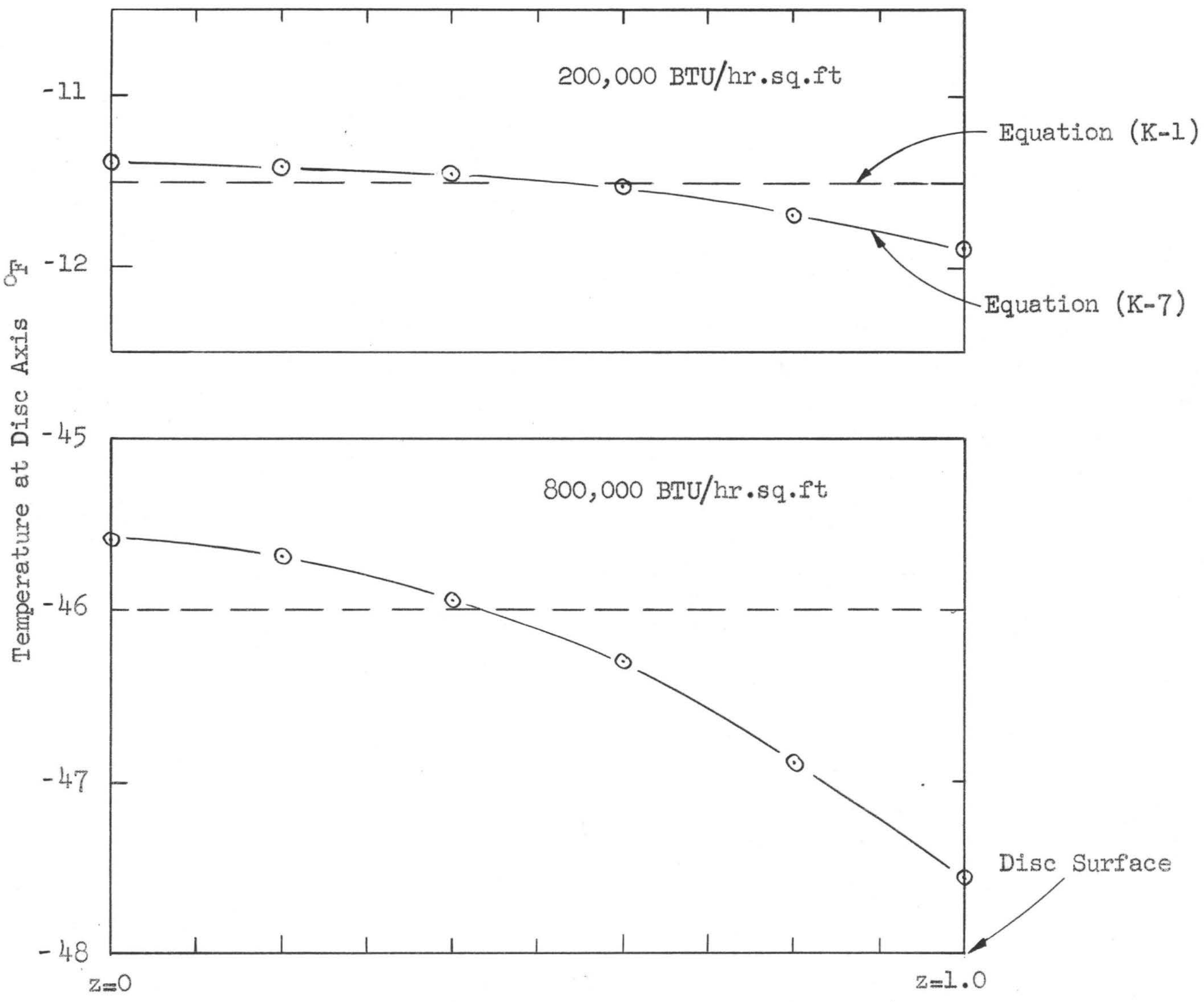

FIGURE 73

TEMPERATURE PROFILE OF THICK COPPER DISC

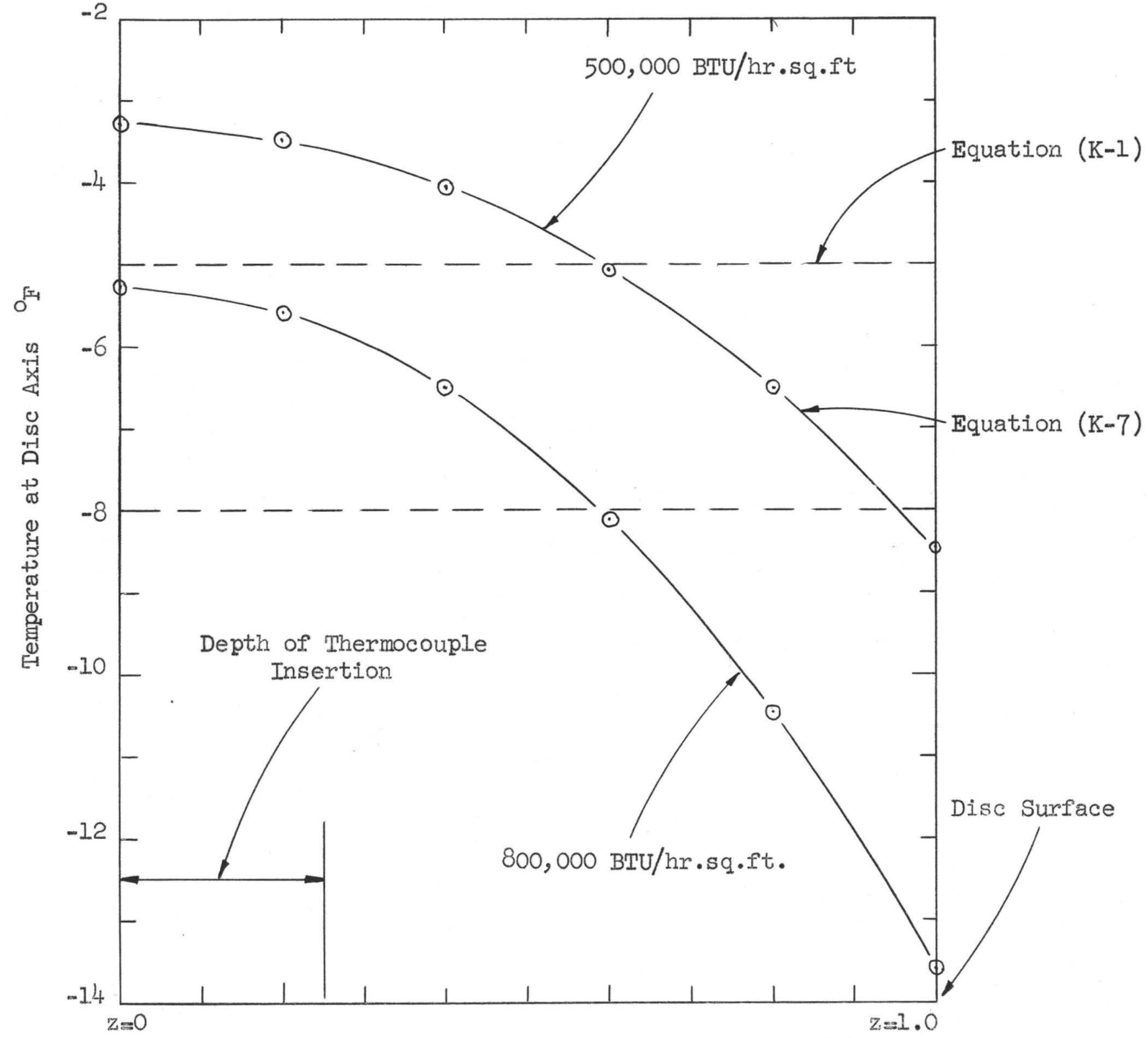

FIGURE 74

Equation (K-7) reduces to equation (K-1) when the average temperature $T_{℄\mathrm{ave}}$ along the axis of the disc is calculated. The summation in the equation shown in Figure 69 equals 1/8. However the thermocouple e.m.f. is not directly related to this average temperature, because the e.m.f. is not a linear function of temperature. Thus the three-dimensional equation is necessary for the proper evaluation of the heat flux from the measured e.m.f., when the temperature gradient along the axis is large (as in the thick disc heat-flux meter).

Unsteady-state analysis

The equation (K-5) may also be written

$$\frac{\partial^2 T}{\partial r^2} + \frac{1}{r}\frac{\partial T}{\partial r} + \left(\frac{R_o}{t}\right)^2 \frac{\partial^2 T}{\partial z^2} = \frac{\partial T}{\partial \theta} \qquad \text{(K-8)}$$

where $T = T'' - T_{ss}$ $\qquad T_{ss} = T'(r, z) - T_W$

$T'' = T'(r, z, \theta) - T_W$

and T_{ss} is the steady-state temperature distribution given by equation (K-7).

The boundary conditions in this case are

(i) $r = 0$ $\quad \frac{dT}{dr} = 0$ $\quad$ for all θ and z

(ii) $z = 0$ $\quad \frac{dT}{dz} = 0$ $\quad$ for all θ and r

(iii) $z = 1$, $0 \leq r \leq r_1$ $\quad \frac{dT}{dz} = 0$ $\quad$ for all θ, since $\frac{dT''}{dz} = \frac{dT_{ss}}{dz} = -\frac{(q/A)t}{k}$

(iv) $r = 1$ $\quad T = 0$ $\quad$ for all θ and z

(v) $\theta = 0$ $\quad T = -T_{ss}$ $\quad$ i.e. $T'' = 0$ for all r and z.

By the separation of variables with

$$T\ (r,z,\theta) = R\ (r)\ .\ F\ (z,\theta)$$

the following differential equations are obtained

$$\frac{d^2R}{dr^2} + \frac{1}{r}\ \frac{dR}{dr} + \lambda^2 R = 0$$

$$\frac{\partial F}{\partial \theta} - \left(\frac{R_o}{t}\right)^2 \frac{\partial^2 F}{\partial z^2} = -\lambda^2 F$$

Applying the separation of variables technique a second time with

$$F\ (z,\theta) = \mathcal{Z}\ (z)\ .\ \Theta\ (\theta)$$

the result is

$$\frac{d\,\Theta}{d\ \theta} + \Gamma^2\ \Theta = 0$$

$$\frac{d^2\mathcal{Z}}{dz^2} + (\Gamma^2 - \lambda^2)\left(\frac{t}{R_o}\right)^2 \mathcal{Z} = 0$$

Remembering that

$$T\ (r,z,\theta) = R(r)\ .\ \mathcal{Z}(z)\ .\ \Theta\ (\theta)$$

$$R = C_1\ J_o\ (\lambda r) + C_2 Y_o\ (\lambda r)$$

$$\mathcal{Z} = C_4 \sin\left[(\Gamma^2 - \lambda^2)^{1/2}\left(\frac{t}{R_o}\right) z\right] + C_5 \cos\left[(\Gamma^2-\lambda^2)^{1/2}\left(\frac{t}{R_o}\right) z\right]$$

$$\Theta = C_3\ e^{-\Gamma^2\theta}$$

From boundary conditions (i) $C_2 = 0$ and from (ii) $C_4 = 0$. Applying boundary condition (iii) then

$$\Gamma^2 = \left[\left(\frac{R_o}{t}\right) n\pi\right]^2 + \lambda^2$$

Boundary condition (iv) yields

$$J_o\ (\lambda_m) = 0$$

and hence

$$\Gamma^2_{m,n} = \left[\left(\frac{R_o}{t}\right) n\pi\right]^2 + \lambda_m^2$$

Boundary condition (v) is applied to the remaining equation for T with the result, in which the constant of integration $A_{m,n}$ remains to be evaluated:

$$- T_{ss} = A_{m,n} J_o (\lambda_m r) \cos n\pi z$$

In order to represent the steady-state temperature profile T_{ss} by a Fourier-Bessel series both sides are multiplied by $r J_o (\lambda_i r) \cos j\pi z$

$$-T_{ss}\, r\, J_o (\lambda_i r) \cos j\pi z = A_{m,n} J_o(\lambda_m r) \cos n\pi z . r J_o(\lambda_i r) \cos j\pi z$$

Integrating

$$\int_0^1\int_0^1 -T_{ss} \left[r J_o (\lambda_i r)\, dr\right] \cos j\pi z\, dz$$

$$= \int_0^1\int_0^1 A_{m,n} \left[r J_o (\lambda_m r) J_o (\lambda_i r)\, dr\right] \cos n\pi z . \cos j\pi z\, dz$$

Both double integrals are equal to zero unless $m = i$ and $n = j$. By substituting equation (K-7) for T_{ss} and performing the necessary integrations $A_{m,n}$ can be evaluated.

Then

$$A_{m,n} = \frac{4\ (q/A) R_o}{k \lambda_m^2 r_1} \cdot \frac{J_1(\lambda_m r_1)\ (-1)^n}{\left[J_o^2(\lambda_m r_1) + J_1^2 (\lambda_m r_1)\right]} \frac{\left(\frac{R_o \lambda_m}{t}\right)}{\left[\left(\frac{R_o\ n\pi}{t}\right)^2 + \lambda_m^2\right]}$$

except when $n = 0$, in which case

$$A_{m,o} = \frac{2 (q/A) R_o}{k \lambda_m^2 r_1} \cdot \frac{J_1 (\lambda_m r_1)}{\left[J_o^2 (\lambda_m r_1) + J_1^2 (\lambda_m r_1)\right]} \left(\frac{R_o}{\lambda_m t}\right)$$

TIME RESPONSE OF HEAT FLUX METER

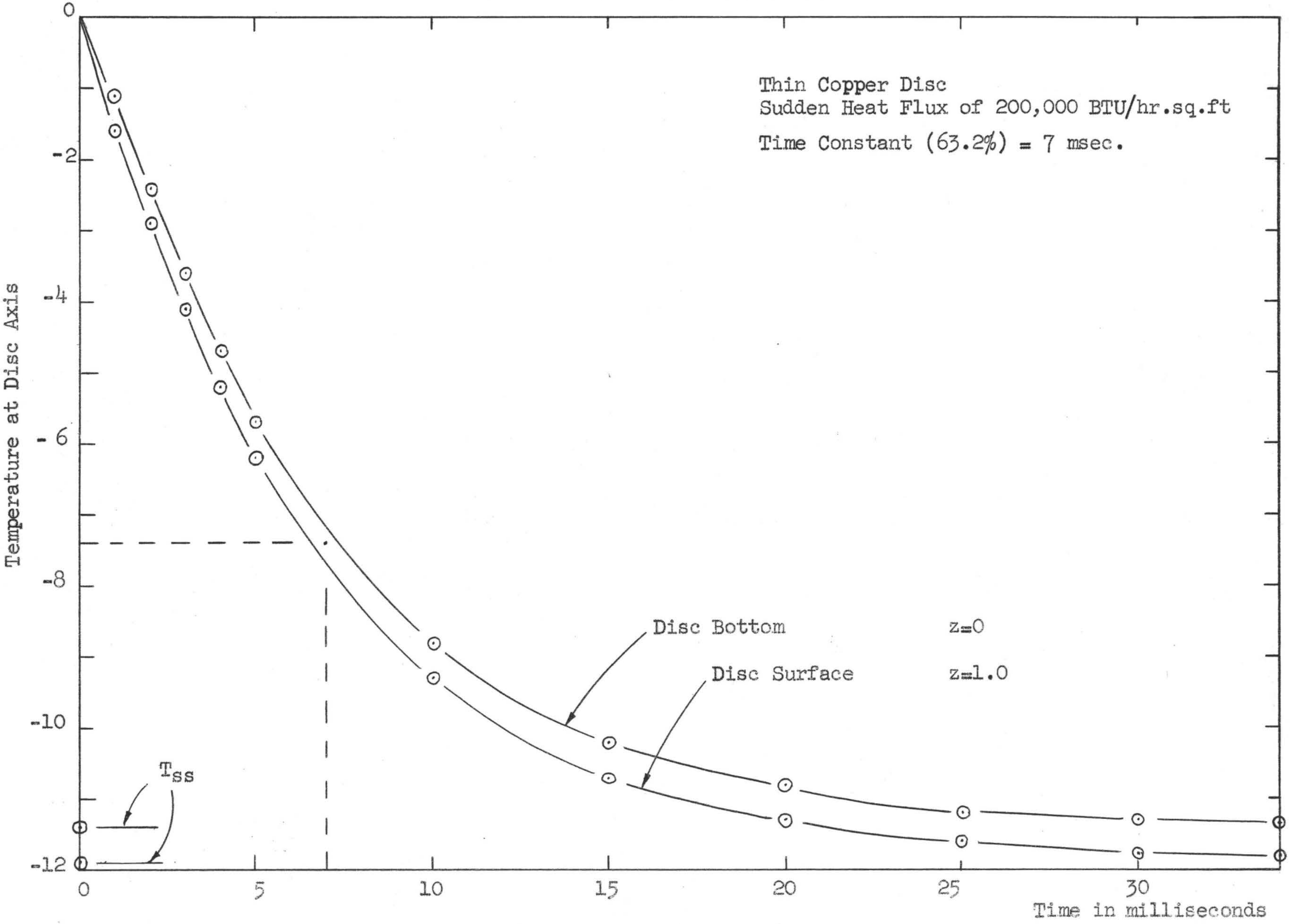

FIGURE 75

Therefore

$$T\ (r,z,\theta) = \sum_{m=1}^{\infty} \frac{2(q/A)R_o}{k\lambda_m^2\ r_1} \cdot \frac{J_1(\lambda_m r_1)\ J_o(\lambda_m r)}{\left[J_o^2\ (\lambda_m r_1) + J_1^2\ (\lambda_m r_1)\right]} \left(\frac{R_o}{\lambda_m t}\right) \exp\left(\frac{-\Gamma_{m,o}^2 \alpha\theta}{R_o^2}\right)$$

$$+ \sum_{m=1}^{\infty} \sum_{n=1}^{\infty} \frac{4(q/A)R_o}{k\lambda_m^2\ r_1} \frac{J_1(\lambda_m r_1) J_o(\lambda_m r)(-1)^n}{\left[J_o^2(\lambda_m r_1) + J_1^2(\lambda_m r_1)\right]} \frac{\left(\frac{R_o \lambda_m}{t}\right) \cos n\pi z}{\left[\left(\frac{R_o\ n\pi}{t}\right)^2 + \lambda_m^2\right]} \exp\left(\frac{-\Gamma_{m,n}^2 \alpha\theta}{R_o^2}\right) \tag{K-9}$$

With $r_1 = 1$ the equation describes the behaviour of each point in a normally operated heat-flux meter at any instant of time. Although it does not have the same form as equation (K-7) it does yield the same prediction of the steady-state temperature at zero time.

The equation (K-9) was used to predict the time constant of the thin disc meter used in the present study. Figure 75 shows a plot of the centre surface temperature as a function of time, when a uniform heat flux of 200,000 BTU/hr.sq.ft is suddenly applied. The time constant is predicted to be approximately 7 milliseconds, when based on 63.2% of the steady-state temperature difference.

1.5 Thermocouple Conduction Error

The results obtained with the heat-flux meter were always lower than those obtained with the vapour collection method in the steady-state pool boiling of benzene. (Figures 58 and 61). The difference was of the order of 10,000 to 20,000 BTU/hr.sq.ft. Also a change in the zero position of the galvanometer was frequently observed, particularly during an accidental dry-out in the pool boiling experiments, (Figure 68). The zero deviation was always negative and was found to be approximately -0.025 mV (15,000 BTU/hr.sq.ft) for boiling benzene and -0.060 mV (35,000 BTU/hr.sq.ft) for boiling water. Heat conduction into the thin disc by conduction along the centre thermocouple wire could lead to "low" measured heat fluxes and to such negative deviations.

The actual boiling heat fluxes of benzene were about 60,000 BTU/hr.sq.ft^2. Then the temperature gradient across the copper plate was

$$60,000 = 220 \frac{\Delta T}{1/12} \qquad \left(q/A = k \frac{\Delta T}{\Delta x}\right)$$

$$\Delta T = 23 \ {}^{o}F$$

Under these conditions the chromel-alumel thermocouples indicated a copper block temperature of 420°F. Thus for the heat transfer resistance between the copper block and the copper plate a value of 130°F was estimated. This figure increases with time due to increasing oxidation and distortion of the contact areas; this is the position where the thermocouples leads are embedded. The heat flux through the constantan thermocouple wire was then approximately

$$q/A = 15.0 \ \frac{(23 + 130)}{1/12}$$

$$= 27,000 \text{ BTU/hr.sq.ft}$$

Figure 76 shows the increase of the centre temperature of the thin copper disc with the heat flux through the constantan wire. This graph was obtained by solving equation (K-7) and setting $r_1 = 0.038$. It is shown that a heat flux of 27,000 BTU/hr.sq.ft through the constantan wire increases the centre temperature by about 1.7 °F.

THERMOCOUPLE CONDUCTION ERROR

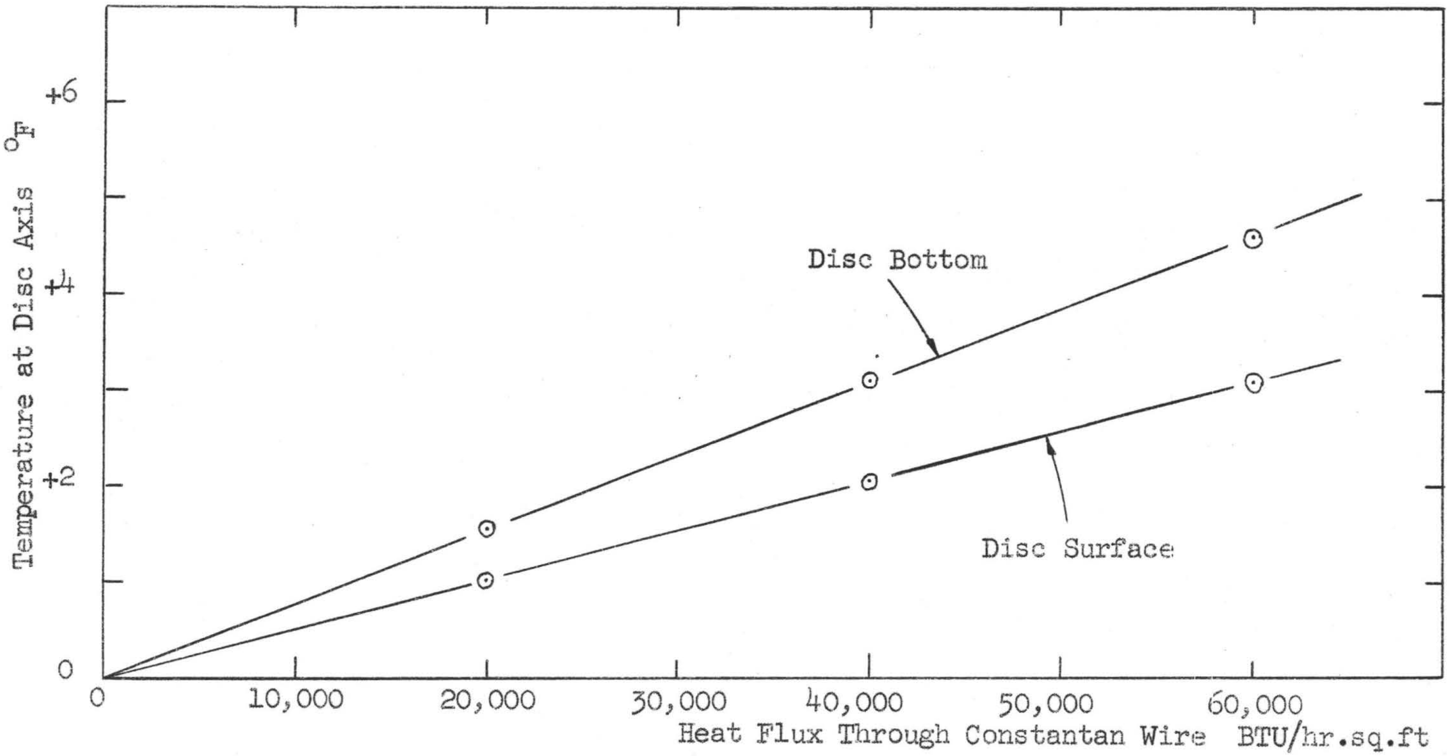

FIGURE 76

Such an error would decrease the measured heat flux by approximately

$$q/A = 17{,}700 \times 1.7 = 30{,}000 \text{ BTU/hr.sq.ft}$$

using equation (K-3). Hence the "low" heat fluxes indicated by the heat-flux meters and the negative deviations can be accounted for by heat conduction along the centre thermocouple. However, no quantitative correction can be applied to the heat fluxes because the temperature gradient in the constantan wires is not exactly known at any time. Since in most experiments the copper block temperature was about 450°F the calculated correction of 30,000 BTU/hr.sq.ft represents roughly the maximum correction.

Experiments were performed in which the boiling plate was rapidly heated with the electric heater. Both were initially at the same temperature. The Honeywell Deviation Amplifier, calibrated in the range 0-0.1 mV, was used to measure the zero shift. During rapid heating a negative deflection of the zero position was observed, which amounted to a maximum of -0.025 mV. When heating was discontinued and the boiler assembly attained a uniform temperature again the negative deflection was found to decrease markedly. However it not necessarily returned to the initial zero position after 1 hour, but sometimes required much more time. Unfortunately no accurate evaluation of the zero-shift with the temperature gradient across the boiling plate could be made, because no proper thermocouples were located at the bottom of the boiling plate. This effect was reproducible, but was not obtained during slow heating of the boiler assembly.

The problem of thermocouple conduction errors for thermocouples attached to an infinite slab has been treated by Burnett (B15). The method however is not recommended for correction purposes.

2. Electric Heater Design Data

The electric heater was designed to sustain a nucleate boiling heat flux of 310,000 BTU/hr.sq.ft over an area of 6 in. x 4 in. The electric heater was divided into 6 indpendently controlled sections, each capable of supplying 8,600 BTU/hr (2.52 KW).

Three windings, each 2 ft long, were fitted into each section (Figure 21). Two windings in series were used for 2.52 KW operation and the three windings in series were used for 1.0 KW operation. Each section was designed with 4 copper fins, 2 1/2 in. long, 6 in. wide and 1/8 in. thick. The temperature at bottom of the fin at the maximum heat load was calculated to be 650°F using the equation applicable to rectangular fins. The design data are shown in Table 3.

3. Experimental Difficulties

The surface thermocouples introduced into the boiling plate necessitated a separation between the electric heater and the boiling plate. The contact surfaces were machined flat and tinned together for good thermal contact. However over long periods of steady-state runs with water the tin oxidized and formed a heat transfer resistance. The electric heater was subsequently overheated leading to slight deformation. During the unsteady-state runs these difficulties were not so significant.

TABLE 3

Operating Power KW	Winding No.	Length of Winding ft	Resistance Ω	Surface Loading watt/sq.in.	Ω/ft	$\frac{\text{sq.in.}}{\Omega}$	Kanthal "A"-1
2.5 { 1.25	1	2	0.114	35.0	0.057	315	3/4 in. x 0.015 in.
1.25	2	2	0.114	35.0	0.057	315	3/4 in. x 0.015 in.
1.0 { 0.2	1	2	0.114	-	-	-	3/4 in. x 0.015 in.
0.2	2	2	0.114	-	-	-	3/4 in. x 0.015 in.
0.6	3	2	0.348	33.4	0.174	50	3/8 in. x 0.015 in.

Some of the surface thermocouples proved unreliable. The electroplated, press-fitted thermocouples worked very well near the bottom of the boiling plate, where they were not subjected to the large temperature gradients. Some of the surface thermocouples near the thin section of the boiling plate failed after a few runs and sometimes mushroomed out of the boiling plate. Unfortunately the silversoldered thermocouples were not silversoldered properly and gave erratic readings. This difficulty however can easily be overcome.

Due to the high temperatures of the boiling plate the teflon deformed extensively. The leakage of benzene vapour into the room was a safety hazard although substantial ventilation was provided.

The connections of the cables to the electric heater oxidized leading to large contact resistances. This limited the power of the electric heaters considerably.

Further difficulties were experienced in the synchronisation of the camera with the flash stroboscope. A modification of the camera pick-up was suggested.